University of Sheffield

Development of composite electrospun scaffolds for tissue engineering.

A thesis submitted in application for the award of PhD in materials science and engineering.

August 1, 2011 - March 31, 2014

Author:
Frazer James Bye

Supervisors:
Professor Sheila MacNeil
Professor Anthony Ryan

The results, discussions and conclusions presented herein are identical to those in the printed version.

This electronic version of the thesis has been edited solely to ensure conformance with copyright legislation and all excisions are noted in the text.

The final, awarded and examined version is available for consultation via the University Library.

Contents

List of Figures

List of Tables

Outputs

0.1 Publications

BYE, F. J. Wang, L. Bullock, A. J. Blackwood, K. Ryan, A. & MacNeil, S. Post production processing of electrospun fibres for tissue engineering. J. Vis. Exp., 2012, e4172.

BYE, F. J. Bissoli, J. Black, L. Bullock, A. J. Puwanun, S. Moharamzadeh, K. Reilly, G. C. Ryan, A. J. & MacNeil, S. Development of bilayer and trilayer nanofibrous/microfibrous scaffolds for regenerative medicine Biomaterials Science, Royal Society of Chemistry, 2013, 1, 942-951.

0.2 Presentations

A tissue engineering approach for the treatment of cleft palate. BITEG Work in Progress, 17/12/2010, University of Leeds, Leeds, UK.

Using a tissue engineering approach for the treatment of cleft palate. TCES Annual Meeting, 19/07/2011-21/07/2011, University of Leeds, Leeds, UK.

Electrospun biaxially distensible bilayer membranes to treat cleft palate. EPPP, 21/03/2012-22/03/2012, Institute of Physics, London, UK.

Tissue engineering of the Cleft Palate. Geoset, 15/12/2012, Kroto Research Institute, University of Sheffield, Sheffield, UK. `http://www.geoset.info/presentation/tisue-engineering-of-the-cleft-palate/`

0.3 Posters

Tissue engineering for Cleft Palate. BITEG Work in Progress, 20/12/2011, University of Sheffield, Sheffield, UK.

Electrospun biaxially distensible bilayer membranes to treat cleft palate. 3^{rd} TERMIS world conference, 05/09/2012-08/09/2012, Vienna, Austria.

Glossary

α**MEM** α-modified Eagles medium. 50, 51

β**FGF** β-fibroblast growth factor. 51

ϵ permittivity. 22, 24, 68

λ_{em} emission wavelength. 52, 53, 55, 147

λ_{ex} excitation wavelength. 52, 53, 55, 147

BMDMEM buffer modified Dulbecco's modified Eagle's medium. 124, 125, 128

DAPI 4',6-diamidino-2-phenylindole. 52, 93, 94, 98, 117, 118, 157, 173

DCM dichloromethane. 24, 59, 63, 68, 69, 71, 74–78, 90, 92, 147, 172, 198, 199

DED de-epithelised dermis. 146

DMEM Dulbecco's modified Eagle's medium. 49, 51, 95, 98, 115, 124, 125, 160

DMF dimethylformamide. 24, 68, 69, 71, 72, 75–77, 198

DMSO dimethylsulfoxide. 52

E Young's modulus. 48, 62, 69, 71, 75–77, 93, 99, 103, 130, 148, 168, 180, 189, 204, 205

ECM extracellular matrix. 49, 88, 93, 130, 131

EDTA ethylenediamine tetraacetic acid. 51, 55

EtOH ethanol. 24, 68, 69, 71, 72, 75, 99, 130

FCS fœtal calf serum. 49, 51

FITC fluorscein isothiocyanate. 53, 173

GTR guided tissue regeneration. 190, 192

HEPES 4-(2-hydroxyethyl)piperazine-1-ethanesulfonic acid. 122–125, 128, 134, 135, 201

hESMPs human embryonic stem mesenchymal progenitor cells. 44, 51, 144, 145, 150, 153, 155, 187, 193, 194, 199, 204

IMS industrially methylated spirits. 110, 113, 132, 135, 200

MeOH methanol. 63, 68, 69, 71, 72, 75, 76, 78, 147, 168, 199

MTT 3-(4,5-dimethylthiazol-2-yl)-2,5-diphenyltetrazolium bromide. 54, 98

PBS phosphate buffered saline. 49, 51–54, 94, 95, 104, 115, 117, 133, 135, 172, 173, 187, 200

PCL poly ϵ-caprolactone. 6, 7, 9, 10, 15, 24, 44, 63, 71, 73, 77, 89–91, 98, 138, 142–145, 147, 148, 150, 153, 155, 187–190, 193, 194, 199

PHA polyhydroxyalkanoate. 11

PHB polyhydroxybutyrate. 6, 11, 13

PHBV polyhydroxybutyrate-co-hydroxyvalerate. ix, 6, 7, 9, 11–13, 15, 24, 25, 44, 68, 69, 71–76, 90, 91, 96–98, 103, 115, 138, 141, 143–148, 153, 155, 160, 164, 187–190, 193, 194, 198, 199

PHV polyhydroxyvalerate. 6

PLA poly L-lactide. ix, 5–10, 14, 23, 24, 44, 59, 62, 63, 68, 71, 73, 76, 89–91, 97, 98, 103, 115, 138, 141, 143–148, 153, 155, 162, 164, 165, 167, 168, 172–176, 178, 180, 182, 187, 189, 190, 192–194, 198–200

PLGA poly lactic-co-glycolic acid. 7–9, 67, 78, 88, 90, 92, 98, 99, 103, 130, 199

PMSSQcoPFPA polymethylsilsesquioxane-polypentafluorophenylacrylate. 16, 18, 172, 174, 189, 190, 194, 199

RAFT reversible addition fragmentation chain transfer. 16–18

RPM revolutions per minute. 48, 56, 57, 59, 63, 67, 69, 74, 91, 110, 167

SEM scanning electron microscopy. 48, 59, 62, 63, 67, 69, 73, 75, 96, 143, 165, 168, 180

TCP tissue culture plastic. 62, 72, 150, 153, 157, 173–175, 178, 188

UTS ultimate tensile strength. 48, 62, 99, 103

Acknowledgements

I would like to thank:

The BBSRC for providing the funding for my PhD.

Patrick Theato for providing the PMSSQ-co-PFPA.

Julio Bissoli, and Sasima Puwanun, for conducting the experiments for and providing Figures 4.14 and 4.16.

Keyvan Moharamzadeh, and Gwendolen C. Reilly for their advice and input on Chapter 4.

Linge Wang, and Keith A. Blackwood for conducting the experiments for and providing Figures 3.3, 3.3, and 3.8.

Sheila MacNeil, I cannot say how much I have enjoyed my time as one of her students, the excitement this project has brought me, and how I will never look at a balloon the same way again.

Anthony Ryan for his inspirational meetings.

Anthony Bullock, for all his support in written and lab work, coffee breaks, "meetings"and for his advice and input on Chapters 3 and 4.

All my friends at the Kroto who have added to my enjoyment during my studies.

Finally, I would like to thank my wife Emma Bye for all the time spent listening to me practice presentations to the point where she knew them off by heart.

Abstract

The aim of this project was to design and evaluate biocompatible and biodegradable membranes. These membranes must be suitable for treating conditions where two tissues are required to coexist but would normally compete, and also for conditions where the target tissue must cope with distension. Two clinical conditions were considered in the design of materials -repair of major defects of the hard palate and a tissue engineered membrane for repair of the weakened pelvic floor where this tissue is subject to dynamic distension on a daily basis.

Cleft palate is a condition that affects one in every 500-700 live births worldwide. Its current treatment is slow and multi-staged over at least 15 years. This is due to the difficulty of trying to replace both the fast-growing soft tissue and the much slower growing hard tissue, in the hard palate in a child. There are two immediate problems: soft tissue overgrows the area where bone is required; and the defect in the hard palate expands with the growth of the child. A scaffold/membrane is required, which supports soft tissue growth and hard tissue growth, by keeping them segregated, and which can also expand with the growth of the child.

The approach undertaken was that of composite membrane production based on the use of electrospinning. First it was shown that monolayers of microfibres and nanofibres could be created in random, aligned and pseudo woven layers. These scaffolds were shown to have mechanical properties suitable for the treatment of a range of conditions, such as pelvic organ prolapse and bladder repair. These scaffolds were then further processed to produce multi-layered scaffolds, combining micro and nanofibres to make bi and trilayer membranes. Scaffolds were characterised by SEM and evaluation of mechanical properties.

Cell culture was then evaluated on these scaffolds. It was demonstrated that fibroblasts can infiltrate and fill microfibrous scaffolds, while nanofibrous scaffolds were shown to act as a barrier to cell entry for up to six weeks, but were still porous enough to allow nutrients to pass through membranes. Experiments showed that co-cultures of bone forming and soft tissue forming cells were kept segregated on multi-layered microfibrous/nanofibrous scaffolds.

Novel balloon collectors and fibre orientation were used to make scaffolds with low Poissons ratios in an attempt to create a scaffold that does not contract when distended. Finally, it was shown how proof of concept bioreactors can be used to multi-axially stress cells in culture to induce extracellular matrix production.

In summary, the techniques developed in this thesis lay the foundations for the creation of complex multi-layered scaffolds for tissue engineering, with tailored and novel mechanical properties. Furthermore, the research demonstrates that cells cultured on these scaffolds will respond well to distension on these scaffolds.

Chapter 1

Introduction

1.1 Biomaterials

Biomaterials show promise as carriers for new tissue and potentially, can be tailored to specific tissue types. They are also used to provide the mechanical properties desired of a particular tissue and to ensure that new tissue forms as it should. These materials must be biocompatible to be successful as invoking an immune response is undesirable. A desirable quality is for the material to biodegrade, leaving behind a fully functioning tissue with no evidence of intervention. Biodegradable devices also negate the necessity for a second surgical operation to remove the implant.[1] There are many polymers that can be used to create a biocompatable and degradable implant (Table 1.1).[2,3]

Material	Molecular weight / Da	Melting point /°C	Tensile strength / MPa
Poly(hydroxy esters)[2]	21k-500k	57-210	16-50
Poly(ortho-esters)[2]	99k-130k	Amorphous	20-27
Polyanhydrides[2]	-	66-240	-
Poly(hydroxybutyrates)[2]	230k-530k	137-171	16-36
Polydioxanones[2]	48k	Amorphous	0.5
Poly(fumarates)[2]	2.6k-14k	25-40	1-70
Polystyrene[4]	-	-	30-100
PHBV[4]	-	-	40
PLA	101K[5]	-	70[4]
Poly ϵ-caprolactone	65k[5]	60[5]	-
PLGA[5]	40k-240k	-	-
Titanium	48	-	700[6]
Steel 316L[6]	N/a	-	1000[6]
Magnesium[4]	24	649	185-232
Bone	N/a	N/a	200[6]
Skin	N/a	N/a	83 ± 40[7]

Table 1.1: Table of polymers currently used for medical applications with implant metals and tissues.

Biomaterials come in many different forms and types and can be formed from natural products such as collagen, synthetic polymers such as PLA or even biodegradable metals (magnesium alloys).[8]

Metals have long been used for hard tissue replacement and include the use of steel, titanium and cobalt alloys. Such materials are used to replace load

bearing tissues due to their high strength and good corrosion resistance (Table 1.1). The major drawback of non-degradable metals is that once the tissue has sufficiently healed it is necessary to remove such implants, causing extra distress and risk to a patient via a secondary operation. Biodegradable metal implants based on magnesium (which is already abundant in the body and has similar mechanical properties to bone, Table 1.1) are promising but present a challenge due to the highly corrosive environment of the body decaying the implant too rapidly. This can lead to rapid evolution of hydrogen gas. Hence, current research is focusing on the use of Mg alloys incorporating calcium and zinc (to prevent the creation of a Galvanic circuit and reduce the rate of corrosion).

With respect to polymers, PLA is an example of a semi-crystalline thermoplastic polymer with high crystallinity (60-70%) and mechanical properties similar to polystyrene (Table 1.1). Applications outside of biomedicine include food packaging, envelope windows and floral wrap.

Polyhydroxybutyrate (PHB) is also a melt-processable semi-crystalline thermoplastic. The polymer is stiff and brittle with very high crystallinity (Table 1.1). When melt processed, PHB degrades quickly.

PHBV copolymers are used over PHB due to their lower melt processing temperatures vs. stiffness and toughness. Polyhydroxyvalerate (PHV) contents of 5-10% produces a copolymer with properties similar to polyethylene and polypropylene. Typical uses of PHBV include biodegradable containers such as shampoo bottles, disposable razors and medically contaminated items.

Poly ϵ-caprolactone (PCL) is a semi crystalline polymer with mechanical and physical properties that can be varied with the polymer's molecular weight (Table 1.1). PCL has found many uses such as packaging, drug delivery, microelectronics, adhesives and tissue engineering.[9,10] PCL degrades in a similar fashion to PLA, by ester hydrolysis and its degradation products can be excreted from the bodies of rats.[11,12] The degradation time of the bulk polymer is longer than PLA (30 months compared to 20). However, porosity, crystalinity, surface area and molecular weight all play critical roles in the time required for the polymer to degrade as discussed later.

1.1.1 Rate and mechanisms of material biodegradation

The rate at which materials breakdown is dictated by a combination of factors. The first factor is the rate of chemical decay. The mechanism of a material's chemical degradation is dependent on each material's specific chemistry. It can be as simple as ester hydrolysis by exposure to water and wet environments, or require a more complicated enzymatic pathway. The second factor is material processing. This is simply explained by surface area. A highly porous implant will degrade faster than a compressed implant of the same mass. Using these factors the rate of a material's decay can be customised and materials adapted for specific purposes. A material used in a bone screw will need to last longer than in a resorbable suture, and materials can be selected to suit these purposes. One example is that PLA screws are noted to last up to 5 years *in vivo* compared to poly lactic-co-glycolic acid (PLGA) based scaffolds that can decay in as short a time as 3 weeks.[13–15] Finally, the degradation products of the materials must be known as some materials can degrade into

toxic metabolites. The degradation of specific polymers used in this project are discussed in more detail later.

Bulk degradation vs. surface degradation

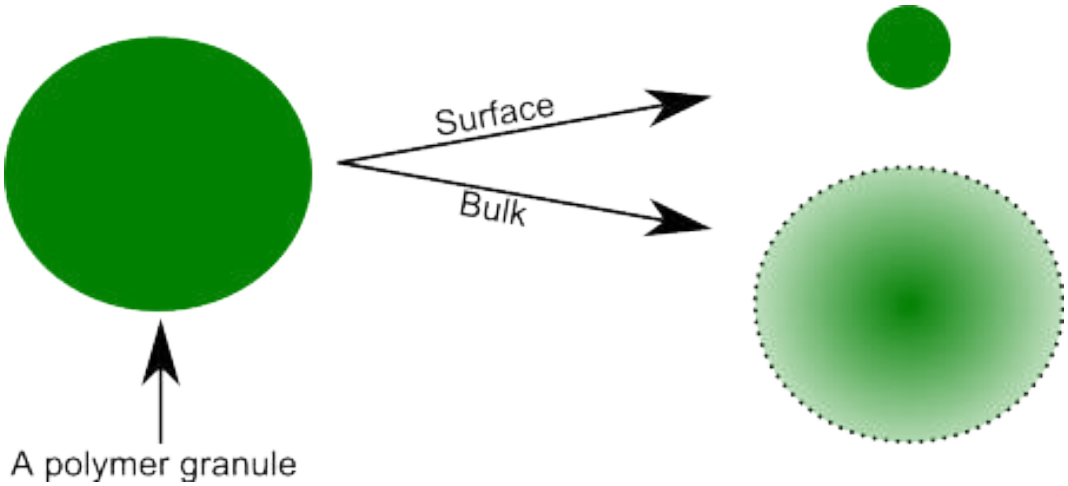

Figure 1.1: Modes of degradable water insoluble polymer breakdown. A polymer may undergo surface or bulk erosion. The material density is maintained during surface erosion, thus the particle decreases in volume as it loses mass. A polymer that undergoes bulk degradation maintains a constant volume, but decreases in density as it loses mass.

A water insoluble degradable polymer may degrade in a number of ways. Surface degradation is where the polymer loses volume (i.e. gets smaller, Figure 1.1) but maintains a constant density. Bulk degradation is where the polymer's density decreases (i.e. the volume stays constant but the material looses mass, Figure 1.1). A theoretical model was developed by Burkersroda, Schedl and Göpferich to predict the mechanism of such degradation pathways.[16] How water diffuses through a polymer matrix governs which of these two pathways is followed, along with other considerations such as dimensions, and degradation rate of the polymer's functional groups. Although it is essential to understand how such polymers degrade with respect to drug release or mechanical stability, the mechanism of bulk or surface degradation is poorly understood. Polyesters

(such as PLGA, PLA, PHBV, and PCL) have been traditionally thought to undergo bulk erosion.[17] However, Burkersroda *et al.* demonstrated that such polyesters (the poly(α-hydroxy esters) PLA and PLGA in their study), depending on processing, can undergo both of these mechanisms. The cross over point between these two mechanisms was quantified by dimension of the polymer granule under investigation. Under a critical dimension bulk erosion can occur. Above the critical dimension surface erosion predominates. For poly(α-hydroxy esters) Burkersroda *et al.* estimated the critical dimension to be 7.4 cm and in PCL to be 1.3 cm. As electrospun scaffolds consist of fibres with diameters of μm and smaller, the predominant degradation mechanism will be bulk erosion. This is due to the ability of water to sufficiently diffuse and penetrate polymers that are processed into dimensions smaller than their critical dimension. It must be noted that such estimates are subject to normal polymer variables such as molecular weight, crystallinity, and polydispersity which would all affect the diffusion of water.

Enzymatic degradation

Enzymatic degradation is hugely important for materials that may be implanted into the body. Polyesters in particular are susceptible to many polymerases found in the environment.[18] PHBV can be enzymatically degraded.[19] This degradation is strongly influenced by comonomer composition and proportion. The degradation of PLA hollow fibres in the body has been well studied, and enzyme activity characterised.[20] PLA invokes a foreign body response with a minor macrophage and giant cell response. A day after implantation alkaline phosphatase and β-glucuronidase activity was detected. ATP-ase, acid phosphatase, and esterase activity was noted from day three,

these enzymes are specifically associated with degradation of PLA into lactic acid. Finally, lactate dehydrogenase was detected at day 7, this enzyme is particularly associated with the conversion of lactic acid produced from the degradation of PLA. PLA does not degrade rapidly in the body, exponential increase in degradation rate was not observed until after a year, after bulk degradation reduced the molecular weight of the polymer to around 5000 Da. Likewise, the *in vivo* enzymatic degradation of PCL has also been well studied.[12] PCL is noted to have a long degradation period in the body which can be split into two stages, first is a decrease in molecular weight without deformation (bulk degradation) followed by rapid surface degradation (PCL capsules lost strength and broke into pieces). Low molecular weight PCL pieces were metabolised and then excreted through urine and faeces.

The hydroxyl free radical and degradation

The hydroxyl free radical ($^{\bullet}OH$) has been cited as important in the degradation process of both PCL and poly(D,L-lactic acid).[11,21] The hydroxyl radical is produced *in vivo* during acute inflammatory response to materials. Suitably stimulated macrophages produce superoxide ($^{\bullet}O_2^-$ radicals) and hydrogen peroxide (H_2O_2).

In the presence of iron or another metal suitable as a catalyst the $^{\bullet}O_2^-$ and H_2O_2 react to form the toxic $^{\bullet}OH$ radical. If produced near polymer implants, the polymer can then be attacked by the $^{\bullet}OH$ radical. This can cause the polymer chains to break up into smaller segments via homolytic bond fission. This mechanism preserves the free radical (i.e. it is not terminated), thus this

reaction can occur repeatedly, leading to the premature decay of a polymer implant.

1.2 Biomaterials used in this project

Several biodegradeable polymers were selected for investigation in this project, principally PLA, PCL, and PHBV (a polyhydroxyalkanoate (PHA)). These are discussed in the following section.

1.2.1 Polyhydroxyalkanoates

Polyhydroxyalkanoates are fatty acid derived polymers produced by microbes to act as an energy store.[22] They are biodegradable and known for their biocompatibility.[23,24] Industrially the bacterium *Alcaligene eutrophus* is used due to ease of culture and high polymer yield.[25] If these bacteria are cultured in conditions where phosphorous is limited, they can divide to a point, until the phosphorus is used up, at which point they attempt to store glucose as an energy reserve as polyhydroxybutyrate.[26] Once 70-80% biomass has been reached the polymer is extracted using an aqueous based process (Figure 1.2).

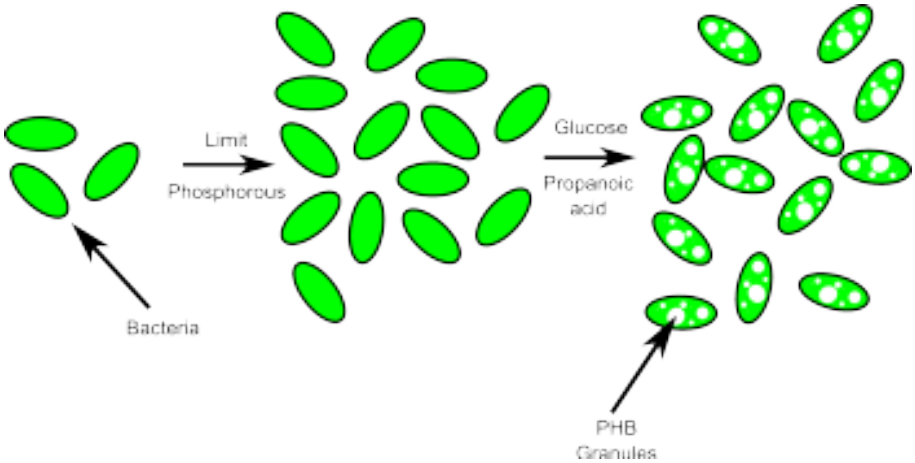

Figure 1.2: Synthesis of PHBV. Stage 1, culture bacteria under phosphate starved conditions until maximum population achieved. Stage 2, feed bacteria a definied concentration glucose and propanoic acid until 70-80% biomass achieved. Stage 3, lyse the bacteria and harvest the polymer.

There are reportedly 150 monomers that can form polymers in the PHA family.[22] Therefore a great variety of structures, chemistries and mechanical properties are available. In general, PHA polymers are thermoplastic, biodegradable, piezoelectric, chiral, and hydrophobic. The polymers produced are not restricted statistical copolymers either. Depending on bacterial species and culture conditions homopolymers and block copolymers can also be synthesised.

PHA polymers can be brittle or elastic with PHB being brittle due to the ready formation of a crystal lattice. PHA polymers that consist of other monomers or PHB polymers that include hydroxyvalerate monomer (to form PHBV) are more elastic as the secondary monomer breaks up the crystal lattice structure producing a more amorphous material. The extensive in-press review conducted by Laycock *et al.* considers that the connection between composition and mechanical properties, in particular for high hydroxyvalerate containing PHA polymers, is not well understood.[27]

PHBV

PHBV is a polymer with a high degree of crystallinity regardless of the hydroxyvalerate content (Figure 1.3). Laycock *et al.* reference PHBV as a example of isodimorphism, i.e. irrespective of the concentration of hydroxyvalerate in the PHBV polymer, the degree of crystallinty is in the range of 45% - 65%, predominantly above 52% and only falling below when the composition of hydroxyvalerate is between 40% and 60%.

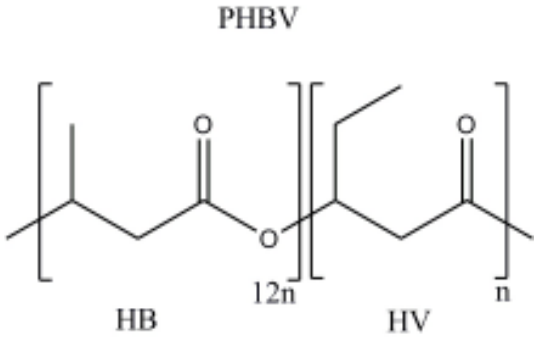

Figure 1.3: Structure of PHBV.

A statistical copolymer of hydroxybutyrate-hydroxyvalerate can be created by including propanoic acid in the media fed to the bacteria. The ratio of hydroxyvalerate to hydroxybutyrate can be predictably controlled by changing the concentration of additional propanoic acid.

Degradation of PHBV occurs naturally in microbially active environments, with the products being CO_2, H_2O and humus. This has been profiled over time in a number of different environments. There are many factors governing the rate of decay of the polymer, including processing method, polymer processing melt temperature, porosity, ambient temperature, media composition and most importantly molecular weight.[28,29]

Low molecular weight polymers have shorter degradation times than high molecular weight polymers, as it takes longer to break a large chain molecule down. Temperature affects the molecular weight, hence processing at high temperatures significantly reduces the polymers' molecular weight, leading to a decrease in longevity. Processing the polymer in such a way that it has a high surface area leads to a reduction in decay times. The high surface area exposes more of the polymer allowing more bacteria to access it at one time, hence compressed polymer disks have a shorter life than a injection moulded disk of the same mass.

The environment contributes to the rate of decay. Polymers in a warm wet environment decay faster than those in a dry environment, or where there is little microbial life, such as sea water. The polymer composition affects the crystallinity of the final material, a more crystalline compound is stronger and requires more energy to break down. PHB is a highly crystalline polymer, the addition of hydroxyvalerate into the polymer chain decreases this and leads to a shorter lifespan. However the crystallinity of PHB makes it difficult to process, requiring a high temperature, which reduces the molecular weight and hence a shorter decay time. So there is a benefit to including hydroxyvalerate, although it decreases the lifespan compared to pure PHB. The fact that it can be processed at lower temperatures allows it to have a longer lifespan than similarly treated PHB, due to the preservation of higher molecular weights.

Toxicological reviews of the polymer *in vitro* and *in vivo* have shown no negative effects or resultant abnormalities in the physiological and biochemical nature of single cells or whole lab animals, and it has been patented for use as bioabsorbable sutures.[23,30,31]

1.2.2 Poly lactic acid

PLA (Figure 1.4) is well known as a biomaterial and for being biocompatible.[2,32–36] It has been used often in the MacNeil group, and a knowledge base has been built up, making it a good candidate for initial investigation.[15,37]

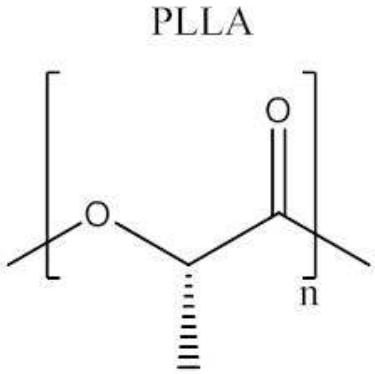

Figure 1.4: Structure of PLA.

The synthesis of PLA is multi-stage. Lactic acid is produced by fermentation of corn starch. The lactic acid molecules are condensed (ester formation) to form oligomers. A high molecular weight polymer is not formed at this stage due to the water liberated during the condensation reversing the reaction. Oligomers are formed initially to reduce the water formed when high molecular weight chains are produced. The oligomers are heated to induce a rearrangement and then form lactide dimers (Figure 1.5). Lactide dimers exhibit isomerism and have two chiral centres. The most common occurring form is the L-lactide, followed by the racemic DL-lactide. D-lactide is not naturally occurring, this makes it expensive so it is not regularly used in research. L-lactide easily undergoes polymerisation with the use of a metal catalyst such as stannous octanoate to produce isotactic (crystaline) poly L-lactic acid. This name is misleading as the polymer itself is a polyester.

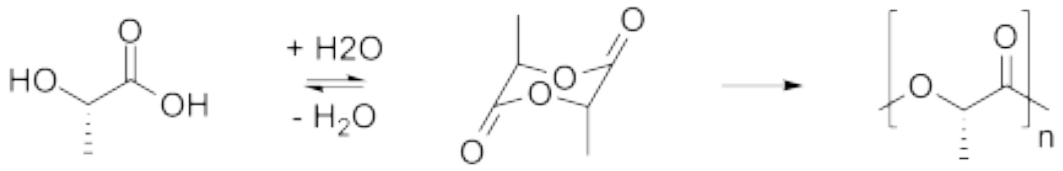

Figure 1.5: Two stage synthesis of PLA. First the lactic acid molecules form lactide dimers, that then undergo ring opening polymerisation to form PLA.

The degradation of PLA *in vivo* has been been well studied; no abnormal response is observed in rats and the polymer completely degrades over a period of 2 to 5 years.[13–15] The degradation times are dependent on molecular weight, method of polymer processing, surface area, crystalinity and porosity, much the same as for PHBV.[38–40]

1.2.3 Poly ε-caprolactone

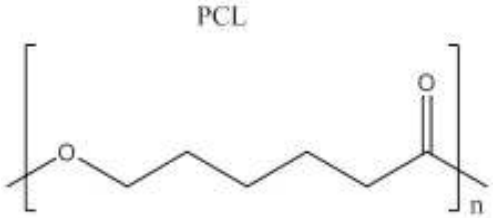

Figure 1.6: Structure of PCL.

PCL is derived from the ring opening polymerisation of ε-caprolactone (Figure 1.6). The polymer can be synthesised in a number of ways, including the use of enzymes, metal catalysts and organic methods.[41] Ring opening polymerisation is the most common methodology due to the cost and quality of the produced product. The ε-caprolactone monomer is formed in industry by the

oxidation of cyclohexanone by peracetic acid via the Baeyer-Villiger oxidation mechanism (Figure 1.7).

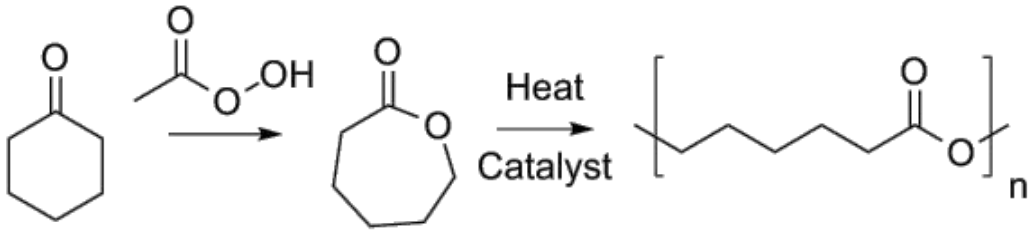

Figure 1.7: Synthesis of PCL. ϵ-caprolactone monomers undergo ring opening polymerisation to form PCL.

1.2.4 Poly (methylsilsesquioxane)-poly (pentafluoropheny-lacrylate)

This hybrid inorganic-organic block co-polymer shows promise as a surface coating for implants based on inorganic materials such as silicon and silicon oxides. Such surfaces can be very hydrophobic and do not wet well, a coating agent can be used to overcome this problem (Figure 1.8). Polymethylsilsesquioxane-polypentafluorophenylacrylate (PMSSQcoPFPA) is able to coat a wide range of substrates compared to other siloxane based coatings.[42] It has been shown that PMSSQcoPFPA allows the easy functionalisation of substrates in order to tune how surfaces interact with water and even protein binding.[42,43]

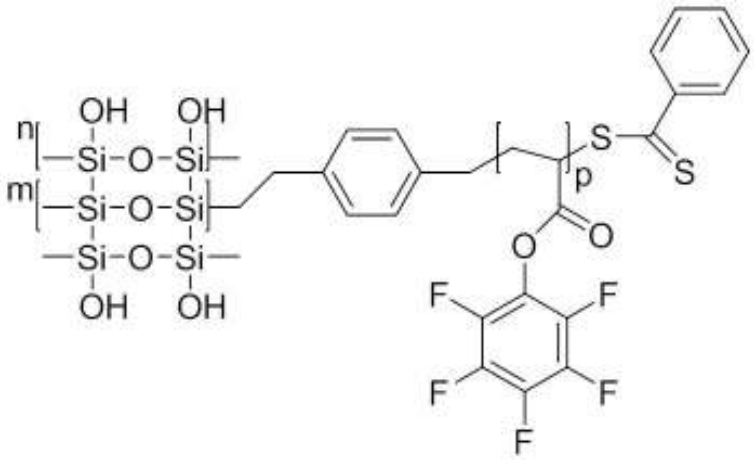

Figure 1.8: Structure of PMSSQ-co-PFPA.

Precise control over contact angles with water has been demonstrated by changing the reacting monomers and their respective ratios, or reacting the polymer with amines to produce a temperature responsive smart polymer whose contact angle changes with temperature.[42–45] The aspect of this polymer that interests tissue engineers is the possibility to use it as a protein immobiliser to encourage the binding of proteins to a scaffold made with/incorporating the polymer.[46]

PMSSQcoPFPA is synthesised in a multistage reversible addition fragmentation chain transfer (RAFT) polymerisation mediated process (Figure 1.9). RAFT polymerisation is a method for the controlled use of free radicals to synthesise polymers. RAFT is an example of living polymerisation, and as a result, polymers synthesised *via* RAFT have low polydispersities, can accept a great variety of monomers, can be performed at low temperatures ($\leq$60 °C), and are insensitive to acidic monomers. The general mechanism RAFT proceeds by is shown in Figure 1.9. The R and Z groups determine how the reaction proceeds. The RAFT process is subject to the following conditions; the Z group of the dithioester must activate the carbon - sulphur double bond

to allow free radical attack. Moieties that form suitable Z groups include aryl and alkyl groups.[47] Attempts at using other groups such as dialkylamino or alkoxy groups (dithiocarbamates and xanthates for example) have produced lower transfer constants and as a result are far less effective.[47] The presence of lone electron pairs on Z groups that can conjugate with the carbon - sulphur double bond are similarly less effective RAFT agents than those that incorporate electron withdrawing groups that can significantly increase the reactivity of RAFT agents.[48]

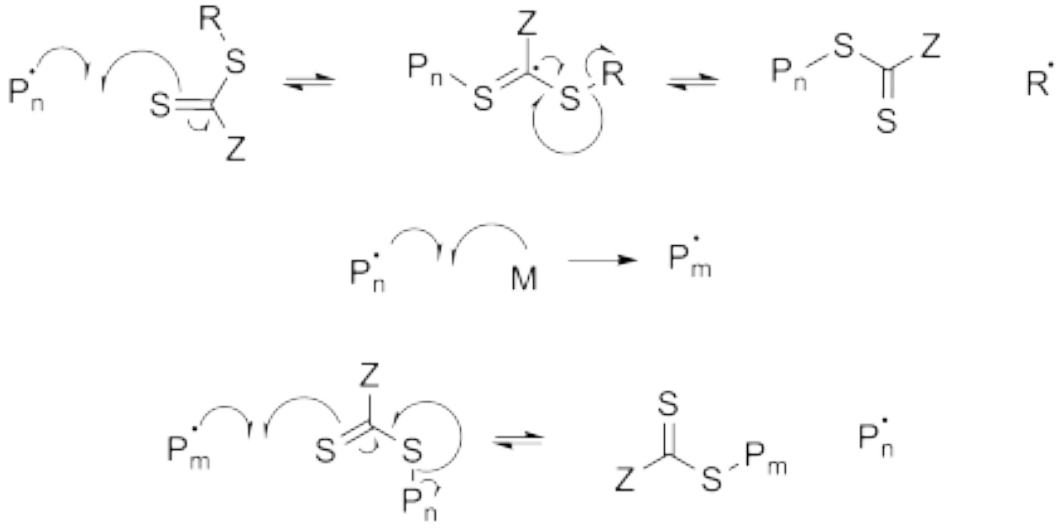

Figure 1.9: General mechanism reversible addition fragmentation chain-transfer polymerisation.

The R group facilitates the progression of the polymerisation by functioning as a leaving group from the dithioester. The R group then proceeds to initiate the next monomer. To be an effective R group many factors such as polarity, sterics, and radical stability must be considered.[49]

First the inorganic poly (methylsilsesquioxane) is produced by polymerising methyltrimethoxy silane with dithiobenzoic acid benzyl-(4-ethyltrimethoxy-

silyl) ester (Figure 1.8). This also forms the RAFT agent required to form the block co−polymer.

The poly (methylsilsesquioxane) is then RAFT polymerised again with the monomer pentafluorophenyl acrylate. This final step produces the PMSSQ-coPFPA block copolymer. This second monomer provides the organic component of the polymer and is the key to reactions with biological moieties. The inorganic PMSSQ has been reported to cross link easily, readily forming thin films. This lends itself to coating technologies. It is hoped that by combining organic and inorganic polymers the hybrid will not only share the properties of the components but could also yield new and more interesting properties through their interaction.

Using RAFT polymerisation near mono-disperse (nearly identical chain length) polymers can be produced predictably. The mechanism proceeds through the use of dithioesters, monomer and radical initiator. The dithioester acts as a RAFT agent, controlling the progress of the free radical polymerisation of the monomer. The radical initiator (often azobisisobutyronitrile) starts the reaction. These chemicals normally decompose into radical species when heated to a particular temperature. Free radical polymerisations are susceptible to premature termination from oxygen in the atmosphere, so they must be performed under inert atmospheres such as nitrogen or argon.

1.3 Electrospinning of biodegradable polymers

The polymers used in this project were processed using the technique of electrospinning, into microfibrous and nanofibrous scaffolds.

Electrospinning derives from a phenomenon described in 1914 by Zeleny, observing electrical discharge through water droplets from points.[50] If a syringe needle is continually fed a solution to which an electric current is supplied, the resulting droplet will be repelled from the needle and attracted to a grounded or oppositely charged collector.

The work of Sir Geoffrey Taylor on thunderstorms underpins and explains the electrospinning phenomenon, and it is his name that is used to describe the cone formed at the spinning tip.[51]

When a droplet forms at the end of the spinning needle, surface tension makes the drop assume a spherical form (lowest surface energy). When an electrical field of sufficient strength is applied the droplet is deformed, and at a critical point, disintegrates. At this point the strength of the electric field is greater than the surface tension, and conical points are formed from which jets of solution are then projected. The conical points are known as Taylor cones.

The cones form due to the accumulation of surface charge, and a pressure differential forming between the interior and surface of the droplet. When the surface of the drop is charge saturated, additional charge is enough to cause repulsion between other charges and the droplet vibrates. This is known as Rayleigh instability. Electrospraying occurs when the jets produced from a

droplet breaks up. If the jet remains stable, fibres are formed. This normally relies on the solution being viscous and the solvent volatile.

Electrospinning has been patented on a number of occasions throughout the 21^{st} century but has not become a widely commercial process, with few businesses specialising in it.[52,53] Electrospinning has garnered popularity in research labs due to its small scale flexibility and multitude of variables, allowing the creation of a huge variety of fibres that have potential uses from energy production to food preparation.[54,55] These are the same features which hamper the industrial up-scaling of the process, with bulk production of nanofibres being noted as a particular problem.[56,57]

Electrospinning can create fine fibrous networks with fibre diameters ranging from nm to μm and has found uses from filtration to biodegradable scaffolds for tissue regeneration. Electrospinning is governed by many parameters, including potential difference, distance between needle and collector, solution flow rate, viscosity, solution conductivity, and surface tension (Figure 1.10). Fibre formation occurs in a narrow window of concentration, viscosity and electrostatic charge, these parameters are discussed below.

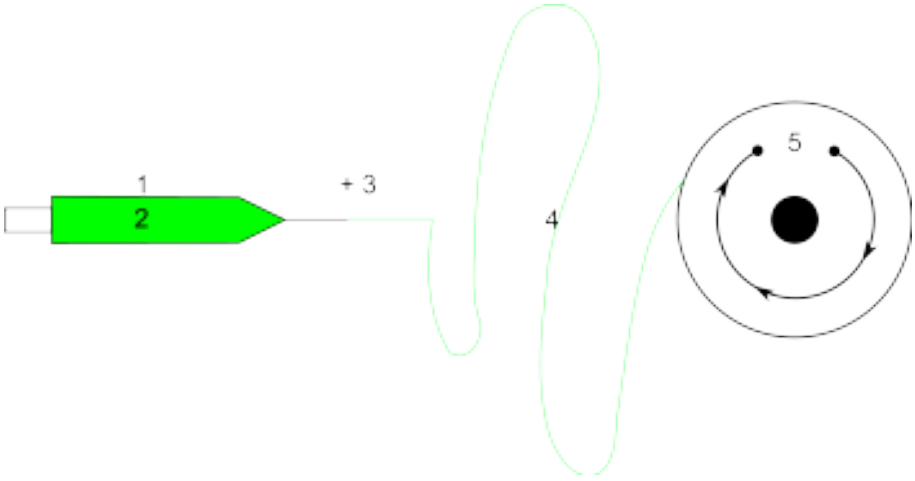

Figure 1.10: Spinning parameters: 1. Flow rate. 2. Concentration. 3. Potential difference. 4. Distance to collector. 5. Rotation speed. Temperature and humidity are also factors.

Voltage

This is the most obvious parameter, the potential difference provides the driving force and must be sufficient to overcome surface tension and produce a Taylor cone for fibre formation. The electric field drives the acceleration of the fibre from the spinner to the collector with fibres reaching velocities of the order of ms^{-1}. The potential difference applied and solution composition appear to be the biggest factors in outcome variability.[58–60] Too great a potential difference has been noted to cause beaded fibres.[61]

Viscosity

Too low a viscosity results in the jet breaking up and electrospraying. Polymer molecular weight directly impacts electrospinning due to its inextricable link

with solution viscosity and thus the required solution concentration to produce fibres. Low molecular weight polymers are more inclined to bead formation. It also appears that polymer chain entanglement has a role here and a critical number of entanglements is required for the formation of a stable jet.[62–64]

Solution concentration also affects viscosity and as a result is closely linked with fibre diameter (concentrated solutions result in thicker fibres). Too low a concentration and electrospraying results, too high and the solution will not spin as its viscosity is too great. This means there is a minimum and maximum concentration in which electrospinning can occur.[58,65]

Surface tension

Surface tension has a key role in bead formation. Solutions prefer to adapt conformations with the lowest surface energy, this happens to be a sphere as it has the highest volume to surface area ratio.[66] Surface tension is predominantly down to the solvent used.[67] Mixing solvents often results in a surface tension less than the sum of the neat solutions' surface tensions.

Flow rate

Flow rate is critical in droplet formation, a sufficient rate is required to maintain a droplet at the end of the spinner for a continuous fibre to result.[67,68]

Conductivity

The permittivity (ϵ) of the solutions is very important in the electrospinning process. A solvent with a low dielectric constant is a poor medium for electrospinning and can mean the difference between a solution spinning or not.[67,69] The conductivity of the polymers themselves also has an effect on their electrospin-ability. Polymers with a low permittivity are unable to accumulate sufficient surface charge density to be drawn to, and deposited on, the collector without fibre break up.[70]

Temperature and humidity

Humidity and temperature both affect the rate of solvent evaporation and solution viscosity. This has a marked effect on fibre morphology.[71] Ideally an environmental cabinet that can fix these two variables solves this problem. It has been shown to improve fibre consistency.[72] However, this is not always available, primarily due to cost.

Access to the rig and surrounding equipment when in an enclosure must also be considered, especially if it is necessary to produce scaffolds in a sterile environment. This can be achieved with an enclosed rig, preferably within an aseptic environment. For experimental purposes currently most electrospinning is conducted in laboratories without fine control of temperature or humidity and this leads to considerable variability in scaffold production.

1.3.1 Novel spinnerets for fibre production

One of the major limitations of current electrospinning rigs and an obstacle to industrial scale up is means of fibre production. Most rigs rely on a syringe pump and needle. Hence, there is a physical limitation on the number of syringes that can be used in one spinning session.

This is further hampered by problems with needles blocking up and even expensive glass syringes seizing after use (due to solvent evaporation). Niu *et al.* report the use of a disc, cylinder and spiral coil as a fibre generator. Each are rotated through a bath of the polymer solution, and fibres, at a critical potential difference are drawn from the spinneret to the collector.[73,74] This technique has the advantage in that many fibres can be formed at once, greatly reducing the time required to electrospin a sheet. This technology has a granted US patent and is sold under the trademark of Nanospider^{TM}.[75] If the collector is motorised such that it's movements match the rate of fibre production, a "direct write" electrospinning rig may be created allowing very fine and controlled deposition of fibres.[76]

1.3.2 Electrospinning of PLA

PLA is well known in the MacNeil group and is normally electrospun as microfibres (10 wt% in dichloromethane).[15,37,77] Nanofibres of PLA can be produced, as shown by Ball *et al.*, when producing electrospun condoms that release anti-HIV and spermicidal agents.[78] The spinning solution used consisted 10-15 wt% PLA dissolved in a mixed solvent system of chloroform and

2,2,2,-trifluoroethanol (1:1). Many groups are electrospinning PLA for use as medical implants and tissue engineering applications.[79–82]

1.3.3 Electrospinning of PCL

PCL is under great inventigation as a material for tissue engineering applications.[83] Hutmacher *et al.* are a particular authority on the electrospinning of PCL.[76,84–88] Nanofibres of PCL have been produced by using a solution of 14wt% PCL in a mixed solvent system of 9:1 chloroform:ethanol.[89,90] PCL can be readily made into microfibres using a solution of 15wt% PCL in dichloromethane.[83]

1.3.4 Electrospinning of PHBV

PHBV has shown promise as a biomaterial, and while less popular as a material choice than PLA and PCL due to its brittle nature. PHBV has previously been electrospun as micro and nanofibres using chloroform as the carrier solvent.[91–94] Zuo *et al.* have published work investigating the use of tetrachloromethane, ethanol (EtOH) and dimethylformamide (DMF) as cosolvents, and also including benzyltriethylammonium chloride in dichloromethane (DCM) solutions of PHBV as a ϵ enhancer.[94]

1.4 Using Bioreactors to test cell culture on scaffolds

Once a biomaterial has been processed into a scaffold, its performance with cells can be evaluated using a bioreactor.

A bioreactor is defined as a device that tightly controls its internal environment for the development of specific biological and chemical processes.[95] The environmental conditions used to guide these processes include temperature, pressure, pH, control of nutrients and waste. Bioreactors are, in one form or another, used to make useful products such as polymers, alcohol, or cells and complete organs.

This definition is very broad, and as a result there are many different kinds of bioreactor, depending on the product that it is designed to produce. Fermentation vessels are bioreactors in their simplest form, essentially a bucket that is kept warm. The environment of the yeast is tightly controlled and adjusted for the production of alcohol. Some polymers, such as PHBV, are created in a similarly fermented fashion as discussed in Section 1.2.1 and nutrients controlled to force the *Alcaligene eutrophus* bacterium to preferentially produce the polymer. Bioreactors for cell culture are the next step up and can contain multiple chambers to precondition medium with growth factors from other kinds of cells.[96] Depending whether the cell is adherent or not, reactors need surfaces for the cell to adhere to.

Going to the problem of producing tissues or even organs, here the biological complexity increases again and there are many more variables to be considered. There are at present very few bioreactors capable of handling complex tissue production. However, several studies point towards the same thing, that it may be necessary to induce stimulation of tissue to produce tissue that is fit for clinical use. Thus for example, corneal cells will be adapted for the conditions of the eye (where they survive under moist but not wet conditions and are subject to constant abrasion from blinking) compared to skin cells (where the upper cells exist in dry, acidic conditions). Also its well established that for hard tissues such as bone and cartilage it isn't enough to grow a tissue under static conditions. These cells need to be cœrced into creating appropriate extracellular matrix and this has now been shown to only be achieved through stimulation of the cells. Stimulation can be achieved through a number of different mediums such as electric pulses or physical mechanical stimulation through pummelling, stretching, and twisting. The kind of tissue produced can be greatly influenced depending on the kind of stimulation administered. This subject has been extensively reviewed.[95,97–101]

In vitro it is now recognised that bone cells require a mechanical stimulus to be induced to deposit calcium for bone formation.[102–105] Likewise, mechanical loading has been shown to be essential for cartilage formation.[106] It is also well known that cells are mechanosensitive and literature has shown there is a relationship between mechanical stimulation and extracellular matrix production, in particular elastin and collagen for fibroblasts.[107–109] This fact is also being exploited by beauty therapists as a nouveau anti-ageing treatment that can "instantly" rejuvenate unhealthy fibroblasts and boost elastin production.[110]

1.4.1 *In vitro* mechanically stimulating bioreactors

Most dynamic stimulation of samples in the lab is in 1D and until recently bioreactors have been custom, purpose built arrangements.[111] Commercial systems are becoming available. The Bose electroforce biodynamic system is perhaps the best well known system. It houses a sample in a chamber while administering a pre-prescribed distension or compression regime.[112] Other systems do exist and are gradually being brought to market, for example the Ebers medical TC-3 bioreactor which while very similar to the Bose system, does not contain force transducers and runs up to 3 samples at once.

For 2D simulation, the options are even more limited, most systems for applying 2D distortions (biaxial distension) to samples are custom made such as those used by Nielsen *et al.*[113–115] However, samples cannot be maintained in culture once they have been analysed. One commercial system that is able to maintain samples in culture while applying biaxial distension is the Flexcell^{TM} tension system that relies on a vacuum pressure to deform an elastic substrate. The deformation of the elastic substrate applies a biaxial distension to cell cultured in the system.[107,116,117] Unfortunately the Flexcell^{TM} system is limited in substrate choice and it not capable of incorporating bespoke substrates such as electrospun scaffold sheets.

1.5 Using biomaterials for Tissue Engineering

1.5.1 What is it and what can be done?

The term tissue engineering as defined by Vacanti *et. al* is "an interdisciplinary field that applies the principles of engineering and the life sciences toward the development of biological substitutes that restore, maintain, or improve tissue function".[118]

A broader definition of tissue engineering is as follows: engineering is concerned with the development and modification of structures, systems and processes using specialized knowledge.[119] Hence, to tissue engineer is to gain knowledge in developing and modification of complex systems that govern tissue growth, repair and replacement. The ultimate goal of tissue engineering is to be able to regenerate or replace degraded tissue and return it to its original healthy and functioning state.[120,121] This will also help alleviate current problems such as dependence on donor tissue. If the patient has a little healthy tissue it would be desirable to expand it in the lab for transplantation. A good example of this was published in 2004.[122,123] An adult male with most of his jaw missing underwent a mandible repair through the use of a "custom vascularised bone graft". Ablative tumour surgery left a gap to be bridged, including his chin. An implant was custom made to bridge the gap. The implant was constructed out of titanium mesh filled with blocks of BioOss bovine derived bone mineral. The mineral blocks had been pre-treated using recombinant human bone morphogenic protein 7 and bovine collagen type 1. To provide a bone precursor cell, bone marrow as extracted from the iliac

crest of the patient, mixed with bovine bone mineral and used to fill the gaps between the BioOss mineral blocks in the titanium mesh.

The implant was surgically implanted into a pocket in the right *latissimus dorsi* muscle in his back, in order to allow the implant to become pre-vascularised. This lead to its successful implantation into the defect region at a later stage. Initial results were promising, with the patient being able to eat his first solid meal in 9 years, bread and sausages. It had a pleasing aesthetic appearance, boosted self confidence, and allowed a return to social interactions. Bone was observed to be developing via a CT-scan, if unevenly, inside the implant after 7 months. Unfortunately due to a life style of heavy drinking and tobacco use, he died of cardiac arrest after 15 months.

Instances like these are important in the development of tissue engineering, demonstrating its successes and illuminating its failures. While the implant technique was successful, failure to treat the underlying causes ultimately resulted in its failure.

This is the type of direction tissue engineering appears to be taking *i.e.* current methods concentrate on using the patient's own tissues in conjunction with scaffolds to regenerate the areas in need of repair.[124–128]

There are still major problems to be overcome. While it is currently possible to use scaffolds to create a habitat for cells, such as the mandibulectomy above, or to graft small sections of epithelium onto a well vascularised wound bed, it has not been possible to construct complete tissues from a small biopsy.[129,130] Each tissue has its own peculiar set of conditions to overcome, for example

liver fabrication has yet to overcome creating the conditions to keep a bulk amount of hepatocytes in a scaffold alive while transferring from *in vitro* to *in vivo*.[124]

1.5.2 Guided tissue regeneration

The aim of guided tissue regeneration is to encourage the preferential growth of one tissue over another, for example bone over epithelium. This is normally achieved through the use of a barrier membrane to mechanically segregate one tissue type from another.[131–133] This is typically useful in instances where one tissue grows much faster than another and will invade, preventing the slower tissue proliferating.

Periodontal defects and gum disease are major causes of tooth loss. Invading bacteria cause the bone which the tooth is seated in to irreversibly erode, resulting in the tooth loosening and eventually falling out. Biomaterials can be used to reverse this damage and yield a stable tooth again. A scaffold to treat this must be mechanically stable, easy to make, sterilise and handle.[133]

Whatever material is selected, it is well known that it must biodegrade and be resorbed by the body. A non-degradable material would require a follow up procedure to remove it, incurring risks of reinfection and disturbing and newly formed tissues.[134] The materials currently in vogue are collagen based, as they are resorbable, easy to manufacture and sterilise, and can be handled with ease during surgery compared to synthetic scaffolds which have been compared to wet cotton wool.[135,136] However, collagen based materials have

been reported to be less successful as a barrier than non-resorbable scaffolds.[137] It is also reported that there is no gain using collagen compared to synthetic resorbable barriers.[138] The main disadvantage to the use of collagen based materials is from the potential for disease transmission such as Creutzfeldt Jakob disease.[136] Manufacturers of such patches have conducted theoretical studies and have concluded, with a small amount of experimental evidence, that their materials are "effectively" protein free.[139]

1.5.3 Bladder repair

Muscle invasive bladder cancer is a condition where the muscles surrounding the bladder become cancerous and need to be removed in order to prevent the cancer from spreading to the rest of the body. The removal normally involves a radical cystectomy, the complete surgical removal of the bladder. This causes a number of problems, primarily the need to create a new way of passing urine.

The current methods for doing this all involve the use of bowel tissue to form a small pouch the ureters can be plumbed into. This is then either fed to a hole in the abdomen known as a stoma which can drain into a bag (this is known as a urostomy). Or a valve can sometimes be implanted into the stoma, preventing the need for a bag, and instead the pouch can be drained at will through a catheter (continent urinary diversion).

Finally, it may be possible for the bladder to be reconstructed from bowel tissue (a cystoplasty), this is known as a neobladder. A section of bowel is formed into a balloon shaped sac with the ureters connected at one end and

the urethra at the other. The patient is then able to pass urine without the need for bags or valves, but the technique needs to be relearned from scratch. The neobladder remains connected to some of the bowel's nerve endings resulting in the sensation of having to pass wind when the neobladder is full and urine needs to be passed.[140] The tissue of the bowel is not ideal for bladder replacement, it is a mucous secreting tissue, and long term complication rates are high (40.8%).[141]

Tissue engineering could provide a solution, and research is being conducted on the use of biodegradable electrospun scaffolds for bladder replacement.[142,143] Such scaffolds could be used to fashion a new neobladder, not involving mucous secreting bowel tissue, and potentially use the bladder's own nerves. However, there are significant challenges to be overcome, the bladder must be able to cyclically fill and empty without putting pressure on the kidneys, nor the material fatigue, this makes bladder tissue engineering a very interesting problem.

Atala *et al.* reported in 2006 treating 7 myelomeningocele (one form of spina bifida) patients ages between 4-19 years old.[144] Spina bifida is the result of a development fault and leaves a gap in the spinal chord, and is linked to folic acid deficiency.[140] Myelomeningocele is the most severe form, the spinal column does not fully close and as as a result the baby's membranes and spinal chord collect in a sac at the baby's back. Myelomeningocele affects 1 in every 1000 live births in the UK.[140] As a result damage occurs to the nervous system, one of the symptoms that can result includes urinary incontinence. The bladder may only store a little urine and if treatment is not given kidney and bladder damage results. If regular treatments fail, a cystoplasty is necessary. However, Atala *et al.* notes the deficiencies of this procedure including metabolic disturbances, increased mucous production and malignant disease.

[144] Atala *et al.* attempted to bypass these problems by creating a tissue engineered bladder from the patient's own urothelial and muscle cells, obtained from bladder biopsies. After subculture and expansion these cells were implanted onto a range of decellularised bladder submucosa, the most successful of which was supplemented with polyglycolic acid and wrapped in omentum (a fold of the peritoneum, the membrane that lines the abdominal cavity covering the organs). Post implantation a catheter was used to cyclically load the new bladder for 3 weeks. Post operation no effect on metabolism or mucous production was observed, and renal function was maintained. In Atala's 2001 and 2011 literature reviews he concludes that acellular implanted scaffolds contract and produce diminished bladder capacities, that "cell-seeded matrices are superior" and that current research is "aimed at developing biologically active and 'smart' biomaterials".[145,146]

1.5.4 Pelvic organ prolapse

Pelvic organ prolapse is a condition where the organs such as the uterus, bowel, and bladder bulge and protrude into the vagina.[140] Symptoms can be a sense of something needing to be pushed back in the vagina, discomfort during sex and problems passing urine. The condition is not life threatening but can affect the patient's quality of life. Prolapse occurs when the vaginal tissues weaken and can no longer support the surrounding pelvic organs. The vaginal tissues weaken with age and also from the strain of childbirth, with half of women suffering from some form of prolapse after having children.[147]

Mild cases of the condition can be treated by weight loss and pelvic floor exercises, more severe conditions may require a vaginal pessary; a device that is inserted in the vagina to hold a prolapsed organ in place. In the most severe cases surgery is required to stitch the the vaginal and pelvic organ tissues in place. This can sometime involve the use of polypropylene mesh as a supporting material. However, long term data on the use of polypropylene meshes show that the repair then later perforates the surrounding tissues (Figure 1.11).[148,149] This is due in part to the mechanical properties of the implant not matching the surrounding tissues. The stiff implant lacerates the surrounding soft tissues.

Figure 1.11: Photograph of bladder perforation caused by use of lower urinary tract polypropylene mesh. Note the "wire fence" arrangement of mesh filaments that when under tension create a saw tooth edge to the implant.[148]

The US food and drug administration have issued a warning on serious complications resulting from these meshes and that they are not rare occurrences. It is unclear if such repairs are more effective than traditional non-mesh repairs.[150] Regardless of this, a better solution is required.

1.5.5 Cleft palate

The formation of the hard palate

The hard palate is formed by the maxilla, the bone found at the roof of the mouth (Figure 1.12).[151,152] The mechanism of the formation is peculiar in that the palatine processes grow down on either side of the embryonic mammalian tongue and then, dramatically "flip up" in a few hours to form the hard palate.[151–153]

Figure 1.12: Formation of the hard palate from a 16 day old rat to embryonic human.[151,152]

Aetiology and treatment

Cleft palate affects 1 in 700 live births in the UK and 1 in 500-700 worldwide.[140,154] A cleft palate occurs when the processes that govern the palates'

formation fail. Clefting can include just cleft lip or cleft palate and can be unilateral or bilateral. The most severe case being bilateral cleft lip and palate (Figure 1.13).[155]

Figure 1.13: Example of unilateral cleft lip and palate in an infant.[155]

The causes may be genetic or environmental, though these are still under debate.[156–159] Cleft palate can present itself as part of a syndrome or it can appear on its own (non-syndromic).

Environmental causes are not definitive, but there are strong links between the heavy use of alcohol, smoking and low folic acid levels.[158,159] These studies can be flawed due to poor separation of factors. Little's study corrects for confounding co-factors such as alcohol and the use of multivitamins.

The argument for folic acid being a cause is that cleft palate develops at approximately the same time as neural tube defects, caused by low folic acid levels.[159,160] However, the evidence here is also flawed due to poor separation of variables. Studies often use a control of mothers on "multivitamins" without

acknowledging most multivitamin products contain folic acid. The majority of studies find no significant link between folic acid and cleft palate.[161–163] The identification of gene mutations that cause cleft palate is still in its infancy. There is a link, with 20% of patients having similar genetic deviations.[156,157] These are for non-syndromic cases of cleft lip and palate only.

There have been many studies on instances where cleft palate goes untreated into later life, the findings of which conclude that deviations from normal growth is greatest just after birth.[164–167] As the sufferer ages the deviations in placement of bones such as the vomer or maxilla reduce. It has also been noticed that more problems can be caused by corrective surgery, with unoperated cases reporting better speech and quality of voice. Maxillary growth in unoperated cases is closer to normal adult growth than operated cases, giving a better facial shape. However, the social difficulties incurred in leaving cleft palate cases untreated are terrible with the majority of suffers having difficulty at school because of speech problems.

The tissues required for the repair of the palate are epithelium, specifically oral mucosa to cover the defect, and bone. The bone needs to provide a hard surface that can allow for suckling and speech development, but also must be able to grow and expand with the child allowing for normal growth patterns. An early repair of the hard palate is desirable to minimise impact on speech development.

Treatment is protracted and cannot deal with all the problems produced by the condition. Soft tissue is used to fill defects where hard tissue should be, fulfilling the aesthetic part of the repair, but this neglects the mechanical

function that the hard tissues provided. Hard tissue repair is a great challenge, hard tissues are required for suckling and subsequent speech development.

Bone grafts to fill the hard palate defect are currently not used as an option. They have actually been found to lead to distortion of the maxilla and the results can be worse than no surgery.[155,168] A bone graft may appear satisfactory to begin with, but then the bone cells fuse and this tissue does not grow with the child's head causing major facial disfigurement. The resulting complications and distortions to the maxilla are unacceptable and explain why the hard tissues of the palate are currently mostly left untreated. The NHS time line for treatment is as follows (Figure 1.14);[140]

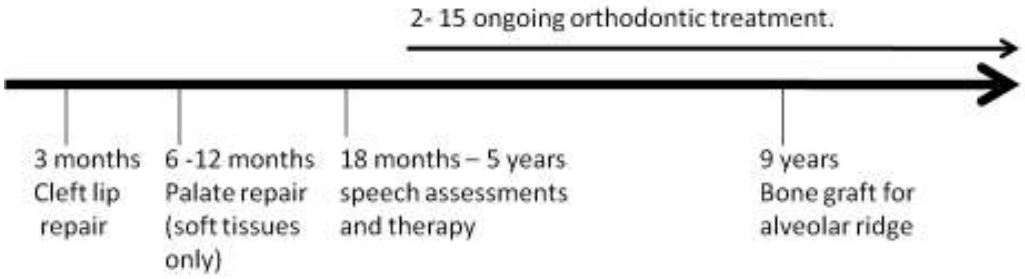

Figure 1.14: The NHS timeline of treatment for cleft lip and palate.[140]

Three months: surgery is carried out to repair the cleft lip and other soft tissues.

Six-twelve months: surgery to cover the hard palate is performed. This only covers the defect with the soft tissues already surrounding the cavity.

Eight-eleven years: a bone graft is used to correct the alveolar ridge if required. This restores the bony ridge at the front of the mouth allowing repair of dentition.

Two-fifteen years: orthodontic treatment is given.

Nothing is done to replace the hard tissues lost in the palate. This causes immediate and ongoing problems including suckling (managed through the use of specially designed soft bottles) and later speech development. Novel teat design helps the child to grasp the bottle, allowing the parent to help by squeezing, which removes the need for the child to suck (Figure 1.15).

IMAGE OF A FEEDING BOTTLE

Figure 1.15: Special bottle designs to aid in feeding infants with cleft lip and palate.

An obturator (a prosthesis used to make speech and feeding easier) is sometimes used, this is an acrylic plate fitted to the roof of the mouth, which replaces the hard palate allowing the child to suckle and aiding speech development (Figure 1.16).

Figure 1.16: An acrylic obturator.

Without a hard palate it is difficult to form sounds such as K, G, T, L, D, N. Obturators are not an ideal solution as they require replacing often because of the very fast rate of child growth. Each obturator has to be specifically moulded to fit each individual since no two instances of cleft palate are the same. The hard palate has proven difficult to repair at an early age, primarily due to the rapid and dramatic rate of growth of a child. Between the ages of 0 and 3 the skull grows exponentially (Figure 1.17).[169] The maxilla undergoes a similar dramatic change, doubling in volume in the first 5 years of life (Figure 1.18).[170]

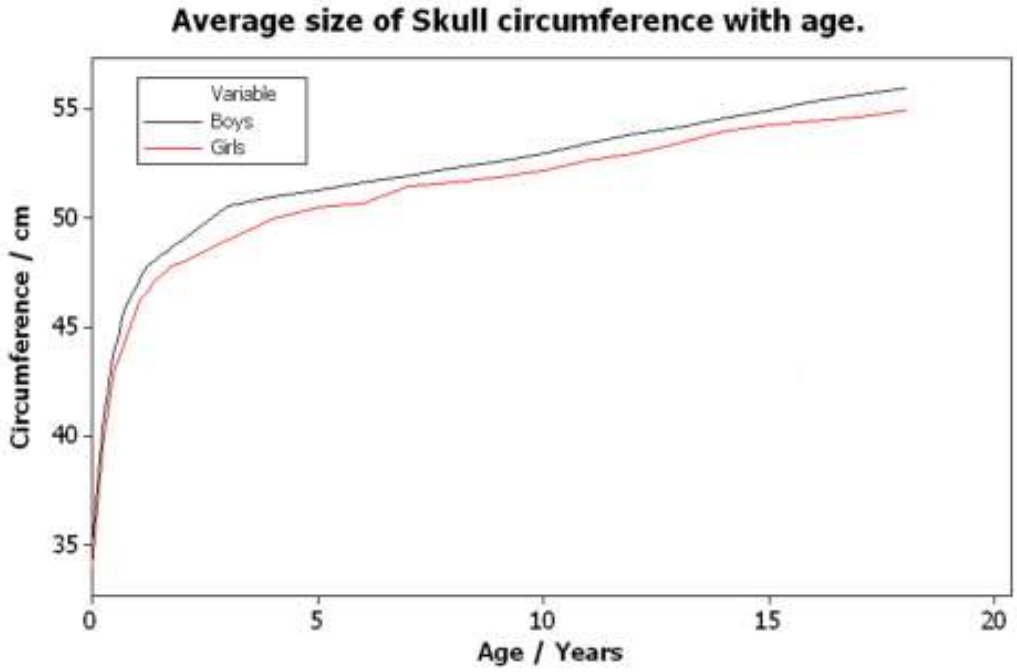

Figure 1.17: Change in skull size with age, note the first portion of the graph is exponential.[169,171]

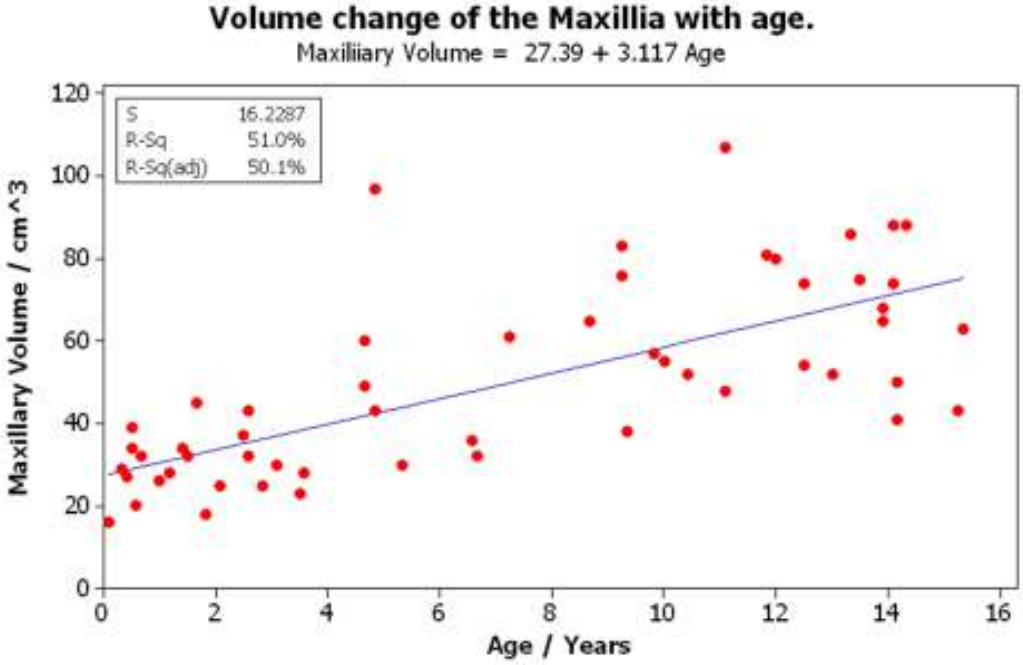

Figure 1.18: Change in maxillary volume with age.[170]

There has been a lot of debate about how best to treat cleft palate patients in the literature, the NHS time line is echoed around the world with the general principles that soft tissues are repaired early and a bone graft to the alveolar cleft is given much later.[155,168,172–178] There are two problems to overcome for the successful replacement of the hard tissues in cleft palate cases.
First, hard tissues grow at a rate far slower than soft tissue. An implant must be able to deal with this and prevent fast growing tissue invading the space where the hard, slow developing, tissues are desired. An aside to this is that the implant must also allow for the flow of nutrients in order to allow the separated tissues to flourish.

Second, the implant must allow for the growth of the patient. Cleft palate defects approximately double in volume from birth to the age of 5. Any construct must have this built in for a procedure to be a single and final solution.[169,170] To fulfil this the implant must be biocompatible and biodegradable. It would be unacceptable to require the removal of the implant at a later stage, disturbing the new tissues and risking the formation of disfiguring scar tissue.

The challenges of cleft palate repair in the context of tissue engineering

The solution to the treatment of cleft palate cases must be an improvement on current treatments, ideally requiring very minimal follow up. In order to fulfil this criterion, it must adapt and cope with the dramatic growth a child experiences, particularly up to the age of five. Currently the cleft defect is only repaired using surrounding soft tissues, this provides an aesthetically pleasing but non-functional repair (Figure 1.19, top). A potential solution to creating a

functional hard palate would be to use barrier membranes. A single operation could be performed early, inserting a soft tissue barrier above and beneath the cleft defect, then repairing the soft tissue as normal. The barrier's role would be to give bone a chance to develop in the defect, while keeping other soft oral tissues (such as oral mucosa) out (Figure 1.19).

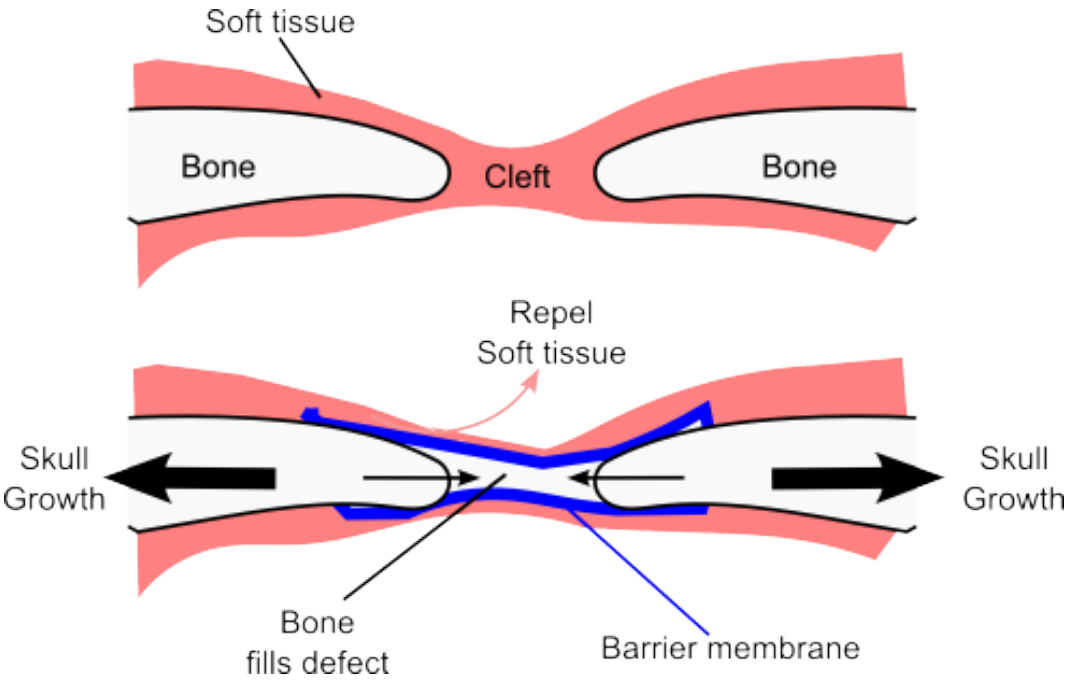

Figure 1.19: Diagram of current treatment (cross section through upper jaw, top) and proposed solution (bottom). The repair currently applied to a cleft defect is to merely fill the void with soft tissues. A better solution would use a barrier membrane to allow bone to develop within the cleft without being overrun with soft tissues. This would ideally require a single operation early on and be able to cope with the dramatic growth of a child.

This would lead to the formation of a normal healthy hard palate, with a complete shelf of bone (allowing speech and suckling) coated with healthy oral and nasal mucosa. The material used to construct the barrier must be biocompatible, and biodegradable at a rate comparable to the rate of bone growth. This will remove the need for follow up surgery to remove a non-degradable material. As it is intended to perform this operation as early as

possible, a mechanism must be included to allow the child's skull to grow as normal without the implant affecting facial shape. Essentially the barrier must be able to cope with and allow for the rapid expansion of the upper jaw.

1.6 Summary

In summary, in tissue engineering there are often needs (as illustrated by the condition of cleft palate where soft tissue and bone must be kept separated) to produce complex composite scaffolds. These scaffolds are often required to be both load bearing and biodegradable, necessitating the design of multifaceted composite scaffolds capable of delivering both concepts. For cleft palate the solution must facilitate the growth of two completely different tissues adjacent to each other. There are other tissues where cells of different types must be separated; a further challenge is that *in vivo* cells in tissues are subject to biaxial distension. Are soft tissues analogous to hard tissues? Will they respond to mechanical stimulation? Do they need mechanical stimulation to form physiologically relevant tissues in the laboratory?

Scaffold design will play an important functional role in tissue engineering. This is a given, a scaffold for bladder repair requires quite different properties to that used in periodontal defects or cleft palate treatments. This work documents the creation and design of scaffolds with multilayers (bilayers and trilayers) made of microfibres and nanofibres. The object is to create artificial basement membranes and barriers to allow different, and normally competing, tissues to develop together in a complementary manner. Further to this the end, the function of the scaffold is considered and the aforementioned membranes are adapted to tackle these issues. Including the incorporation of corrugations and designing of low Poisson's ratio cross linked scaffolds. These are meant to cope with uniaxial and biaxial distension. Such distensions are observed in cleft plate cases, pelvic floor prolapse, and bladder tissue engineering. An emphasis is placed on how the end scaffold is to handle as it must be

suitable for implantation, to this regard pseudo-woven scaffolds (hybrid cospun random-aligned fibre scaffolds) are devised.

What scaffolds do we need to address these issues, and how are we going to culture cells in the laboratory under relevant mechanical stimulation?

To this end several questions are raised. Is it possible to produce synthetic scaffolds that prevent cells from penetrating them, but at the same time allow nutrients to pass through? Is it possible to adapt these scaffolds in order to culture two different, but viable tissues either side without cell crossover? As there is not a one size fits all solution, can methods be developed to produce a range of comparatively complex scaffolds, in different materials, to tackle a range of different tissue engineering problems?

These are the questions this thesis will address.

1.7 Aims and objectives

The overall aim of this project was to develop electrospun scaffolds capable of supporting some of the physiological challenges of tissue engineering not currently met by simple scaffolds. Thus allowing one to co-culture two different cell types successfully, to achieve biomechanical properties close to complex human tissues, and to respond well to culture of cells under dynamic strain. The clinical applications which guided this research were the challenges of developing tissue-engineered materials for cleft-palate repair and repair/support of the weakened pelvic floor

The work is described under 5 related objectives:

1. To use the process of electrospinning to create a range of scaffold architectures, including microfibres and nanofibres, in a range of well known biocompatible polymers, preferably from PLA, PHBV, and PCL.

2. To evaluate the effect of the spinning methodology and scaffold architectures on cell viability and penetration of cells into scaffolds. In particular, do nanofibres prevent cell ingress, and if so maintained over a period of up to 6 weeks?

3. To produce composite and functional electrospun scaffolds that allow one to culture two different cell types under segregated conditions, in particular cells that have been shown to form bone and soft tissue such as human embryonic stem mesenchymal progenitor cells (hESMPs) and fibroblasts.

4. To investigate how scaffold architecture can potentially produce materials with novel mechanical properties e.g. auxetic behaviour under strain. At least the creation of materials with low Poisson's ratios should be investigated through scaffold design.

5. To develop simple bioreactors that can be used to test the effect of multiaxial distension on cells when growing on a 3D scaffold.

Chapter 2

Standard methodology, method creation and optimisation

2.1 Standard methodologies

The following methods were routine procedures used throughout this thesis. Where methods were developed as part of the thesis these are presented in the appropriate results chapters. All materials were acquired from Sigma Aldrich unless otherwise stated.

2.1.1 Arrangement of the electrospinning rig

All electrospinning was carried out in aseptic cleanroom conditions (pharmaceutical grade B. class 100).

Prepared polymer solutions (20 ml) were loaded into 4 × 5 ml syringes, fitted with blunt-tip needles (0.6 mm ID), and placed onto a single syringe pump set to deliver 40 μL.min^{-1} per syringe (Genie Plus, Kent Scientific, Connecticut, US). A mandrel (597 cm^2, radius 63 mm) coated in aluminium foil and rotated at 300 revolutions per minute (RPM), was used to collect the fibres. A working distance of 5-25 cm from the needle tip to the mandrel was used. A potential of +12000 to +30,000 V was applied to the needles (73030P, Genvolt, Shropshire UK).

2.1.2 SEM of electrospun scaffolds

Scaffold fibre diameter and morphologies were analysed using scanning electron microscopy (SEM) (Philips XL-20). Cross sections of bilayer scaffolds were obtained by manually cutting thin (2 mm) slices of scaffold and mounting them perpendicular to the mounting surface.

2.1.3 Tensile testing of scaffold

All scaffolds were cut into rectangles (5 mm × 20 mm) and measured for thickness using a micrometer. These sections were then placed in a Bose Electroforce 3100 instrument equipped with low-force testing grips, of a clamp design, with knurled locking screw, and smooth gripping surface for compliant samples such as biomaterials (8.4 mm maximum sample thickness, 12.5 mm maximum sample width, 12 mm recommended minimum sample length). A load of between 0 N and 22 N was then applied up to a distension of 6 mm at a rate of 1 mm per second. The Young's modulus (E) and ultimate tensile strength (UTS) was then calculated.

2.1.4 Fibroblast culture

All cell culture was conducted inside a class II laminar flow hood (Walker Safety Cabinets, Glossop, UK).

Skin samples were taken from consenting patients undergoing elective abdominoplasty or breast reduction surgery. Tissues were collected and used on an anonymous basis under Research Tissue Bank Licence 12179 as per the Human Tissues Act 2004, Part 1, Section 1(9b) which states research on human tissues may be lawfully conducted if it is;

"carried out in circumstances such that the person carrying it out is not in possession, and not likely to come into possession, of information from which the person from whose body the material has come can be identified."[179]

However, donations were typically from females ($\tilde{8}0\%$) in the age range 18-60. All samples were made anonymous before use. Tissue samples (0.5 cm $\times$ 0.5 cm) were incubated in 0.1% w/v trypsin (Difco Laboratories) and 0.1% glucose in phosphate buffered saline (PBS) (12-18 hours, 4 °C). The dermis was peeled off, minced finely and incubated with 10 ml of collagenase (0.5% w/v in Dulbecco's modified Eagle's medium (DMEM) and 10% fœtal calf serum (FCS) (eBiosera), 37 °C for 18 hours). Following centrifugation of the resulting cell suspension (400 g for 10 mins), pelleted cells were cultured in DMEM supplemented with FCS (10% v/v), streptomycin (0.1 mg/ml), penicillin (100 IU/ml) and amphotericin B (0.5 g/ml), and sub-cultured as necessary. Only fibroblasts of passage 4-9 were used in experiments. This is because primary fibroblasts have a finite lifetime *in vivo* and beyond passage 9 are susceptible to developing altered characteristics. This is well characterised by Hayflick *et al.* in 1961 (Figure 2.1).[180]

Janson *et al.* note that late passage fibroblasts have enlarged cell bodies and positive for myofibroblast markers and also greatly decreased matrix deposition.[181] Late passage is defined by Janson *et al.* as 30 passages. Likewise Janson *et al.* also show that donor age impacts fibroblast proliferation and extracellular matrix (ECM) formation (3 donors, ages 44, 56 and 60 years). Each experiment using fibroblasts in this thesis was performed in triplicate using fibroblasts from 3 anonymous donors each time between the ages of 18-60, therefore some natural variation can be expected.

GRAPH OF FIBROBLAST PROLIFERATION
VS. PASSAGE

Figure 2.1: Diagram showing how fibroblast growth alters with time and passage. Phase I, or the primary culture, terminates with the formation of the first confluent sheet. Phase II is characterised by exponential growth necessitating many passages (subcultivations). Cell alteration can occur at any point during Phase II. Hence, an alteration may occur at any time giving rise to a cell line whose potential life is infinite. Phase III, cells in culture rapidly decline after a finite period of time. Thus, primary fibroblasts used in experiments in this thesis were between passage 4-9, before entry into Phase II to minimise the possibility of cell alteration.[180]

2.1.5 hESMP culture

All cell culture was conducted inside a class II laminar flow hood (Walker Safety Cabinets, Glossop, UK).

Mesenchymal progenitor cells (hES-MP^{TM} 002.5) were obtained from Cellatris®, Göteborg, Sweden. α-modified Eagles medium (αMEM) was from BioWhittaker, Lonza, Switzerland. The hESMPs were seeded into a T75 (EasyFlask^{TM}, Nunc, US). αMEM supplemented with penicillin (100 IU/ml), streptomycin (0.1 mg/ml), β-fibroblast growth factor (βFGF) (4 ng/mL) and L-glutamine (100 mg/ml) until confluent. Only hESMPs of passage 2-9 were used in experiments.

2.1.6 Keratinocyte culture

All cell culture was conducted inside a class II laminar flow hood (Walker Safety Cabinets, Glossop, UK).

Keratinocytes were obtained from skin samples obtained from patients as above, washed with streptomycin and penicillin (100 mg/mL and 100 IU/ml respectively in PBS). The tissue samples were refrigerated overnight (12 hrs) at 4 °C in trypsin and glucose (0.1% w/v and 0.1% w/v respectively in PBS). The epidermal and dermal layers were separated, and keratinocytes were scraped off of the lower surface of the epidermis and the upper surface of the dermis with a scalpel blade. Keratinocytes were then seeded at a density of 2×10^6 per T75 culture flask pre-seeded with 5×10^5 i3T3 cells in Greens medium (3:1 v/v DMEM and Hams F12 medium supplemented with 10% v/v FCS, 10 ng/mL EGF, 0.4 μg/mL hydrocortisone, 1×10^{-10} mol/mL cholera toxin, 1.8×10^{-4} mol/L adenine, 5 μg/mL insulin, 2×10^{-3} mol/L glutamine, 0.625 μg/mL amphotericin B, 100 IU/mL penicillin and 10 μg/mL streptomycin).

Keratinocytes were maintained in culture to passage 2 then used in experiments.

2.1.7 Preparation of cultured cells for seeding

Cell suspensions were prepared for seeded by adding trypsin/ethylenediamine tetraacetic acid (EDTA) (5 ml, 5 mg/ml trypsin, 2 mg/ml EDTA in saline) and incubating for 5 minutes at 37 °C. The resulting suspension was centrifuged for 5 minutes (150 g). The cells were re-suspended in 5 ml of cell appropriate medium and counted using a haemocytometer, and the concentration adjusted for seeding.

2.1.8 Staining of cells with fluorescent vital dyes

Where required, cells were prelabeled using CellTracker green (CMFDA) and CellTracker red (CMTPX, Invitrogen) prior to seeding. The cells to be labelled were washed (3 × 5 ml PBS) and a 10 mM solution of the appropriate CellTracker was added (CellTracker was dissolved in dimethylsulfoxide (DMSO) (0.001% v/v) and added to 10 ml serum free cell-appropriate medium). The cells were subsequently incubated for 45 minutes at 37 °C. After incubation, the cells were washed (3 × 5 ml PBS) following which, they were seeded onto the appropriate scaffold. An Axon ImageExpress microscope (Molecular Devices, Sunnyvale, US) set to 570 nm excitation wavelength (λ_{ex}) 620 nm emission wavelength (λ_{em}) (CellTracker red) and 480 nm λ_{ex}, 533 nm λ_{em} (CellTracker green) was then used to image samples.

2.1.9 Cell nuclei staining

Samples to be stained with 4',6-diamidino-2-phenylindole (DAPI) were fixed in 1 ml 3.7% formaldehyde in PBS at 37 °C for 20 minutes. Samples were then washed with 3 × 1 ml PBS and incubated in a solution of DAPI (1 μg/ml in PBS) for 30 minutes. Afterwards the samples were washed with 3 × 1 ml PBS. The stained samples are then imaged on an Axon ImageExpress fluorescent microscope using 365 nm λ_{ex}, 460 nm λ_{em}.

2.1.10 Cell cytoplasm staining

Samples to be stained with fluorscein isothiocyanate (FITC) were fixed in 1 ml 3.7% formaldehyde in PBS at 37 °C for 20 minutes and then washed with 3 × 1 ml PBS. Samples were then incubated in a solution of FITC (1 μg/ml in PBS) for 30 minutes. After the samples were washed with 3 × 1 ml PBS, the stained samples were then imaged on an Axon ImageExpress fluorescent microscope using 480 nm λ_{ex}, 533 nm λ_{em}.

2.1.11 Elastin staining

Samples to be stained for elastin were fixed in 1 ml 3.7% formaldehyde in PBS at 37 °C for 20 minutes and then washed with 3 × 1 ml PBS. 200 μL of elastin primary antibodies were added to each sample (5% v/v in PBS, rabbit anti human alpha elastin, AbDserotec, Kidlington, UK) and incubated at 37 °C for

30 minutes. Samples were then washed with 3 × 1 ml PBS and incubated in a solution of secondary antibody (0.5% v/v goat anti rabbit IgG (FC):FITC) in PBS for 30 minutes. After the samples were washed with 3 × 1 ml PBS. The stained samples were then imaged on an Axon ImageExpress fluorescent microscope using 480 nm λ_{ex}, 533 nm λ_{em} for the secondary antibody.

2.1.12 Measuring cell viability using the resazurin salt assay

The resazurin salt assay is a colorimetric growth indicator that detects metabolic activity. The resazurin dye is a oxidation-reduction indicator. When viable cells are exposed to blue resazurin dye for a fixed time the cells reduce the dye to a pink product whose optical absorbance can be read.[182] As the product can permeate the membrane of the cells the culture remains viable and the assay does not destroy the experiment. If the concentration of the dye is fixed then a measure of the number of viable cells can be made by recording how much of the dye is reduced in a given time.

A resazurin stock solution was made in PBS (5 μg/ml). After removal of residual media, 1 ml of solution was added to each substrate and incubated for 1 hour, following which 150 μL was taken from each sample and the optical density read (570 nm, Bio-Tek ELx800). The media was then replaced if required (1 ml per sample).

2.1.13 Measuring cell viability using the MTT assay

The 3-(4,5-dimethylthiazol-2-yl)-2,5-diphenyltetrazolium bromide (MTT) assay is a colorimetric growth indicator that detects metabolic activity.[183] Like the resazurin salt assay the yellow MTT dye is an oxidation-reduction indicator. When viable cells are exposed to yellow MTT dye for a fixed time the cells reduce the dye to a blue product that is insoluble in PBS. The cells can then be lysed, the dye liberated, and dissolved in a known quantity of solvent, and the mixture's optical absorbance read. The number of viable cells can be determined by how much of the dye is reduced in a given time.

0.5 ml of MTT solution (0.05 mg/ml in PBS) was added to each sample and incubated for 1 hour at 37 °C. The solution was removed. 2-Ethoxyethanol (500 μL) was added to each substrate to lyse the cells and solubilise the dye. 150 μL was pipetted from each sample into a 96 well plate, and the optical density read (560 nm, Bio-Tek ELx800).

2.1.14 Measuring total DNA using PicoGreen

The picogreen assay was performed by first washing the samples with PBS (3 $\times$ 1 ml). A digestion buffer was then added (250 μL) to each sample and left for 10 minutes. The cells were mechanically separated and lysed from the plate by scraping with a pipette. The cell lysate was then collected and placed into 0.5 ml Eppendorf tubes and vortexed for 1 minute. The Eppendorfs were then subjected to 3 rounds of freeze thawing between 37°C and -80°C and then centrifuged for 5 minutes (150 g). Picogreen (180 μL, 1:200 picogreen, 1:20

trypsin EDTA buffer in distilled water) was added to the supernatent (180 μL) of each eppendorf and then read on a fluorescence plate reader (485 nm λ_{ex},− 528 nm λ_{em}).

2.1.15 Statistics

Statistics presented, unless otherwise stated, are calculated using Student's unpaired t-test. The significance of the results is denoted using $*$ symbols where;

$*$ Denotes that P<0.05 was recorded and the results are significantly different.

$**$ Denotes that P<0.01 was recorded and the results are very significantly different.

$***$ Denotes that P<0.005 was recorded and the results are extremely significantly different.

2.2 Methodologies created and optimised in this thesis

The following methods had to be created and optimised during the course of this project.

2.2.1 Calculating the RPM of the electrospinning drum

The speed of the electospinning mandrel currently used in the MacNeil laboratory is described using arbitrary units from 0 to 10 displayed on the motor. 0 is not stationary but the minimum speed and 10 is the maximum. In order to understand the effect of rotational velocity on fibre characteristics this had to be translated into speed. It has been previously observed that the creation of aligned vs. randomly oriented fibres is facilitated by accelerating the speed of the collector.

A plastic splint (2 mm × 5 mm × 50 mm) was taped tangentially to the surface of the drum, perpendicular to the axis of rotation. The mandrel was then set to spin at the arbitrary units of 0, 2, 4, 6 and 8. A plastic "shatter proof" ruler was placed in the path of the plastic splint resulting in a "tick" sound with every rotation. This sound was recorded as a .wav file using Adobe audition audio software on a wireless pc for 10 seconds per each setting. The error bars are calculated from the counts in 1 second ±1 multiplied for every second in 1 minute. Hence readings are ±60 counts. Plotting speed setting vs. measured RPM gives a linear plot where a setting of 0 results in a mandrel speed of 300

RPM and a setting of 8 gives a top measured speed of 1700 RPM (Figure 2.2).

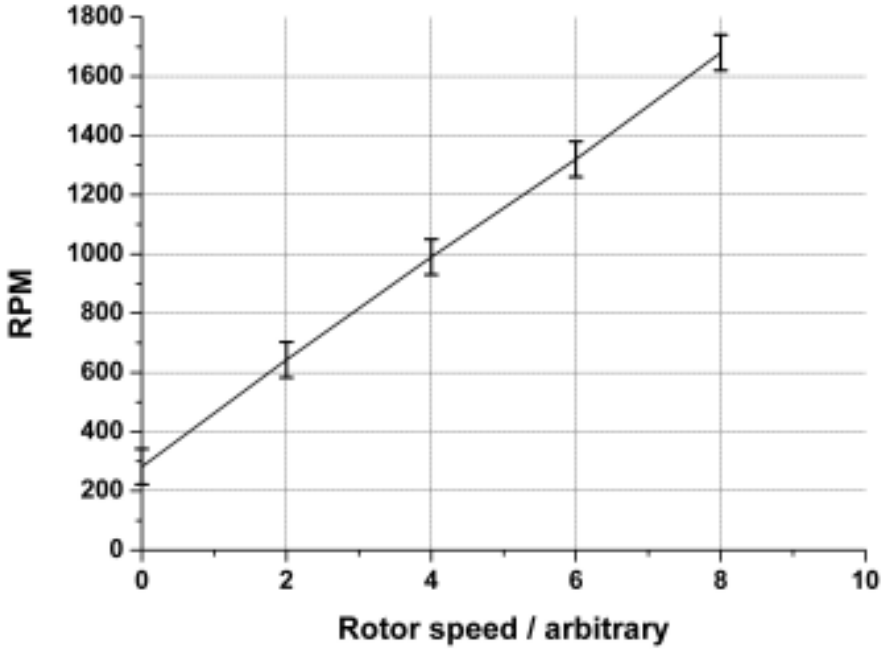

Figure 2.2: Graph of rotor setting vs. RPM. Error bars calculated from error propagation in method.

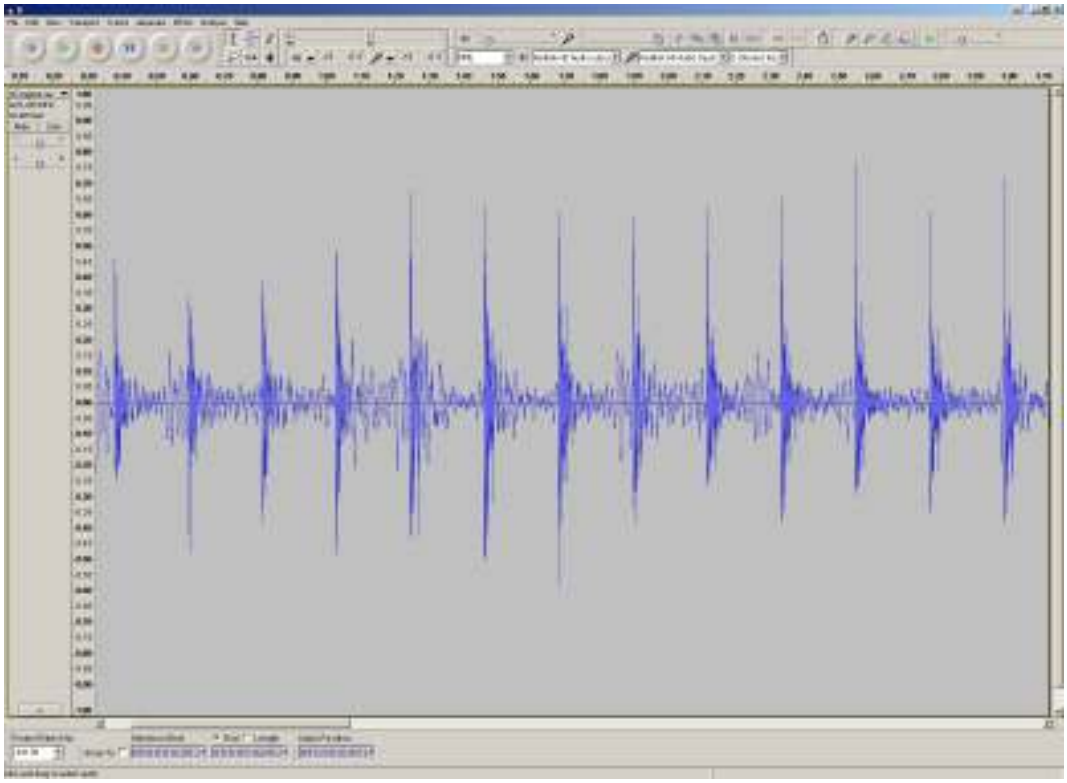

Figure 2.3: Peak counting in Audacity to calculate the RPM.

The resulting .wav file was analysed using Audacity 1.2.6, Dominic Mazzoni, US. This software was used to remove noise from the track and allowed the RPM to be calculated from the 'ticks' per minute counted at each speed setting (Figure 2.3). Extrapolating for the top predicted speed, at a setting of 10 the RPM would equal 2300±60.

$$y = mx + c \tag{2.1}$$

$$y = (\frac{(1600 - 300)}{(7.5 - 0)})10 + 300 \tag{2.2}$$

(Gradient values read directly from Figure 2.2.)

$$y = 2300 \tag{2.3}$$

Error in value as calculated via error propagation;[184]

$$\sqrt{(\frac{60}{1600})^2 + (\frac{60}{300})^2} + \sqrt{60^2} = 60.2 \tag{2.4}$$

This was necessary as the mixer used to rotate the mandrel only defines its rotational velocity on an arbitrary scale of 0 to 10. It's interesting to note that 0 isn't stationary. In the literature it's been shown that random architectures are obtained at lower RPM (around 200-300 RPM) and that aligned fibres can be achieved at 1000 RPM and over.[185,186] From this experiment we now know we are electrospinning in the random range (300 RPM) and also that we have the ability to spin in a range suitable for aligned fibres.

2.2.2 Electrospinning of PLA

PLA (Goodfellow, Huntingdon, UK, molecular weight unavailable, please see data sheets in Appendix A.1) solutions were made by dissolving the bulk polymer in DCM (10 wt%, Sigma Aldrich, Dorset, UK). The polymer solutions (20 ml) were loaded into 4 × 5 ml syringes, fitted with blunt-tip needles (0.6 mm ID), and placed onto a single syringe pump set to deliver 40 μL.min^{-1} per syringe (Genie Plus, Kent Scientific, Connecticut, US). A mandrel (597 cm^2, radius 63 mm) coated in aluminium foil and rotated at 300 RPM, was used to collect the fibres. A working distance of 17 cm from the needle tip to the mandrel was used. A potential of +17,000V was applied to the needles (73030P, Genvolt, Shropshire UK).

5, 10, and 15 wt% solutions of PLA were made and electrospun under standard conditions. The resulting scaffolds were then processed for SEM to assess the effect of changing polymer concentration upon fibre morphology (Sections 2.1.2). At 5 wt% nanofibres were achieved, but also present were bulbous artefacts (Figures 2.4 & 2.5). At 10 wt% and 15 wt% fibres were achieved although the fibre diameters reduced with increasing polymer concentration (Figure 2.6). PLA microfibres can be easily and reproducibly obtained. The scaffold produced was white and considerably fluffy. This made them difficult to handle as they easily stuck to anything, and easily deformed. SEM images showed the fibres to be 3 μm in diameter on average (Figure 2.4).

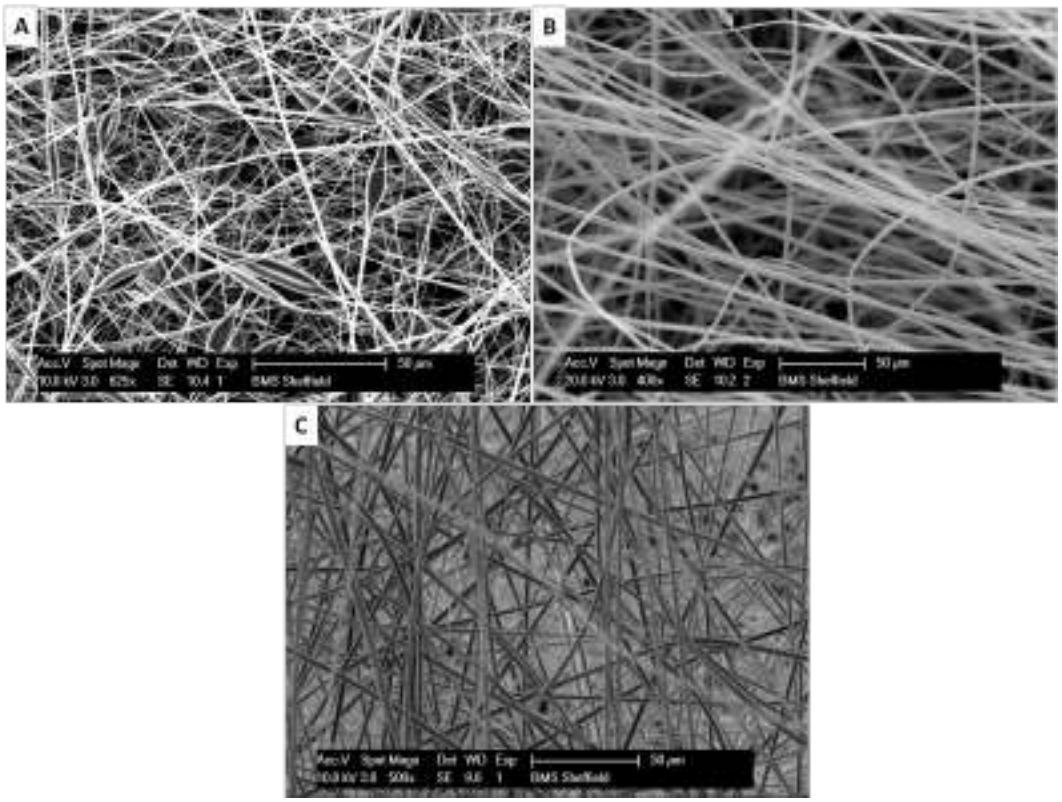

Figure 2.4: SEM image of PLA electrospun at A. 5 wt%, B. 10 wt% and 15 wt% concentrations in DCM. Fibre morphology changes as the concentration of PLA is increased.

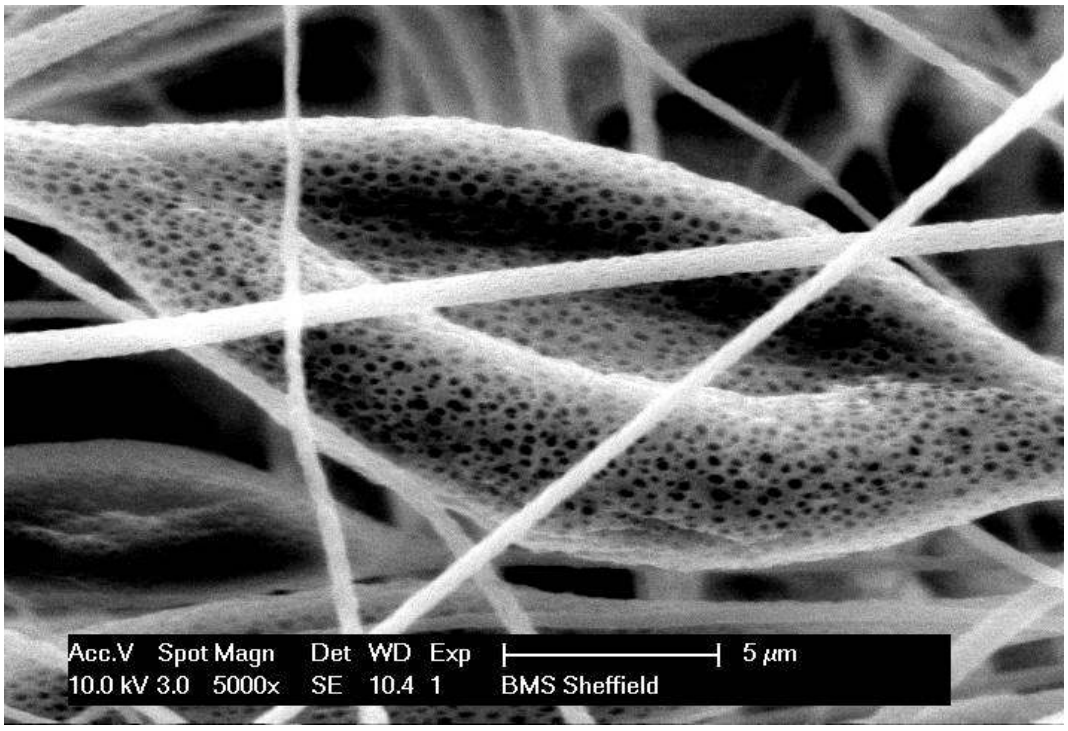

Figure 2.5: Close up SEM image of spinning artefacts that occurred when electrospinning 5 wt% solutions of PLA.

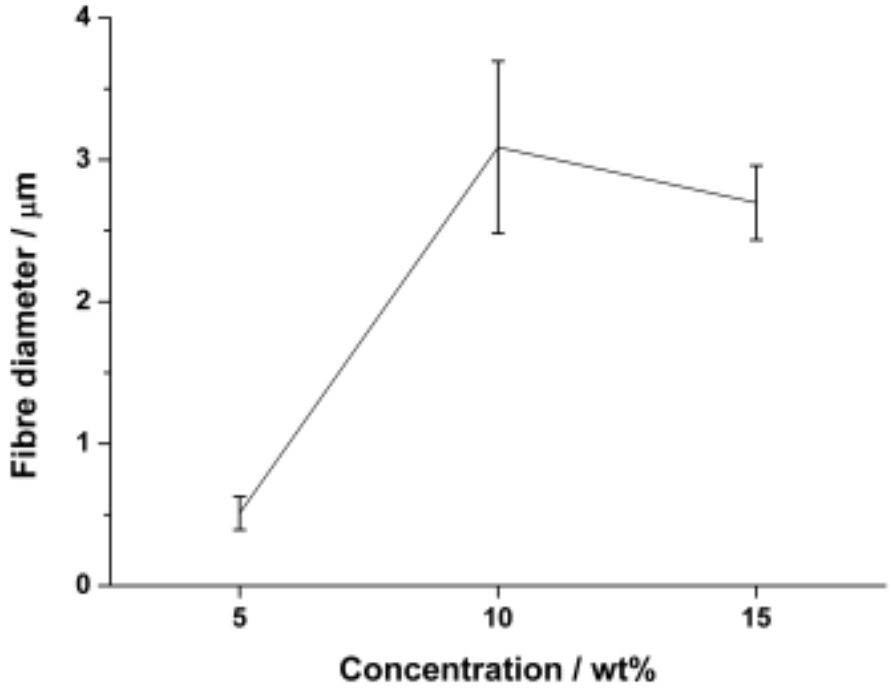

Figure 2.6: Average fibre diameter of PLA produced from 5 wt%, 10 wt% and 15 wt% solutions. Error bars are ± SD, n=5.

Evaluating Goodfellow PLA vs. Aldrich PLA

This may seem an odd thing to include in this report, but with projects working to a tight budget seeking economy is necessary. As of 22/7/2012 PLA bought from Aldrich costs £161 for 10 g. From Goodfellow it costs £151 for a kilogram! This works out at £16.10 per gram from Aldrich and £0.15 per gram from Goodfellow. To ensure that this swap could be made it was necessary to compare the two materials to find any differences before making the transition. The molecular weight of the Aldrich PLA was 10100 g/mol and the molecular weight of the Goodfelllow PLA is unavailable (please see data sheets in Appendix A.1). Sheets of Goodfellow PLA and Aldrich PLA were consecutively

electrospun (Section 2.2.2). Fibre diameter and morphology were analysed using SEM (Philips XL-20, Section 2.1.2), tensile strength (Bose electroforce tensiometer, Sections 2.1.3), and assayed for cell viability (50,000 fibroblasts, resazurin salt assay, Sections 2.1.4 & 2.1.12).

Figure 2.7 shows SEM photographs taken of electrospun Goodfellow and Aldrich PLA. Fibre diameter and morphology was the same for the two samples.

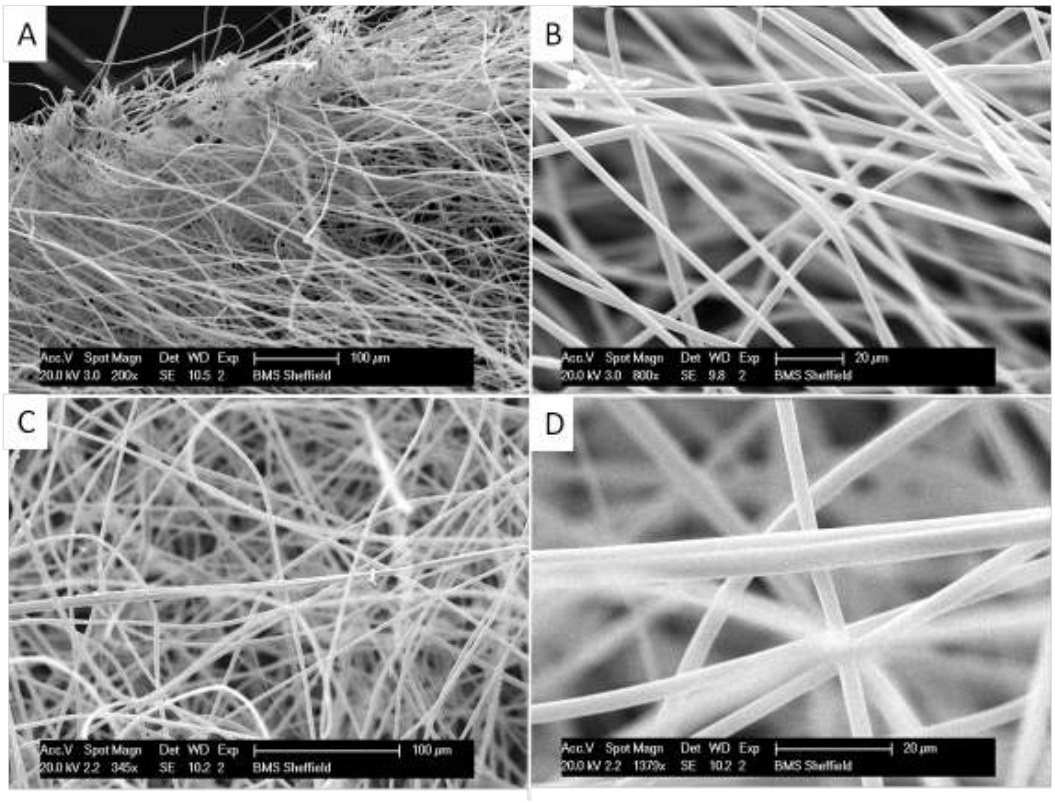

Figure 2.7: SEM images of Aldrich (A & B) and Goodfellow (C & D) PLA electrospun fibres.

E and UTS measurements between the Goodfellow and Aldrich PLA had little difference between them (Figure 2.8). The E and UTS measurements for both polymers are not significantly different ($P>0.05$). Figure 2.9 shows the cell viability of fibroblasts cultured on Goodfellow and Aldrich PLA compared to tissue culture plastic (TCP) for one week. Cell populations increased equally

on all three substrates in this time. Goodfellow PLA was comparable to TCP. Tensile measurements are identical, and Goodfellow PLA performs as well as Aldrich's in regard to cell viability. When electrospun under the same conditions identical scaffolds were produced with the same morphologies and fibre diameters. So it makes good financial sense to use the Goodfellow PLA, purely on grounds of cost.

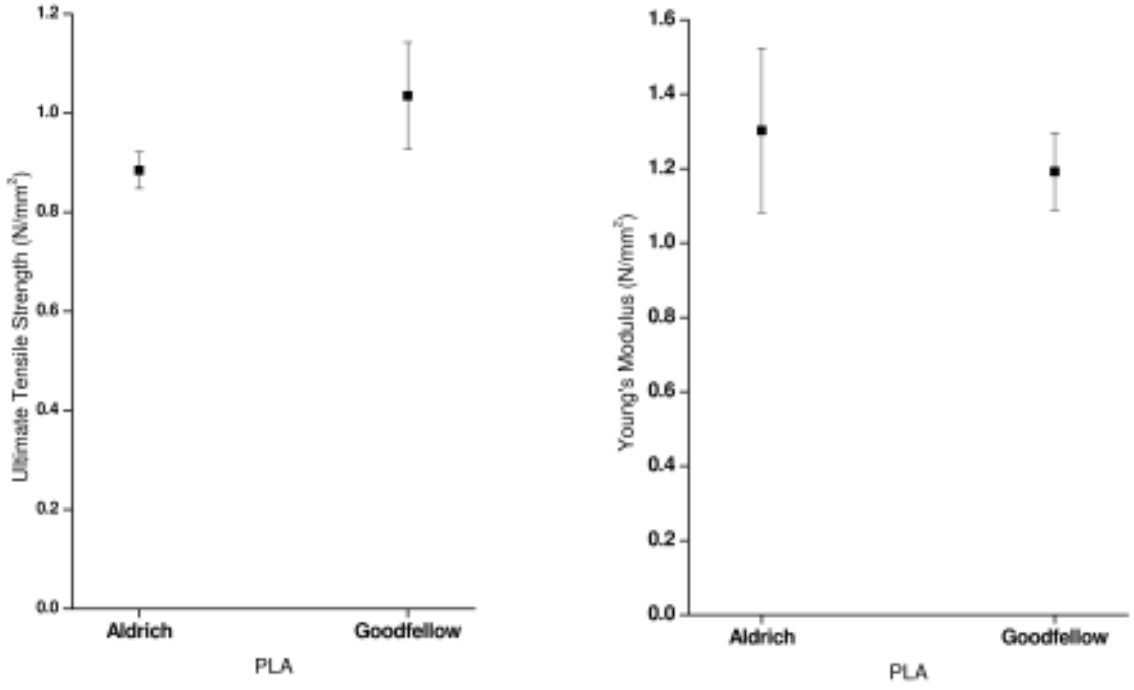

Figure 2.8: Ultimate tensile strength and Young's modulus of elasticity (E) of Goodfellow and Aldrich PLA. Values are expressed as mean ±SEM, n=3. There is no significant difference between the data recorded.

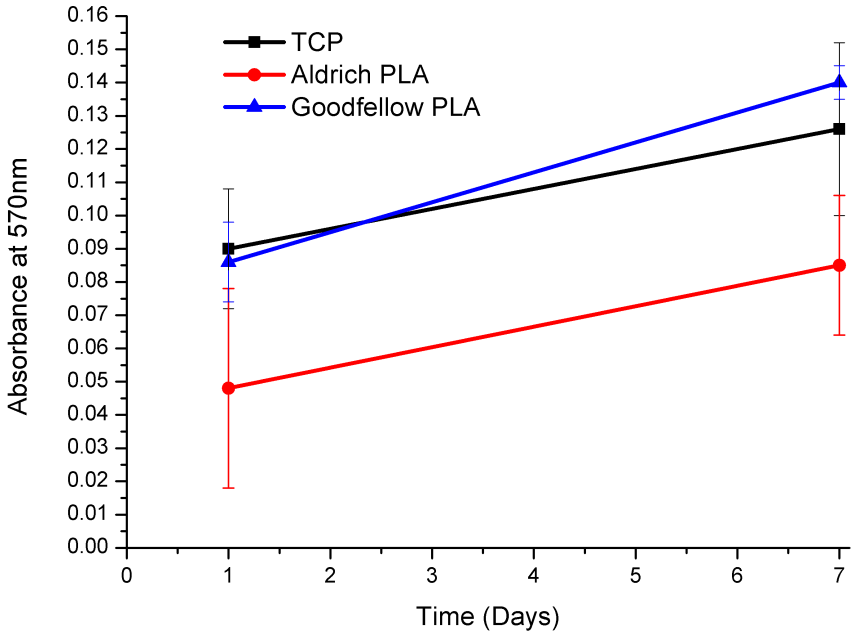

Figure 2.9: Attachment of culture of 50,000 fibroblasts to Goodfellow and Aldrich PLA compared to TCP after 1 week measured by resazurin salt assay. Values are absorbance at 570 nm expressed as mean ±SEM, n=3.

2.2.3 Electrospinning of PCL

PCL solutions (70-90 kDa) of concentration 5 and 10 wt% in DCM were made. This solution was then electrospun (17 cm distance, 40 μL per minute flow, 300 RPM, 17 kV) onto a rotating collector (63 mm radius, 597 cm^2).

SEM images were taken to assess fibre morphology. Two futher PCL sheets were spun but methanol (MeOH) (10 wt%) was added as a cosolvent.

PCL micofibres can be reproducibly electrospun. The scaffold is visually identical to the PLA scaffold and exhibits the same difficulties in handling. There

was a small reduction in fibre diameter when MeOH was used as a cosolvent (1500 nm in diameter without cosolvent, 1250 nm in diameter with MeOH as a cosolvent, Figure 2.10). Both 5 wt% solutions produced pearl necklace morphologies regardless of the presence of a cosolvent (Figure 2.11). Fibre diameters between "pearls" was the same regardless of solvent system (250 nm, Figure 2.10). PCL spun with 5 wt% MeOH cosolvent presented an interesting "pock marked" macro morphology (Figure 2.12).

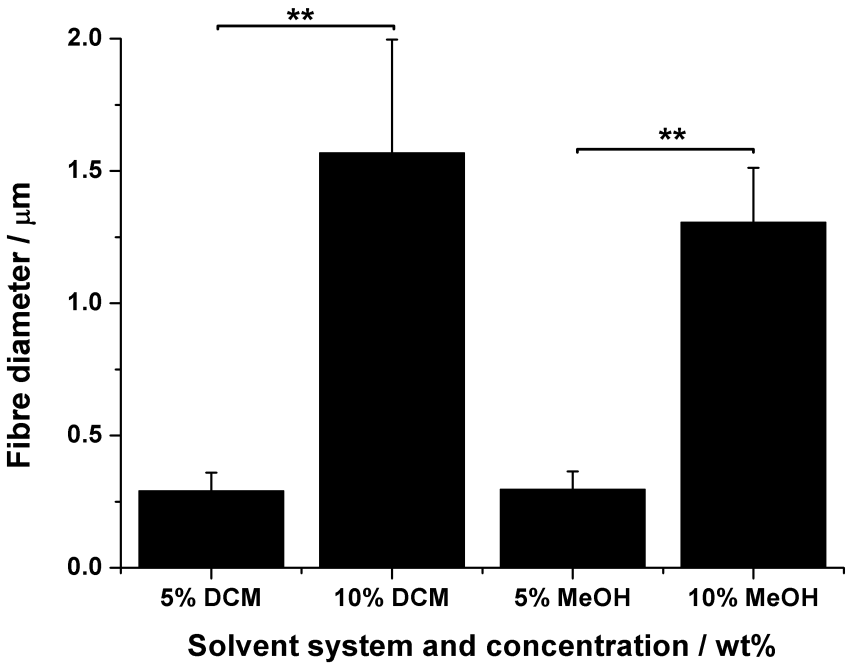

Figure 2.10: Average fibre diameter of PCL fibres produced from A. 5 wt% in DCM, B. 10 wt% in DCM and C. 5 wt% in DCM/MeOH, D. 10 wt% in DCM/MeOH solutions. Error bars are mean ±SD, n=5

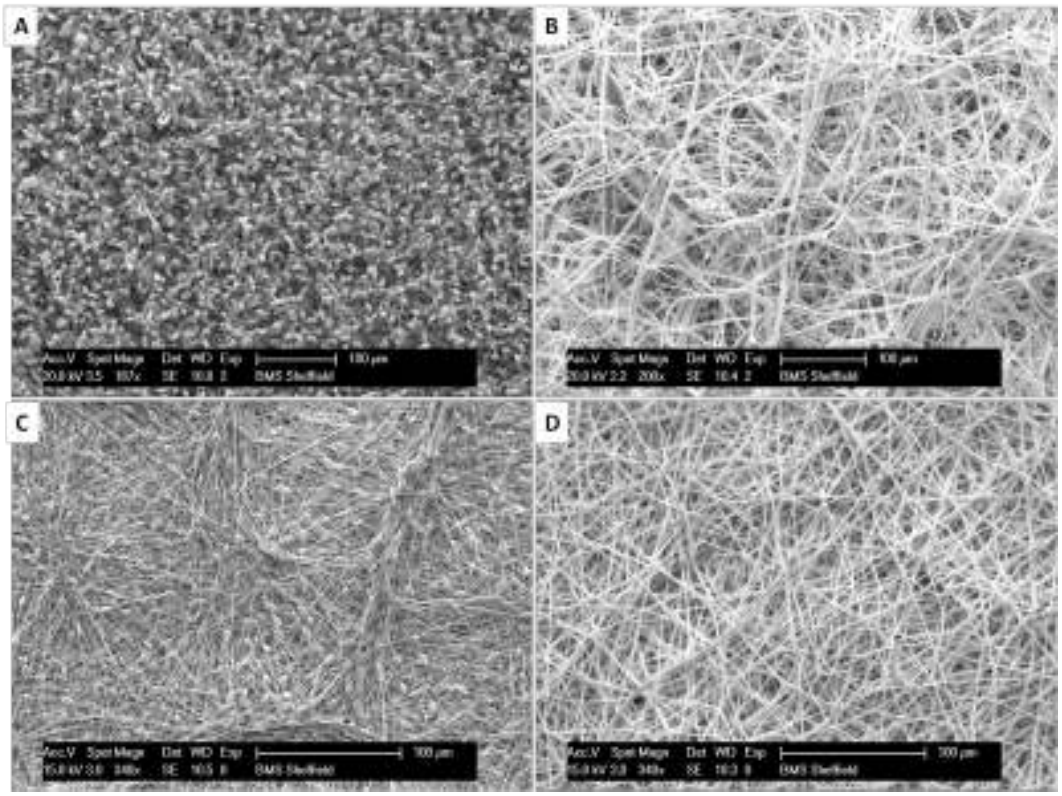

Figure 2.11: SEM images of PCL electrospun using a solely DCM solvent system (A & B, 5 wt% and 10 wt% respectively) and a DCM/MeOH mixed solvent system (C & D, 5 wt% and 10 wt% respectively).

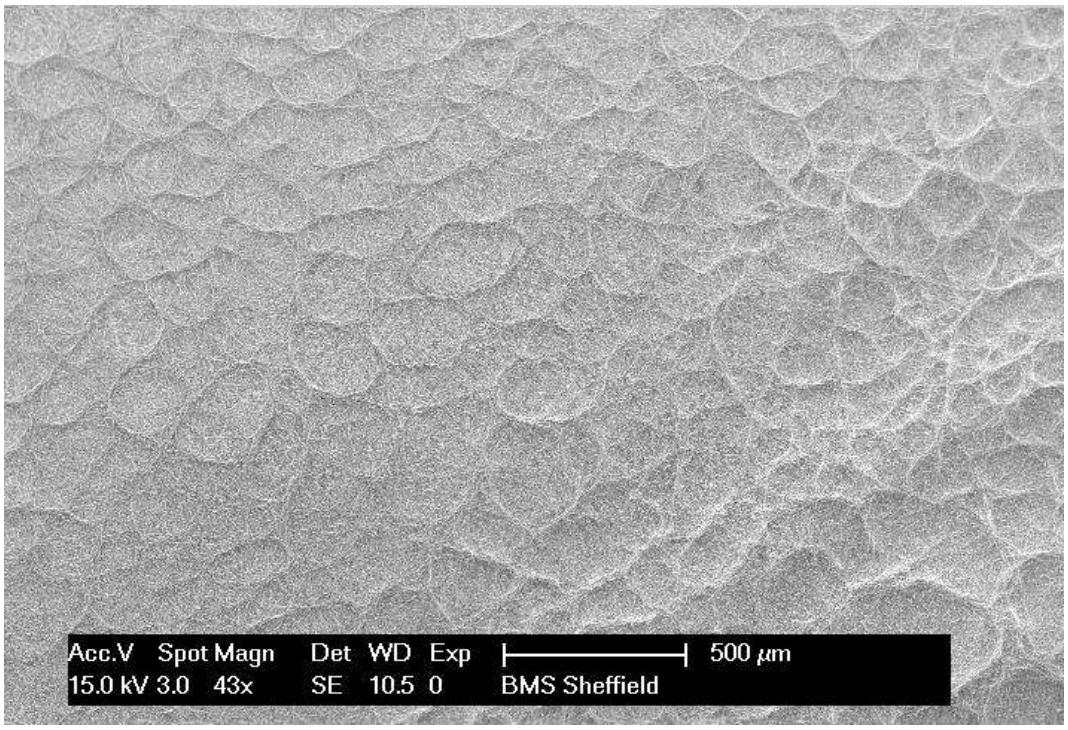

Figure 2.12: SEM image showing macro morphology that formed when electrospinning a 5 wt% solution of PCL with 10 wt% of a MeOH cosolvent.

2.2.4 User friendly electrospinning of PLGA nanofibres

PLGA is a rapidly decomposing polymer and notoriously tedious to electrospin. At the time of starting this work the current method produced a great deal of waste through Taylor cone build up and also the end product adhered strongly to the collector. It was decided to apply the above methods to PLGA spinning in order to determine if detachable nanofibres of PLGA could be easily electrospun with less waste.

A 15 wt% solution of PLGA was created (15 wt% in 10 wt% MeOH and 80 wt%DCM) and then electrospun onto aluminium foil (17 cm needle tip to collector, 30 kV, 300 RPM, 4 $\times$ 5ml syringes pumped at 40 μLmin^{-1}). The solution was noticeably less viscous than the regular method (20 wt% in DCM) and the spun polymer produced an even white coverage across the collector. The resulting scaffold had the texture and durability of tissue paper, but it could be readily peeled from the backing foil. SEM images were taken (Section 2.1.2, Figure 2.13) and fibre diameter measured and found to be 1.02 μm $\pm$0.19 SD, n=5.

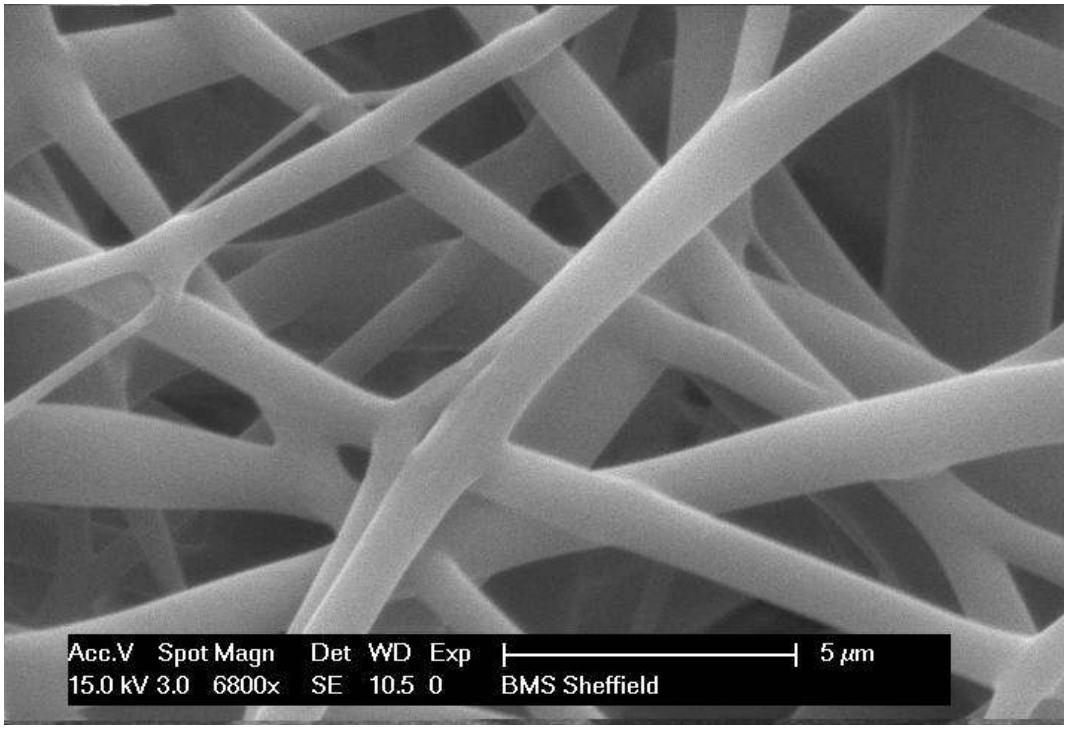

Figure 2.13: SEM image showing fibres formed formed when electrospinning a 15 wt% solution of PLGA with 10 wt% of MeOH as a cosolvent.

2.2.5 Electrospinning of PHBV

As PHBV had not been electrospun in the MacNeil laboratory before, tests were carried out to find the set of conditions from which fibres could be electrospun. The electrospinning conditions normally used for PLA were taken as a starting point (Section 2.2.2). Upon electrospinning PHBV it became apparent that a much closer working distance was required as the fibres would not deposit on the collector at 17 cm. A 10 cm working distance was selected as this was the greatest distance fibre deposition was noted at. Samples were processed for scanning electron microscopy (Section 2.1.2). The scaffold produced was a "pearl necklace" with microfibrous spheres connected by nanofibres (Fig-

ure 2.14 A). It was decided to enhance to spinning solvent by increasing its permittivity.

Permittivity is a measure of how much a substance (or nothing in the case of vacuum permittivity) interacts with an electric field. ϵ is measured in Farads per meter (Fm^{-1}), essentially the capacitance of the substance over 1 meter. Naturally solvents with a high ϵ are great for electrospinning as they polarise when introduced to the electric field, this increased interaction maximises the chance of a stable spinning jet forming and fibres being deposited. Chloroform and DCM are poor solvents with regard to ϵ (4.8 Fm^{-1} and 8.9 Fm^{-1} respectively).[187] Adding a co-solvent with a higher ϵ should increase the interaction the solution has with the surrounding electric field and make fibre formation possible. Some common solvents and their ϵ are listed in Table 2.1.[187] The ϵ of a vacuum and water are included for comparison. MeOH, EtOH, and DMF were selected to be investigated as co-solvents for spinning PHBV because of their greater ϵ.

Solvent	ϵ /Fm^{-1}	Temperature /°C
Methanol	33.0	20
Ethanol	25.3	20
DMF	38.3	20
Chloroform	4.8	20
DCM	8.9	25
Water	80.0	20
Vacuum	8.85×10^{-12}	N/A

Table 2.1: Permittivity of some common solvents.

2.2.6 Selection of solvent for spinning PHBV

PHBV (12:1 hydroxybutyrate:hydroxyvalerate, Goodfellow Corporation, U.K.) solutions of concentration 10 wt% in 80 wt% DCM were created. The additional 10 wt% was then made up using one of three cosolvents; MeOH, EtOH or DMF. A PHBV solution (10 wt% in DCM) was also made and spun as a control for comparison. These solutions were then electrospun (17 kV, 10 cm from the needle point to the collector, 40 μL per minute solution flow, onto a collector of area 597 cm^2, radius 63 mm, spinning at 300 RPM). Scaffolds were then assessed for cell viability using the resazurin salt assay, and mechanical properties determined using a tensile testing machine. Finally samples were processed for scanning electron microscopy (Sections 2.1.12, 2.1.3 and 2.1.2). The SEM images show a marked change in morphology when a cosolvent is used compared to spinning solely with DCM. Electrospinning PHBV in DCM alone produced a pearl necklace morphology with nanofibres joining larger globules of polymer in-between 5 μm and 20 μm in diameter. Upon addition of the cosolvent, fibres were produced without globules (Figure 2.14). SEM images did not display a significant variation in fibre diameter. All of the samples measured gave an average fibre diameter in the nanometre range, when DCM was used, fibre diameters were significantly smaller compared to the other solvents (Figure 2.15).

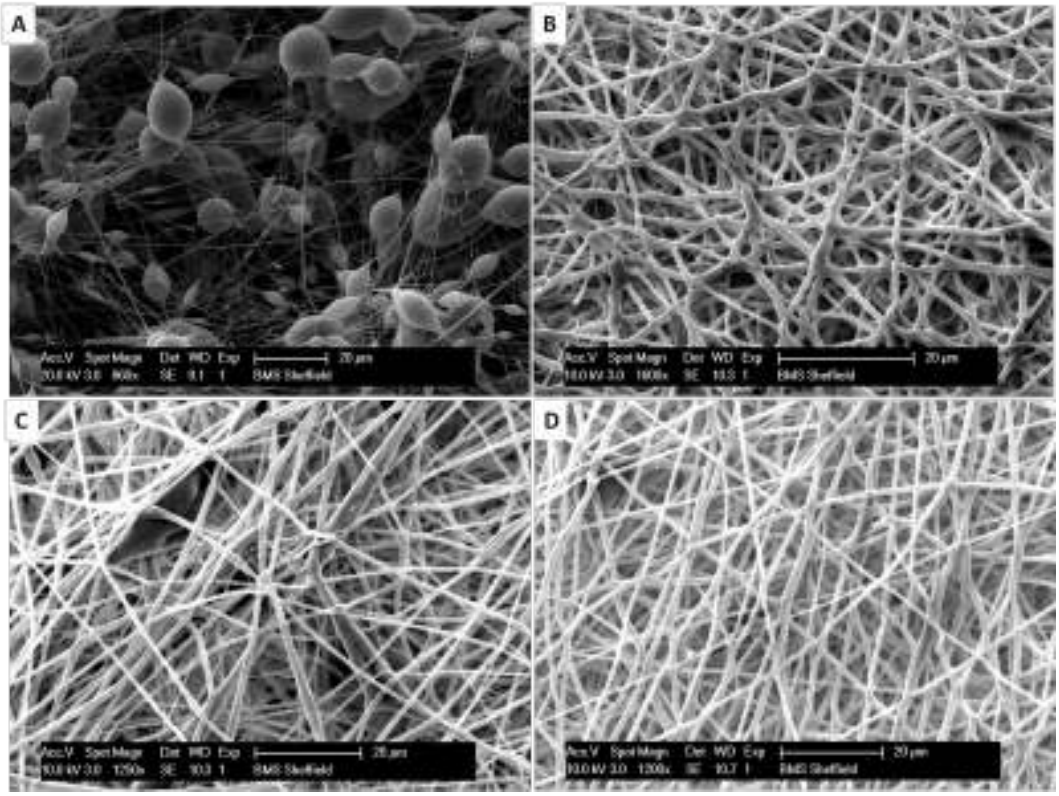

Figure 2.14: Effect of solvent selection on morphology of PHBV fibres produced. A. No cosolvent, DCM only. B. 10 wt% DMF cosolvent. C. 10 wt% EtOH cosolvent. D. 10 wt% MeOH cosolvent.

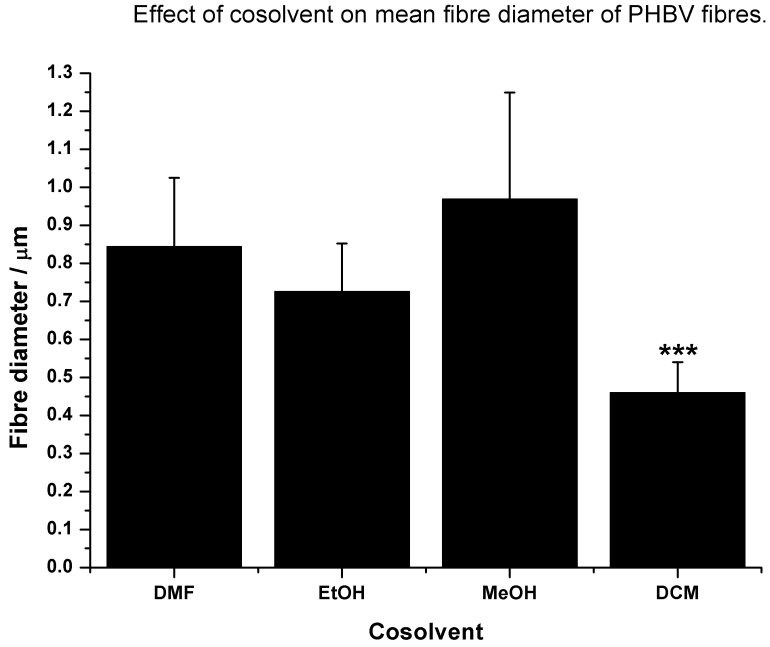

Figure 2.15: Fibre diameter of PHBV fibres resulting from different solvent systems. Error bars are mean ±SD, n=3.

The E of the resulting scaffolds did change significantly depending on the cosolvent, except for MeOH, which was not significantly different to just DCM (Figure 2.16).

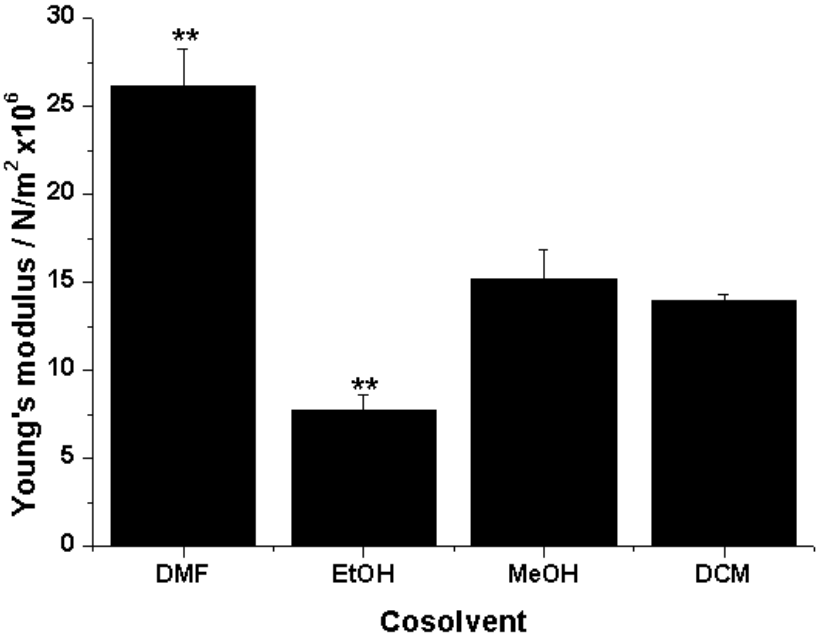

Figure 2.16: Effect of solvent selection on Young's modulus of PHBV fibres produced. Error bars are ±SD, n=3.

The addition of EtOH produced a scaffold with half the E of DCM alone or with MeOH. Using DMF as a cosolvent produced a scaffold with around double the E compared to DCM alone. All PHBV scaffolds produced were white and the sheets of fibres were noticeably flatter than PLA or PCL microfibres. None of the PHBV scaffolds were fluffy (as for PLA) but almost paper like. The paper-like sheets had radically different handling properties depending on the cosolvent. The scaffolds produced using EtOH or no cosolvent were very brittle and difficult to remove from the backing aluminium foil in one piece. When DMF or MeOH were used the scaffold could be readily peeled off in their

entirety and they were very easy to handle, much more like a sheet of paper or a plastic bag.

Fibroblasts were cultured on the scaffolds and cell viability measured (50,000 fibroblasts cultured as per Sections 2.1.4 and 2.1.12). Cells performed best on PHBV when MeOH was used as a cosolvent (20% better, but not significantly better, than TCP). When DMF was used the cells performed significantly worse (80% less metabolic activity than on TCP, Figure 2.17).

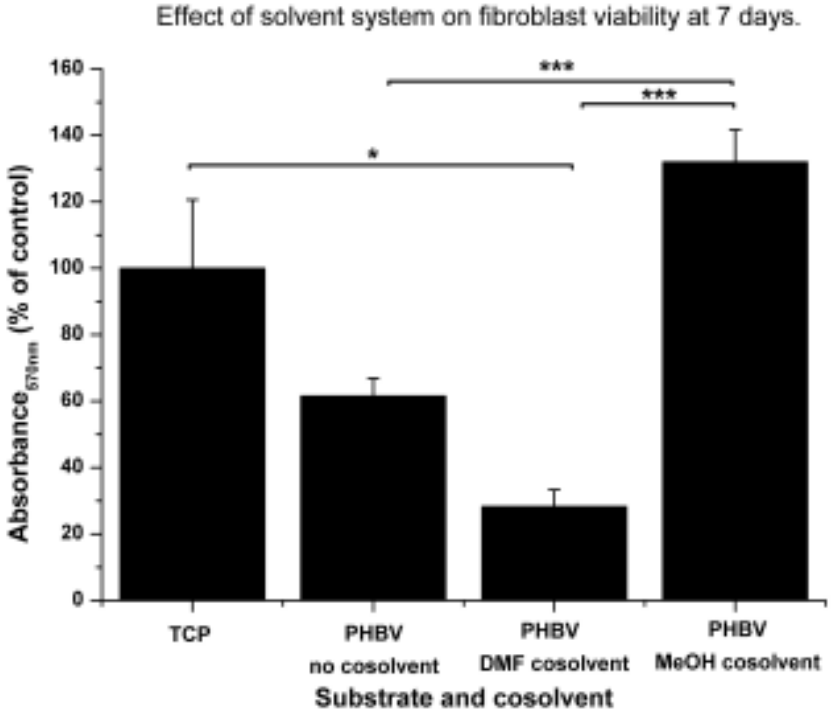

Figure 2.17: Recorded cell viability measured by resazurin salt assay on scaffolds spun with different cosolvents. The substrate PHBV was electrospun using DCM only. Values are absorbance at 570 nm, error bars are ±SD, n=3

Scaffolds spun using EtOH as a cosolvent were discarded at this point as their handling properties were too poor to conduct further experiments on.

Fibroblasts grown on PHBV (50,000 cells per well, Section 2.1.4) spun with MeOH as a cosolvent exhibited the same viability as cells cultured on TCP. Where cells were grown on PHBV spun without a cosolvent, the viability dropped by one third, and where DMF was used the viability dropped by two thirds of that seen on TCP alone. MeOH was chosen as a cosolvent with which to electrospin PHBV due to the good cell viability achieved, retention of nanofibrous architecture, mechanical properties and ease of handling.

All subsequent PHBV scaffolds were electrospun using a 10wt% cosolvent of MeOH.

2.2.7 Scaffold porosity determination

Scaffolds were cut into discs (14 mm diameter) and weighed on a balance. Scaffold thickness was determined by measuring cross section thickness of SEM images. SEM image cross sectional thickness was chosen as it prevents scaffold deformation unlike other methods such as using a micrometer, thus allowing the actual volume of the scaffold to be calculated. The density of each scaffold was then calculated. This was done by dividing the recorded mass of the scaffold by the calculated scaffold volume. The volume was calculated using the SEM determined cross sectional thickness (thickness $\times 2\pi 7^2$). The scaffold density was then divided by the bulk polymer density and expressed as a percentage, giving the bulk porosity of the material.[188]

Porosity measurements were conducted in order to establish if fibre diameter impacted on the density of the scaffolds. As fibre diameter decreased so did

porosity (Figure 2.18). PHBV nanofibrous scaffolds (Section 2.2.6) exhibited the lowest porosity, significantly less (around 20%) than microfibrous PLA or PCL.

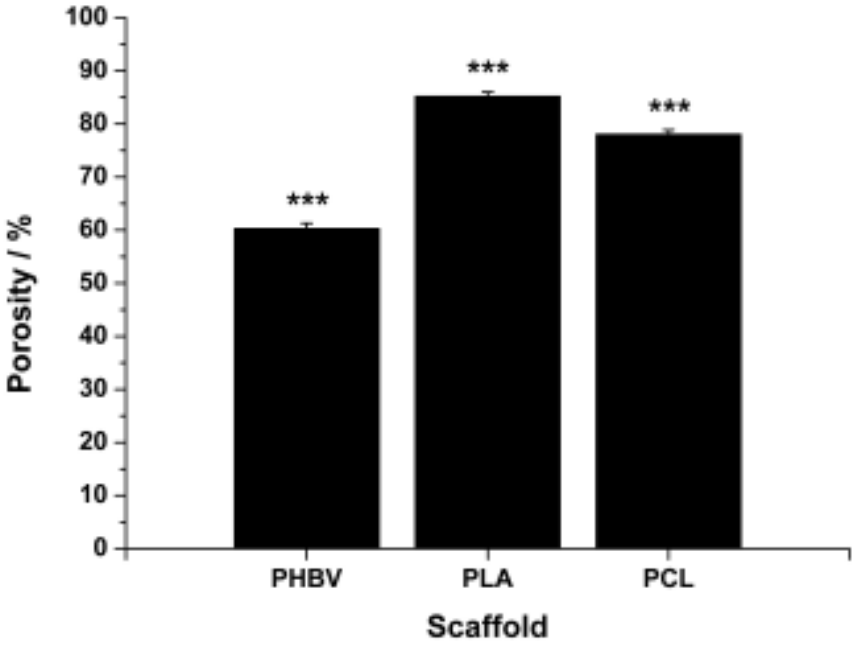

Figure 2.18: Calcuated percent porosity for nanofibrous PHBV and microfibrous PLA and PCL scaffolds. Error bars are mean ±SD, n=3.

2.3 Discussion: Production of a variety of electrospun scaffolds

2.3.1 Determination of the speed of mandrel rotation

It was first necessary to calculate the mandrel's RPM as the mixer used to rotate the mandrel only defines its rotational velocity on an arbitrary scale of

0 to 10. It's interesting to note that 0 isn't stationary. In the literature it's been shown that random architectures are obtained at lower RPM (around 200-300 RPM) and that aligned fibres can be achieved at 1000 RPM and over.[185,186] Taking the dimensions of their mandrels into account, randomly oriented fibres were formed at linear surface velocities of around 17000 cm/min and aligned fibres at 69000 cm/min. The linear surface velocity of the mandrel used in the experiments presented could be set in the range of 9000 cm/min to 62000 cm/min, adequately matching the velocities achieved in the literature for the production of both random and aligned fibres. Hence, knowing the speed of the mandrel is vital for the creation of aligned and random fibres. The mandrel used in this work was capable of matching reported velocities required for aligned and random fibre formation.[185,186]

2.3.2 Electrospinning PLA

Varying the concentration of the PLA solution from 5% to 15% produced a range of different fibres. 5 wt% PLA in DCM produced a pearl necklace structure, probably due to the rate of solvent evaporation and solvent permittivity, as explained above. What was interesting was that the fibre diameter decreased when the concentration of polymer was increased from 10 wt% to 15 wt%. The change is small, and not significant, but it is present (Tables 2.2 and 2.3 at the end of this section). This is due to the effects of increasing viscosity preventing thicker fibre formation.[66,189]

Goodfellow PLA vs. Aldrich PLA

The cost saving implications of a switch of polymer suppliers made this a worthwhile exercise. There was a good correlation of fibre diameter, morphology, E, and cell viability between fibres spun from both polymer sources. A definitive measure or similarity would be given by the polydispersity index (how uniform the polymer chain lengths are) and the polymer molecular weight. However, these were unavailable from Goodfellow (Appendix A.1). These should be measured in future. While the cell viability appeared lower on Aldrich's PLA, the viability rose to that of TCP and Goodfellow PLA over seven days of incubation.

2.3.3 Electrospinning of PCL

Varying the concentration and solvent system of PCL solutions produced both micro and nanofibres (Tables 2.2 and 2.3). Nanofibres were produced with a pearl necklace morphology regardless of the solvent system used. Nanofibres of PCL have been reported using a mixed DCM (80 wt%) and DMF (20 wt%) system with 8 wt% of PCL.[190] It is not ideal to use DMF as an electrospinning solvent due to its low vapour pressure, and hence any scaffolds produced would require an additional solvent removal step such as vacuum drying. Thus all following scaffolds produced during this project do not include DMF as a cosolvent.

2.3.4 Electrospinning of PLGA nanofibres

A mixed solvent solution was once again employed to create nanofibres of PLGA. While nanofibres of PLGA are not a new phenomenon, this is the first time a MeOH and DCM mixture has been used in their creation. Also, it is uncommon for a 50:50 lactic acid:glycolic acid polymer to be used due to its fast degredation rate (Tables 2.3).[191]

2.3.5 Electrospinning PHBV

PHBV has previously been electrospun as micro and nanofibres using chloroform as the carrier solvent.[91–94] DCM was selected as the solvent for spinning PHBV as it was the common solvent already in use in the MacNeil laboratory. It also has a higher permittivity than chloroform and hence it should produce a solution that reacts more intensely to an electric field (9 Fm^{-1} and 5 Fm^{-1} respectively).[187] However, it is clear from the work presented here that using DCM alone is insufficient to produce the desired fibres. In the literature a conductivity enhancing salt (benzyltriethylammonium chloride) is used to improve fibre formation. Using benzyltriethylammonium chloride as an additive does improve chloroform as a solvent choice. However, this particular salt is stated to cause skin irritation, serious eye irritation and may cause respiratory irritation.[5] As it is a salt, it is likely that it will remain within the fibres and potentially be in a scaffold if implanted. This is not desirable, and as shown in this project the inclusion of a cosolvent such as MeOH can achieve the same effect, but without the toxicity, as any residual solvent will evaporate.

Zuo *et al.* have published work investigating the use of tetrachloromethane, EtOH and DMF as cosolvents and also including benzyltriethylammonium chloride in DCM solutions of PHBV.[94] Their findings show that EtOH as a cosolvent produces fibres with no beads or other morphological aberrations. However, this paper does not investigate any further properties of the scaffold. In the course of this PhD project EtOH did produce fibres of PHBV but the scaffold had very poor handling properties compared to those made with MeOH and DMF, preventing EtOH being a candidate solvent. The Young's modulus measurements reflect this. This could be due to inter fibre connections forming in scaffolds where DMF and MeOH have been used, but not in those spun with EtOH. This kind of behaviour has been noted in other electrospun polymer scaffolds, and can also be clearly observed in the SEM presented in Figure 2.15.[192,193]

There is a considerable difference in E measurements of the PHBV scaffolds produced with different solvent systems. Figure 2.14 shows the reason for this, when DMF is used there is significant inter-fibre adhesion, effectively cross linking the fibres together. This would produce the greater E observed compared to the other solvent systems.

With regard to the suitability of these scaffolds for cleft palate repair, the greatest concern would be the potential for growth disturbances. This could occur if the implant was too stiff compared to the surrounding tissues. The E of a child's skull is around 4-16 MPa.[194] As all the scaffolds produced have a E less than this value it is likely that the scaffolds would not cause growth disturbances. When used in cleft palate repair, bone grafts taken from the iliac crest cause major growth disturbances and are no longer used. The clinical experience as reported by surgeons with experience in using such grafts (Pro-

fessor Julian Yates, BSc, BDS, PhD, MFDSRCPS, FDSRCPS (Oral Surgery), FDSRCS, Manchester, UK, and Dr. Kevin S. Hopkins, MD, FACS, Texas, US) is that initial results are very good but that the implanted bone then fails to expand with the growth of the child's mandible, leading to distortion of the jaw requiring corrective surgery. Indeed for this reason hard palate defects are often not closed at all in many patients. This may be due to a mismatch of E. Infant iliac crest E has been reported to be of the order of 17 GPa ±3 GPa, which is considerably stiffer than the observed range for a child's skull, explaining why iliac crest bone fails to expand.[195]

Comparing cell viability on PHBV electrospun scaffolds using different cosolvents, it is clear that DMF has a detrimental effect on cell viability. This is most likely to be due to residual solvent in the scaffold. This would be due to the very low vapour pressure of DMF (2.7 mmHg) compared to MeOH (97.68 mmHg) and chloroform (160 mmHg). This means that DMF does not readily evaporate.[5] Cells cultured on scaffolds where MeOH is used as a cosolvent exhibit a greater viability than on scaffolds spun using just chloroform. However, this could also be explained by the increased fibre diameter of the PHBV spun with MeOH, providing a substrate that is more compatible with cell attachment (Figure 2.15, Tables 2.2 & 2.3).

Polymer	Solvent system	Mandrel velocity / RPM	Voltage / kV	Collector distance / cm	Flow rate / μLmin^{-1}	Mass of Polymer / wt%
PHBV A.	DCM /MeOH	300	17	10	40	10
B.	DCM	300	17	10	40	10
C.	DCM /EtOH	300	17	10	40	10
D.	DCM /DMF	300	17	10	40	10
PCL A.	DCM	300	17	17	40	5
B.	DCM /MeOH	300	17	17	40	5
C.	DCM	300	17	17	40	10
D.	DCM /MeOH	300	17	17	40	10
PLGA	DCM /MeOH	300	30	17	40	15
PLA A.	DCM	300	17	17	40	5
B.	DCM	300	17	17	40	10
C.	DCM	300	17	17	40	15

Table 2.2: Table of electrospinning parameters used to spin PHBV, PCL, PLGA and PLA.

Polymer	Fibre diameter / nm	Young's modulus /1.0^{+7} Nm^{-2}	Porosity / %	Cell viability	Cell migration
PHBV A.	950	1.5	60	+++	− − −
B.	Pearl Necklace	1.25	N/A	++	−−
C.	700	0.75	N/A	N/A	N/A
D.	850	2.5	N/A	+	N/A
PCL A.	Pearl Necklace	N/A	N/A	+++	N/A
B.	Pearl Necklace	N/A	N/A	N/A	N/A
C.	1500	N/A	80	+++	+
D.	1250	N/A	N/A	N/A	N/A
PLGA	1000	N/A	N/A	N/A	N/A
PLA A.	500	N/A	N/A	N/A	N/A
B.	3000	1.2	85	+++	+++
C.	2750	N/A	N/A	N/A	N/A

Table 2.3: Table of scaffold properties resulting from the parameters used in Table 2.2.

2.4 Bioreactor enclosure design

This section of the project was devoted to finding an inexpensive, but workable method to keep cells in culture on a biomaterial, in a bespoke bioreactor, outside a conventional incubator.

The criteria for this next step was to create a system that could easily accommodate, and apply loading to, multiple replicates simultaneously. It had to also be easily accessible, adjustable, and not involve a "spaghetti junction" of tubing. It was very quickly identified that the typical front loading incubators were not suitable or convenient for bioreactor use; both because of their communal use, and the front loading multi-shelf design. This results in poor access and added complications of dealing with different height levels and feeding tubes through ports and between shelves.

This lead to the first question to be answered; can a cheap top loading container be sourced that can incubate a potential bioreactor at 37 °C continuously? Broadly speaking, cells in culture require three things from their environment, warmth (37 °C), nutrients (provided by their media), and pH regulation (provided by a buffer system included in the medium).

Warmth is straight forward, through the use of a heating element or radiator system a constant temperature can be achieved and maintained. Humidity is also straight forward. If a reactor is sealed then this is not an issue, as no liquid is lost.

Open reactors would require a reservoir in the environment to increase the humidity and reduce net evaporation from the system. However, achieving a constant pH is a little more difficult, requiring either a CO_2 supply for bicarbonate buffering of media (this is the most common system) or a bespoke media that uses an entirely different buffer system.

2.4.1 Investigation of the thermal stability of two potential incubator chambers

The aim of this was to create a chamber suitable for housing a bioreactor. The main requirement for this was that it must be possible to regulate the temperature and allow pumps/rockers to act on the bioreactor without affecting the temperature, or ruining the equipment. Equipment can be damaged when placed in an incubator, either by the temperature or humidity. There must also be provisions ensuring easy access for tubing and other external devices.

A seed propagator (Stewart, Wilkinsons Hardware stores Ltd.) was placed into a polystyrene box (1 m × 0.5 m × 0.5 m with 5 cm thick walls) with small access holes (one either side, 1 cm × 1 cm through the box wall) cut into the sides to allow piping in (Figure 2.19). Distilled water (56 °C, in a water bath) was pumped through tubing into the access holes of the polystyrene box and tubing coils placed in the propagator to achieve an internal temperature of 37 °C. Extra access holes were made as required to plumb in media circulation tubing. An R-COM® King Suro egg incubator (P & T poultry Ltd., Figure 2.20) was also set to 37 °C and allowed to reach temperature.

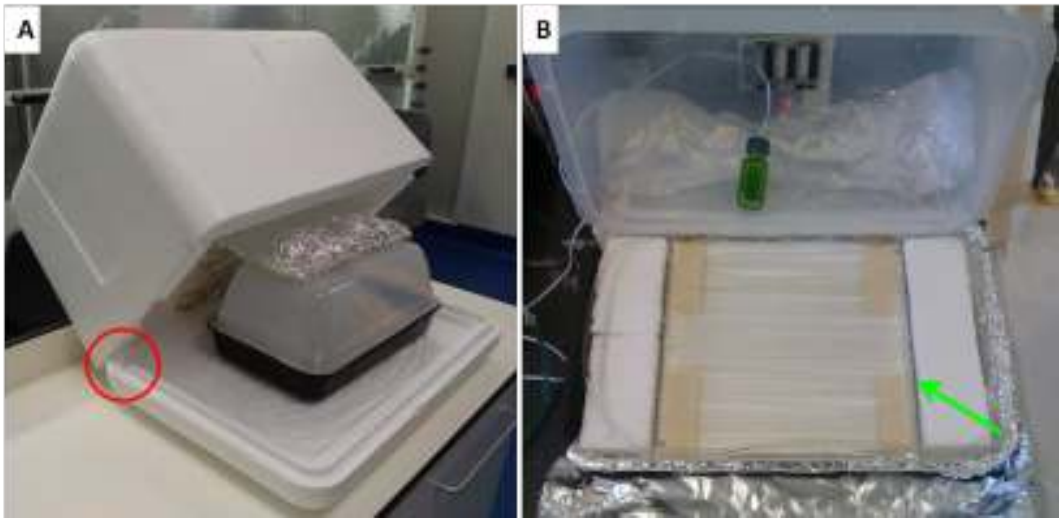

Figure 2.19: (A) The propagator is insulated by using tin foil lagging and housing inside a thick-walled polystyrene box. The box has access holes cut in the side to allow tubing to enter and exit (red ring). (B) Inside the propagator, coiled tubing (green arrow) is perfused with water at 37 °C to provide "under-floor" heating.

Figure 2.20: R-COM King Suro egg incubator. The system promises temperature and humidity control as well as the option to apply a rotation through 90°every hour.

The temperature was measured inside the propagator, King Suro egg incubator, and a normal incubator using a temperature data logger (EL-USB-1, LASCAR electronics, Hong Kong) every 2 minutes for 48 hours.

Monitoring the temperature of a water heated propagator shows that there was no variation in the temperature, even in the early, coldest, hours of the morning (Figure 2.21). The average temperature was 34 °C and the greatest deviation, ignoring initial warm up was by 0.5 °C. Comparing this to a regular incubator (Figure 2.21), the average temperature was 36 °C and the greatest deviation was 1 °C. The egg incubator oscillated by ± 1-2 °C about a mean temperature of 37 °C (Figure 2.21).

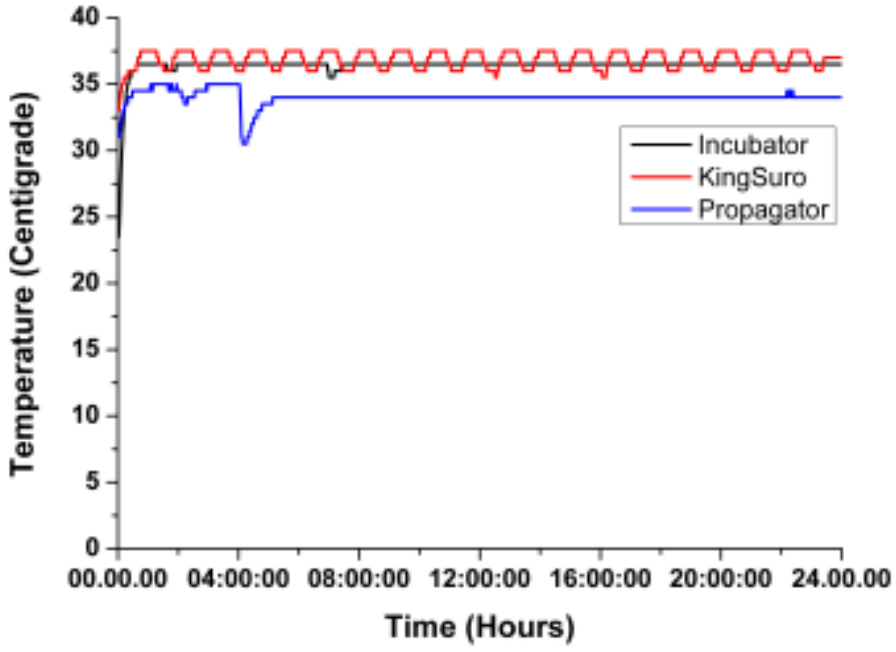

Figure 2.21: Thermal stability of an incubator, propagator and R-COM King-Suro egg incubator over a 24 hour period. Average temperatures were 36.5 °C, 34 °C and 37 °C respectively. The dips at 4 hours (propagator) and 8 hours (incubator) are due to the door/lid being opened in order to observe the temperature drop, and measure how swiftly each would return to operating temperature.

In order to understand how mechanical stimulation affects growing cells, a system that maintains cells in culture for two weeks and allows them to be continuously exercised is required. The use of a propagator has shown that for a low cost, a viable, and immensely flexible system can be easily created. There are no restrictions to the equipment that could be incorporated and there are no problems with overheating. This set up would also prevent damage of delicate equipment by humidity.

2.5 Summary and conclusions

This chapter summarises methods for electrospinning a range of different polymers into scaffolds comprising of varying architectures. These range from microfibres, to nanofibres and pearl necklaces. Culturing cells on these scaffolds shows the impact of different architectures, solvent choice and dopant on cell behaviour.

Microfibres allow cells to penetrate and fill a scaffold, whereas nanofibres prevent cell infiltration and act as a barrier. Solvents and the method of spinning can greatly affect the viability of cells on scaffolds. Care must be taken when designing spinning methods to remember that such scaffolds are intended to ultimately be used in patients. This data is summarised in Tables 2.2 and 2.3. Table 2.2 is a summary of the polymers spun and the conditions used. Table 2.3 summarises the properties of the scaffold produced by using the conditions given in Table 2.2.

Finally, the need for a method to keep cells under ideal culture conditions, while having access to valuable and sensitive equipment is investigated. Such systems are becoming more important as more control over the environment of the cell is sought.

The use of a propagator or an egg incubator has shown that for a low cost, a viable and immensely flexible system can be easily created. Both systems were capable of holding a constant temperature for at least 24 hours. There are no restrictions on the equipment that could be incorporated, as access ports can be readily made. There are no problems with overheating of incubators from machinery, or delicate equipment being affected by humidity. This allows experiments that were not feasible in an incubator to be performed. Multiple pieces of sensitive equipment can be readily plumbed in, and a constant temperature maintained.

Chapter 3

Post production processing of electrospun fibres for tissue engineering

3.1 Introduction

Please see the accompanying video by visiting

www.Jove.com

or

www.youtube.com.

Once biomaterials have been refined into electrospun scaffolds, these can be processed post production for tissue engineering applications. Described here

are methods for spinning complex scaffolds (by consecutive spinning), for making thicker scaffolds (by multi-layering using heat or vapour annealing), for achieving sterility (aseptic production or sterilisation post production), and for achieving appropriate biomechanical properties.

Electrospinning is a commonly used and versatile method to produce scaffolds (often biodegradable) for 3D tissue engineering.[15,36,37] Many tissues *in vivo* undergo biaxial distension to varying extents such as skin, bladder, pelvic floor and even the hard palate as children grow. In producing scaffolds for these purposes there is a need to develop scaffolds of appropriate biomechanical properties (whether achieved without or with cells), which are sterile for clinical use. Electrospinning tends to produce thin sheets as the electrospinning collector becomes coated with insulating fibres it becomes a poor conductor, such that fibres no longer deposit on it. Hence, described here are approaches to producing thicker structures by heat or vapour annealing, increasing the strength of scaffolds, but not necessarily the elasticity. Sequential spinning of scaffolds of different polymers to achieve complex scaffolds is also described.

Sterilisation methodologies can adversely affect strength and elasticity of scaffolds. Three methods are compared for their effects on the biomechanical properties on electrospun scaffolds of PLGA.

Imaging of cells on scaffolds and assessment of production of ECM proteins by cells on scaffolds is described. Culturing cells on scaffolds *in vitro* can improve scaffold strength and elasticity, but the tissue engineering literature shows that cells often fail to produce appropriate extracellular matrix when cultured under static conditions. There are few commercial systems available that allow the culture of cells on scaffolds under dynamic conditioning regimes.

One example is the BOSE Electroforce 3100 which can be used to exert a conditioning programme on cells in scaffolds held using mechanical grips within a media filled chamber.[105] An approach to a budget cell culture bioreactor for controlled distortion in 2 dimensions is described. This work shows that cells can be induced to produce elastin under these conditions. Finally, assessment of the biomechanical properties of processed scaffolds cultured with or without cells is described.

As introduced in Section 1.5.3, bladder tissue engineering encounters many similar problems seen in cleft palate and is therefore a good source of literature for comparison.[142,143] Like cleft palate, a bladder must be able to undergo a plastic deformation biaxially and increase its volume many times in a day. In contrast the palate must undergo this transformation only once over a few years, whereas a bladder must be able to do this cyclically. Most literature examines cell compatibility with a given material and asks if it shrinks under cell culture. For example, a composite collagen, PLA, and PCL composite scaffold that does not shrink through cell culture and is "slightly elastic" has been produced.[33] The greater mechanical problems posed are not often looked at. A bladder is unique in that it must expand to more than 15 times its deflated volume, while not increasing the pressure of the liquid inside it to protect the function of the kidneys. It must do this in a water tight and repeatable fashion. An elastic material is not suitable, it would increase the pressure on the kidneys causing damage. The material needs to expand and contract plastically.

Aside from this a bladder expands in 2 dimensions, in the x and y planes. Most equipment used in mechanical testing only test in a single plane. There are few examples of literature that have attempted to deal with this problem.[196]

Scaffold creation on balloons can circumvent and test some of these problems. A crinkly scaffold can be synthesised by allowing the balloon to deflate with the scaffold pre-spun on it.

3.2 Electrospinning of random and aligned fibres

Electrospinning creates fine fibrous networks by using electric potential to draw a polymer solution towards an earthed collector. Collectors can be in very many shapes and can be static or, more commonly, rotating. The solvent evaporates before the solution arrives at the collector and the jet solidifies into a fibre.

Each polymer requires its own set of conditions to produce a given type of fibre. The concentration of the polymer, the solvent, the distance between the pumped solution and the earthed collector, the potential difference between the two, the velocity of a rotating collector, the flow rate, temperature, and humidity will all affect electrospinning. There are many studies describing the selection of electrospinning parameters and how these impact on the scaffolds produced (e.g. fibre diameter, morphology, and orientation).[58,59,61,197] In these experiments scaffolds were spun based on conditions selected in our previous studies.[37,198] PLGA, PLA and PCL and nanofibrous PHBV scaffold with micro-sized beads ("pearl necklace" morphology) were electrospun as per Sections 2.2.2– 2.2.5. In summary:

1. Coat the rotating mandrel collector with aluminium foil, with the polished/shiny side facing outwards. Our mandrel was 20 cm wide, and 10 cm in diameter.

2. Prepare polymer solutions; PLA, PCL and PHBV are made up as a 10 wt% solution inDCM. PLGA is made up as a 20 wt% solution in DCM.

3. Place 4 syringes of 5 ml volume on a syringe pump. Syringes are loaded to contain 5 ml of the polymer each, giving 20 ml in total.

4. For PLA, PCL and PHBV use a flow rate of 40 μLmin^{-1} per syringe.

5. For PLGA use a flow rate of μLmin^{-1} per syringe.

6. For PLA, PCL and PLGA use a working distance of 17 cm from needle tip to mandrel.

7. For PHBV use a working distance of 10 cm from needle tip to mandrel.

8. Charge the syringe needles to +17000 V (73030P, Genvolt, Shropshire, UK) and electrospin from the appropriate distance onto the aluminium foil coated mandrel.

9. For random fibres rotate the mandrel at 200 RPM.

10. For aligned fibres rotate the mandrel at 1000 RPM.

11. Scaffolds can be stored on the aluminium foil under dry conditions. Recommended storage is in a sealed container at 4 °C in the presence of desiccant. In our experience scaffolds remain stable for at least 4 months (possibly much longer) under these conditions (the MacNeil group was not aware of any published studies on long term storage conditions for scaffolds at the time of writing).

3.3 Production of complex scaffolds by sequential spinning

Sequential spinning provides a method of combining the properties of different materials to create a material that has the best of both properties. PHBV produces a flat, dense, brittle sheet, whereas PLA or PCL spinning produces low density elastic sheets. Both materials support cell attachment. Consecutively spinning these materials results in a dense cell-impermeable membrane that is elastic. In summary:

1. Set up the electrospinning rig as per Section 3.2, with PHBV spinning conditions.
2. Electrospin PHBV as above.
3. Without changing the aluminium foil, electrospin a second polymer on-top using the parameters and normal conditions for that polymer (e.g. 17 cm drum to needle, 17000 V, 200 RPM for PLA). This additive process builds up a double layer of scaffold producing a bilayer.

3.4 Production of multilayered scaffolds by annealing several layers together

Scaffolds can be multilayered through the use of heat annealing. To do this 4 sheets of PLGA are placed on top of each other and then heat annealed at

60 °C for 3 hours. Scaffolds can also be annealed by vapour annealing. Here 4 sheets of PLGA are placed on top of each other and suspended 2 cm above a pool of DCM (10 ml) for 1 hour. This is performed in a sealed container at room temperature.

3.5 Aseptic production and post production sterilisation of electrospun scaffolds

Aseptic scaffold production can be achieved by electrospinning in an aseptic environment of a laminar flow hood, inside a clean room environment. To do this either sterile polymers of medical grade, or polymers sterilised by incubation in DCM can be used. Once dissolved, polymers are electrospun onto sterile foil wrapped around a sterilised mandrel. Scaffolds are then handled aseptically. Sterility is verified by incubating samples of the scaffold in growth media free from antibiotics for the appropriate period. For ethanol disinfection (this is of use experimentally but is not a recognised methodology of sterilisation which could be taken to the clinic) scaffolds are placed briefly (15 min) in a 70% v/v solution of ethanol in distilled water. For practical experimental purposes this is usually sufficient to disinfect scaffolds so that they can then be combined successfully with cultured cells. For peracetic acid sterilisation scaffolds are immersed in peracetic acid (0.1% v/v in PBS) and incubated for 3 hours at room temperature, as described in Selim *et al.*[198] For gamma sterilisation scaffolds are irradiated with a dose of 3 kGy using a caesium source, as described in Selim *et al.*[198]

3.6 Biomechanical testing of scaffolds

Scaffolds are cut into rectangles 5 mm × 20 mm, measured for thickness using a micrometer, and placed into a Bose Electroforce 3100 instrument. This machine applies a force of 0-22 N up to a displacement of 6 mm and plots the load vs. displacement as a stress/strain curve. This allows the E and elasticity to be calculated.

3.7 Visualising cells on scaffolds and assessing ECM production

Cells can be stained with vital fluorescent dyes which allow one to see cells on the scaffolds as they attach, migrate and proliferate. Post culture the presence of cells on scaffolds can be determined by staining for cell nuclei with DAPI. The production of ECM by cells on the scaffold can be assessed by staining cells for a range of ECM proteins including elastin as shown in this example. All scaffolds used were measured to have a thickness of at least 0.2 mm and cut into squares 1.5 cm × 1.5 cm prior to seeding. In these studies human dermal fibroblasts are used throughout because of the role they play in soft tissue reconstruction which is our laboratory's primary research interest. In summary:

1. Culture cells as per Sections 2.1.4 − 2.1.6.

2. If required, prior to seeding cells on the scaffold, cells can be pre-labelled using CellTracker red or green (Section 2.1.8).

3. Post culture samples are fixed in 1ml 3.7% formaldehyde in PBS at 37 °C for 20 minutes and then washed with 3 × 1 ml PBS .

4. Cells can be analysed for DAPI and elastin as per Sections 2.1.9 & 2.1.11.

3.8 Subjecting cells on scaffolds to biaxial dynamic conditioning

To examine the effect of dynamic conditioning on fibroblast ECM production, a simple proof-of-concept bioreactor was developed to explore this.

Electrospinning onto liquid filled balloons for use in bioreactors

In order to perform cell culture on balloons a method of sterilising and then aseptically coating the surface with electrospun scaffolds was required. Balloons (as above) were autoclaved and then filled with sterile PBS (until just turgid, 30 ml, OXOID^{TM} 8 g/L NaCl, 0.2 g/L KCl, 1.15 g/L $Na_2PO_2(OH)_2$ and 0.2 g/L $K_2PO_2(OH)_2$ in 1 L distilled H_2O). The balloon was then hung in place in a laminar flow hood. An earthing cable was inserted into a branch pipe containing PBS connected to the flow regulation apparatus (Figure 3.1). The balloon was then spun onto while being manually rotated (Section 2.2.5).

Spun fibres adhered to the entire surface of the balloon and gave an even coating, unlike non-graphite coated air filled balloons where fibres could be seen deflecting from the surface. Using an earthing cable inserted into the balloon at a branch pipe on the filling mechanism was essential to ensure that it would act as a collector.

Figure 3.1: Examples of electrospinning PHBV onto a balloon filled with PBS.

SEM images of PHBV scaffold on balloon pre and post deflation

In order to observe if there was any change in the scaffold fibre arrangement on the balloon post deflation, two balloons were prepared as described in section 3.8. After the PHBV was electrospun onto the balloons, one was immediately processed for SEM. The second balloon was then deflated to half the surface area and then the scaffold also processed for SEM analysis (Philips XL-20). Figure 3.2 shows SEM images of the PHBV scaffold electrospun onto a balloon, before and after the balloon is deflated. The two images contrast

greatly. The deflation causes the scaffold to ruffle and become visibly denser than the scaffold before deflation.

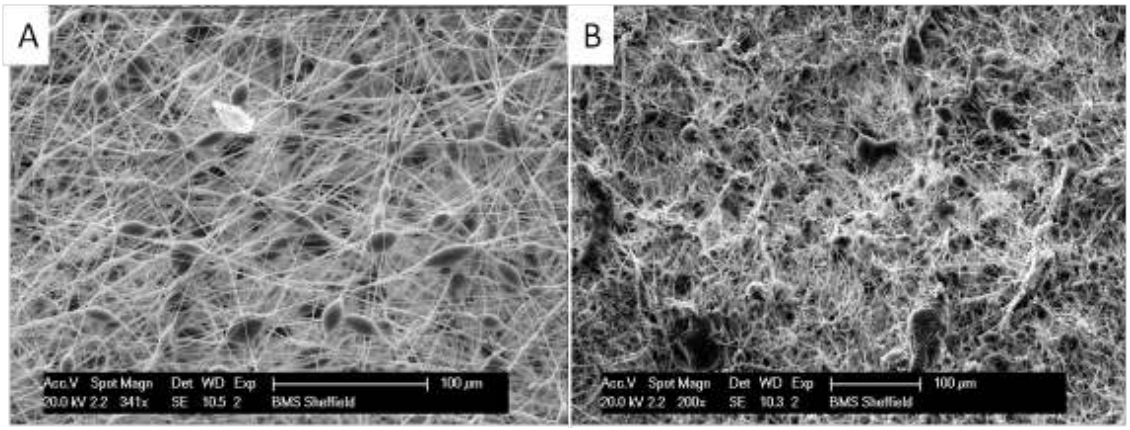

Figure 3.2: SEM photographs of PHBV scaffold electrospun onto a balloon. A. before deflation of balloon and B. post-balloon deflation.

Elastin production on biaxially distended scaffolds

Once methods for creating a sterile, scaffold coated, balloon and an appropriate distension were calculated, it was then possible to study the effect of multiaxial distension on cellular production of extracellular matrix. A balloon and flow regulation apparatus were autoclaved (122 °C, 220 mBar for 1 hour). Under clean room conditions the apparatus was unpacked in a laminar flow hood and placed in position for electrospinnig.

The balloon was inflated with 28 ml (double the required final surface area) of PBS, and the apparatus connected to an electrical earth at the branch pipe on the 3-way tap (a point in the apparatus that does not need to be sterile). PHBV was then electrospun onto the balloon (8 ml, 17 kV, 40 μL.min^{-1}, working distance of 10 cm, Section 2.2.5).

The balloon was then deflated by 14 ml and a second coating of PLA was spun on (8 ml, 17 kV, working distance of 17 cm, 40 μL.min^{-1}), and the scaffold allowed to dry for 1 hour. The balloon was then placed into a sterile vessel (500 ml Schott-Duran bottle) and transported to a laminar flow hood suitable for seeding the cells prior to culture (Figure 3.9). The balloon was removed from the vessel and placed onto a sterile surface (Petri-dish), and its surface basted (1 ml every 20 seconds for 20 minutes) by pipetting a cell suspension (1×10^6 cells in 5 ml of DMEM) using a Pasteur pipette.

The balloon was placed back into the culture vessel pre-filled with 500 ml of pre-warmed culture medium (Section 2.1.4). The inflation apparatus was connected to a syringe pump (Kent Scientific, Genie Plus, Connecticut, US) and the balloon inflated by 14 ml over 5 days (0.0034 ml/min). The culture vessel was placed in an oil bath heated to 37 °C for the duration of the experiment using a hotplate/stirrer.

A second similar balloon was also prepared using the same method, but not inflated by the syringe pump. This was used as a static control. Post culture, each balloon was cut in half (Figure 3.10), one half was stained for elastin and cell nuclei (DAPI) and the other half assayed with MTT (Sections 2.1.11, 2.1.9 & 2.1.13).

Figure 3.11 shows fibroblasts cultured on a balloon. MTT (left) shows viable cells are present and coating a large section of the balloon. The presence of cells is confirmed by DAPI staining (cell nuclei, blue dots). Immunostained elastin was detected on the exercised balloon (green fibres). No elastin was detected on the static balloon (no green substances visible, Figure 3.11 C) .

3.9 Representative Results

The following figures are representative results that can be expected if the above methods are followed. Electrospinning can be utilised to create scaffolds with random and ordered architecture (Figure 3.3), this is repeatable and the fibres are uniform. Many types of polymers can be electrospun with characteristics which can vary considerably, as shown in Figure 3.4 for PHBV, PLA or PCL. Electrospinning can produce light fluffy scaffolds or dense cell impenetrable membranes (see Figure 3.5).

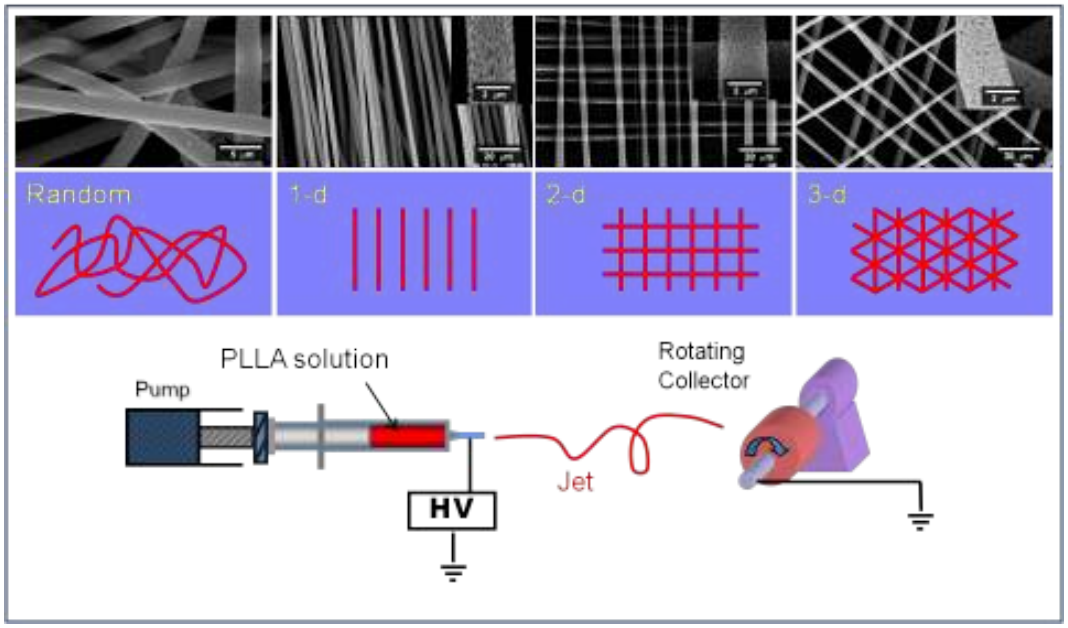

Figure 3.3: A cartoon of an electrospinning rig, the spinning of random and parallel fibres, and then layers of fibres placed over each other.

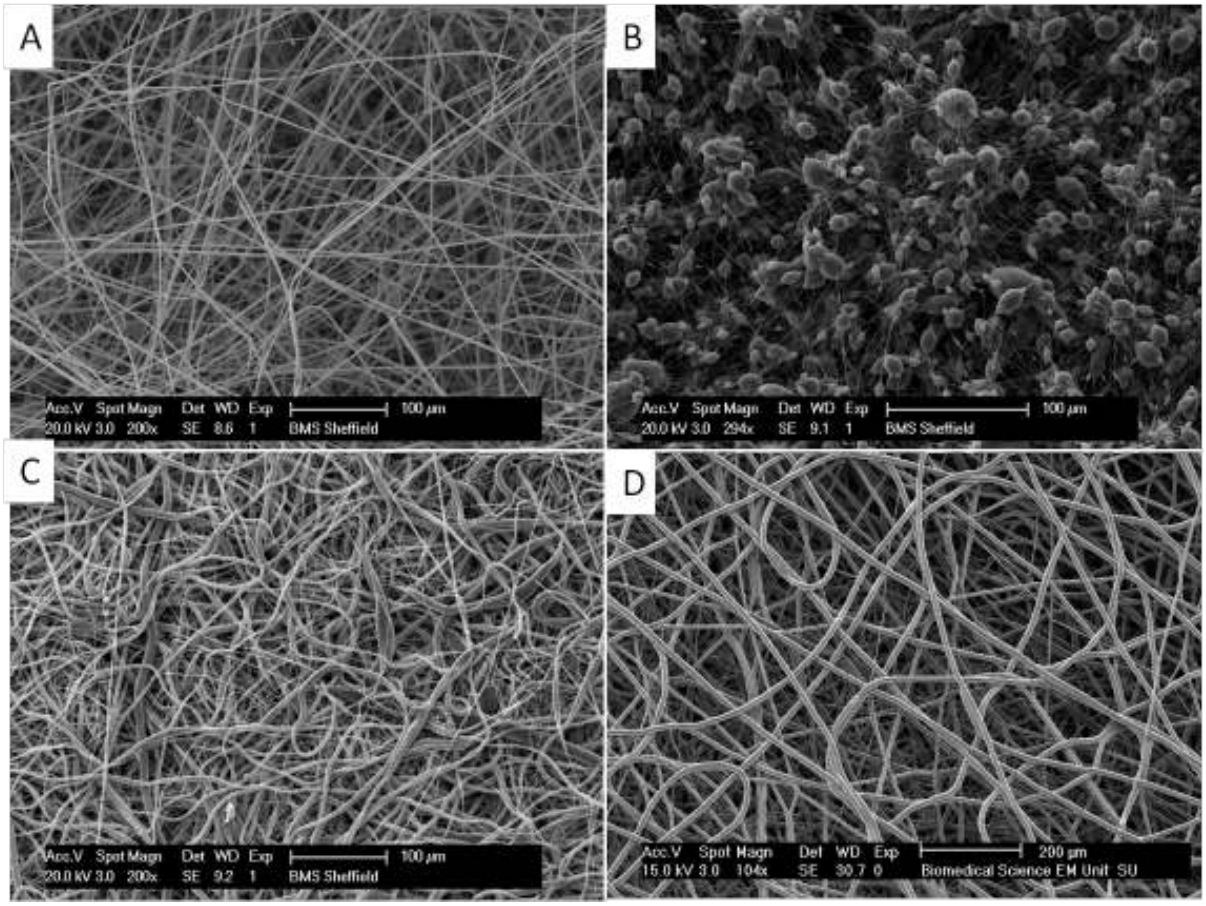

Figure 3.4: Shows the morphology of random electrospun mats of (A) PLA, (B) PHBV, (C) PCL and (D) PLGA.

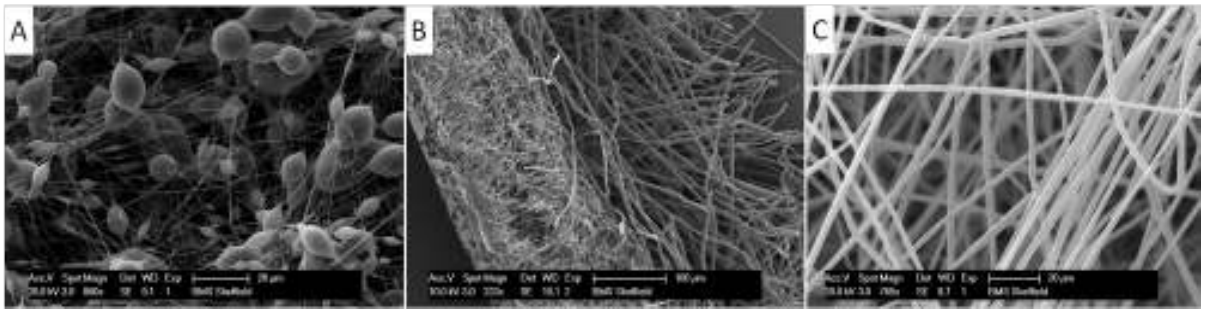

Figure 3.5: Production of a multilayered scaffold. Here the scaffolds were initially spun using PHBV and then syringes filled with PLA or PCL were used, which was spun on top of the PHBV scaffold. The figure shows the appearance of these multilayered scaffolds, (A) PHBV layer, (B) Bilayer cross section, showing dense PHBV layer and more open PLA layer and (C) PLA layer.

All scaffolds shown here facilitated cell attachment and proliferation. For PLA the average fibre diameter was 3 μm; for PHBV it was 0.3 μm; for PCL it was 3 μm; and for PLGA it was 11 μm.

If thicker scaffolds are required vapour and heat annealing can be employed to anneal layers of scaffolds together (Figure 3.6). This work shows that bilayer membranes can be made where cells A and B can each be cultured on a separate membrane without intermingling (Figure 3.7).

This is demonstrated by using fibroblasts coloured with two different fluorescent cell tracker dyes. Such a bilayer membrane would be useful when culturing cells, for example, to form a hard tissue such as bone or cartilage on one side, separated from cells designed to form a soft (and usually faster growing) tissue on the other side.

With respect to the impact of sterilisation on electrospun scaffolds the MacNeil group have previously reported that the method of sterilisation impacts on the scaffold.[198] This is illustrated in Figure 3.8 which shows the effects of peracetic acid, gamma irradiation and EtOH on the fibre diameter and UTS and E of a PLGA (85:15) scaffold.

Gamma irradiation has no significant effect on fibre diameter whereas peracetic acid and ethanol reduce fibre diameter by approximately 50%. Each of the methods of sterilisation changed the ultimate tensile strength and the elasticity of the scaffolds. Culture of cells on these scaffolds further reduced the ultimate tensile stress, but increased the elasticity.

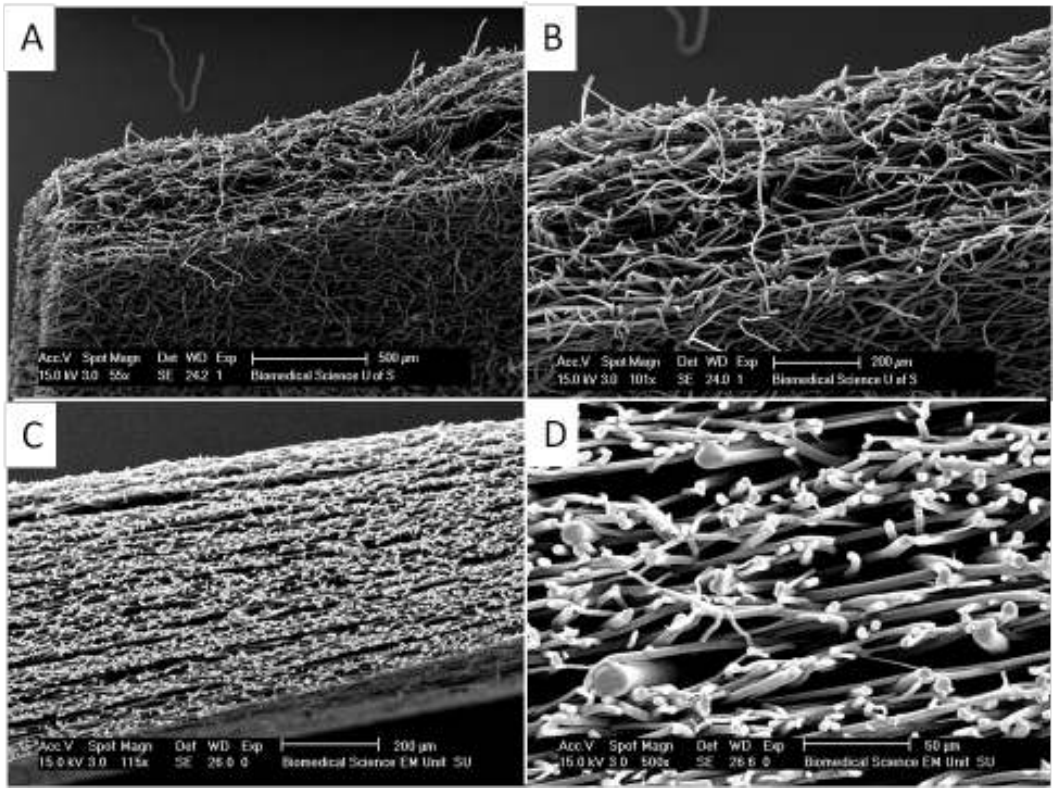

Figure 3.6: Thicker scaffolds can be produced by heat annealing and vapour annealing. (A) and (C) Show a section through a PLA scaffold where initial fibrous scaffolds of approximately 150 μm have been placed together and heat or vapour have been used to make much thicker scaffolds of up to 500 μm. In (B) and (D) one can see that the scaffold consists of layers of much thicker fibres interspersed with layers of thinner fibres. This approach can be used to produce scaffolds of complex mechanical properties.

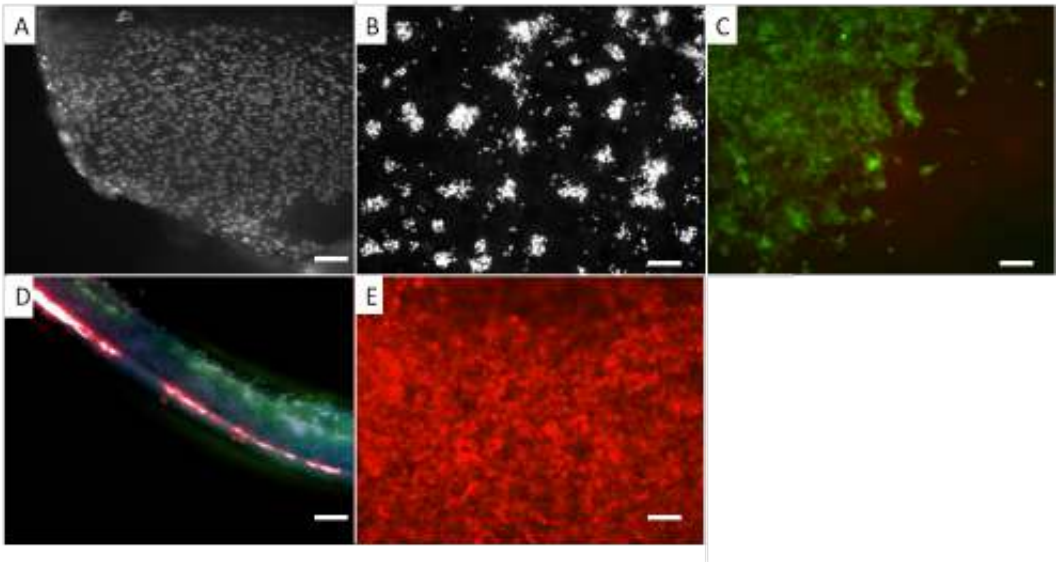

Figure 3.7: Appearance of cells on a bilayer scaffold. In all cases the cells present are skin fibroblasts. (A) Fibroblasts on electrospun PLA where the cells have been fixed and stained with DAPI. (B) DAPI stained cells stained on PHBV. In (C) the fibroblasts have been pre-stained with a vital dye CellTracker green and you can see the appearance of them on the PLA side of the bilayer. (D) A section through the bilayer with red stained fibroblasts on the lower PHBV surface and green stained fibroblasts on the upper PLA surface. (E) Fibroblasts pre-stained with CellTracker red grown on the PHBV surface. The use of vital fluorescent dyes provides a convenient methodology for looking at the distribution of cells on the scaffold while the cells are still growing. One can routinely use these dyes for at least 7 days. However, the concentration of dye becomes diluted as the cells divide. Scale bars are equal to 0.1 mm.

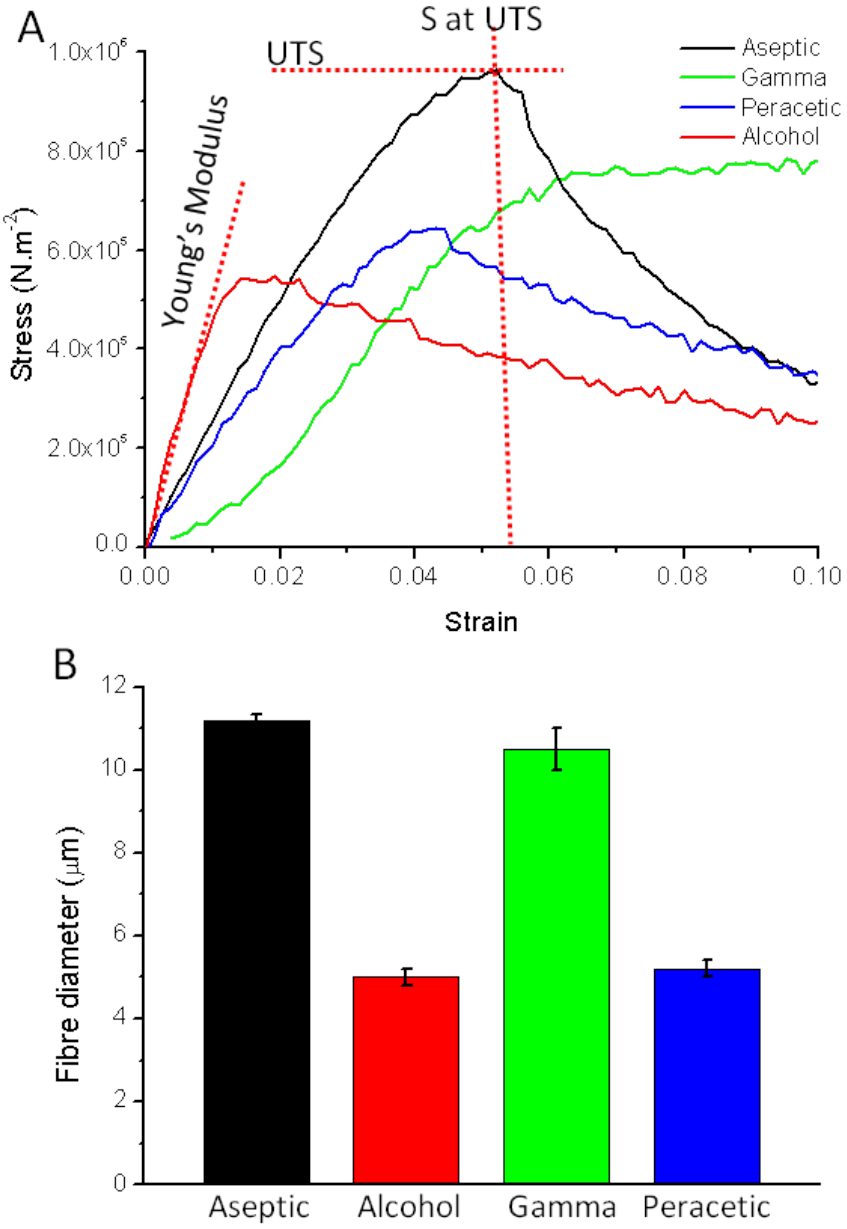

Figure 3.8: Biomechanical properties of electrospun scaffold obtained using a Bose electroforce tensiometer device. (A) Stress/strain curves of PLGA scaffolds sterilised by gamma irradiation, alcohol, peracetic acid, or aseptically produced. Three measurements can be obtained from such a graph, the ultimate tensile stress to which the fibre can be subjected before it breaks, the UTS and the E. The latter gives an indication of the elasticity of the scaffold. (B) The effect of each sterilisation method on PLGA fibre diameter in μm. Each sterilisation methodology decreased UTS. Both peracetic acid and Gamma irradiation decreased the E giving a more elastic scaffold, alcohol made the scaffold particularly brittle.

Finally, a method of testing the effect of dynamic biaxial distension on cells cultured on electrospun scaffolds, is presented. This proof-of-concept approach shows that cells remain viable during dynamic distension but also produce increased amounts of elastin under these conditions. This contrasts markedly to the lack of elastin when the same cells on the same scaffold are maintained under static conditions (Figures 3.9, 3.10, and 3.11).

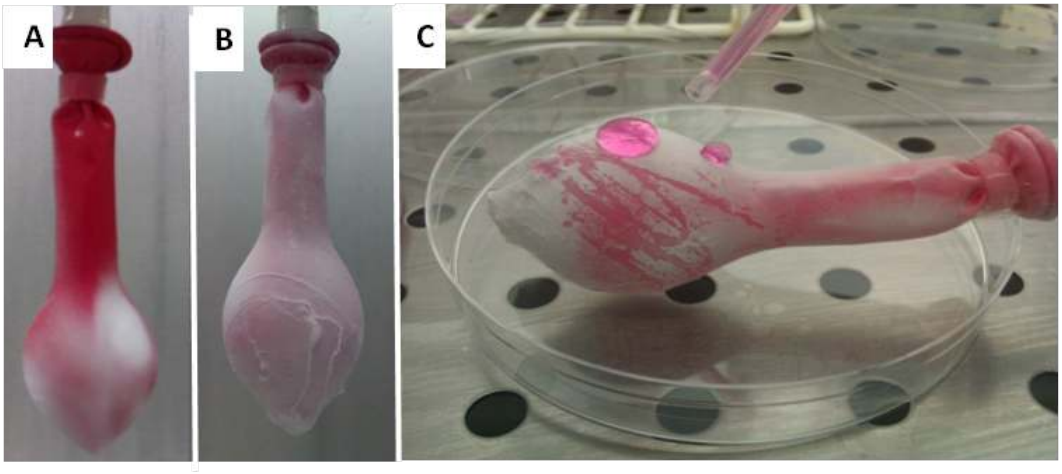

Figure 3.9: (A) A deflated balloon onto which electrospun fibres, PHBV, have been deposited. At this stage the balloon is partially covered with fibres. (B) A balloon fully coated with PHBV and PLA fibres. (C) The balloon is basted with a cell suspension.

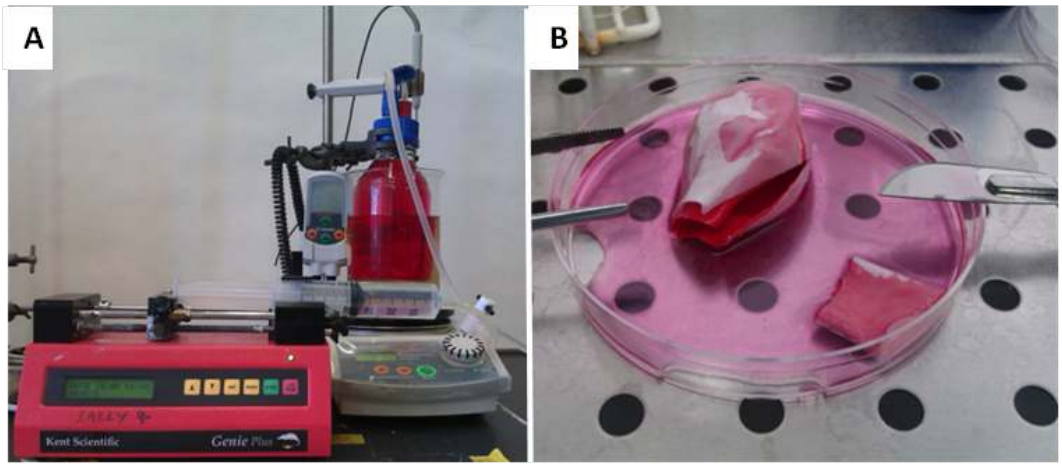

Figure 3.10: (A) A balloon placed within a bottle of sterile media where the balloon is connected to a syringe pump, and PBS (used as a conducting electrolyte) is used to gently inflate and allow deflation of the balloon against a programmed schedule. (B) Cells on scaffolds being removed from the balloon at the end of the experiment, and analysis undertaken for cell viability shown in Figure 3.11.

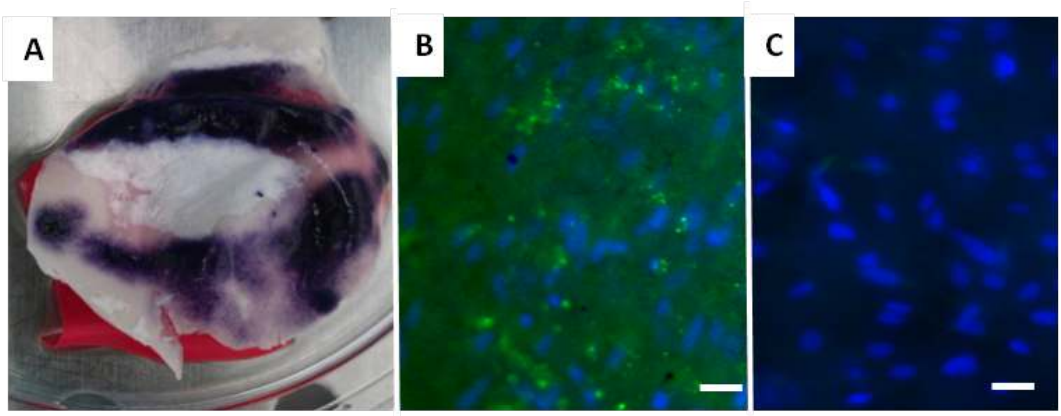

Figure 3.11: A. MTT staining of fibroblasts cultured on a balloon for 1 week. Purple regions show patches of viable cells on the surface of the scaffold. DAPI and immunostained elastin stained balloon sections of exercised (B) and static balloons (C). Cell nuclei (blue) are visible in both, whereas elastin (green) is only present on the exercised balloon (B). Scale bar is equal to 0.025 mm.

3.10 Reasoning for the use of, and the development of, balloons as bioreactor substrates

A crinkly scaffold should be able to change volume without an increase in pressure, when inflated and return to its original shape, by the corrugations unfurling (Figure 3.12). The materials used to create these scaffolds are already well known for their biocompatibility.

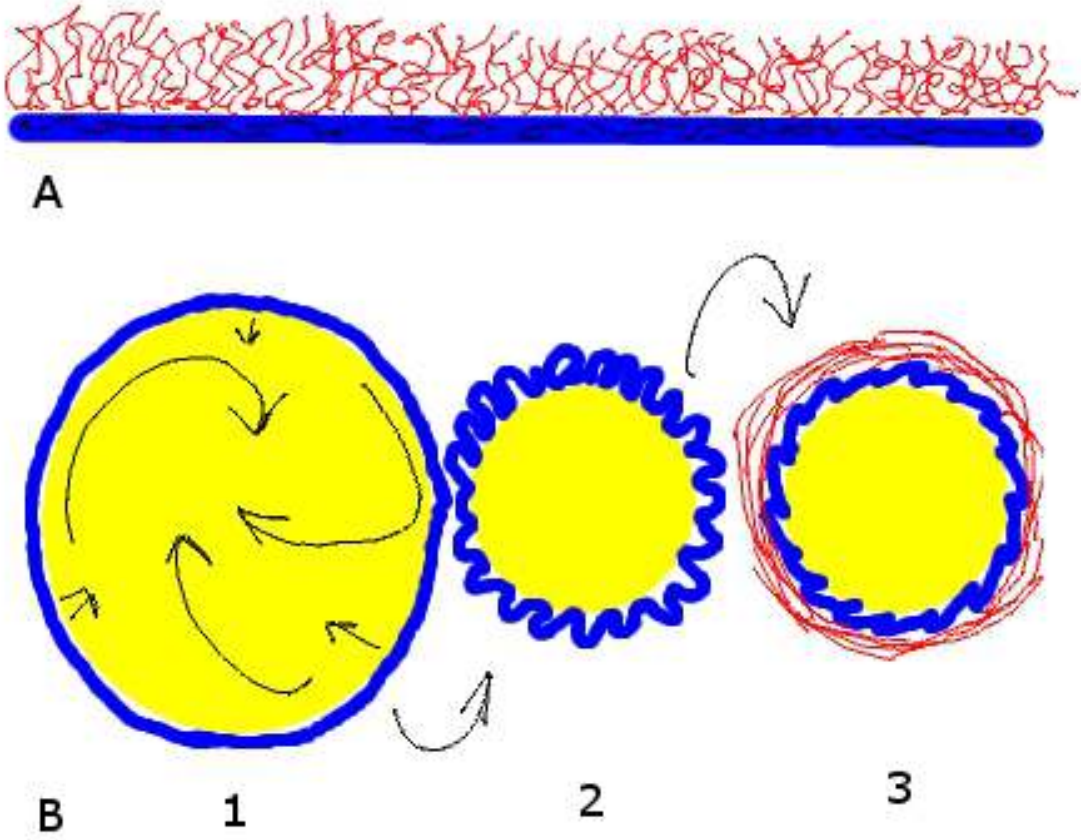

Figure 3.12: A. Flat bilayer. B. Schematic of creation of bilayer capable of distending with a child. 1. PHBV is electrospun onto a balloon. 2. The balloon is deflated, and the scaffold ruffles up. 3. PLA is finally spun on top to create a bilayer.

A balloon can also overcome the limitations of uniaxial mechanical testing equipment. When inflated a balloon will expand biaxially, allowing a stress to be applied in 2 dimensions to a scaffold. An assumption does have to be made that a balloon will inflate uniformly, a low quality balloon may expand significantly more in one area than another and this should be investigated.

The first question that arises is how much distension should be applied? Inevitably this question has different answers depending on the tissue under culture. If bladder tissues were in culture a cyclic regime of expansions and contractions would be required. With respect to cleft palate, a healthy maxilla will double in volume as a child ages from 0-5 years. There isn't physically enough time to keep a construct in culture for 5 years, but if the model can be designed to expand as much as a cleft palate defect in a fortnight, the cells in culture may respond in an appropriate fashion. A model that can distend to twice its original surface area is required (Appendix A.2).

A simple way to achieve this is to use a child's party balloon. Balloons are cheap, non toxic (they are given to children as toys) and they stretch in 2D when inflated. The question here is, do they expand equally in all directions as they are inflated?

3.10.1 Measuring the strain on the surface of an inflating balloon

How a balloon inflates needed to be characterised in order to understand how this will impact any scaffold placed onto a balloon's surface. It cannot be

assumed balloons are equibiaxial (i.e. expand equally in two dimensions). It is not known what kind of 2D strain tissues undergo, and most likely this will vary depending on the tissue under investigation. However, it is useful to characterise it.

Three unadulterated balloons were pre-filled with distilled water (14 ml) and purged of air by connecting to a syringe (50 ml, Plastipak Ltd, UK), and a 3-way tap with 3 mm diameter tubing (Figure 3.13). The balloons then had 9 dots drawn on them in a cross-hair pattern (Figure 3.14).

Figure 3.13: Schematic of apparatus used to suspend and inflate balloons with liquid.

Each balloon was then inflated by injecting 30 ml of distilled water using a syringe pump (Genie Plus) in increments of 5 ml and then deflated back to it's original starting volume. The distance between sets of points was measured at each increment. Displacement and strain in x and y were calculated (Figures 3.14 and 3.15).

Figure 3.14: Balloon undergoing 2D strain analysis. Nine points are drawn on the balloon in a cross-hair pattern. As the balloon is inflated the change in distance between the points is recorded.

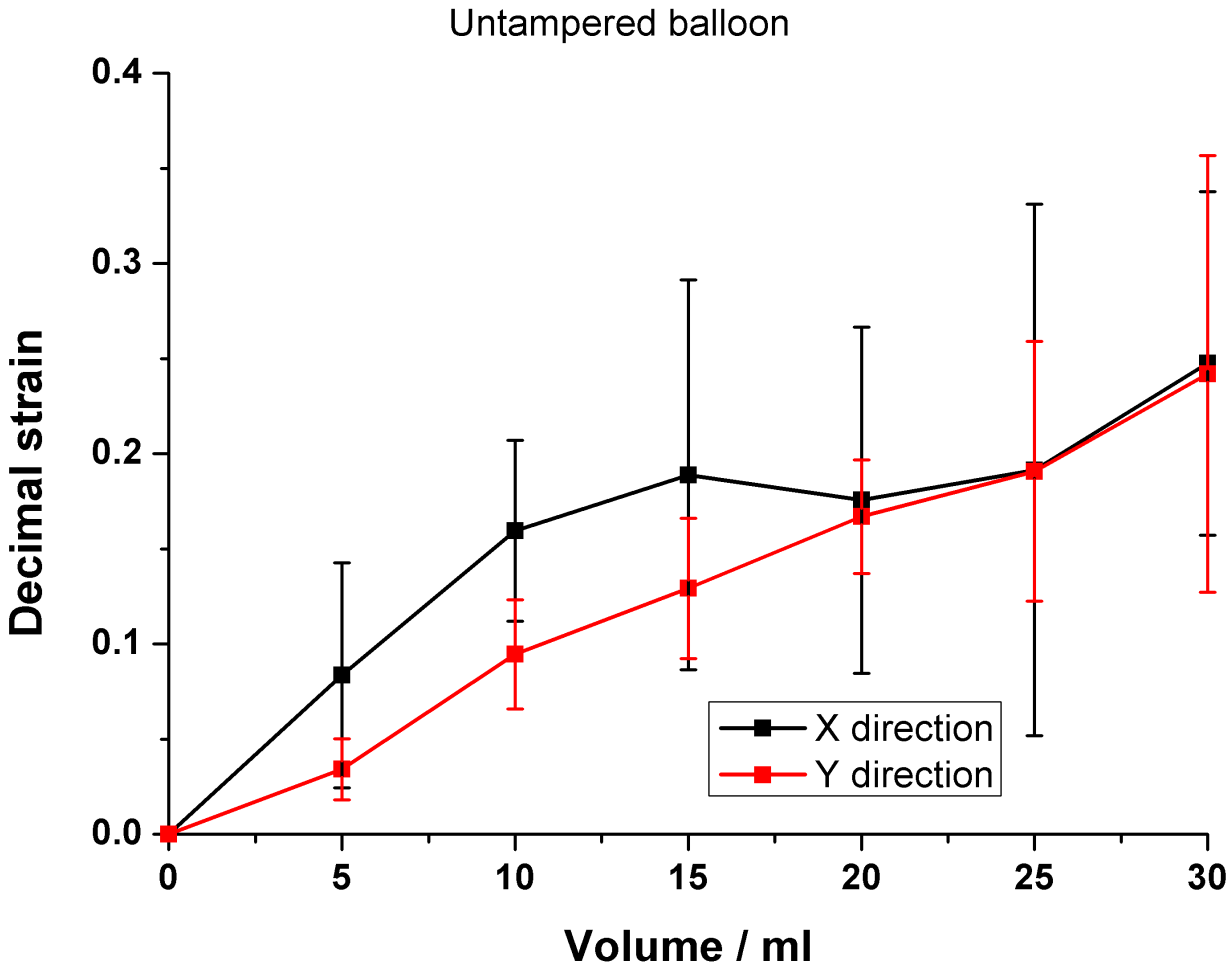

Figure 3.15: A graph to show the change in strain in x and y on the surface of a balloon as it is inflated from 0 ml to 30 ml. Error bars are equal to the mean ±SD, n=3.

It can be seen that balloons do not inflate equally in the x and y planes, with the greatest change occuring in the x axis. The variance between balloons is also large (Figure 3.15).

When balloons are inflated fully, on deflation, it is often obvious that the balloon does not return to its original dimensions. In order to determine how great this change is, the experiment described above was repeated, except the

three balloons were pre-strained by inflating with air until taut (1 L) and held for 30 seconds before deflating and then their surface strains analysed. This was performed 3 times using separate balloons.

A plot of strain in the x axis verses strain in the y axis shows that strain in both directions increases with inflation up to 30 ml. So balloons do distend multiaxially (Figure 3.16). When the balloons are pre-inflated the variance is less, and the difference in strain between the x and y planes narrows. However, the total strain applied to the surface of the balloon is about 50% less than on a fresh, unadulterated balloon.

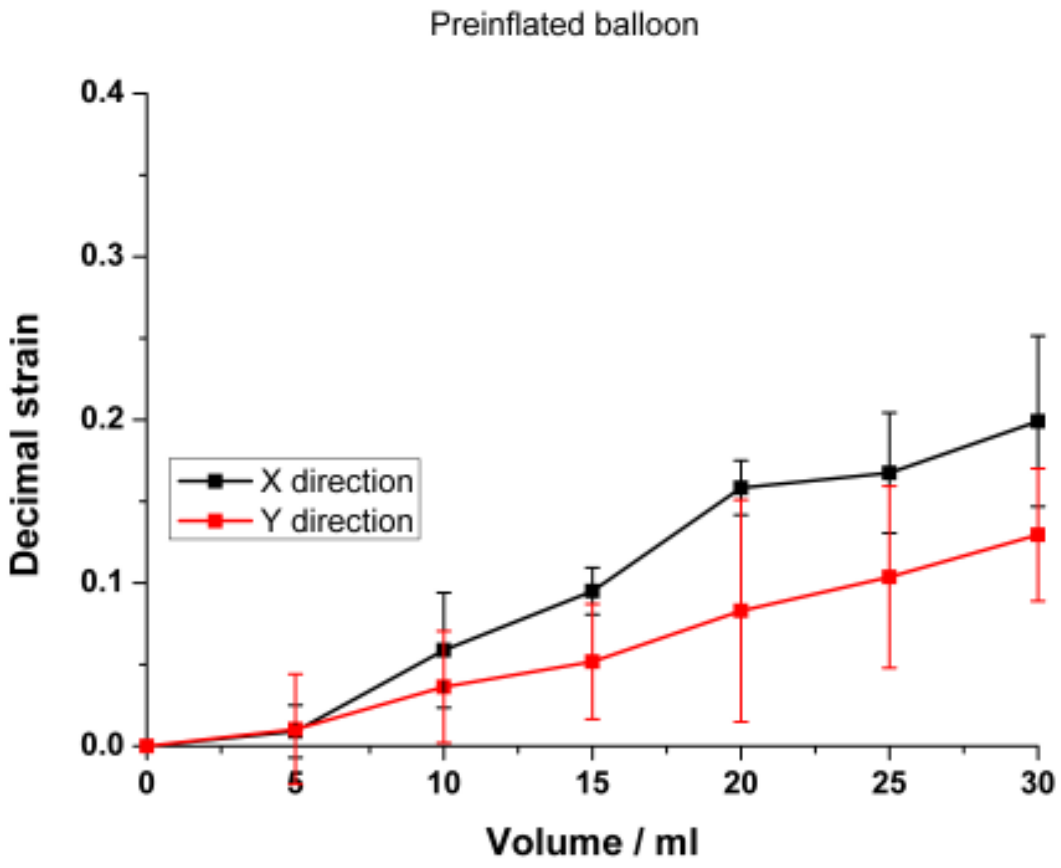

Figure 3.16: A graph to show the change in strain in x and y on the surface of a balloon as it is inflated from 0 ml to 30 ml. Error bars are equal to the mean ±SD, n=3.

The degree of strain in the x axis is not equal to the y axis. The greatest increases are observed in the x axis (equatorial around the balloon). The error in taking these measurements is small, around ± 0.025 in decimal strain. However, the variance between balloons is huge, up to ± 0.150 decimal strain. The balloons fresh out of the packet do not return to their original dimensions on deflation back to the starting volume. This diminishes when the balloon is pre-strained to within ± 0.100 decimal strain. This variation seems to peak at around 20 ml inflation, it is considerably lower for all balloons below this value at ± 0.03 decimal strain. The pre-strained group do return to their starting dimensions upon deflation.

Given that this is a proof of concept model, it was decided to use pre-strained balloons in future models. The strain in x and y may not be equal, likewise the variance between balloons is significant.

To achieve the doubling in surface area required by this model, a balloon must be inflated by at least a factor of $2\sqrt{2}$ (Appendix A.3).

3.10.2 Electrospinning onto balloons

A method was required to fix scaffolds under investigation to the balloon. The most direct method of achieving this was to electrospin the scaffold directly onto the surface of the inflated balloon.

Electrospinning onto air filled balloons

Air filled balloons seemed an obvious starting point, although a couple of hurdles needed to be overcome. Firstly a method of mounting and earthing the balloon was required, and secondly overcoming the positive surface charge that is inherent in balloon latex. The positive surface charge prohibits the direct electrospinning of scaffold onto the balloon as it repels the positively charged polymer jet, preventing deposition. Party balloons (mixed bag of 50, Wilkinsons Hardware Stores Ltd) were inflated with air to the required surface area (597 cm^2). 5 ml of industrially methylated spirits (IMS) (70% v/v in distilled water) was placed inside and then the balloon tied up. The inflated balloon was then mounted on a knitting needle ($3\frac{1}{4}$ mm diameter, anodised aluminium core, Wilkinsons Hardware Stores Ltd) by pushing it through the surface of the balloon and out the opposite side (Figure 3.17).

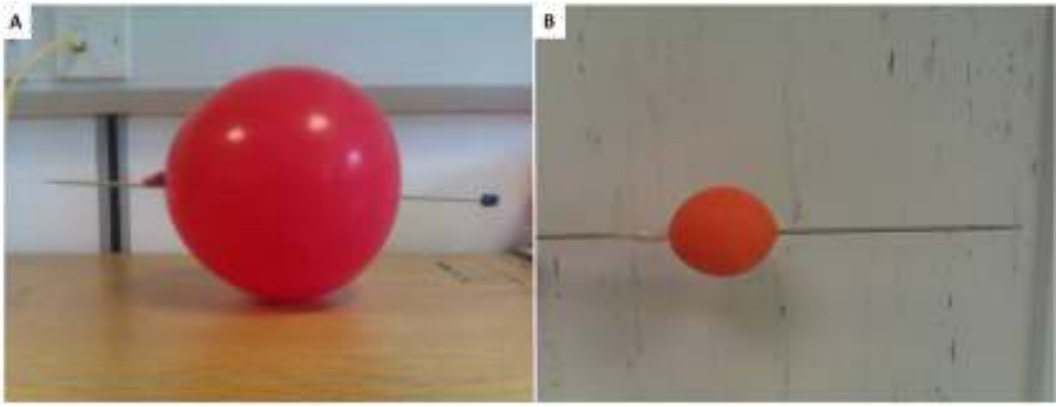

Figure 3.17: Inflated balloons mounted on knitting needles.

The knitting needle was then fitted into the chuck of the electrospinning rotator, replacing the normal rotating collector (balloon rotated at 300 RPM). The IMS acts as an electrolyte, allowing the balloon to act as an earth, and become a collector suitable for the deposition of fibres. The knitting needle

provides a stable spindle on which to mount the balloon, a physical earthing point, and prevents the collector from wobbling.

Graphite coating of air filled balloons

Another method of overcoming the positive surface charge of a balloon is to coat the surface with a conductor. Graphite was selected due to its non-toxic and conductive properties. Once mounted on the knitting needle the balloon was coated with a graphite suspension in IMS (<20 μm particles, 70 wt% IMS in distilled water), completely covering the surface of the balloon. Once the IMS had evaporated the graphite was polished until the balloon surface was lustrous (Figure 3.18). This ensures even and complete coverage.

Without any liquid in, or graphite on, the balloon, the latex would repel the positively charged polymer jet resulting in a clean balloon and a fibre coated cabinet. Once the balloon became a conductive, earthed collector, then fibres evenly coated the surface during spinning. Once a complete coverage of fibres was achieved and dried, the balloon could be deflated and removed leaving a ball of scaffold behind (Figure 3.19).

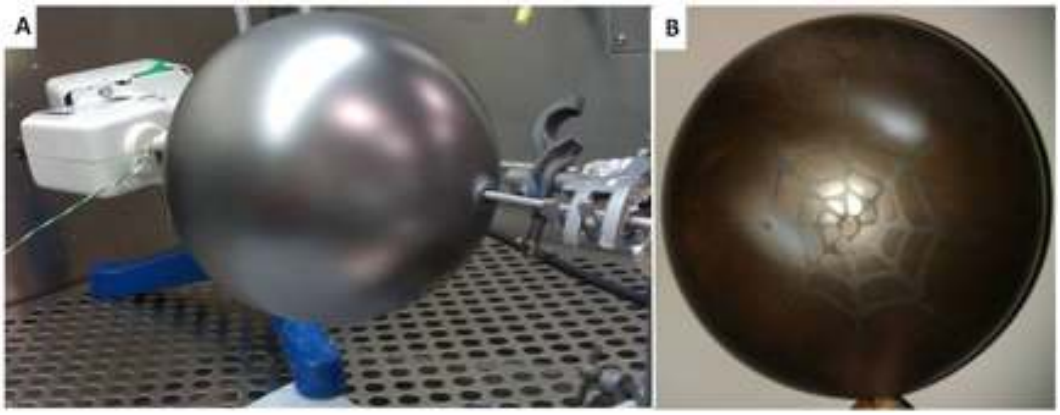

Figure 3.18: Balloons coated with graphite after polishing.

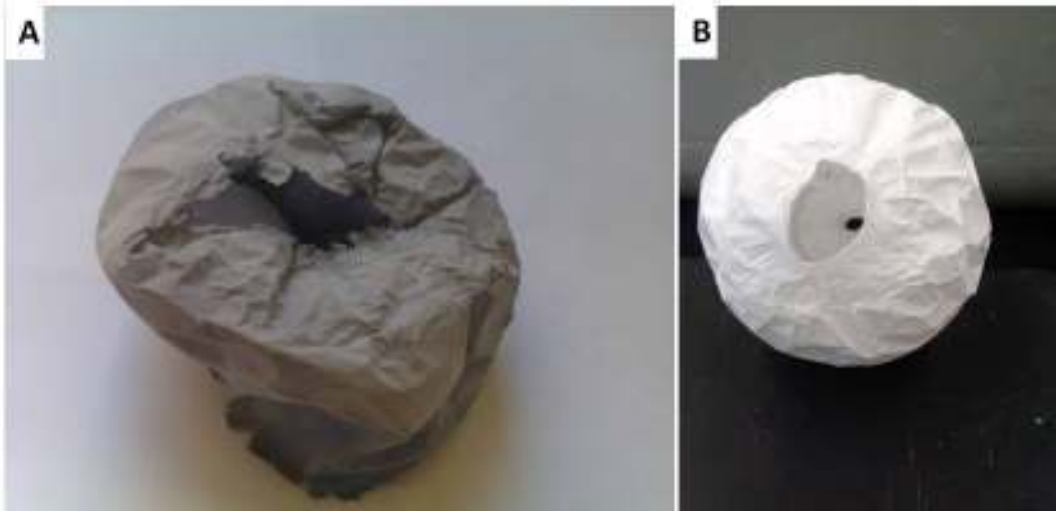

Figure 3.19: Polymers are spun onto balloons and then the inner balloon was removed to leave an electrospun sphere. Electrospun spheres from A. Graphite coated balloon. Graphite staining can be seen on the sphere from the graphite coated balloon. B. Air inflated balloon with 5 ml of IMS inside.

Electrospinning onto predefined areas on graphite coated balloons

As the balloon latex is repulsive to positively charged streams of polymer, but a graphite coating can transform this into a collector, tracks can be drawn on the balloons surface allowing selective deposition of scaffold. Using an 8B pencil (Staedtler®), patterns were drawn onto a balloon, areas where deposition was

required were shaded in with pencil. These areas were then connected up by pencilling lines to connect them to ground. The balloon was then electrospun onto (Figure 3.20, Section 2.2.5).

Figure 3.20: Examples of patterns spun onto balloons by shading specific areas with graphite.

Due to the knitting needle compromising the structure of the balloon, and the desire to be able to inflate/deflate the balloon post spinning, air filled balloons were abondoned. Liquid filled balloons do not have these limitations. Hence, were used for the duration of the project (as per Section 3.8).

3.11 An alternative embodiment of a balloon based bioreactor: Mechanical stimulation of scaffolds using Ebers P3D perfusion chambers

Once a suitable enclosure for a bioreactor had been created attention could be turned to the system itself (Section 2.4). The goal of this section was to create a system that avoided an excess of tubing but could also handle multiple

replicates simultaneously. An emphasis was placed upon user-friendliness of the system.

Ebers P3D 6 mm (Zaragoza, Spain) perfusion chambers were chosen to be adapted, to create mini exercising bioreactors, due to their inexpensive nature and clip-lock design, allowing scaffolds to be easily inserted (Figure 3.21). Their plastic construction also favoured them for adaptation. The use of Luer lock ports on either end of the chamber also made them compatible with most other lab equipment. In order to create a chamber that could distend a membrane at one end, but also circulate medium, a third port was added using epoxy resin (Wilkinsons Hardware Stores Ltd, UK) and hypodermic needles (BD, New Jersey, USA, Figures 3.21 and 3.22).

Eight adapted chambers were connected using branch trees (in order to minimise complexity and total tubing). This in turn was connected to a reservoir of media and a PBS filled syringe to provide the stimulus (Figure 3.23). In a laminar flow hood, balloon disks (6 mm diameter, autoclaved prior to use) were placed in the base of the chamber.

PLA-PHBV scaffold disks (6 mm diameter) were then placed inside and any air bubbles were purged. 10,000 fibroblasts were seeded in DMEM into the chambers, and then the chambers were sealed. The scaffolds were left overnight at 37 °C for the cells to attach (Section 2.1.4). The chambers were then placed inside the propagator set up as described in Section 2.4.1.

Figure 3.21: An Ebers P3D chamber adapted to accommodate a third port. Scaffold can be seen at the base, on a section of orange balloon.

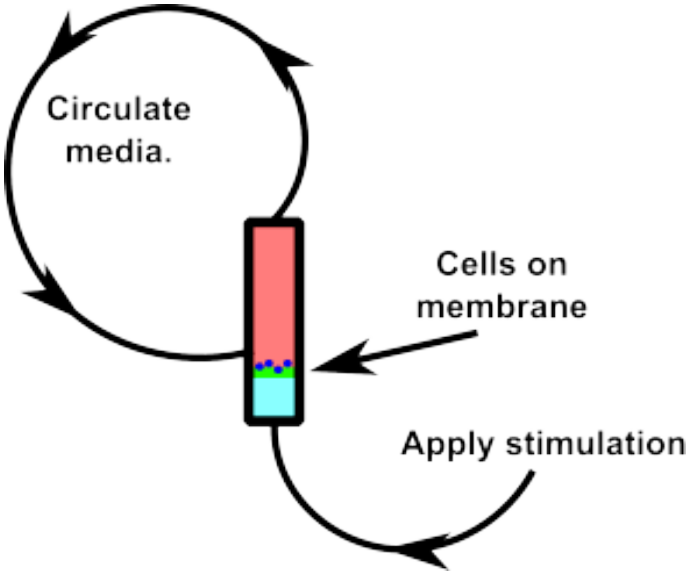

Figure 3.22: Diagram of chamber set up. Media flows in and out through the top two ports, while a mechanical stimulus is applied to the balloon membrane using the bottom port.

Figure 3.23: Eight Ebers P3D chambers are connected together using a branching system. This minimises tubing and requires only two pumps. One to circulate media, and the second to mechanically stimulate the cells. Green and blue dyed liquid is alternately pumped through to check there is liquid flow through all 8 chambers.

Media was circulated using a peristaltic pump (90 rpm) and the PBS filled syringe cyclically infused/withdrew 0.4 mlmin^{-1} applying 0.05 ml to each chamber. This cyclically inflated each balloon section into a hemisphere, doubling, then halving the surface area every two minutes. The cells were cultured for 14 days and then the scaffolds assayed using the resazurin salt assay (Section 2.1.12).

Following this, the samples were immunostained for elastin and cell nuclei with DAPI (Sections 2.1.9 and 2.1.11). A second similar reactor was set up where the samples were not mechanically stimulated. This constituted our static control.

Figures 3.24 and 3.25 show the cell viability in the Ebers perfusion chambers after 2 weeks of culture. The static chambers show a higher absorbance indicating a greater number of viable cells than the dynamic chambers. There was a high variation (at least 50%) across all chambers, for both static, and dynamic culture in the number of viable cells.

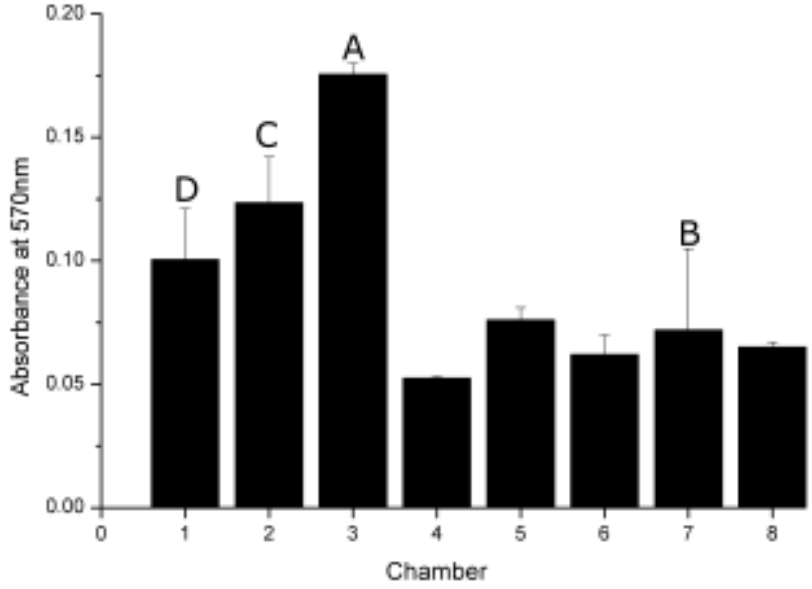

Figure 3.24: Viability of cells cultured under static conditions in 8 connected Ebers P3D chambers for 2 weeks. Viability was assessed by the resazurin salt assay. The change in readings between systems shows the variability of culture conditions in the system. Values are absorption at 570 nm expressed as mean ± SE, n=3. The chambers labelled A, B, C, & D correspond to panels A-D of Figure 3.26

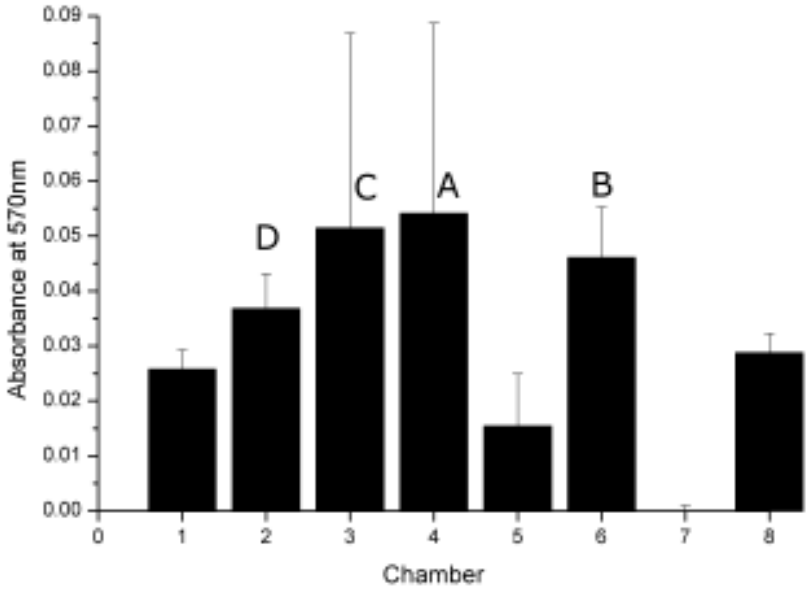

Figure 3.25: Viability of cells cultured under dynamic conditions in 8 connected Ebers P3D chambers for 2 weeks. Viability was assessed by the resazurin salt assay. The change in readings between systems shows the variability of culture conditions in the system.Values are absorption at 570 nm expressed as mean ± SE, n=3. The chambers labelled A, B, C, & D correspond to panels A-D of Figure 3.27

Staining the substrates for elastin and DAPI highlights the difference between static and dynamic cultures (Figures 3.26 and 3.27). Even with the dynamic culture having fewer viable cells at the end of the culture there is visibly more elastin (stained "green" in the Figures) than in the static system.

This smaller system, if perfected, should allow for more replicates, especially inside an inexpensive propagator. It would be possible to have rows of these each running multiple experiments. This "proof of concept" design does show the effect of mechanical stimuli on fibroblasts, in spite of the uneven cultures obtained. Elastin in varying amounts was produced in the dynamic system.

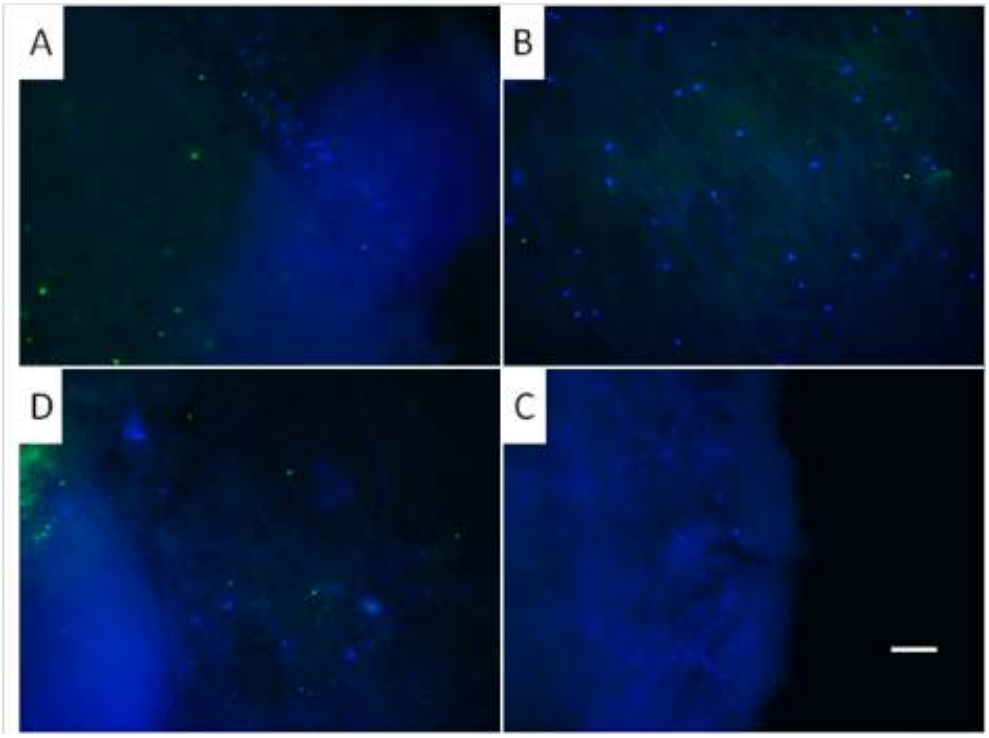

Figure 3.26: Immunostained elastin (green) and DAPI (blue) stained scaffolds after 2 weeks of static culture in an Ebers P3D chamber. A-D are images from 4 different chambers. Scale bar is equal to 0.1 mm.

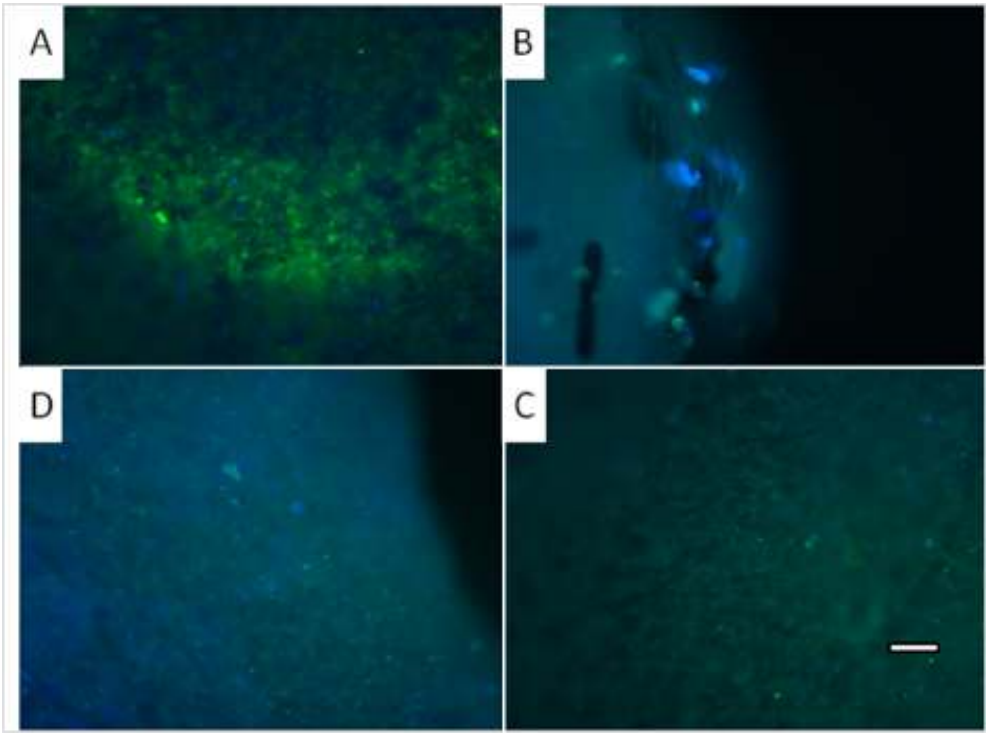

Figure 3.27: Immunostained elastin (green) and DAPI (blue) stained scaffolds after 2 weeks of dynamic culture in an Ebers P3D chamber. A-D are images from 4 different chambers. Scale bar is equal to 0.1 mm.

3.12 Investigation of keratinocyte culture in non-CO_2 perfused systems

While the above described bioreactors and enclosures (Section 2.4) are a step forward, one parameter had not so far been taken into account: pH buffering. With the balloon and Ebers systems pH buffering for fibroblasts was not a problem as there was a great surplus of medium compared to the number of cells. However, cells that require more precise pH conditions or an expensive culture medium are a potential problem. A pH regulation system that did not rely on volume alone needed to be included. This could either be a CO_2 gas perfused system (for bicarbonate buffering) or another, alternative CO_2 "free" system.

3.12.1 Action and kinds of pH buffer systems

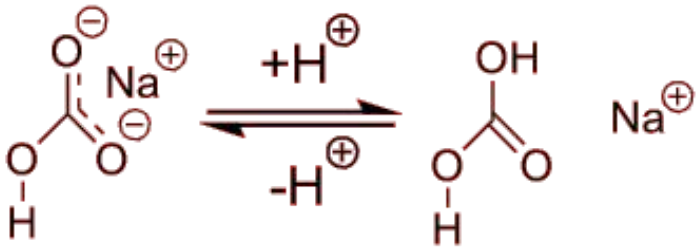

Figure 3.28: Chemical structure of sodium bicarbonate.

Sodium bicarbonate is commonly used as a pH buffer in cell culture (Figure 3.28).[199] Its method of action is well known, and it is responsible for pH regulation in the worlds oceans.[200,201] The system works by the following

chemical equibibria;

$$H_2O_{(l)} + CO_{2(g)} \rightleftharpoons H_2CO_{3(aq)} \tag{3.1}$$

$$H_2CO_3 \rightleftharpoons HCO_3^- + H^+ \tag{3.2}$$

$$HCO_3^- \rightleftharpoons CO_3^{-2} + H^+ \tag{3.3}$$

The result of these equations is a pH buffering effect, where excess acid can be converted into water and CO_2, and excess base converted into the carbonate ion (HCO_3^-). The buffer mechanism relies on gaseous CO_2 exchange. In the laboratory this means a CO_2 supply is essential, and incubators require CO_2 regulation apparatus to effectively buffer the pH.

In some bioreactors this dependence on gaseous CO_2 is either impractical to plumb in or undesirable (if a sealed bioreactor system is required). As shown earlier a large volume of medium can overcome this issue. However, in smaller bioreactor systems, where the total medium volume is less than 100 ml, a different buffer system is required. One such system uses 4-(2-hydroxyethyl)piperazine-1-ethanesulfonic acid (HEPES) (Figure 3.29).

Figure 3.29: Chemical structure of HEPES.

HEPES is an example of a zwitterion, that is a molecule that can have a positve and negative change, but remain neutral overall (the charges cancel each other out). This lends itself to being a buffer. HEPES was first identified as a potential buffer by Norman Good in 1966, and is known as one of Good's buffers.[202] Good designed buffers to meet the following criteria:

1. The molecules' pH buffer midpoint (the pK_a) should lie between 6 and 8, to function correctly in standard pH biological reactions (pH 7.4).
2. The substance must be very water soluble to maximise the ability of the buffer.
3. The molecule should be poor at, or better still, unable to penetrate the membrane of a cell so as not to interfere with the cells' biochemistry.
4. The buffer should not produce a salt upon reaction.
5. Buffer dissociation should be independant of buffer concentration, temperature, and ionic composition of media.
6. The buffer should not form any insoluble products upon dissociation.
7. The buffer should be resistant to enzymatic and chemical degradation, nor act as an enzyme inhibitor.
8. The buffer should be radio opaque in the UV/vis specturm in order to avoid interference with spectrophotometric assays.
9. Ideally the buffer should be inexpensive, easily synthesised, and purified.

These points become more important in the environment of a bioreactor. Should a buffer, for example, precipitate a solid dissociation product there

would be risk of a reactor's tubing clogging. HEPES functions as a buffer because of it's Zwitterionic nature, it can donate and accept hydrogen and is thus able to counteract changes in pH as required (as shown by the equilibrium in Figure 3.29). HEPES meets these requirements and has been shown to be an effective buffer that does not require external gaseous CO_2.

The aim of this section was to determine if keratinocytes can be cultured without the need to perfuse the medium with CO_2 to maintain the pH. HEPES does not need a gas supply to effectively buffer a medium to the correct pH. However, our (and other) groups' historical experience with HEPES indicate that keratinocytes do not like it. Perhaps the normal bicarbonate media buffering system fulfils a secondary roll. Bicarbonate is used by cells to regulate intracellular pH. If bicarbonate is absent from the medium, then cells that use pH as a controlling factor in differentiation may be greatly effected. It has been shown that sodium bicarbonate does form part of keratinocytes pH regulation system.[203,204] Perhaps bicarbonate is essential in keratinocyte medium regardless of the pH regulation system used.

3.12.2 Keratinocyte culture using different buffer systems

DMEM was made from DMEM powder and dissolved in distilled water (Sigma Aldrich, 1 L) according to the manufacturers instructions. The mixture was then split into 3 lots of 333 ml. $NaHCO_3$ (1.47×10^{-2} mol) was added to one third of the original DMEM solution to make the regular CO_2 dependent medium. HEPES (8×10^{-3} mol) was added to the second third of the original

DMEM, and finally both $NaHCO_3$ and HEPES (1.47×10^{-2} and 8×10^{-3} mol respectively) were added to the final, third buffer modified Dulbecco's modified Eagle's medium (BMDMEM). These bespoke DMEMs were then used to make bicarbonate buffered, HEPES buffered, and BMDMEM buffered Green's medium as in section 2.1.6.

Keratiocytes were cultured and then seeded into 24 well plates, pre-seeded with i3T3 cells (25,000 keratinocytes per well, 100,000 i3T3's per well, Section 2.1.6). The cells were then allowed to attach overnight. Cell viability was then measured using the resazurin salt assay (Section 2.1.12). One pair of plates was stored in a regular CO_2 gassed incubator. One of the pair of plates was sealed using parafilm to prevent gas exchange. A second pair of plates was also placed in a propagator set up as described earlier (Section 2.4.1). One of the pair of plates was sealed using parafilm to prevent gas exchange. The medium was then replaced with the three bespoke media (1 ml per well), and cultured for seven days. The pH and cell viability were recorded on days 1, 3, and 7 (resazurin salt assay), and then the media changed. Total DNA was measured using picogreen on day 7 (Section 2.1.14).

Three different buffering systems were compared for the culture of keratinocytes in Green's medium. When used in a gassed incubator bicarbonate buffered DMEM is the standard for making Green's medium. pH measurements over the course of the cell culture show an initial increase to nearly a pH of 8 on day 1, then tailing off to 7.25 (Figure 3.30). This was for both gassed and ungassed samples. Hepes buffered medium exhibited a significant drop in pH from 7.4 at day zero, to pH 7 at day one, and continued to decrease to pH 6.8, likewise for both gassed and ungassed samples. The mixed buffered system, BMDMEM, shows the least deviance from pH 7.4, except for the system sup-

plied with CO_2 which dropped to pH 6.8 at day 7. The ungassed BMDMEM system's final pH was 7.4 (Figure 3.30).

When used in a heated propagator with atmospheric gassing only the outcome was similar but more exaggerated. The mixed buffer systems regulated the pH most effectively, maintaining a pH of between 7.5 and 8.5 (Figure 3.31). The bicarbonate systems, sealed and open to atmospheric gas exchange failed to maintain the pH, which increased to around pH 9. The HEPES only buffered systems become more acidic dropping to as low as pH 5.5 on the 7^{th} day.

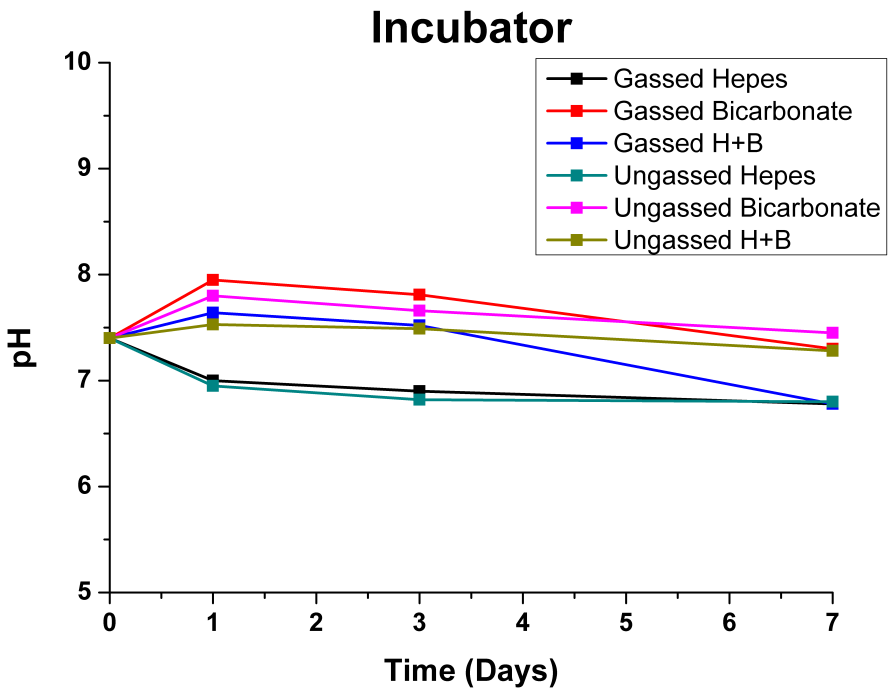

Figure 3.30: pH change of medium used to culture keratinocytes, buffered with HEPES, bicarbonante and both HEPES/bicarbonate over 7 days. The plates were kept inside a CO_2 perfused incubator. Ungassed plates were sealed with parafilm to prevent gas exchange.

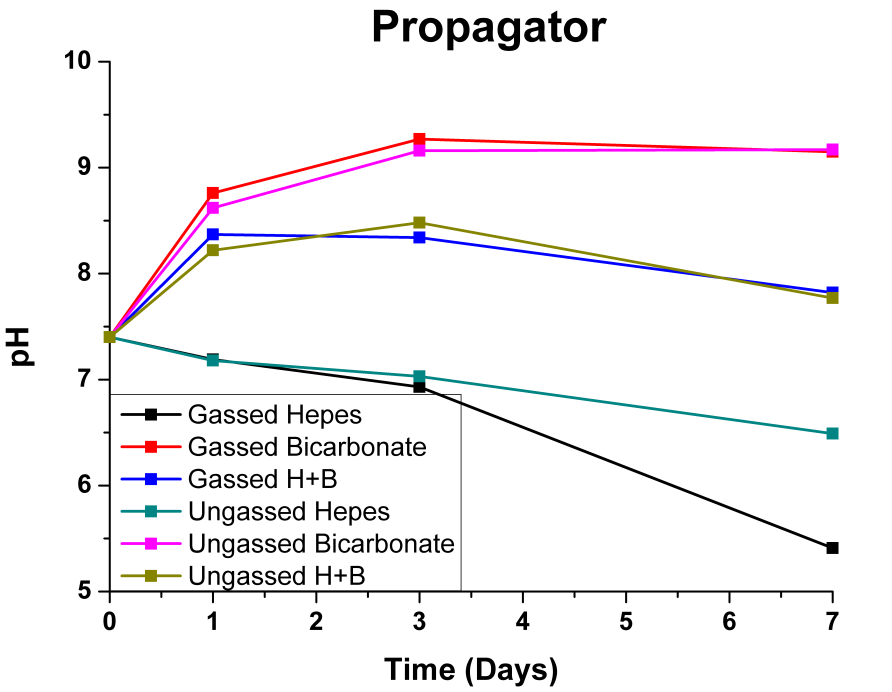

Figure 3.31: pH change of medium used to culture keratinocytes, buffered with HEPES, bicarbonante and both HEPES/bicarbonate over 7 days. The plates were kept inside a non-CO_2 perfused propagator. Ungassed plates were sealed with parafilm to prevent gas exchange.

While there was no significant trend observed in cell viability by resazurin salt assay, the best performing keratinocyte cultures were those using the mixed HEPES/bicarbonate, or just bicarbonate systems (Figures 3.32 and 3.33). This was consistent regardless of supply of CO_2 or incubation method. Cell viability recorded in the propagator was lower overall than in the incubator, particularly for the bicarbonate buffered cultures only. This is most likely due to the lack of sufficient CO_2 for buffering. Cultures buffered by HEPES only also performed poorly.

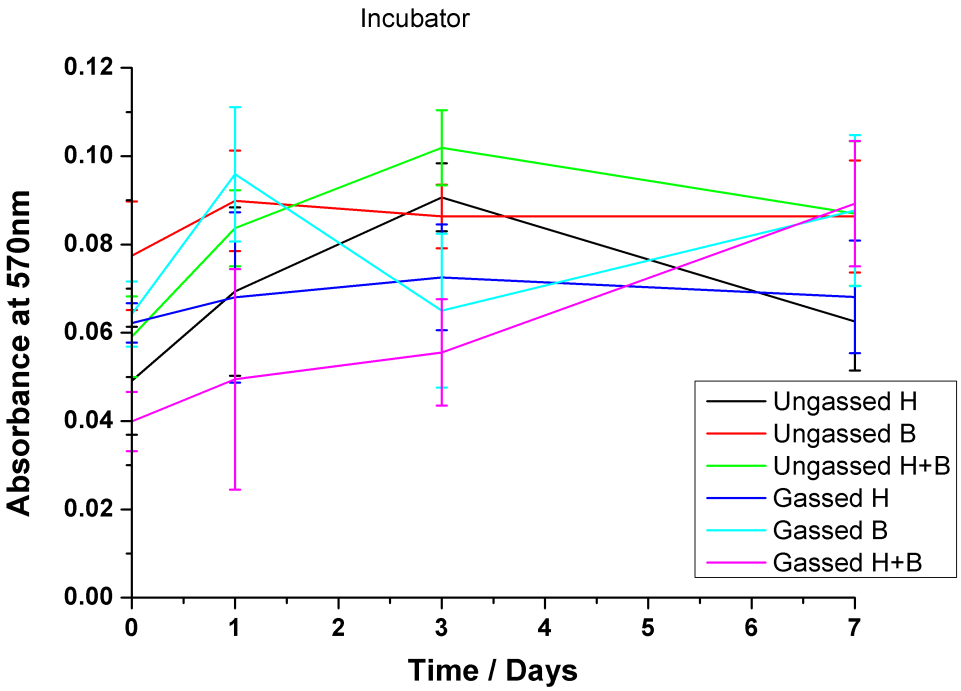

Figure 3.32: Keratinocyte viability in HEPES, bicarbonate, and both HEPES and bicarbonate buffered culture medium, in a CO_2 gassed incubator, over 7 days by resazurin salt assay. Error bars are mean ± SD, n=3.

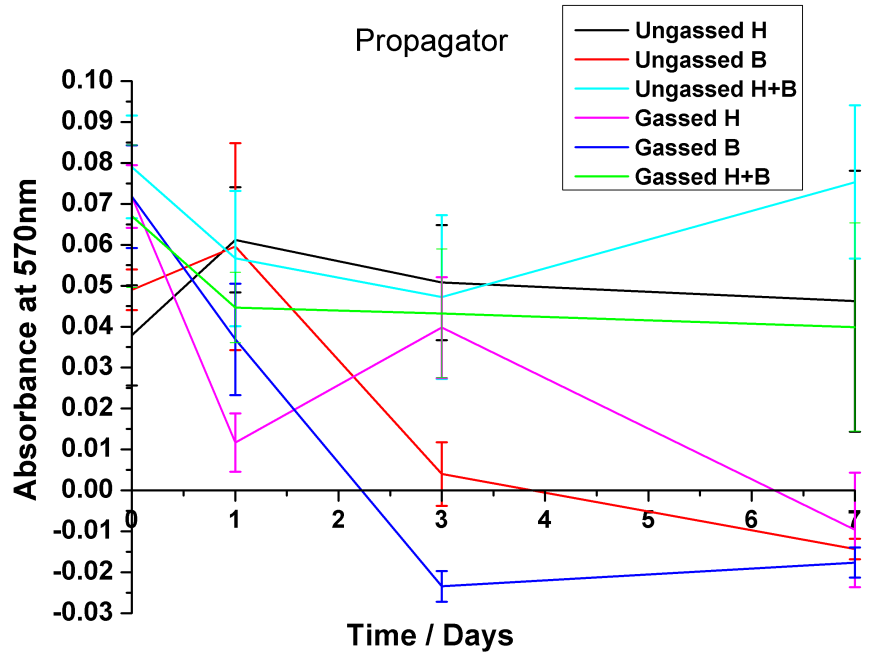

Figure 3.33: Keratinocyte viability in HEPES, bicarbonate and both HEPES and bicarbonate, buffered culture medium, in a propagator with only atmospheric gas exchange, over 7 days, by resazurin salt assay. Error bars are mean±SD, n=3.

The total DNA was measured to check if the observed viabilities were directly connected to the number of cells (Section 2.1.14, Figures 3.34 and 3.35). The HEPES only buffered systems gave significantly less DNA than the other buffer systems, regardless of incubation method or CO_2 supply. There was no significant difference between gassed or ungassed samples for bicarbonate buffered or BMDMEM systems. Cultures kept in an incubator contained more DNA than those in a propagator. Overall, cultures in mixed HEPES/bicarbonate medium, or bicarbonate only systems, performed best.

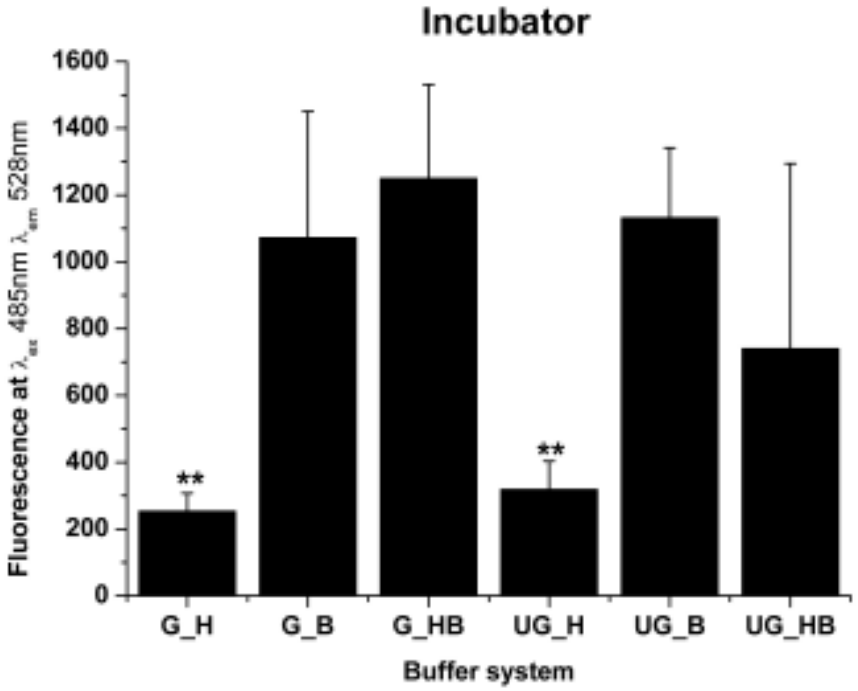

Figure 3.34: Total DNA assessed by Picogreen assay for keratinocytes cultured for 7 days, in gassed (G) and ungassed (U) medium, in an incubator. Medium is buffered using HEPES (H), bicarbonate (B) or both (HB). Error bars are mean±SD, n=3.

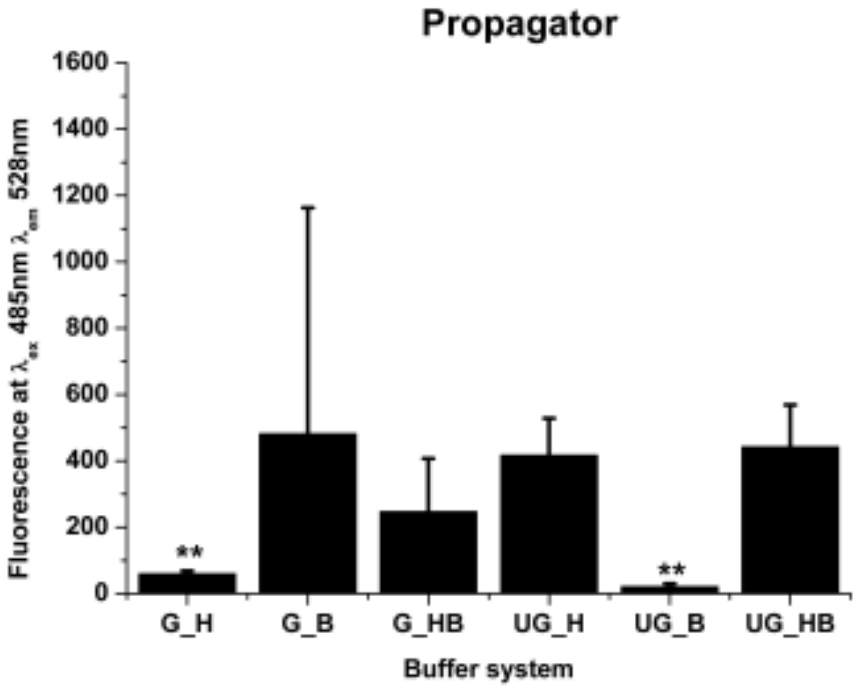

Figure 3.35: Total DNA assessed by Picogreen assay for keratinocytes cultured for 7 days, in gassed (G) and ungassed (U) medium, in an propagator. Medium is buffered using HEPES (H), bicarbonate (B) or both (HB). Error bars are mean±SD, n=3.

3.13 Discussion

Electrospinning is a very popular technique for producing scaffolds for tissue engineering.[58,59,197] While it is relatively simple to produce basic electrospun scaffolds for experimental use, there are considerable challenges post production to make scaffolds of appropriate architectures and mechanical properties. Such properties are intended to encourage cells within the scaffolds to make extracellular proteins to achieve tissue fit for implantation in man. Electrospinning is also complex and multifaceted with many variables.[61]

The aim of this chapter is to describe methods to equip readers to design and characterise scaffolds for a wide range of purposes. In this work is described methodologies to make complex and thicker scaffolds, and to sterilise scaffolds for experimental and clinical use. Imaging cells on the scaffolds and the induction of elastin fibre production by subjecting cells to biaxial distension is also described. Many of the desired features of scaffolds can be achieved post production (such as annealing several layers) and sterilisation. However, these in turn will affect the mechanical properties of scaffolds.

Sterilisation methodologies all tend to change ultimate tensile strength and E to varying extents. A recent study from our group compared gamma irradiation, peracetic acid, and EtOH for their effects as potential sterilising regimes for PLGA scaffolds.[198] The adverse effects of sterilisation techniques can be avoided by producing scaffolds under aseptic conditions. The latter requires the use of a cleanroom. Different users may select different methodologies but all should be aware that current sterilisation methodologies will impact negatively on the properties of the scaffolds.

Culture of cells on scaffolds also affects the scaffold's mechanical properties. Induction of ECM production by subjecting cells on scaffolds to biaxial distension may be used to affect the mechanical properties.

The methodology of spinning one scaffold over another to make a bilayer membrane is easily understood and bilayer scaffolds capable of supporting two diverse populations of cells is illustrated in this chapter by relabelling cells with two vital cell tracker dyes. These were used to illustrate that the bilayer membrane achieved its stated purpose.

Finally, the budget biaxial distension rig described in this study can be used to deliver a range of regimes. Cyclic, linear, and random regimes can be readily programmed and applied. This versatility will allow the system to be utilised for many of the problems faced in tissue engineering such as, cleft palate, pelvic floor, bladder, and skin.

In the tissue engineering literature the use of uniaxial testing systems for culturing cells on scaffolds has been reported.[105] However, at the time of writing the MacNeil group were unaware of any published literature dealing with how soft tissues respond to biaxial distension. This simple approach demonstrates that cells respond to biaxial distension with the production of elastin, a key component of the ECM which gives soft tissues their elastic recoil. This gives a clear indication of how conditioning soft tissues as they grow in the laboratory offers a route to the production of tissues appropriate for implantation. Such as for areas of the body where the native tissues have intrinsic elasticity. This is an area where further development will clearly be merited by the tissue engineering community and bioreactor manufacturers.

3.13.1 Change in surface strain as a balloon inflates

This research was necessary to characterise what kind of multiaxial distension a scaffold on the surface of the balloon would undergo. While these experiments do show that the strain does not change uniformly as a balloon inflates, or between balloons, there is no viable culture system available on the market that can strain a sample multiaxially and maintain the conditions required to keep cells in culture.

Further work is required in creating such a system, and these experiments confirm that there is an effect to investigate. The closest commercial product currently available is the Flexcell® circular foam culture plate.[205] This device does allow for biaxial strain of cells in culture, but is restricted in the range of substrates that can be used, preventing its use for scaffolds and other substrates intended to ultimately be implanted. This restriction is simply due to a lack of any method to fix a scaffold to the flexible membrane used in the Flexcell® system. This means cells can only be cultured on the membranes available for the Flexcell® system.

Balloons were selected as they can expand in 2 dimensions as they are inflated, and they are children's toys (hence non-toxic). Balloons are made from isoprene and have been thoroughly studied for their toxicoloigcal effects. Isoprene monomer has been found to have toxic effects in rats when exposed to >70 ppm for 6 months.[206] Free isoprene monomer in balloon latex should be investigated and quantified. However, as balloons are described as toys and given to children it can be anticipated that free monomer concentrations are kept to an absolute minimum.

3.13.2 Electrospinning onto graphite coated and non-graphite coated air filled balloons

Graphite was selected to coat balloons, as it is well known as a conductor, and because there is evidence that it is non-toxic . Graphite has been used as a " DIY" tattoo ink for many years, and is well known in dentistry for causing oral tattoos (when a young child chews on a pencil and stabs themselves; this can often leave a permanent graphite stain).[207–210] Hence, a balloon coated in graphite could be electrospun onto and the scaffold produced could be potentially used with cells. One interesting side effect of this was that graphite can be used to form conductive tracks, and complex patterned mats of electrospun scaffold created.

However, coating balloons with graphite was abandoned when it was found a small volume of IMS (5ml) inside the balloon could produce a viable collector and produce large, clean scaffolds. The main downside to using air filled balloons to spin on is that a knitting needle is required to stabilised the rotating balloon. The two punctures this creates renders the balloon useless for further experimentation (such as observing the effects of inflation on cell culture). The PBS filled system was developed to keep the balloon intact, and allow it to be inflated when cells are cultured upon its surface.

3.13.3 Elastin production on biaxially distended scaffolds

It is well known that cells are mechanosensitive, and the literature reports a relationship between mechanical stimulation and extracellular matrix production, in particular elastin and collagen for fibroblasts.[107–109] This fact is being exploited by beauty therapists as a nouveau anti-ageing treatment that can "instantly" rejuvenate unhealthy fibroblasts and boost elastin production...[110] There is little literature on mechanically stimulating cells in two dimensions. Most is focused on uniaxial stretching.

The balloon bioreactor mechanically stimulates cells in 2D. Elastin staining, after 2 weeks of mechanically stimulated dynamic culture, reveals how much of a difference there is compared to static culture. Exercise dramatically stimulates extracellular matrix production. Though only elastin deposition was examined in this study, the amount of collagen deposited could also be investigated in future.

3.13.4 Mechanical stimulation of scaffolds using Ebers P3D perfusion chambers

This smaller system, if perfected, should allow for more replicates, especially inside an inexpensive propagator. It is conceivable that rows of these chambers could be set up, all running multiple experiments. This proof of concept design does show the effect of mechanical stimuli on fibroblasts in spite of the uneven

culture obtained. Elastin is produced in the dynamic system, whereas no observable elastin is produced in the static system.

3.13.5 Investigation of buffering systems in order to perform non-CO_2 perfused keratinocyte culture

From the results shown in Figures 3.30 and 3.31 it is clear that using a double buffer system maintains the pH of culture media better than a single buffer system. HEPES buffered systems tend to become relatively acidic, which explains the poor cell viability. Bicarbonate buffer systems tend to be more alkaline overall. The pHs observed in the propagator are quite different to the incubator, this could be due to the lack of a tight CO_2 concentration control system. CO_2 incubators have hardware built in them to tightly manage CO_2 levels.

The viability of cells closely match these pH values, HEPES buffered systems result in poor viabilities, lower than the other systems. This is a good indication that bicarbonate may be essential for keratinocyte viability, aside from its role as a pH buffer. In the incubator the viability of cells cultured with bicarbonate buffered media, without gas exchange, is comparable with the gassed bicarbonate system. This could be due to a poor gas seal on the apparatus used, or perhaps a momentary exposure to air accompanied by media changes being enough to sustain the cells. In the propagator this is not the case, the ungassed bicarbonate system fails, and cell viability drops off. In the context of a bioreactor these findings have interesting implications. A gas tight, sealed system could be used for long periods (1 week) between media changes as long

as a binary HEPES/bicarbonate system is used. The two together maintain the pH more effectively than on their own, and the bicarbonate is essential in keratinocyte culture.

3.14 Summary

Cells respond to mechano-stimulation by up-regulating production of extracellular matrix. This was determined using proof of concept biaxial bioreactors.

The design of these was based on the estimated worst case expansion expected for a cleft palate defect (a doubling in surface area). Children's toy balloons were selected as they are inexpensive, can be sterilised by autoclave, and expand multiaxially when inflated. It was shown that balloons expand anisotropically on inflation, and that the expansion varies between balloons.

Balloons can be used as electrospinning collectors by coating with graphite, adding a small volume of a conducting liquid (such as IMS), or inflating with PBS. Sterile balloons filled with PBS could be aseptically coated with a bilayer scaffold and fibroblasts subsequently cultured on the surface.

A syringe pump was used to administer multiaxial distension. Increased elastin deposition was observed in the exercised system compared to a static control. This research highlighted the need to design a better culture system, with more replicates.

This necessitated investigations into alternative incubation chambers, that could be adapted to include equipment to administer multiaxial distension. It was shown that an inexpensive propagator, or an egg incubator were capable of maintaining the required temperature for cell culture.

A different proof of concept bioreactor, based on Ebers P3D chambers was investigated, to attempt to create a system with increased replicates. Although variability between chambers was high, increased elastin deposition was observed in the exercised system compared to the static system.

Finally, different pH buffer systems were investigated in order to determine if it was feasible to culture keratinocytes in a sealed bioreactor with no gaseous CO_2 exchange. It was shown that bicarbonate is essential in keratinocyte culture medium, regardless of the pH buffer system used. A double buffer system of HEPES and bicarbonate was found to be the most effective pH buffer system, and could be used to create isolated bioreactor systems.

Chapter 4

Development of bilayer and trilayer nanofibrous/ microfibrous scaffolds for regenerative medicine

4.1 Introduction

Many biomaterial scaffolds have been developed for use in tissue engineering, usually for populating with a single cell-type. This chapter demonstrates the production of, bilayer and trilayer, nanofibrous/microfibrous, biodegradable scaffolds suitable for the support, proliferation and yet segregation of different tissues. These scaffolds are intended to be used to separate soft tissue from

bone forming tissue, and keratinocytes from fibroblasts. Essentially, described here is a nanofibre barrier membrane which is permeable to nutrients coupled with attached microfibres (either on one side or both sides) to support the proliferation of different cell types either side, but prevents migration of cells across the barrier. Such membranes would be suitable for guided tissue regeneration in areas where one wishes to support both soft and hard tissues but keep them separated. This chapter describes a sterile bilayer membrane electrospun from PHBV (nanofibres) and PLA or PCL (microfibres), and a trilayer membrane electrospun in layers of PLA, PHBV, then PLA. These membranes are biocompatible, biodegradable, and capable of supporting two different cell populations.

Biomaterial scaffolds are extensively used as carriers for cells, and as 3D scaffolds for the regeneration of new tissue. They are commonly tailored to specific tissue types. Thus, they are designed to have the necessary mechanical properties for the tissue that they are seeking to repair or replace. To be successful post implantation, all scaffolds must be biocompatible to avoid provoking an adverse immune response. The majority of scaffolds (but not all) are designed to be biodegradable, with the intention that cells introduced to the scaffolds will form a new tissue and supporting tissue matrix, replacing the implanted scaffold as it degrades, for a long term and successful repair. Biodegradable devices also negate the necessity for a second surgical operation to remove the implant.[1] There are many polymers that can be used to create a biocompatible, and degradable implant.[2,3]

The ultimate goal of tissue engineering is to be able to regenerate, or replace, diseased or damaged tissues.[120,121] Tissue engineering, based on autologous laboratory expanded cells and scaffolds, is most commonly used but some-

times scaffolds are designed to promote the ingrowth of the surrounding tissue *in vivo*.[122,123] Here the approach is essentially to concentrate on using the patient's own tissues in conjunction with scaffolds to regenerate the areas in need of repair.[124–128]

Thus, in tissue engineering very often the patients own tissues are biopsied, cells expanded in the laboratory and combined with scaffolds, to regenerate tissues for repair of damaged areas. However, there are many conditions when one needs to look at replacing both soft tissues and adjacent hard tissues, or to introduce a scaffold that could promote the intrinsic repair of soft tissues and hard tissues.[129,130]

While it is entirely possible to culture skin cells, or even epithelia, it has been difficult to make more complex tissues. The last decade has seen a growing realisation that the 3D environment of the extracellular matrix in which cells live is far from passive. Not only are the cells receiving signals from the extracellular matrix proteins, but the composition of the matrix, and its stiffness, give major signals which guide the differentiation and performance of cells within the matrix.[211] Thus, bone was originally repaired using metal splints, providing the structural, and mechanical support while allowing the bone to heal.[212] There are now ceramics and osteoinductive materials which can be used to aid bone repair. Tissue guidance membranes have been developed, for example for use in periodontal defects, seeking to achieve guided tissue regeneration.[131–133] The problem of one tissue growing much faster than another, invading and preventing the appropriate expansion of the slower growing tissue needs to be considered.

As previously described, one area where tissues require segregation is in the treatment of cleft palate. The current standard treatment is protracted, involving many stages. While soft tissue defects can be readily repaired within a few months, defects of the hard tissue of the alveolar ridge (which bears teeth) and the hard palate, are much more challenging.

Bone grafts to fill the hard palate defect are currently not used as an option, as they have actually been found to lead to distortion of the maxilla, and the results can be worse than no surgery.[155,168] Bone grafts appear to be satisfactory, immediately after implantation, but then the bone cells fuse and this tissue does not grow at the rate of the childs head, causing major facial disfigurement. The subsequent complications and distortions to the maxilla are unacceptable, and explain why the hard tissues of the palate are currently mostly left untreated, and an obturator used.

The problem of treating hard tissue defects in the cleft palate is twofold. Firstly, hard tissues grow at a rate far slower than soft tissue. An implant must account for this, and prevent the invasion of the much faster growing soft tissues into regions where the hard tissues are desired. The implant must also allow for the flow of nutrients in order to allow the separated tissues to proliferate. Secondly, the implant must be compatible with the growth of the patient. The area of a cleft defect approximately doubles in volume from birth to the age of 5, and this must be taken into consideration in developing materials and procedures for treatment of hard palate defects.[169,170] Also for the reasons discussed previously (undesirable post implantation operations), the implant must also be biocompatible and biodegradable.

An ideal solution would be an approach that could treat both soft and hard palate defects early in the childs life, requiring very minimal follow up. To achieve an early stage repair for soft and hard palate, the biomaterial to be introduced must be able to cope with the dramatic growth of the childs palate up to the age of five. For bone to form, it is highly likely that the bone forming tissue or cells will need to be introduced into the defect. One common source for similar surgery are bone chips from the femoral head. It would be quite possible to culture bone forming cells (bone marrow mesenchymal stem cells for example) on a scaffold for use in the hard palate. However, the introduction of soft tissue, such as tissue engineered buccal mucosa, or the ingrowth of soft tissues from the periphery of the defect, could threaten the development of hard palate bony tissues. This is due to the fact that soft tissues will grow throughout such a scaffold, almost certainly forming a fibrotic scar. Scar tissue can contract extensively, distorting the growth of the palate. Hence, one requirement in developing materials for treatment of soft and hard palate defects is a biocompatible and resorbable tissue segregating membrane, which should separate, and yet still allow the proliferation of soft tissues on one side, and hard tissues on the other, without allowing ingrowth of soft tissues into the hard palate area.

A second area where segregation is desirable, is the tissue engineering of skin for burns or diabetic ulcer repair. A biopsy of healthy skin is taken, cultured, and expanded in the laboratory on a scaffold ready for implantation back on the patient. Normally in the laboratory, keratinocytes are cultured under long-established conditions, using murine fibroblast feeder cells and media with bovine foetal calf serum.[213] However, for use in the clinic, it would be preferable. The MacNeil group has had some success previously, using autologous fibroblast feeder cells (instead of murine cells), and omitting bovine serum

in the initial expansion of keratinocytes.[214,215] Building on this, a scaffold designed to provide a synthetic basement membrane would be advantageous, as it would give the cells a framework around which to start producing the required extracellular matrix. If the scaffold was designed to be porous, fibroblasts cultured on the lower surface could act as a feeder layer, and culture may be achieved without the need for animal products.

With respect to choice of scaffolds, PHBV was selected for use as a barrier membrane due to its slow degradation time, and easy synthesis through phosphate starving the bacteria *Alcaligene eutrophus*.[25,28,29] Toxicological assessment of the polymer *in vitro* and *in vivo* has shown no negative effects or abnormalities when tested with cultured cells or in animal experiments, and it has been patented for use as bioresorbable sutures.[23,30,31] PLA is well known as a biodegradable biomaterial with good biocompatibility.[2,32–36] As previously discussed, it has been used for several years in the MacNeil group and a knowledge base has been established, making it a good candidate for further investigation.[15,37] PCL was included in this study as it has been successfully used as a scaffold for production of bone, as extensively reviewed by Woodruff and Hutmacher.[216–220] The MacNeil group has experience of culturing autologous buccal mucosa based on de-epidermised acellular human dermis, and of taking this to the clinic for replacing scarred tissue of the urethra.[129,130,221] The MacNeil group also has previously developed synthetic electrospun scaffolds for soft tissue reconstruction.[15,198]

Against this background, our approach to designing a tissue barrier membrane is to harness electrospinning to produce: bilayer and trilayer, nanofibrous/microfibrous, scaffolds suitable for separating, yet promoting, independent proliferation of two distinct tissue types. Such tissues could soft tissue on

one side, and bone tissue on the other side. These scaffolds are designed for culturing a range of tissues under different situations. Thus, this chapter describes a bilayer structure made to segregate bone and soft tissues. A trilayer structure intended to support soft tissue growth either side is also described. For example, two populations of cells, such as epithelial and stromal cells as shown here, require an open, porous network (microfibres) to grow into, but still require segregation (nanofibres). These scaffolds are also designed to be capable of plastic deformation so that they can grow with the growth of the child's skull.[222] These scaffolds are the first step towards developing a synthetic solution to tissue separation.

Once monolayers of scaffolds with differing morphologies had been created, their compatibility with cells shown, and methods for turning them into cell impermeable barriers developed, the project turned to utilising these structures to form more complex scaffold architectures. Unfortunately, most clinical applications are multifaceted and require several, and often different solutions to tackle various aspects of them. Taking cleft palate as the primary example again, it is not enough to simply have a barrier membrane. Tissues must be encouraged to proliferated either side of it so that regeneration may occur. A nanofibrous scaffold that only acted as a cell barrier would be poor for this end. A microfibrous, cell friendly scaffold, would fill this requirement by providing a structure for cells to grow into and fill. This section of the PhD thus focused on combining different scaffold structures in order to create composite structures, that could be used for different purposes, and to check if these qualities were maintained.

4.2 Methods

4.2.1 Electrospinning of a PLA/PHBV composite bilayer scaffold

The obvious place to start was to create a simple two layer structure, incorporating cell permeable and cell impermeable layers (Figure 4.1). Electrospun nanofibrous PHBV was selected for the barrier layer, due to its long degradation time and ease of use when spun. PLA and PCL were selected for the microfibrous layers due to the previous experiences of the group and user base, demonstrating them to be candidates that showed good cell viability and compatibility.

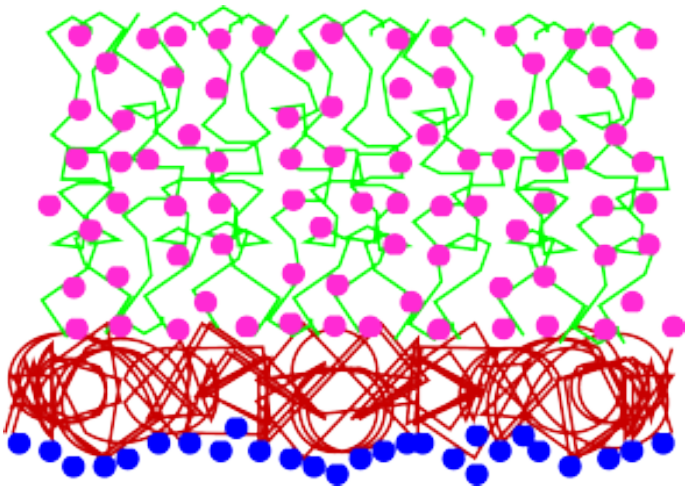

Figure 4.1: Schematic of proposed bilayer. Nanofibres (red) with a layer of microfibres (green) on top. The nanofibres will act as a cell barrier restricting cell A (blue) to one face and cell B (pink) to the opposite face. The microfibres act as a cell permeable region, encouraging proliferation on the membrane (cell B, pink).

The method used to create this bilayer was an additive approach. First a PHBV layer was spun (10 wt%, Section 2.2.5). On completion, PLA or PCL

was immediately spun on top (10 wt%, Section 2.2.2), to create a two layer structure.

On handling this scaffold, there was a noticeable difference between the opposing faces. One side was dull and velutinous. This gossamer face was much like the respective flocculant PLA and PCL monolayers. The opposing face was smooth and glossy. Samples of the scaffold were processed for SEM and tensile testing (Sections 2.1.2 and 2.1.3).

4.2.2 Cell migration into scaffolds at 7 days

Aseptic electrospun scaffold squares (1.5 cm × 1.5 cm) were fitted into Scaffdex Cellcrowns24 (Tampere, Finland), in a laminar flow hood, and placed into a 24 well plate. TCP, and PLA-PHBV, PCL-PHBV bilayers were used. The PHBV face of the scaffold was seeded, with 50,000 hESMPs, and left for 24 hours to allow attachment (Section 2.1.5). The cell crown was then turned over, and the opposite face (PCL or PLA) seeded with 50,000 fibroblasts, and left for 7 days, media was replaced after 3 days (αMEM, 37°C, 5% CO_2, Figure 4.2, Section 2.1.4).

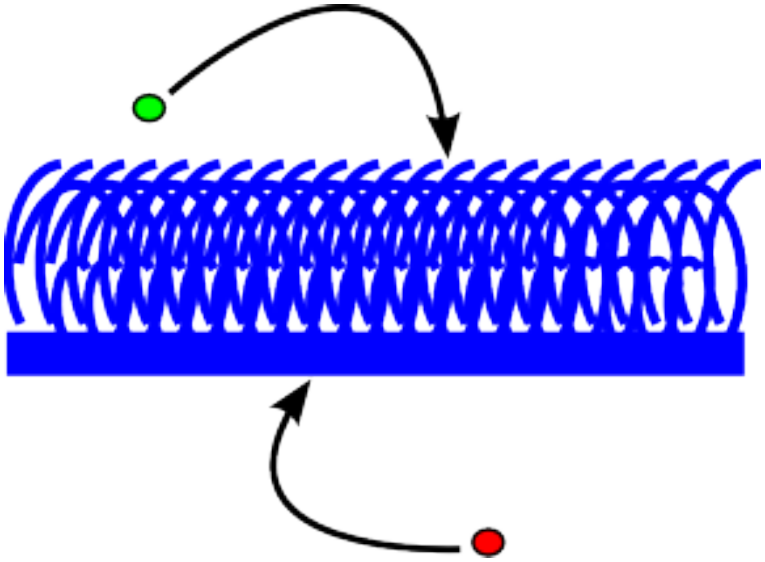

Figure 4.2: Diagram of how cells were seeded onto bilayer membranes. One cell type labelled with red cell tracker is placed on one face of the bilayer membrane. A second cell type labelled with green cell tracker is placed on the opposing side. The construct is then cultured for 7 days.

CellTracker red (CMTPX) or green (CMFDA) were applied to the hESMPs and fibroblasts respectively, prior to seeding as per Section 2.1.8. These bilayers of PLA/PCL and PHBV were assessed for their ability to maintain cell segregation.

4.2.3 Sequential electrospinning of a PLA/PHBV/PLA composite trilayer scaffold

Once a bilayer had been constructed and shown to work, the next logical step was to create a trilayer (Figure 4.3). This scaffold should have the barrier function inbuilt, but support cell proliferation on either side.

A bilayer membrane was electrospun (Section 4.2.1). Immediately after this, the membrane was peeled off from its aluminium foil backing, turned over

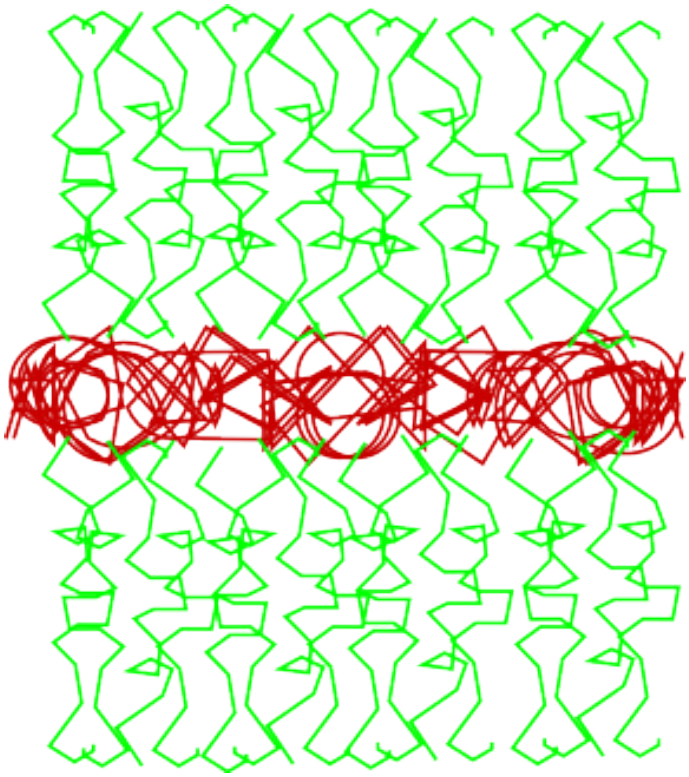

Figure 4.3: Schematic of proposed trilayer. Nanofibres (red) with a layer of microfibres (green) top and bottom. The nanofibres will act as a cell barrier and the microfibres as a cell friendly region, encouraging proliferation on both sides of the membrane.

(PHBV face now facing up), and fixed back on the electrospinning drum using two 1 cm^2 masking tape sections. A further layer of PLA was then electrospun on top creating a PLA-PHBV-PLA sandwich (Section 2.2.2). The resulting scaffold felt sturdier than PLA microfibres alone.

4.2.4 Culture of keratinocytes and fibroblasts on the PLA-PHBV-PLA trilayer

Due to the incorporation of cell-friendly microfibres on both sides of this scaffold, it lends itself for the development of soft, delicate tissues either side. One

example of this is skin, or at least the creation of an alternative 3D skin model. The current gold standard is de-epithelised dermis (DED), reconstituted with fibroblasts and keratinocytes. However, DED is limited in supply because it relies on use of donor tissue. There is also the risk of disease transmission for this reason.

PLA-PHBV-PLA trilayers and PLA monolayers (2 cm $\times$ 2 cm) were sterilised in peracetic acid (0.1% v/v in distilled water) for 3 hours and washed three times in PBS (1 ml). The scaffolds were then placed in 6-well plates. Stainless steel rings with an internal diameter of 1 cm were placed on top of the scaffolds. Human dermal fibroblasts (1×10^5 cells), pre-labelled with CellTracker green (Sections 2.1.4 & 2.1.8), were then seeded inside the steel rings and the medium topped up to 3 ml. The scaffolds were incubated for 2 days (37°C, 5% v/v CO_2). Following this, the scaffold was turned over. Human keratinocytes (3×10^5 cells per scaffold, Section 2.1.6), pre-labelled with CellTracker red (Section 2.1.8), were seeded on the reverse side of the scaffold. The steel rings were then removed on the 4^{th} day of incubation. On the 5^{th} day the constructs were raised to an air liquid interface on stainless steel grids, and incubated for 7 days. Culture medium was replenished twice a week. Cell viability using resazurin was assessed (Section 2.1.12). Samples were then fixed by incubating at 37°C, in formaldehyde (3.7% v/v in PBS), and then labelled with DAPI (Section 2.1.9).

Fluorescence images were taken following the culture period (365 nm λ_{ex} 460 nm λ_{em} for DAPI, 570 nm λ_{ex} 620 nm λ_{em} for CellTracker red, and 480 nm λ_{ex} 533 nm λ_{em} for CellTracker green).

4.3 Results

Figures 4.4 and 4.5 show the fibre diameters that were obtained when a 10 wt% polymer solution was used. Electrospinning 10 wt% PHBV in DCM/MeOH produced fibres of 700 nm in diameter. In contrast, a 10 wt% concentration of PLA and PCL in DCM produced 2.5 μm and 4 μm diameter microfibres respectively.

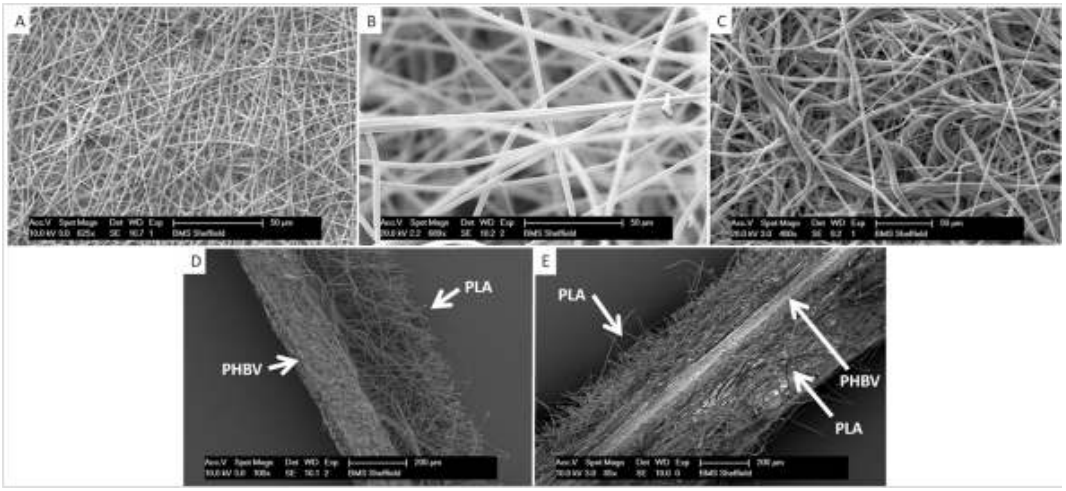

Figure 4.4: Scanning electron micrographs (SEMs) of electrospun scaffolds A. PHBV. B. PLA. C. PCL. D. Representative cross-section of PHBVPLA. The PHBV region on the left is dense, while the PLA region has a more open structure. E. Representative cross section of a trilayer of PLAPHBVPLA

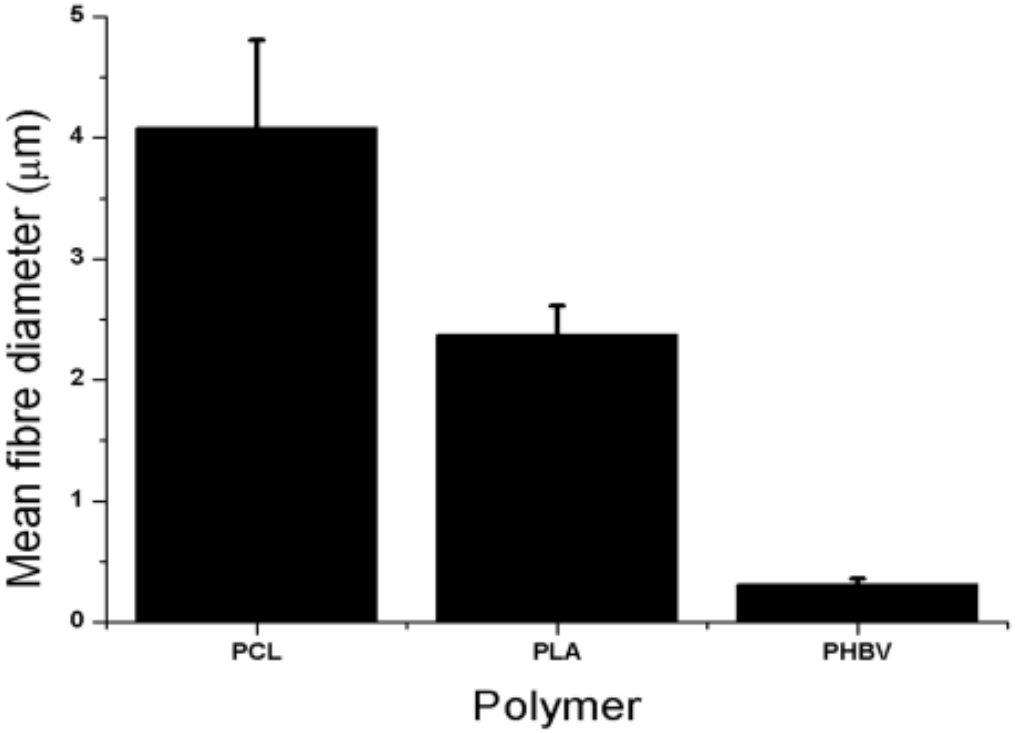

Figure 4.5: Mean fibre diameters for PCL, PLA and PHBV of 4 μm, 2.5 μm and 700 nm respectively. Values are taken from measurement of SEM images, presented as average±standard error of the mean, n=5.

Table 4.1 shows porosity and mechanical data for the bulk polymer and electrospun scaffolds. Porosity measurements show a significant difference between the microfibrous scaffolds of PLA and PCL, compared to the nanofibrous PHBV, with the microfibrous scaffolds being around 20% more porous. The E of the bulk polymer is higher than the measured E of the scaffolds in all cases. The highest E was recorded for the PLA-PHBV-PLA trilayer and is approximately 33% more than the next nearest (PHBV). Scaffolds containing PCL had E values of around 50% of those scaffolds not containing PCL.

Scaffold	Bulk E / GPa	Scaffold E / GPa	Bulk density / $g.ml^{-1}$	Scaffold density / $g.ml^{-1}$	Porosity / %
PLA	3.6	0.012 ± 0.001	1.25	0.18	85 ± 0.8
PCL	0.3[223]	0.008 ± 0.003	1.145	0.25	78 ± 0.8
PHBV	0.5	0.015 ± 0.002	1.25	0.50	60 ± 1
PHBV-PLA	N/A	0.014 ± 0.008	N/A	0.24	N/A
PHBV-PCL	N/A	0.004 ± 6×10^{-5}	N/A	0.30	N/A
PLA-PHBV-PLA	N/A	0.0021 ± 0.001	N/A	0.21	N/A

Table 4.1: Mechanical properties and porosity of scaffolds and their bulk polymers. Bulk polymer and porosity data is not available for bilayer and trilayer structures as these are composite scaffolds. Porosity measurements are the ratio of scaffold density to bulk density, subtracted from 1, and turned into a percent. Bulk polymer E data is from the respective manufacturers where available or referenced. Values are the mean±SEM, n=3

4.3.1 Cell viability on scaffolds at 7 days

Cell viability on scaffolds was demonstrated using a resazurin salt assay. Figures 4.6 − 4.11 shows cell viability on the scaffolds after 7 days of culture compared to the same cells cultured on TCP. With respect to the attachment and expansion of fibroblasts all scaffolds compared reasonably well to TCP. Cells on PCL performed significantly worse than on TCP, but only by approximately 30%, while cells on PHBV-PCL did significantly better (by approximately 20%). Scaffolds were less supportive of hESMPs attachment and expansion. hESMPs performance on all scaffolds being only approximately 50% as good as on TCP (Figures 4.6 − 4.11).

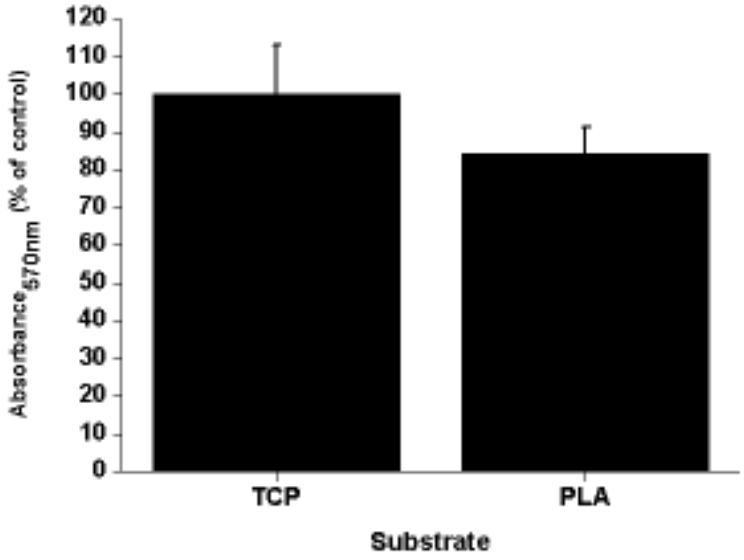

Figure 4.6: Cell viability of fibroblasts measured by resazurin salt assay on TCP and a monolayer of PLA. Values are absorbance at 570 nm as a percentage of control (TCP). Error bars are mean±SD, n=3.

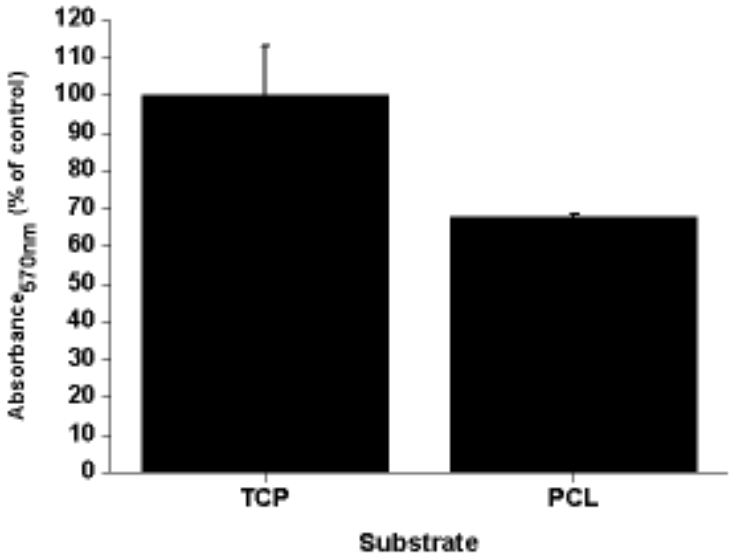

Figure 4.7: Cell viability of fibroblasts measured by resazurin salt assay on TCP and a monolayer of PCL. Values are absorbance at 570 nm as a percentage of control (TCP). Error bars are mean±SD, n=3.

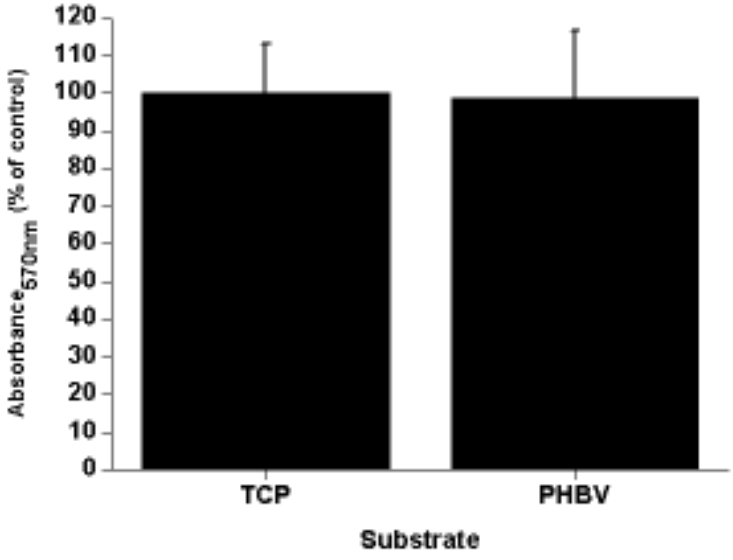

Figure 4.8: Cell viability of fibroblasts measured by resazurin salt assay on TCP and a monolayer of PHBV. Values are absorbance at 570 nm as a percentage of control (TCP). Error bars are mean±SD, n=3.

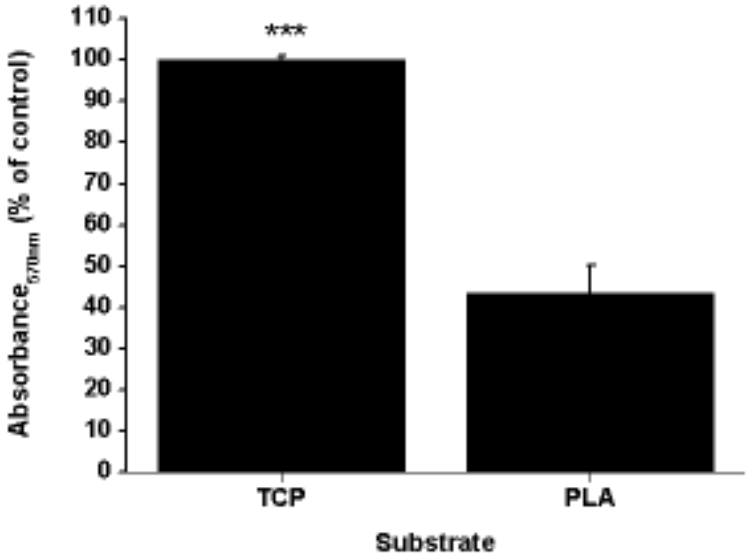

Figure 4.9: Cell viability of hESMPs measured by resazurin salt assay on TCP and a monolayer of PLA. Values are absorbance at 570 nm as a percentage of control (TCP). Error bars are mean±SD, n=3.

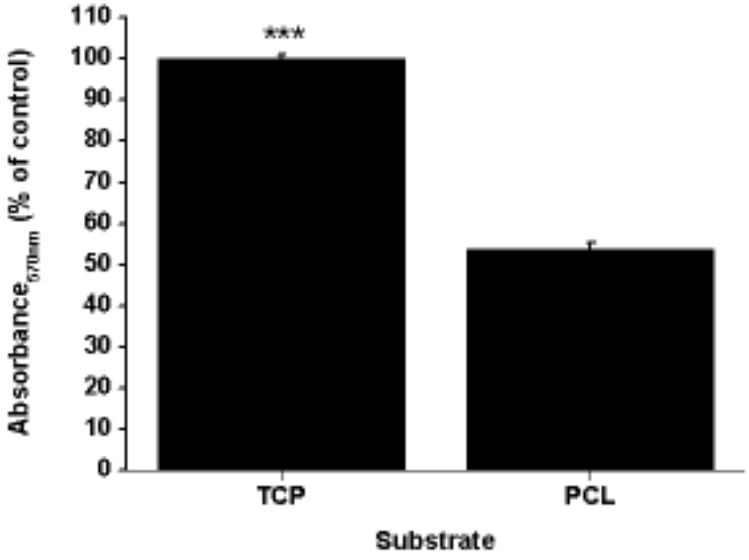

Figure 4.10: Cell viability of hESMPs measured by resazurin salt assay on TCP and a monolayer of PCL. Values are absorbance at 570 nm as a percentage of control (TCP). Error bars are mean±SD, n=3.

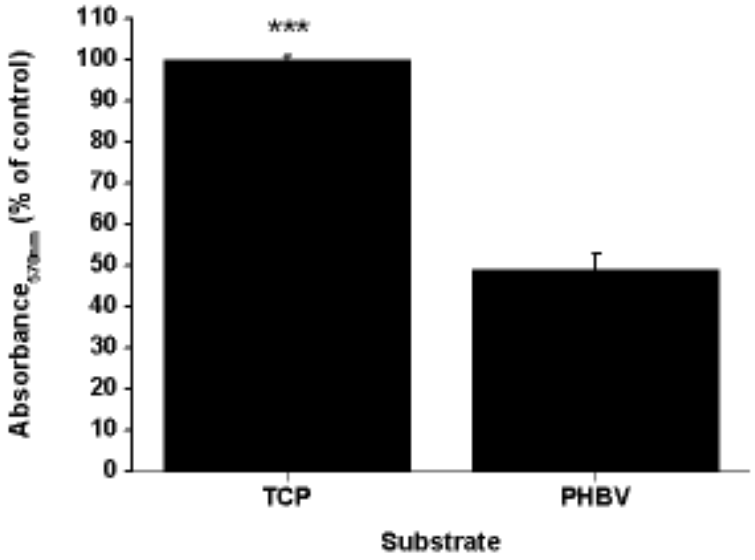

Figure 4.11: Cell viability of hESMPs measured by resazurin salt assay on TCP and a monolayer of PHBV. Values are absorbance at 570 nm as a percentage of control (TCP). Error bars are mean±SD, n=3.

Figure 4.12 shows fluorescent images of the cells on TCP (Figure 4.12A) and on scaffolds (Figure 4.12B-F). When seeded together, there is clear mixing of the cells on TCP, PLA and PCL. On these PLA and PCL scaffolds it is evident that fibroblasts and hESMPs have migrated through the scaffolds, as each face of the scaffold shows both cell types. With PHBV, however, there is a clear segregation of cell types. Even after 7 days of culture of fibroblasts on one face and culture of hESMPs on the opposite face of the PHBV, the cells remain segregated (Figure 4.12D for fibroblasts, and Figure 4.12E for hESMPs). Figure 4.12F is a cross section of the PHBV with the cells on their respective surfaces. As there was no mixing of the red and green fluorescently labelled cells it appears that PHBV has been successful at both supporting cell attachment, and keeping the two cell types segregated for at least 7 days.

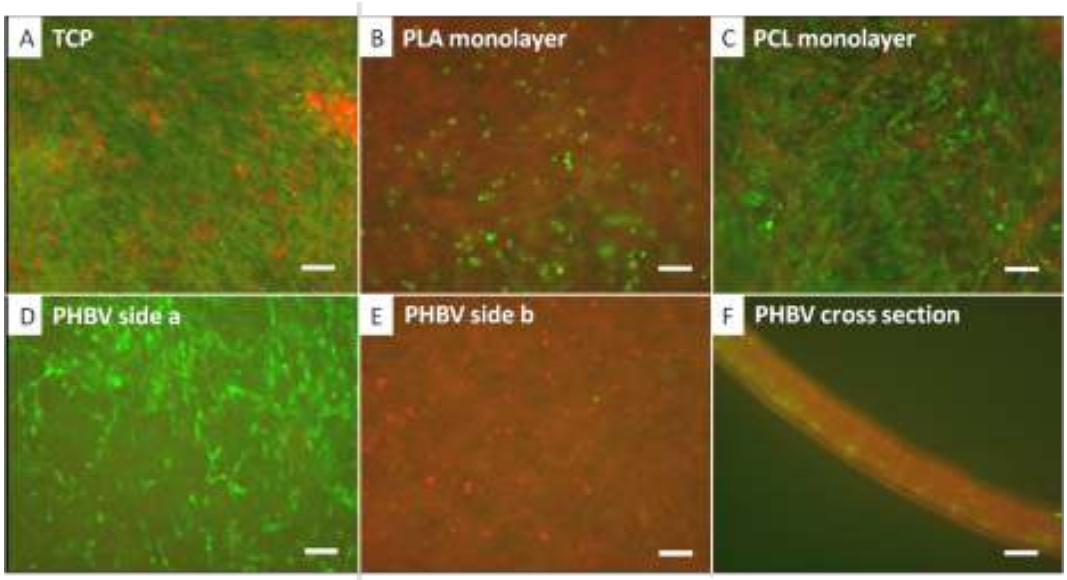

Figure 4.12: Co-culture of CellTracker labelled fibroblasts (green) and hESMPs (red) on a range of scaffolds. In A hESMPs were seeded on day 1 (red) followed by an equal ratio of fibroblasts on day 2 (green), and cultured for 7 days on TCP. In BF hESMPs were seeded on one side of the scaffold on day 1, and then fibroblasts on the other side on day 2 and these were then cultured for a further 7 days. The scaffolds used were PLA in B, PCL in C and PHBV in D, E and F. In A, B and C there is a clear mixture of red and green cells. In D and E however, cells remain segregated. All fibroblasts (green) are shown on the surface shown in D and all hESMPs (red) are seen on the opposite side (E). F shows a cross section of the PHBV scaffold with clear separation of the hESMPs and fibroblasts. Scale bars are equal to 0.1 mm.

PHBV-PLA and PHBV-PCL bilayers were assessed for their ability to maintain cell segregation. Figures 4.13 A and D show the fibroblasts seeded on the PLA and PCL faces of the bilayers respectively. It is clear that hESMPs have not migrated through to this face. Likewise, Figure 4.13 B and E show the hESMPs seeded onto the PHBV faces of each bilayer respectively. Figure 4.13 C and F show cross sections through both bilayers, with both the hESMPs and fibroblasts contained on their respective side. The bone forming potential of hESMPs is demonstrated in Figure 4.14. Continuous culture under appropriate conditions resulted in the cells differentiating into bone forming osteoblasts (increased alkaline phosphatase activity with time), and depositing calcium containing bone mineral (alizarin red staining).

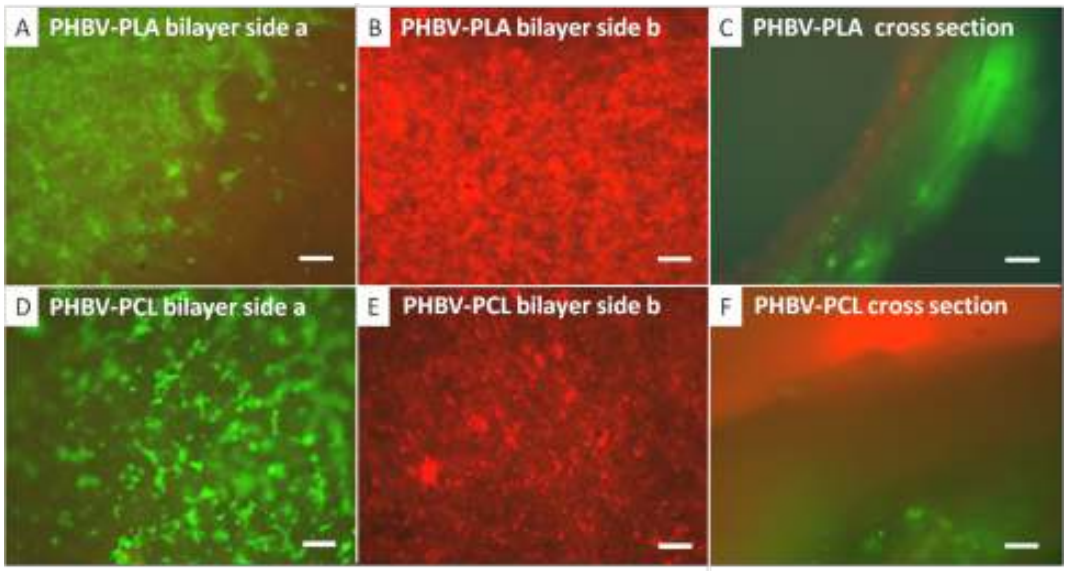

Figure 4.13: Co-culture of CellTracker labelled fibroblasts (green) and hESMPs (red) on bilayer membranes of either PHBVPLA or PHBVPCL. hESMPs were seeded on day 1 (red) onto the PHBV face of each bilayer. Fibroblasts were seeded on either the PLA or PCL face of the bilayer on day 2 (green) and then cultured for a further 7 days. In A, fibroblasts (green), are confined to the PLA face after 7 days with no sign of hESMPs (red). On the opposite face (B, PHBV), hESMPs (red) are also present once again with no fibroblasts. A cross section of the PHBVPLA membrane is shown in C showing each cell type on its respective side after 7 days of culture. In D and E, fibroblasts (green) and hESMPs (red) are shown on the PCL and PHBV faces respectively, and there is no mixing across these faces. F shows a cross section of the PHBVPCL membrane, and clearly shows each cell type still confined to their respective faces after 7 days of culture. All scale bars are equal to 0.1 mm.

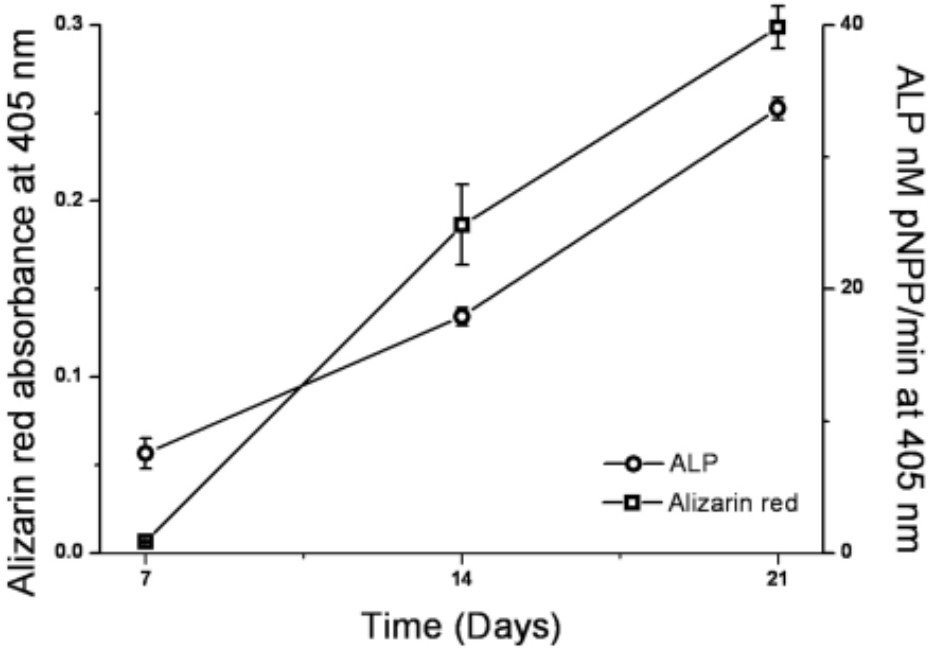

Figure 4.14: Alkaline phosphatase activity and quantification of alizarin red staining of hESMPs after 7, 14 and 21 days on TCP. Increasing alkaline phosphatase activity indicates cell differentiation towards osteoblastic (bone forming) cells and increasing alizarin red indicates increased calcium (present in bone mineral) deposition. Values are mean ± SEM, n=3.

The retained barrier properties of the PLA-PHBV-PLA trilayer scaffold are shown by the fluorescent images in Figure 4.15. DAPI staining of the cell nuclei (blue) has been added to aid with visualising the cell nuclei. There are nuclei on either side of the scaffold, showing that both fibroblasts and keratinocytes adhere and proliferate. The face seeded with fibroblasts (green) shows no sign of keratinocytes (red) having penetrated through the scaffold. Likewise on the keratinocyte seeded face, there are no fibroblasts present. The final image shows a cross section, with both sides well populated by cells, but the fibroblasts and keratinocytes are confined to their respective sides. The recorded cell viability on the PLA-PHBV-PLA trilayer scaffold is good (around 50% compared to those on TCP). This is comparable to the bilayer scaffolds.

Figure 4.15: Co-culture of CellTracker labelled fibroblasts (green) and keratinocyte (red) on trilayer membranes of PLAPHBVPLA. Fibroblasts were seeded on day 1 (green) onto one face of each trilayer. Keratinocytes were seeded on the opposite face of the trilayer on day 4 (green) and then cultured for a further 7 days. In A, fibroblasts (green) are confined to the PLA face after 7 days with no sign of keratinocytes (red). On the opposite face, keratinocytes (red) are present once again without fibroblasts. A cross section of the PLAPHBVPLA membrane is shown in C showing each cell type on its respective side after 7 days of culture. Cell nuclei have been stained using DAPI (blue). All scale bars are equal to 0.1 mm.

Decreasing the amount of the nanofibrous scaffold to 20% and 5% of the original weight does not appear to affect the barrier qualities of these trilayers, with segregation of fibroblasts and keratinocytes maintained after 7 weeks (Figure 4.16).

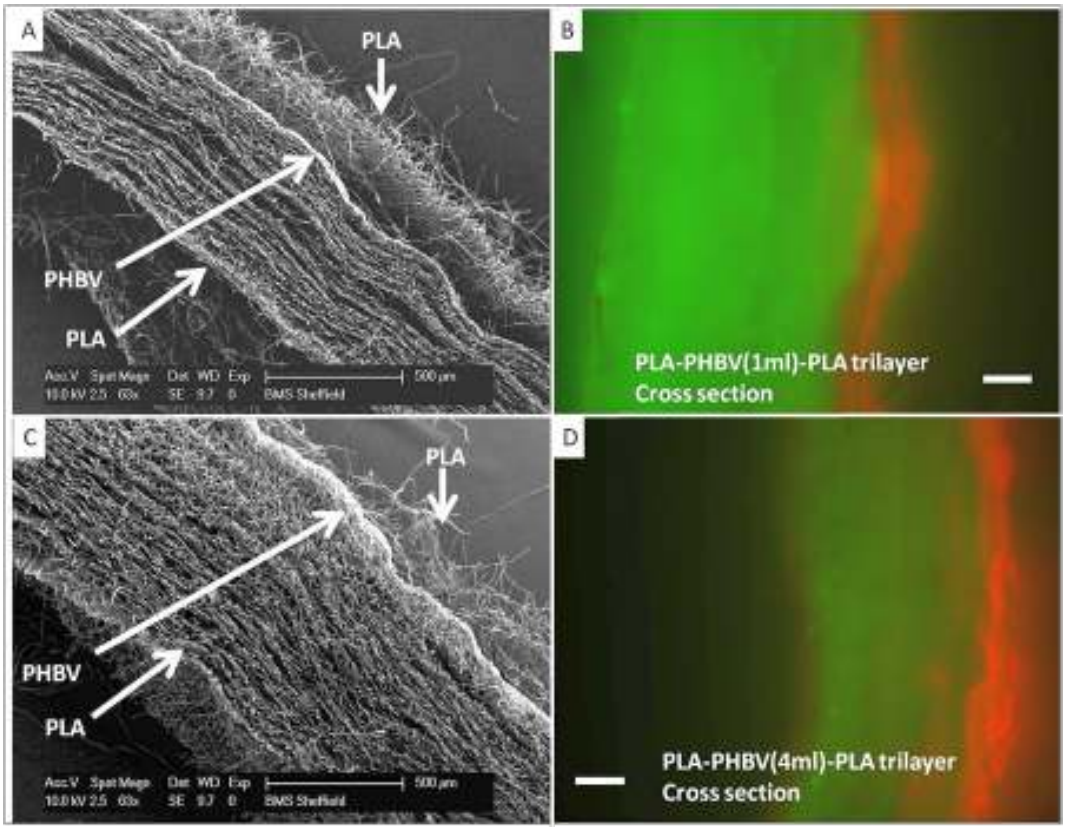

Figure 4.16: SEM and fluorescence microscopy of PLAPHBVPLA trilayers with reduced PHBV layer thickness. Panels A and C shows SEM cross sections of trilayers made using 1 ml and 4 ml of PHBV respectively (5% and 25% of original volume used in Figures 4.12, fig:BT5 and fig:BT7. Microfibrous PLA is present on the top and bottom of each scaffold, with a dense nanofibrous PHBV slither through the middle of each. Panels B and D show fluorescence microscopy of cross sections with fibroblasts (green) cultured on one face, and keratinocytes (red) cultured on the opposite face, with separation maintained after a week (demonstrated by no 'bleed through" of the colours to opposite faces).

4.4 Long term migration of cells into scaffolds

Section 4.3.1 clearly demonstrates that nanofibrous PHBV scaffold are capable of segregating two different cells type for up to 7 days. While this is promising, there are few tissue engineering problems that can be repaired in that time frame. *In vitro* the scaffold must maintain segregation over a long period of time. Henceit is important to show that such nanofibrous scaffolds are capable of segregating cells for a greater period of time. In the 6 week experiment, the underside of the PHBV scaffold was observed over 6 weeks to see if fibroblasts managed to squeeze through. A second nanofibrous scaffold, PCL (5 wt% in DCM) was selected to see if it also had barrier qualities. Cells seeded on TCP were also observed and counted in order to follow their proliferation.

Aseptic electrospun PHBV and nano-fibrous PCL scaffold squares (1.5 cm $\times$ 1.5 cm) were fitted into Scaffdex CellCrowns^{TM}24 (Tampere, Finland), in a laminar flow hood, and placed into a 24 well plate. The interior of each CellCrown was seeded (see Section 2.1.4) with 10,000 or 100,000 fibroblasts (prelabelled with CellTracker green, Section 2.1.8) in DMEM, and incubated at 37°C for 24 hours to allow attachment (Sections 2.1.4 & 2.1.8). Experiments were performed in triplicate with fibroblasts from 3 different patients (36 samples in total). The samples were then incubated and imaged once a week, for 6 weeks (Section 2.1.8). Images collected on an Axon ImageExpress fluorescence microscope were analysed using ImageJ software, in order to count the number of cells visible on the underside of each scaffold (hence those that had migrated through). The results are plotted in Figure 4.17.

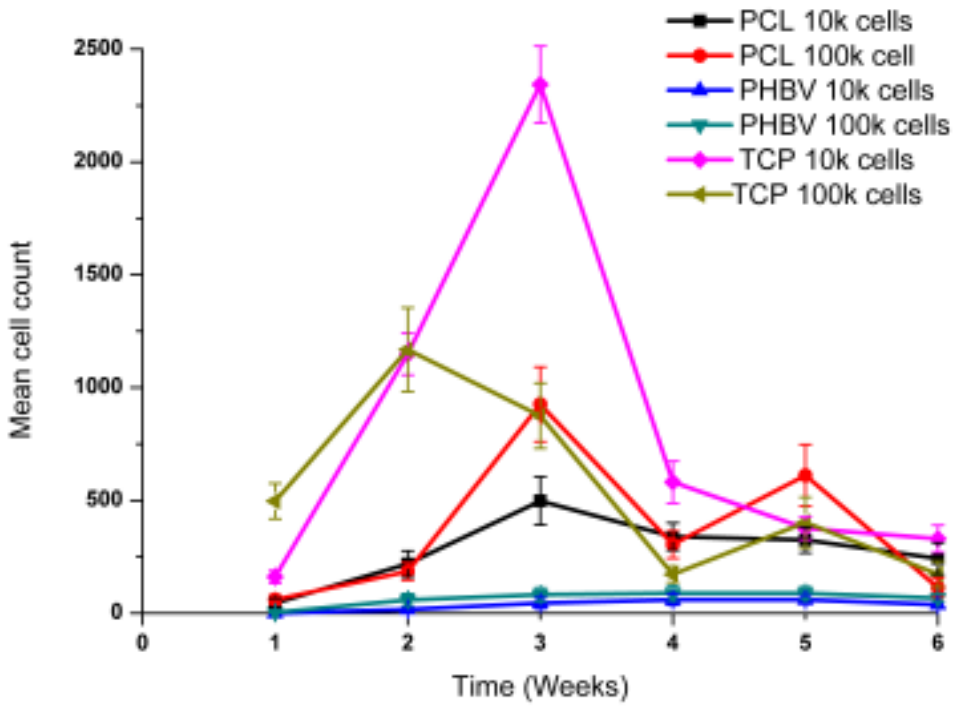

Figure 4.17: Number of cells counted on distal side of membrane during 6 week culture, compared to a layer of cells on TCP. Two initial cell concentrations are plotted for both 10,000 and 100,000 cells. The least number of cells was consistently observed on the bottom of the PHBV scaffold. Values are cell counts expressed as mean ±SEM, n=3.

4.5 Concurrent electrospinning of a PLA/ PHBV-PLA/ PLA composite trilayer scaffold

The trilayer constructed as described in Section 4.2.3 functioned as a barrier to cells and encouraged cell proliferation either side. This scaffold would be suitable as a solution to clinical applications requiring tissue segregation, but it's not perfect. The methodology of producing this led to an unbearable 7.5 hours of electrospinning to produce one sheet. Also it was noticed that while a

conscious effort was required to peel the layers apart, the third and final PLA layer was less well adhered. To tackle these problems, a concurrent spinning method was proposed in order to have a nanofibrous barrier, perforated by microfibres right the way through. This was intended to stitch the three layers together (Figure 4.18).

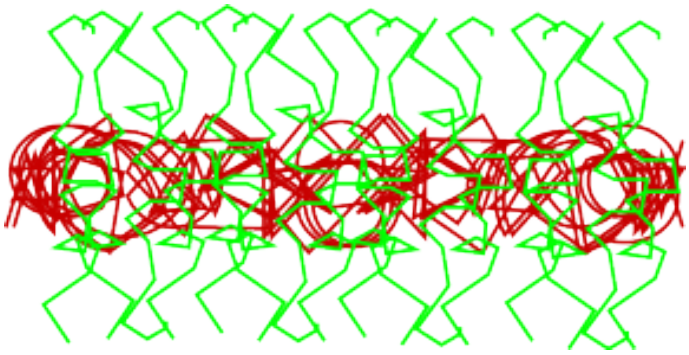

Figure 4.18: Schematic of proposed bilayer. Nanofibres (red) with a layer of microfibres (green) on top. The nanofibres will act as a cell barrier and the microfibres as a cell friendly region, encouraging proliferation and penetration into the membrane.

This scaffold was created by using a double electrospinning rig, consisting of 1 earthed collector (63 mm radius, 597 cm^2), and two syringe pumps either side, connected to two independent power supplies that shared the same earth (Figure 4.19). The right hand pump and power supply was set up for regular PLA spinning (section 2.2.2). The left hand pump and power supply was set up for regular PHBV spinning (Section 2.2.5), except only 1ml of solution was loaded into each of the 4 syringes (4 ml in total).

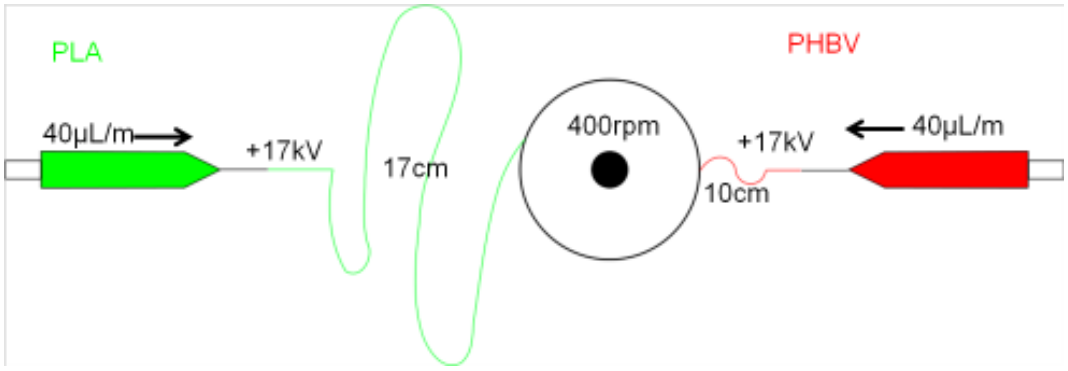

Figure 4.19: Schematic of electrospinning rig used to provide concurrent electrospinning. A layer of microfibrous PLA (green) is deposited first, then microfibrous PLA (green) and nanofibrous PHBV (red) are electrospun together. Finally more PLA is deposited on top to create a trilayered structure.

Spinning progressed as follows; 8 ml of the PLA (2ml from each syringe) was electrospun onto the mandrel. Without stopping the rig the PHBV solution was electrospun consecutively with the PLA (4ml of PHBV and 4ml of PLA). Once the PHBV had been dispensed the rest of the PLA was electrospun on top (remaining 8 ml). The production time for this scaffold was a third of the time required to produce the additive trilayer at 2.5 hours. This reduced the production time to only the time required to produce a monolayer sheet. SEM image cross sections of this scaffold show a tri-layered structure with a dense central region, sandwiched between two open microfibrous layers (Figure 4.20). Examining the dense central region more closely, microfibres can be seen poking through with interweaving nanofibres binding them together.

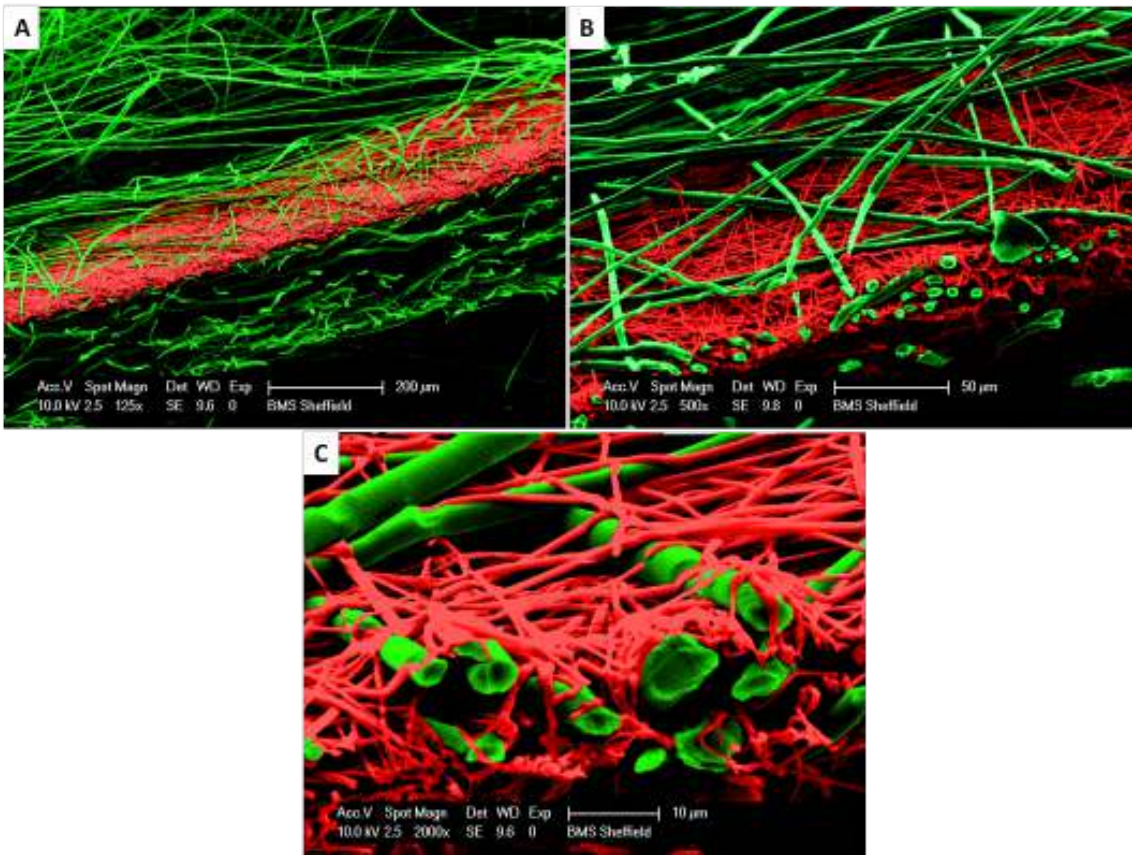

Figure 4.20: SEM photograph of a PLA-PLA/PHBV-PLA trilayer. PLA and PHBV are electrospun concurrently, to create a nanofibrous layer with stitching microfibres, in order to improve layer adhesion and reduce manufacture time.

4.6 User friendly selectively functionalised electrowoven PLA fibres

Given the poor usability of microfibrous PLA it was decided to try to make a more user friendly form of the same scaffold, and also to possibly design a method for the selective functionalisation of only some of the fibres in the scaffold. Such a method is desirable to potentially encourage angiogenesis

along those functionalised fibres, promoting vascularisation throughout the construct. In order to achieve this a woven structure was proposed.

To weave is to "form or fabricate a material by interlacing yarns or other filaments of a particular substance in a continuous web" (Figure 4.21).[119]

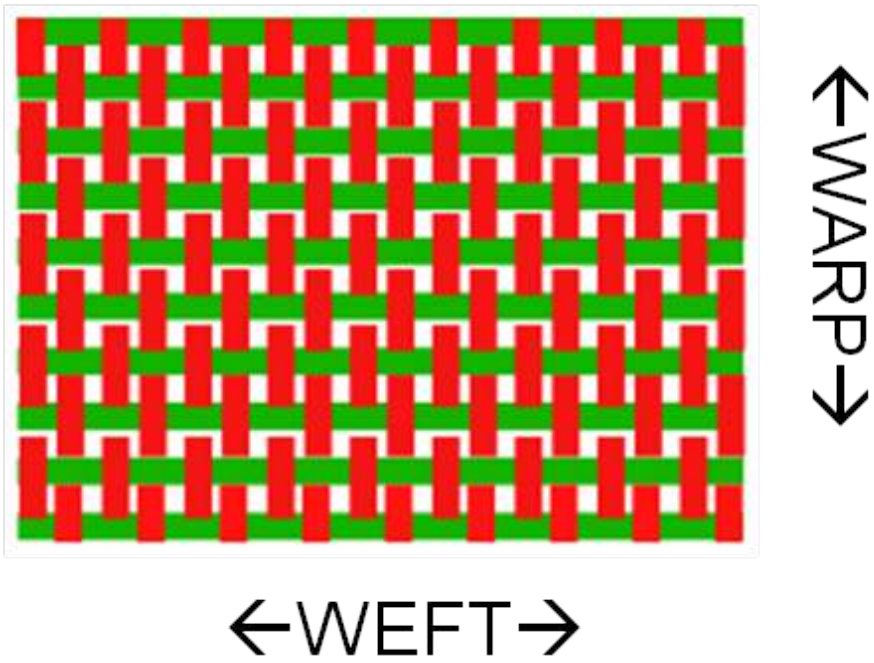

Figure 4.21: Woven fibres, the warp fibres (red) are aligned and run the length of the fabric. Weft fibres (green) criss-cross the warp fibres and form the weave.

A PLA sheet was electrowoven by using a double electrospinning rig (Figure 4.22). This consisted of 1 collector with two syringe pumps either side, connected to two independent power supplies that shared a common earth.

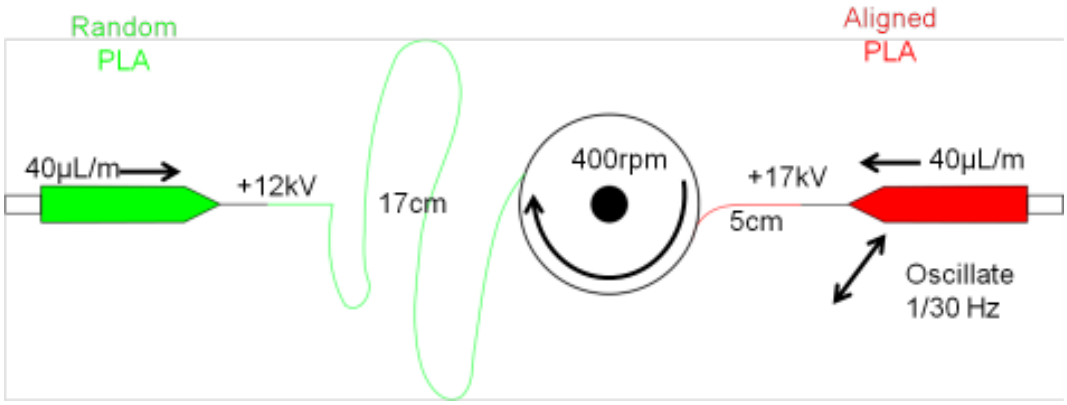

Figure 4.22: Schematic of electrospinning rig set up for the spinning of woven mats.

The right hand set up was adjusted for the formation of randomly oriented fibres (20 ml of solution, 4 syringes, 40 μLmin^{-1}, 12 kV, 17 cm needle tip to drum). The left hand set up was adjusted to favour the formation of aligned fibres (5 ml of solution, 1 syringe, 40 μLmin^{-1}, 17 kV, 5 cm needle tip to drum). In order to ensure an even distribution of aligned fibres across the electrospinning drum, the left hand pump was mounted on a rapid prototype Lego^{TM} robot (Figure 4.23).

Figure 4.23: Photograph of robot used to oscillate electrospinning pump parallel to collector.

The robot was programmed to reciprocate at $\frac{1}{30}$ Hz in front of the collector, and its travel set to the collector's width to ensure even coverage of the aligned fibres. The drum was set to spin at 650 RPM (only one speed setting for both the left and right hand set ups is possible). PLA fibres were labelled using rhodamine and fluorescein fluorophores (0.5 g dissolved in 1 ml of MeOH). 250 μL of rhodamine or fluorescein solution was added to the PLA solutions prior to spinning in order to allow visualisation of the deposited fibres, by confocal fluorescent microscopy (Figure 4.24).

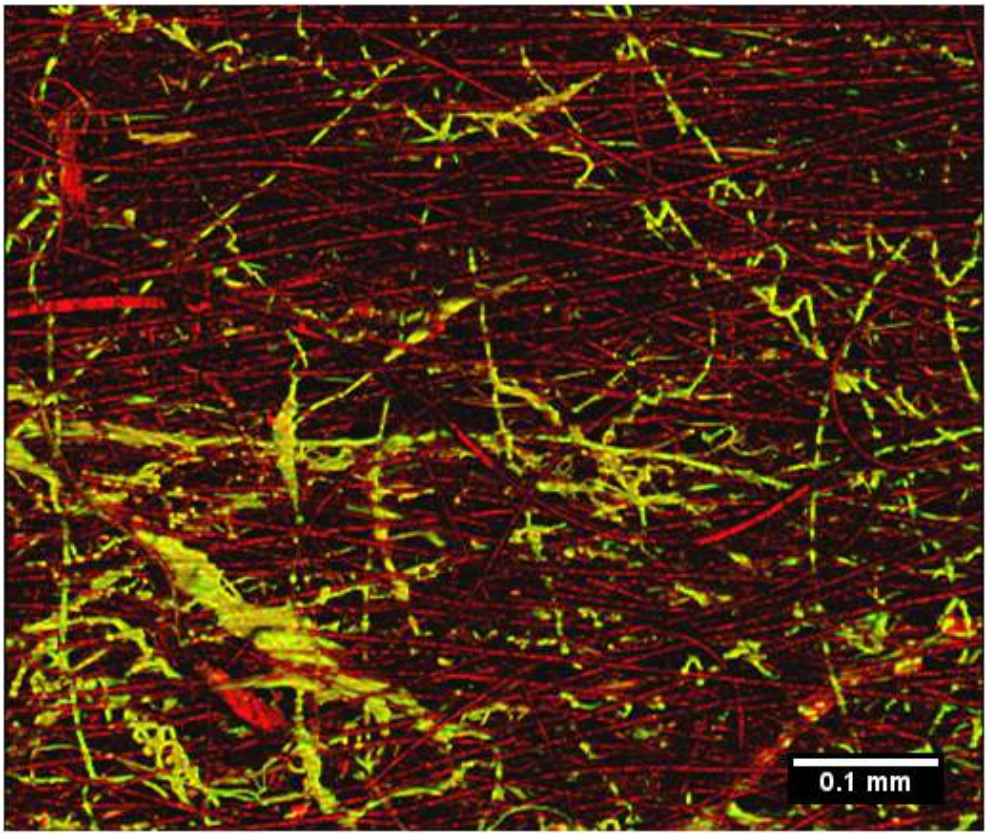

Figure 4.24: Confocal microscopy of fluorescently labelled "electrowoven" PLA fibres, labelled with FITC and rhodamine. Warp fibre (red) form a grain while the weft fibres (green) criss-cross the scaffold. Scale bar is equal to 0.1 mm.

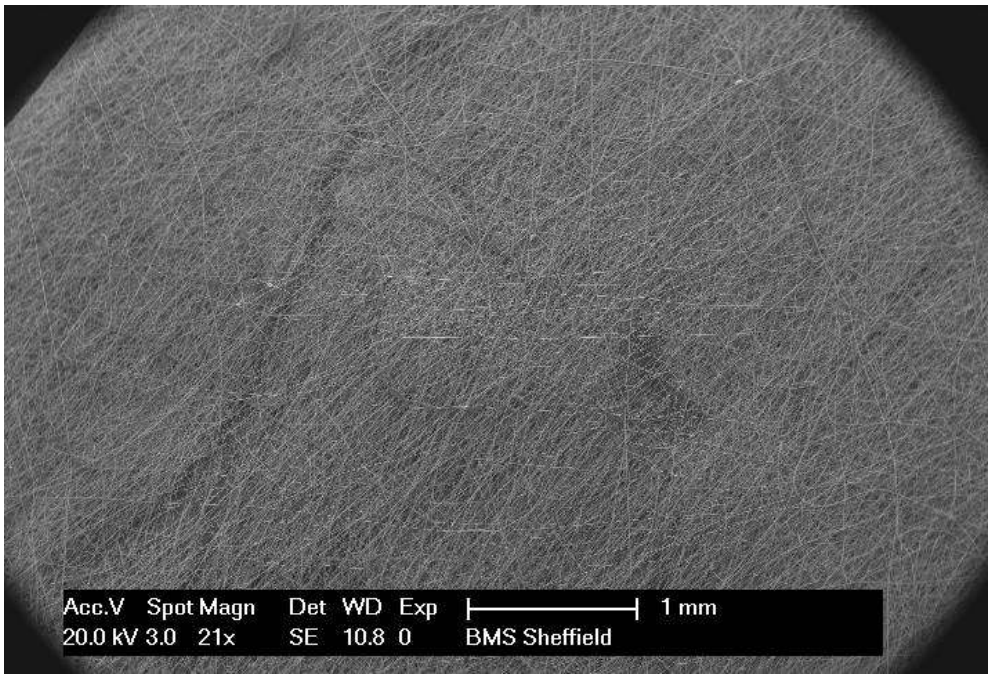

Figure 4.25: SEM image of "electrowoven" fibres.

Scaffolds were assessed for their mechanical properties on a Bose Electroforce tensiometer, and also processed for SEM (Sections 2.1.3 & 2.1.2, Figure 4.25). This method produced a white scaffold. It was noticeably flatter compared to randomly orientated or sandwiched PLA. It could be easily peeled from its aluminium foil backing. When handled it was more characteristic of a woven fabric, than randomly oriented PLA fibres. SEM images show some fibres with a grain, and others randomly orientated (Figure 4.25). There are a mixture of morphologies, either linear or spiral.

ImageJ was used to measure the angles of fibres in the confocal image relative to the x axis of the image. The angles of 50 fibres were measured and the results plotted as histograms for the aligned red warp fibres, random green weft fibres, and a "best practice" aligned scaffold (Figures 4.26, 4.27, & 4.28 respectively). Of the 50 angles recorded, 43 had angles of less than, or equal to 15° from the horizontal. The average fibre angle was 11°, and the standard deviation recorded as 17°. The data is summarised in box-plots in Figure 4.29.

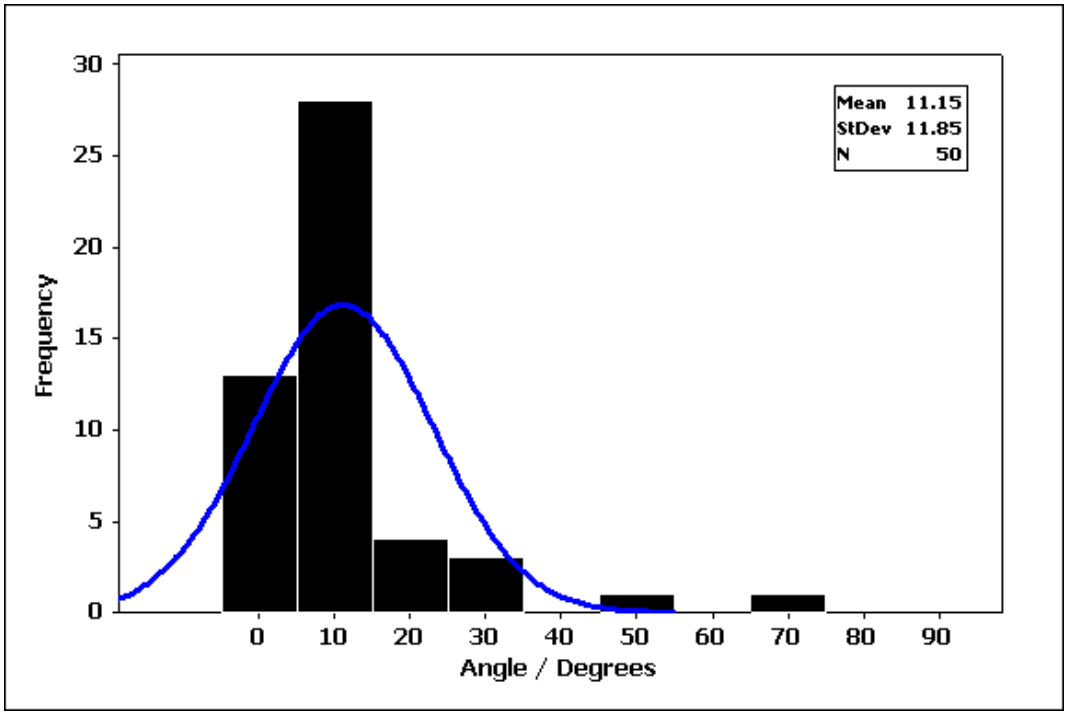

Figure 4.26: Histogram of fibre angle recorded from the aligned red warp fibres of Figure 4.24 with Gaussian distribution superimposed. n=50

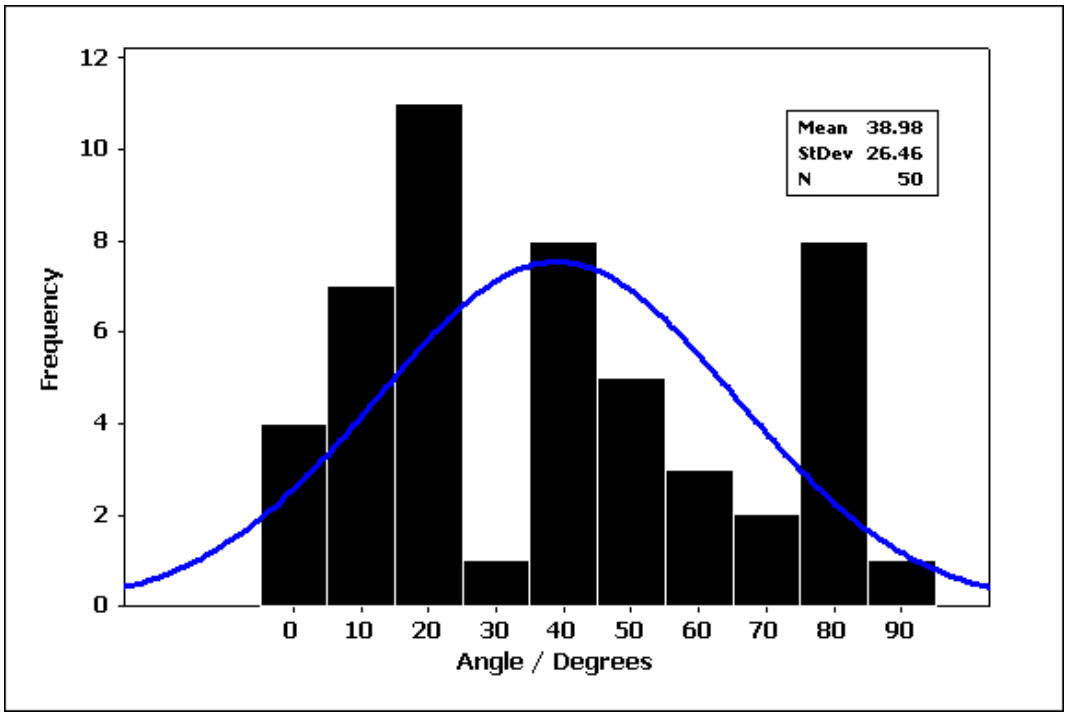

Figure 4.27: Histogram of fibre angle recorded from the random green weft fibres of Figure 4.24 with Gaussian distribution superimposed. n=50

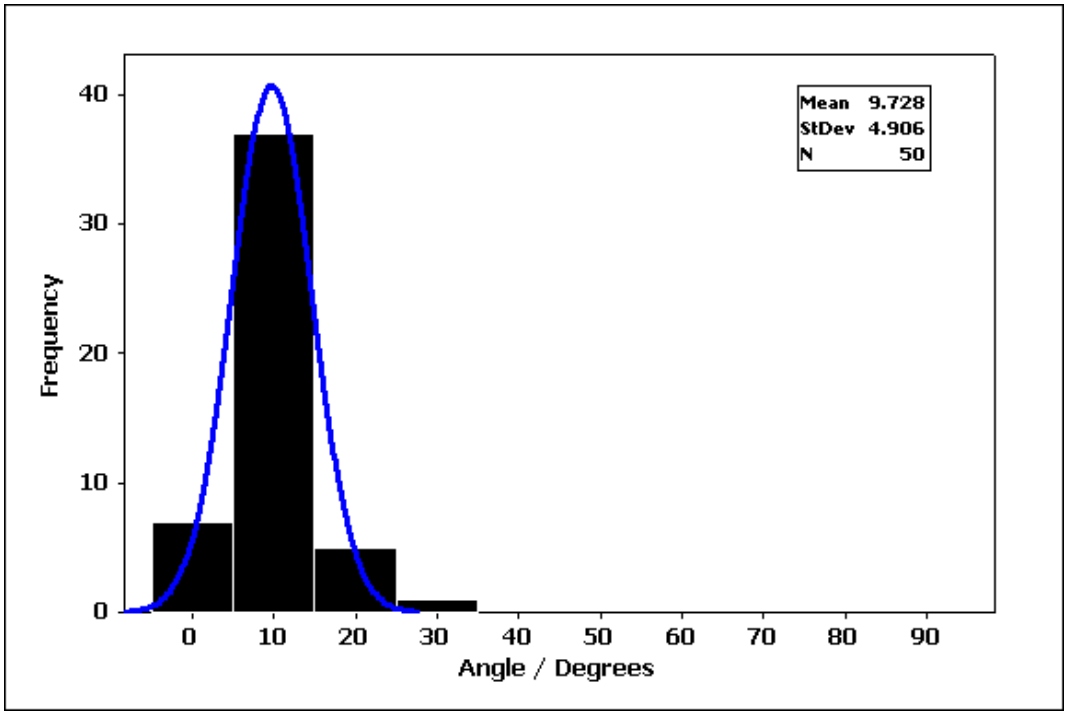

Figure 4.28: Histogram of fibre angle recorded from "best practice" aligned fibres with Gaussian distribution superimposed. n=50

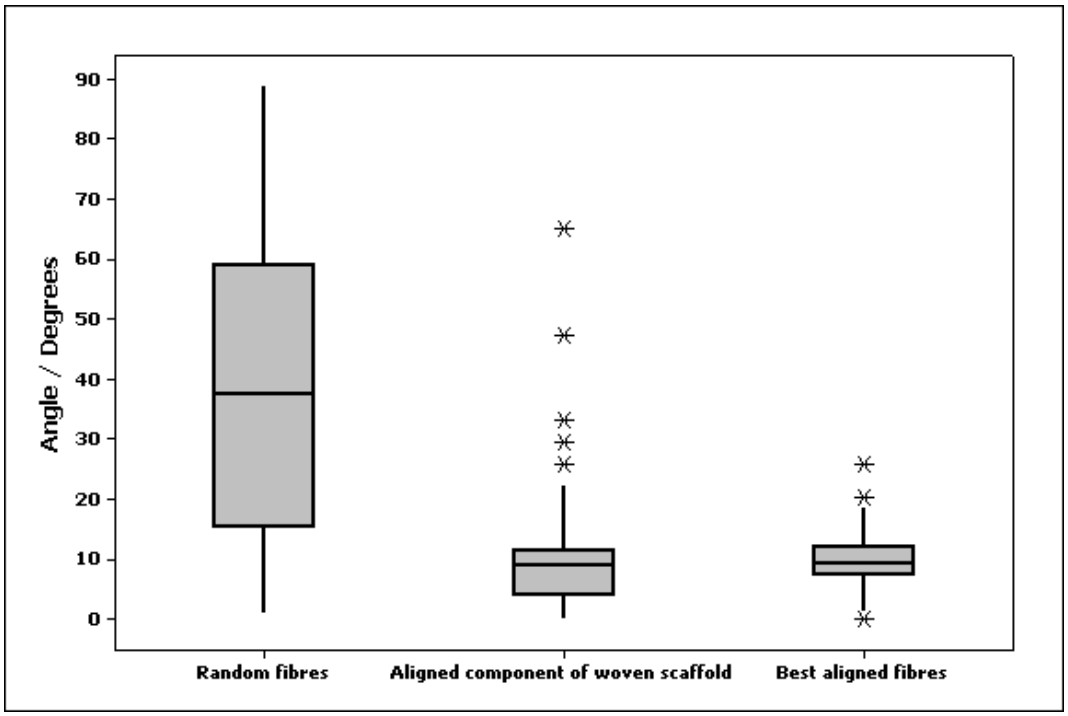

Figure 4.29: Box plot of fibre angles recorded from the random green weft fibres and aligned red warp fibres of Figure 4.24, with "best practice" aligned fibres for comparison. n=50

4.6.1 Electrospinning of a PLA-(PMSSQcoPFPA) blended monolayer

Having shown a user friendly pseudo-woven PLA scaffold could be created, a dopant was then added to either the weft or warp fibres to provide functionality. PMSSQcoPFPA was selected as a proof of concept dopant due to its ability to immobilise proteins as discussed in Section 1.2.4. The protein binding ability allows the polymer to bind heparin, which can be easily detected, and quantified using toluidine blue. Here a plain PLA scaffold is doped with PMSSQcoPFPA to act as a positive control, and ensures the PMSSQcoPFPA still functions when blended with PLA. A solution of PLA (10 wt%) and PMSSQcoPFPA (1 wt%) was blended together in DCM (89 wt%) and then electrospun (Section 2.2.2).

4.6.2 Functionalising PLA and PLA-(PMSSQcoPFPA) blended fibres for selective binding of heparin

A scaffold was woven as per section 4.6, except that the polymer solution used for the aligned fibre component was a solution of PLA (10 wt%) and PMSSQcoPFPA (1 wt%) blended together in DCM (89 wt%). PMSSQcoPFPA was synthesised as described in the literature.[46]

4.6.3 Cell culture on electrowoven, selectively heparin coated scaffolds

A 4:1 PLA (weft) and PLA-(PMSSQcoPFPA) (warp 1:9 PLA:(PMSSQcoPFPA)) scaffold was created as per section 4.6. PLA, PLA-(PMSSQcoPFPA) and electrowoven PLA/PLA-(PMSSQcoPFPA) (80% PLA weft, 20% PLA-(PMSSQcoPFPA) warp) scaffolds were cut into 1 cm^2 sections. These were then incubated overnight in a heparin solution (1 mg/ml in PBS) at 4°C.

Scaffolds were washed three times in 1 ml of PBS. One set of scaffolds was assayed for bound heparin by soaking the scaffold in 1 ml of toludine blue solution (1 mg/ml in PBS) overnight. Excess dye was eluted using distilled water until the diluent ran clear. Scaffolds were allowed to dry overnight, and then 2-ethoxyethanol was used to de-stain the scaffolds (400 μL). The absorbance of the eluted dye solution was then read at 562 nm (Figure 4.30).

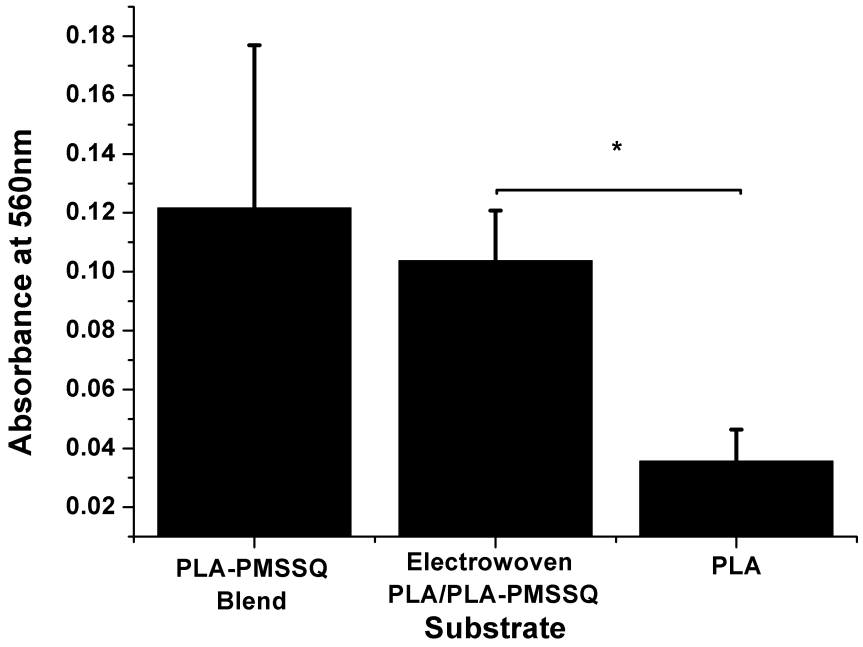

Figure 4.30: Toluidine blue eluted from electrospun scaffolds containing PMSSQ-co-PFPA and bound heparin. The more heparin bound to the scaffold, the more toluidine blue adhered to be eluted. Values are the absorbance at 562 nm presented as the average of 3 experiments in triplicate. Error bars are mean±SD, n=3.

Cell culture wells were created by placing steel rings (inner diameter of 1 cm) on the sterile TCP, and heparin coated PLA, PLA-(PMSSQcoPFPA) and woven PLA/PLA-(PMSSQcoPFPA) scaffolds. Samples were then seeded with 100,000 fibroblasts and cultured for 1 week (Section 2.1.4). On the 7^{th} day cell viability was assessed using the resaurin salt assay (Section 2.1.12, Figure 4.31). Samples were then fixed (3.7% formaldehyde in PBS) and stained using DAPI and FITC (Sections 2.1.9 & 2.1.10). Samples labelled FITC and DAPI were then imaged on an Axon imageExpress fluorescence microscope (Sections 2.1.9 & 2.1.10).

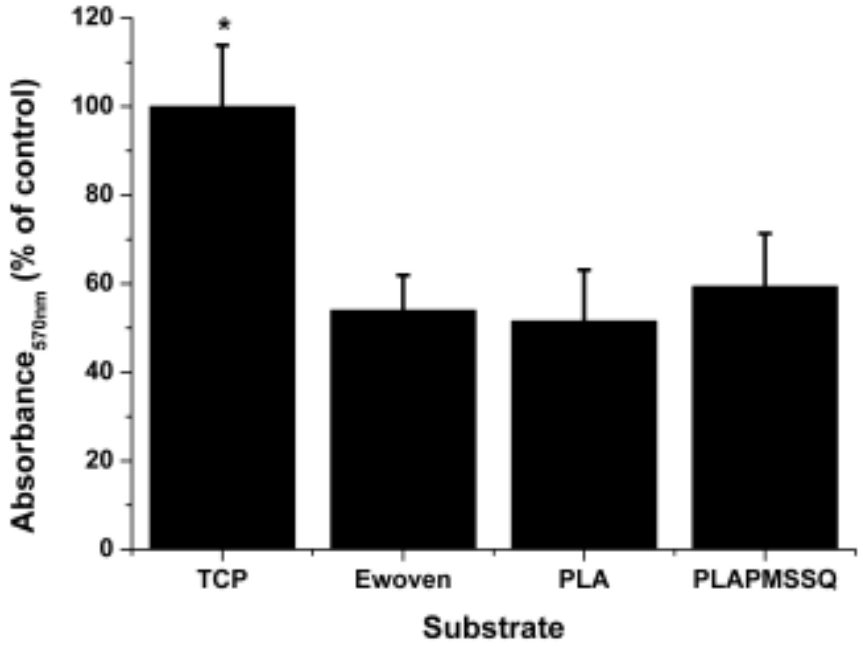

Figure 4.31: Viabilty of fibroblasts cultured on scaffolds coated with heparin. Error bars are mean±SD, n=3.

The optical density measurements of the eluted toluidine blue quantitatively confirmed that scaffolds containing PMSSQcoPFPA bound more heparin than those without PMSSQcoPFPA. Plotting the results shows that the scaffolds of PLA only bound 33% of the toludine blue, compared to scaffolds that contain PMSSQcoPFPA (significantly less, $P<0.05$, Figure 4.30). There was no difference between the scaffold that was completely PLA-(PMSSQcoPFPA) and the scaffold that was only 20% PLA-(PMSSQ) (Figure 4.30).

There was no significant difference in cell viability between cells cultured on PLA, PLA-(PMSSQcoPFPA) or electrowoven PLA/PLA-(PMSSQcoPFPA). All three showed good viability. Cells on TCP gave a reading 33% greater than for cells on electrospun scaffolds (Figure 4.31). Fluorescence microscopy of the samples show normal looking cells on all substrates (Figure 4.32). TCP pro-

duced dense, continuous sheets of cells. Cells on PLA are less densely packed, but grow throughout the scaffold. There was no observable alignment. Fibroblasts can be easily cultured on PLA-(PMSSQcoPFPA) scaffolds and coat the scaffold's surface, although visually there appear to be fewer cells when compared to TCP. When cultured on electrowoven PLA/PLA-(PMSSQcoPFPA) fibroblasts form striations, indicating an alignment with the organised component of this scaffold. The cells are elongated and orientated with the grain of the scaffold (Figure 4.32).

ImageJ was used to measure the angles of the major axis of cell bodies. This was done to determine if there was a general alignment of the cells cultured on TCP, PLA, random PLA-(PMSSQcoPFPA) and electrowoven PLA/PLA-(PMSSQcoPFPA). Angles were measured relative to the x axis of the fluoresce microscope photographs (Figure 4.32). The angles of the major axis of 50 cells were measured for each image and the results plotted as histograms (Figures $4.33 - 4.36$). No statistically significant alignment was recorded, however, it is clear from the histograms that the fibroblasts cultured on electrowoven PLA/PLA-(PMSSQcoPFPA) are more ordered than the random scaffolds of TCP substrates. The data is summarised in box-plots in Figure 4.37.

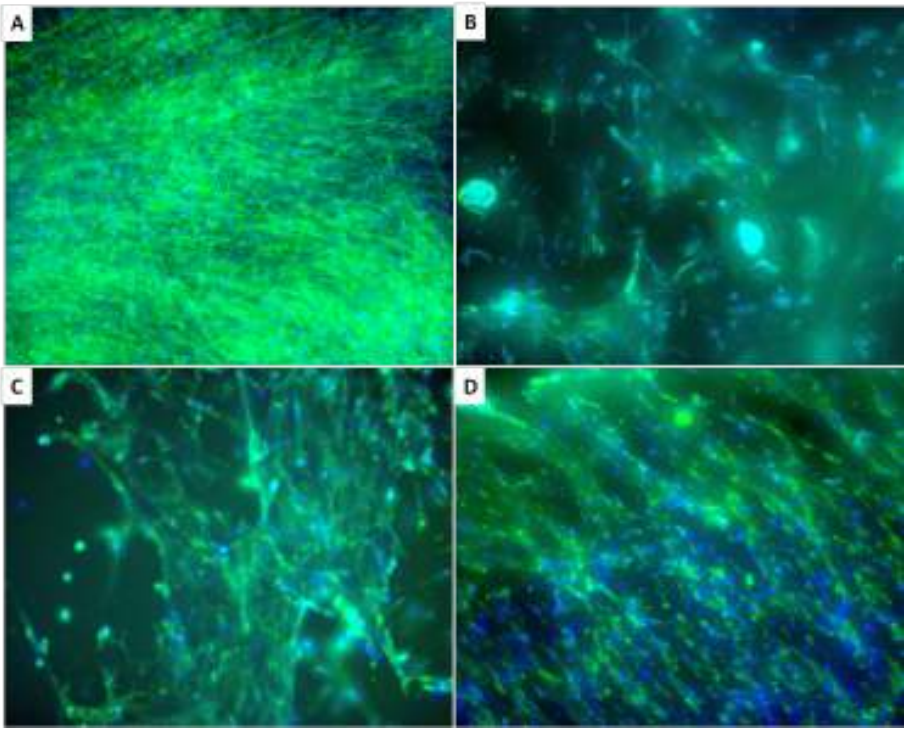

Figure 4.32: Fluorescence microscopy of fibroblasts labelled with DAPI (cell nuclei, blue) and FITC (cytoplasm, green) grown on heparin coated scaffolds. A. TCP B. PLA C. PLA-PMSSQ D. Electrowoven PLA/PLA-(PMSSQcoPFPA). Scale bar is equal to 0.1 mm.

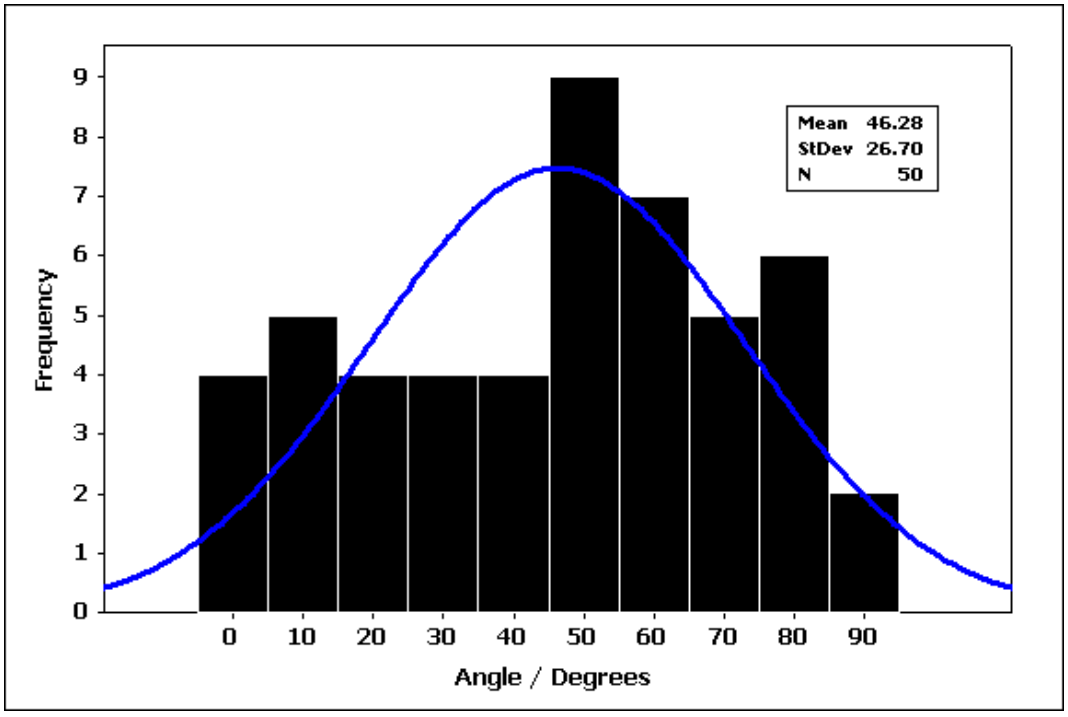

Figure 4.33: Histogram of major cell axis angle on random PLA electrospun scaffold recorded from Figure 4.32. n=50

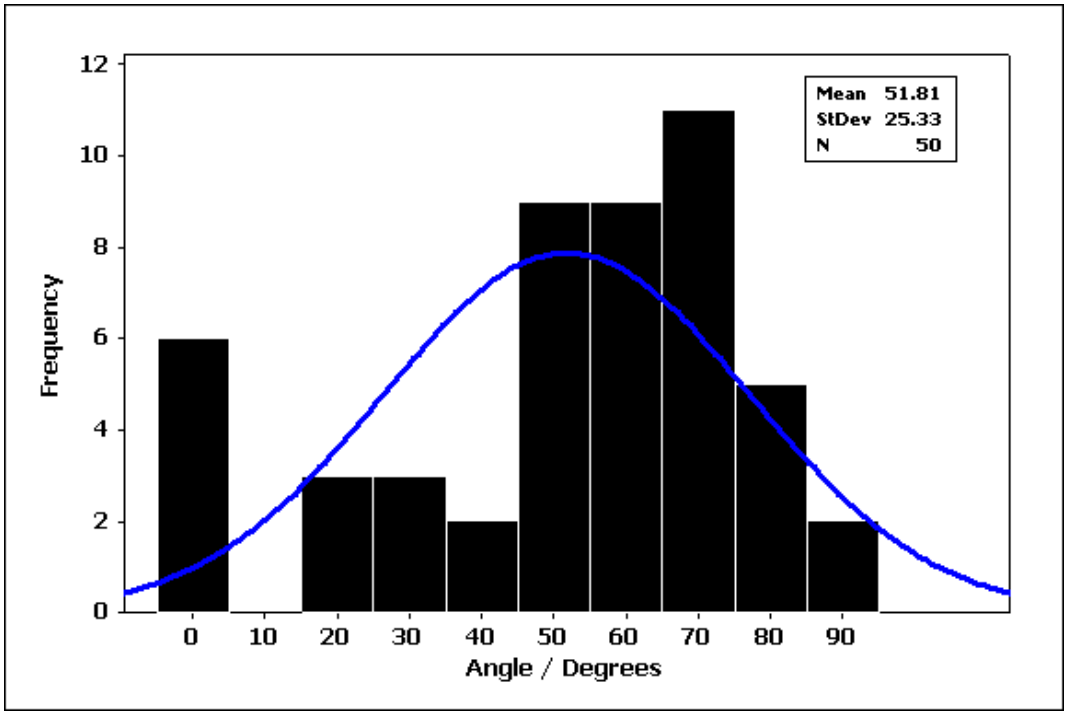

Figure 4.34: Histogram of major cell axis angle on random PLA-(PMSSQcoPFPA) electrospun scaffold recorded from Figure 4.32. n=50

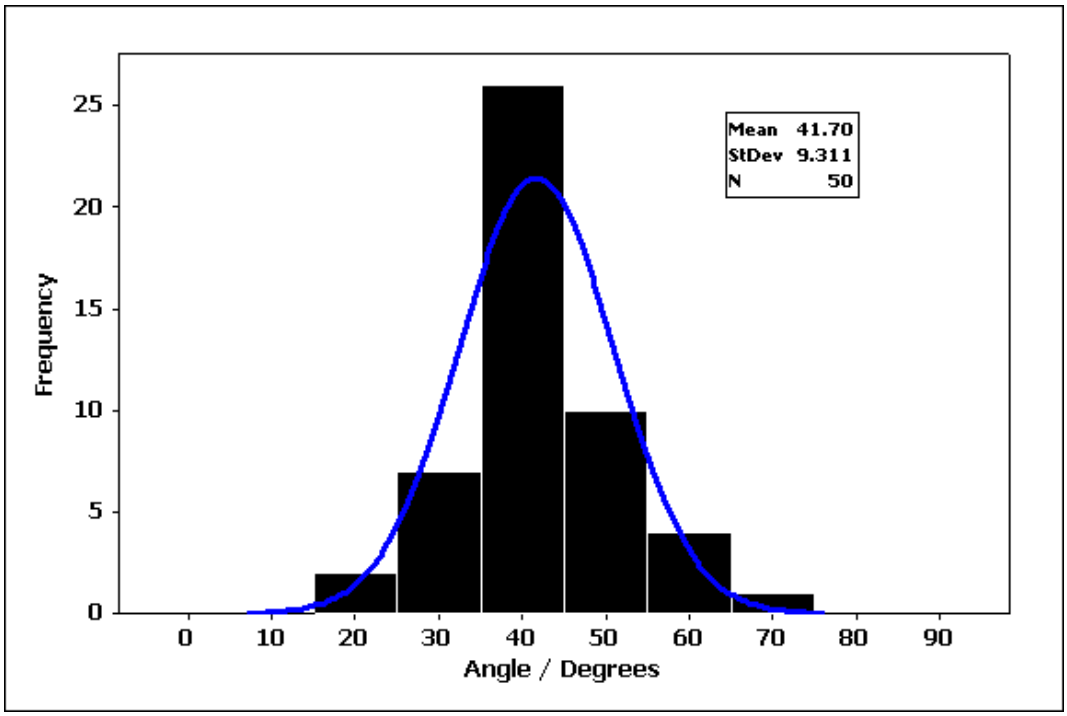

Figure 4.35: Histogram of major cell axis angle on electrowoven PLA/PLA-(PMSSQcoPFPA) scaffold recorded from Figure 4.32. n=50

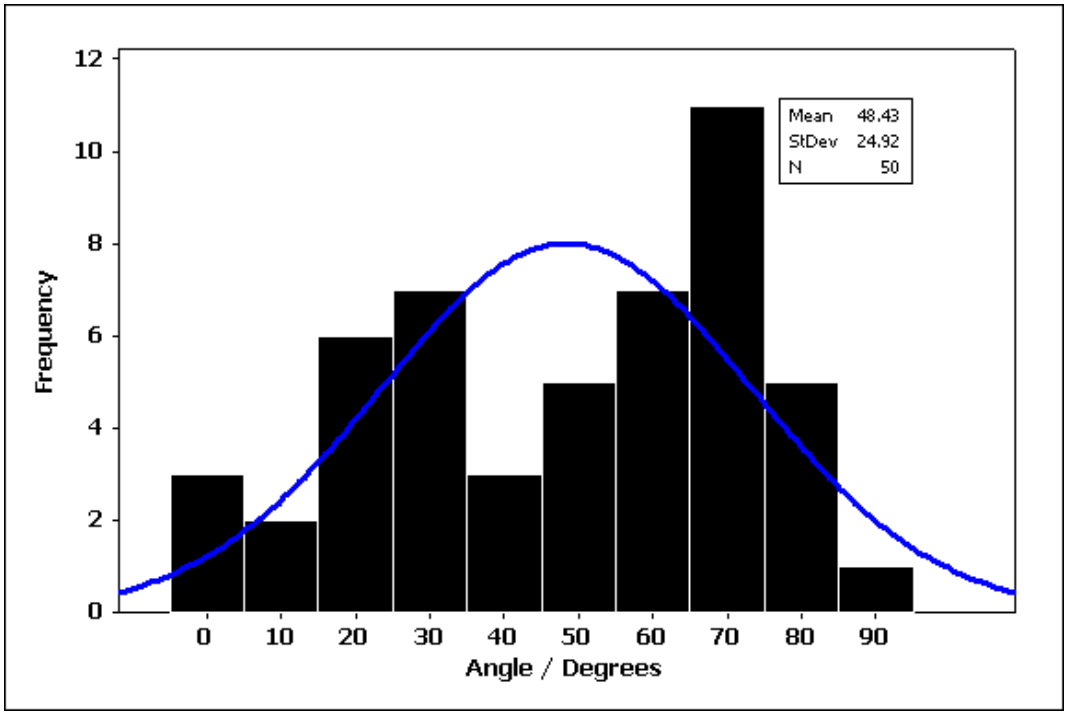

Figure 4.36: Histogram of major cell axis angle on TCP recorded from Figure 4.32. n=50

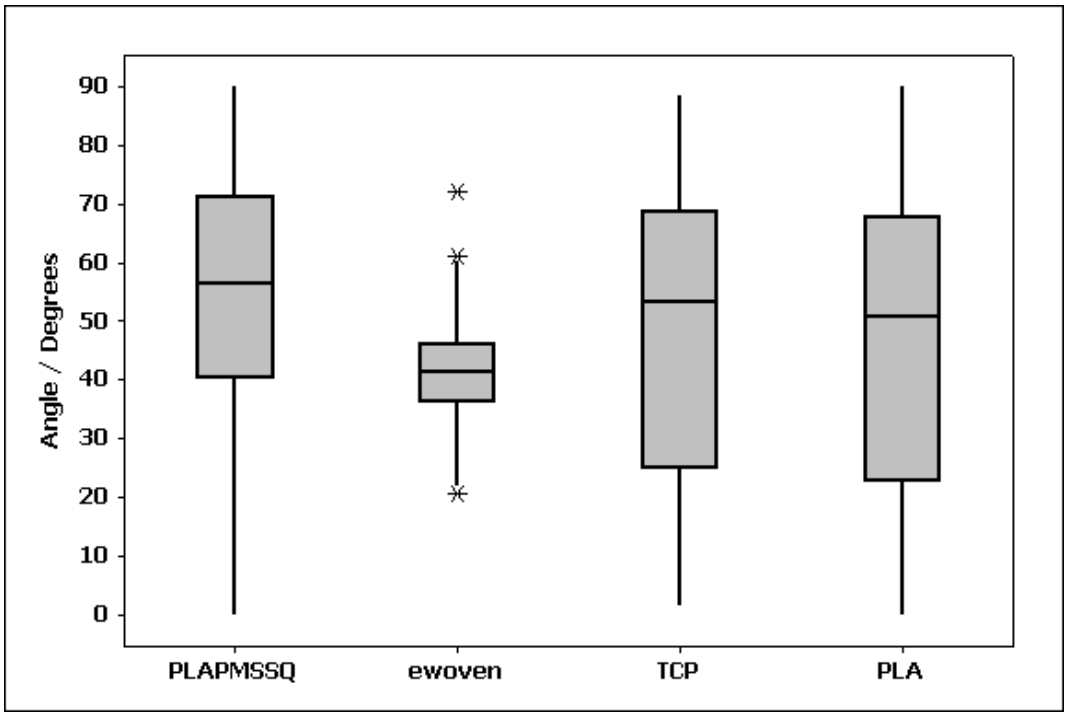

Figure 4.37: Box plots of major cell axis angle on TCP, random PLA, random PLA-(PMSSQcoPFPA), and electrowoven PLA/PLA-(PMSSQcoPFPA) scaffolds recorded from Figure 4.32. n=50

4.7 Designing low Poisson ratio materials; electrospinning of an aligned-random-aligned sandwich of PLA fibres

In some situations scaffolds are being designed to provide support to dynamic tissues, such as the pelvic floor. Materials that would be particularly suitable would exhibit reduced "necking" under strain. The best solution would be to create a scaffold that is auxetic under strain. Necking is observed daily in many materials, when stretched the material thins or "necks". Plastic carrier bags are notorious for this.

With respect to medical devices, this behaviour is undesirable, pelvic floor repair requires a supporting scaffold that can flex with the patient. If the scaffold were to neck it could eventually become too thin to be supportive, and even cut into surrounding tissues, much like a cheese-wire. This effect has already been noted in complications when treating pelvic organ prolapse as described in Section 1.5.4. Auxetic materials expand when put under tension. An everyday, but not obvious example, is paper.[224]

A scaffold created out of such a material would not neck but expand when under tension, providing extra support when it was required. This is a particularly challenging design request, and the work presented here does not produce such a scaffold. However, a cross linked aligned scaffold that exhibits lower Poisson's ratios than scaffolds of purely random fibres is produced and "necks" less than conventional random fibre scaffolds.

Poisson's ratio is used to describe such behaviour in materials, it is the ratio of length to width. Materials that neck have positive Poisson's ratios, auxetic materials have negative Poisson's ratios. Cork is a commonly cited example as a material that has a Poison's ratio close to 0. This is why cork is a popular choice as a bottle stopper, it is easier to hammer into the bottle as it doesn't thicken when compressed.[225]

As electrospun scaffolds have potential as cell carriers, it would be advantageous to be able to design a scaffold with auxetic, or near zero Poison's ratio properties. This is the aim of this section. It was proposed to make a trilayer sandwich of aligned PLA fibres sandwiching random PLA fibres (Figure 4.38).

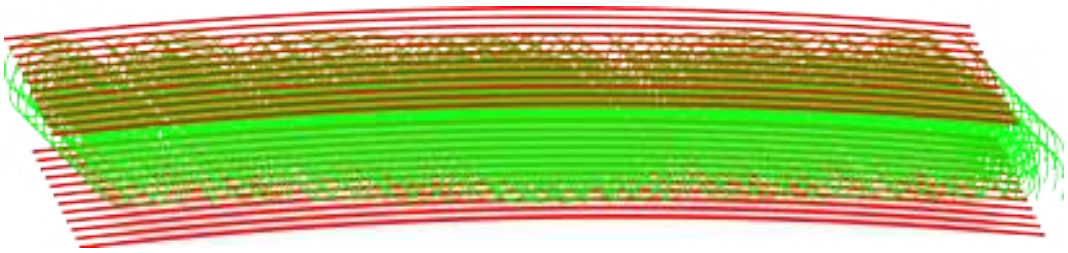

Figure 4.38: Schematic of aligned-random-aligned PLA sandwich. The intention is to make a low Poison's ratio material. As the aligned fibres (red) are put under tension, it was hoped the random fibres (green) would "squeeze out".

A PLA sheet was electrospun as in Section 2.2.2, except the speed of the collector was set to 1700 RPM for the first third of deposited fibres (8ml of the PLA mixture). Following this, the collector speed was reduced to 300 RPM for the second third, and then raised again to 1700 RPM for the final third. The E was then measured on a Bose electroforce tensiometer. The aligned component significantly increased the E compared to random fibres alone (Figure 4.39).

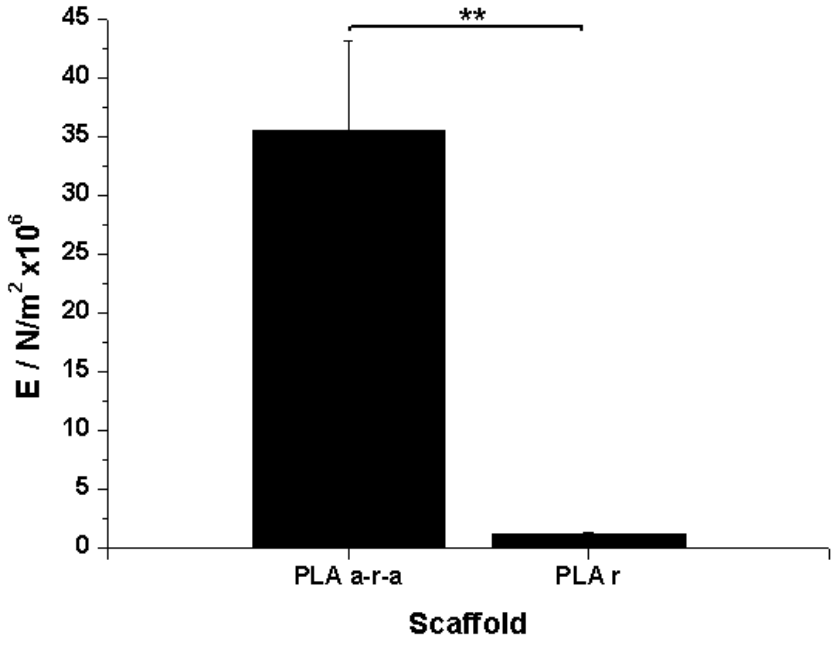

Figure 4.39: E of a trilayer of aligned-random-aligned PLA (a-r-a) compared to a PLA monolayer (r). Error bars are mean±SD, n=3.

A sheet of aligned PLA fibres was electrospun as per Section 2.2.2, except the speed of the collector was set to 1700 RPM for the duration of the spinning. This acted as a solely aligned control. Varying the speed of the collector as the PLA fibres are spun produces a white scaffold with a lustre. The alignment of the fibres makes the scaffold a little easier to use than the comparable randomly orientated scaffold. SEM images show fibres with a distinct grain either side, and a cross sections shows a sandwich of aligned-random-aligned fibres (Figure 4.40). The E of the material is greatly improved compared to solely randomly spun fibres.

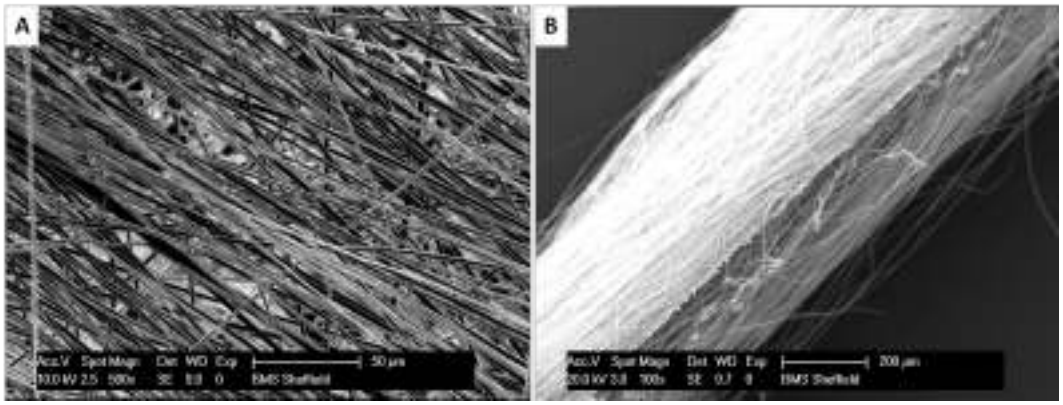

Figure 4.40: SEM photograph of aligned-random-aligned PLA trilayer. A. Top face of scaffold showing the aligned component of the scaffold. B. Cross section of the scaffold, showing aligned fibres above and beneath, with random fibres sandwiched between.

4.7.1 Calculation of Poison's ratio of electrospun PLA aligned-random-aligned sandwiches

A rig was made to fit a syringe pump so that samples of scaffold could be attached and then distended up to 30 mm (Figure 4.41). Three sections of each scaffold were cut (aligned PLA, aligned-random-aligned PLA, and random PLA, 1 cm $\times$ 3 cm, 3 cm side parallel to the direction of the aligned fibres). These samples were then distended by 30 mm at 0.3 cm/s, and were photographed once per second for the duration of the distension. ImageJ was then used to calculate the length and width of the sample, from which their respective strains were calculated, and from that their Poison's ratio.

A plot of scaffold width vs. length shows that the a-r-a PLA neck initially, but then plateaus (Poison's ratio of 0), compared to random PLA which continues to neck (Figure 4.42). Aligned PLA necks very little and has a Poisson's ratio close to 0 throughout.

The Poison's ratio of these materials is not negative, so they are not auxetic (Figure 4.43). However, for aligned-random-aligned PLA, on distension, it was observed that as the material necked "wings" of fibres deployed either side (Figure 4.41 C. and D.). This material has a low Poison's ratio, and is lower overall than random PLA fibres. Aligned PLA is better again and exhibits the lowest Poisons ratio of these three scaffolds.

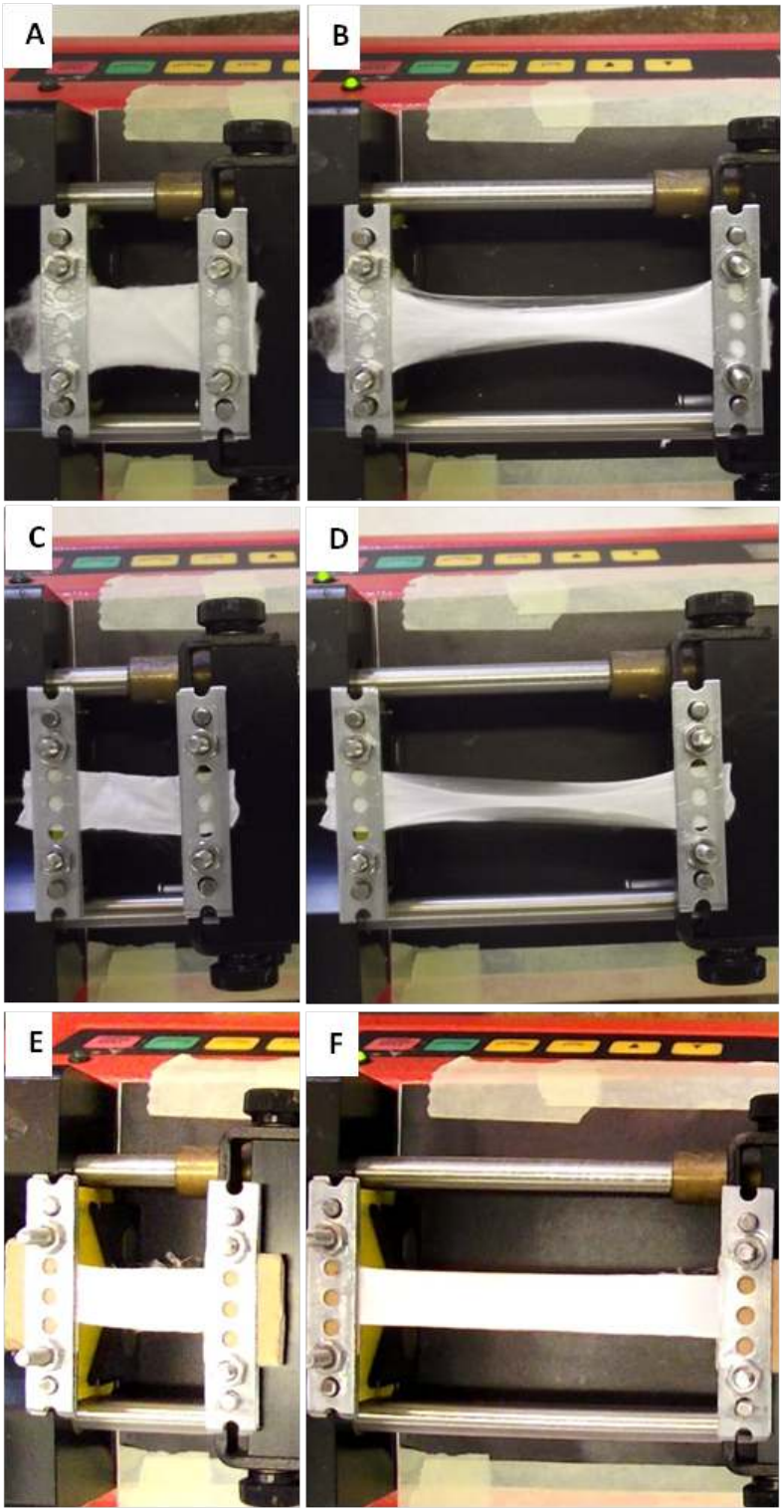

Figure 4.41: Distension of monolayers of aligned PLA, random PLA, and trilayers of aligned-random-aligned PLA. The use of the syringe pump allowed the samples to be distended by up to 5 cm. A and B are a monolayer of random PLA before and after distension respectively. C and D are a trilayer of aligned-random-aligned PLA before, and after distension respectively. E and F are aligned PLA fibres before, and after distension respectively. The length and width at the most narrow point was recorded for each sample, to plot how width changes with distension. The scale bar is equal to 1 cm.

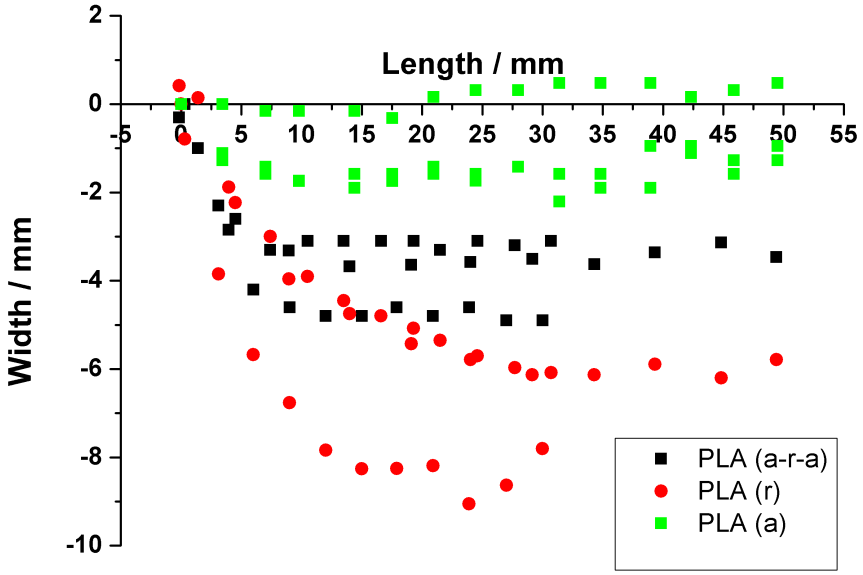

Figure 4.42: A plot of width vs length as scaffold samples are distended. Trilayers of aligned-random-aligned PLA (a-r-a) narrow by around 50% less than random PLA (r) alone, and then reach a plateau, while the random PLA continues to narrow with distension. Aligned PLA monolayers (PLA a) narrow the least.

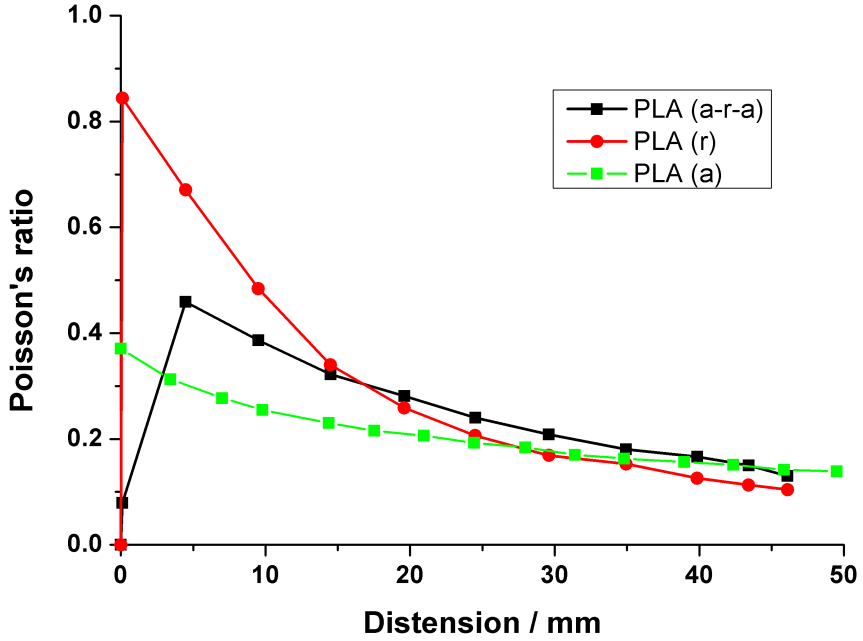

Figure 4.43: A plot of Poisson's ratio vs. distension for a random PLA monolayer (PLA r), an aligned-random-aligned PLA trilayer (PLA a-r-a), and an aligned PLA monolayer (PLA a).

4.8 Discussion

This chapter demonstrates that a nanofibrous scaffold can act as a barrier to cell penetration while providing a scaffold for cell attachment and proliferation. For cleft palate treatment in the clinic, it would be our intention to culture autologous buccal mucosa on one face (as previously demonstrated), and autologous periosteal cells as a bone precursor on the opposite face.[198] These are being investigated for their bone forming ability at present. These could be harvested at the time of a cleft lip repair, expanded in the laboratory, and then re-introduced on a bilayer membrane to encourage the growth of a native hard palate.

The concept of segregating tissue for regenerative purposes is not new. It has been established in dentistry for sometime, where tissue guides have been developed to segregate soft tissue from bone forming tissue in periodontal repairs.[132,133] Commercial materials include collagen-based membranes, biodegradable polymers and Teflon.[2,134,135,226] Collagen has a high biodegradation rate, can be difficult to remove when there are problems, and can introduce the risk of infection as it is an animal derived tissue (usually bovine). Therefore, one must be mindful of the source of the collagen to avoid any risk of prion disease transmission.[135] Teflon is a very successful and effective barrier to cells. However, it cannot be left implanted, and follow up procedures are required to remove it. This is not ideal as it disturbs the newly repaired tissues, risking scar formation and infection.[226] Current biodegradable polymer solutions are commonly based on PLA, however, these are not entirely popular with surgeons as they are difficult to handle.[227]

In the current study the nanofibrous component of the bilayer and trilayer makes the material much more user-friendly. It can be readily picked up, shaped, and handled without tangling, sticking or loss of shape, unlike microfibrous electrospun scaffolds.

The methodology of spinning one scaffold on top of another is reproducible and consistent. Our data show that by using cell tracker labelled cells it is possible to culture two different cell types on these scaffolds, while maintaining segregation for at least 7 days.

The cell tracker fluorescent dyes are very successful at labelling cells through to 7 days, but the intensity of the dye decreases noticeably after longer periods.

In this study fibroblast attachment was examined as a soft tissue model. hESMPs were selected as a model bone forming cell as they are capable of forming bone (see Figure 4.14), and are also an appropriate cell type against which other candidate cells can be compared.[228,229] Here hESMP's bone forming potential is demonstrated on TCP, and other studies have shown similar bone forming potential on other well known biodegradable polymers, such as PCL, PLA and PLGA.[103,230,231] Similarly, it is confirmed that keratinocytes and fibroblasts are effectively segregated when cultured on a trilayer membrane separated by a nanofibrous scaffold layer.

4.8.1 Electrospinning of a PLA/PHBV composite bilayer scaffold

Electrospinning of bilayer materials has been conducted previously, where a PCL under layer was spun first, followed by a PLA layer, to create a 5 mm outer diameter tube, with an interior and exterior of different composition.[185] This tube was designed for use in blood vessel tissue engineering, which requires quite different properties to guided tissue regeneration (GTR) membranes. This did not have a cell segregation aspect, as it had to be populated throughout with cells. The pore sizes created with the tube were up to 15 μm and 10 μm in the PCL and PLA layers respectively. This contrasts to the bilayers synthesised in this project, where pore sizes are much smaller, and allow the material to segregate cells, while the permeation of nutrients and cell cytokine signalling was still possible. The scaffolds synthesised in this project are fit for purpose, the dense PHBV layer has pores to allow the flow of nutrients and cytokines, but gives a sufficient barrier to cells preventing them traversing the material. The PLA layer provides a region that is cell friendly and can be densely populated throughout with cells.

4.8.2 Sequential electrospinning of a PLA/ PHBV/ PLA composite trilayer scaffold

The next step was to create a membrane with separate regions for cells to proliferate within, while remaining segregated. A barrier membrane sandwiched between two microfibrous regions would provide this. Cells can proliferate in the microfibres, but are segregated by the nanofibrous layer. The concept of a

trilayer membrane is not new, electrospun multilayer membranes do exist for periodontal treatment.[232–235] However, these are not without their issues, none of these membranes exhibit a barrier function, and instead rely on a scaffold density gradient to coerce cells to grow in the right place. Such scaffolds become increasingly dense with depth, this allows cells to migrate in to a certain point, until the pore size is too small for further migration. Many such scaffolds are derived from collagen, with its inherent risk of prion transmission, or coatings of expensive protein motifs. The trilayer presented here is simple in it's manufacture, and exhibits a barrier functionality, without the need for expensive or natural products.

4.8.3 Concurrent electrospinning of a PLA/ PHBV-PLA/ PLA composite trilayer scaffold

To simplify and improve the adhesion between the layers of this trilayer scaffold, the method was adapted to spin all three layers in one sitting, as opposed to three separate spinning sessions. A search of the literature shows a similar technique was used before. Microfibres have been used in conjunction with nanofibres, but normally as part of a much more controlled structure, to specifically mimic certain tissues.[236] The other scaffolds created using similar methodology in the literature are sequential with distinct regions of nanofibres or microfibres, whereas the scaffold created here was a mixture with microfibres bound together with nanofibres. One other instance of this is reported in the literature; Shalumon *et al.* electrospun PLA microfibres, and intermittently co-spun PLA nanofibres. However, there is no reference to the proportion of nano to microfibres. Nor is the technique used to create a layered structure.[237]

Equal proportions of microfibres and nanofibres have not been spun together at the same time. Another similar method to this is for the creation of porous scaffolds, where sacrificial fibres are co-spun with supporting fibres into a scaffold. The sacrificial fibres are made of a material that is readily soluble. Hence, when the sacrifical fibres are removed, only the insoluble fibres remain, leaving a scaffold with increased porosity. The fibres used in this technique are of the same dimensions, and not a nanofibrous/microfibrous mix.[238]

4.8.4 Viability of cells on scaffolds

As the scaffolds presented here are intended to be used with soft and hard tissues, two model cells representing each tissue were selected. Human dermal fibroblasts were selected as they are the major cell which comprises the human dermis and are often used as a model cell for methodology development. HESMPs were selected as they have been shown to be capable of forming bone.[227,228] First, the viability of both these cells types on TCP, and simple scaffold monolayers, needed to be determined to check they were compatible.

Resazurin (5 μg/ml in PBS) was used to assess cell viability after 7 days of culture (50,000 fibroblasts and hESMPs respectively, Section 2.1.12). After removal of residual culture media, 1ml of rezasurin solution was added to each scaffold and incubated for 1 hour, following which 150μL was taken from each sample and the absorbance read (570 nm, Bio-Tek ELx800 plate reader, Figures 4.6 to 4.11). The culture media was then replaced (1ml per sample). It has been shown that a variety of different cell types can be grown on PLA, PCL, and PHBV based scaffolds, which agrees with current literature for similar

scaffolds based on these polymers.[239–242] The work completed here agrees with this, and although, in general, the viability of hESMPs was lower than that of fibroblasts on the scaffolds, there were no problems culturing cells on these scaffolds. This may be due to normal hESMPs culture procedure calling for the cells to be seeded onto a bed of gelatin, whereas the scaffolds were left uncoated.[103, 229–231]

The mean cell count per field of view increase with time for all substrates, regardless of the number of cells seeded. Cells were observed on the underside of the nanofibrous PCL scaffold, but the absorbance is far less than that seen on TCP. The rest of the cells were either on the opposite face of the scaffold, or buried within. The cell count was far smaller for PHBV scaffolds regardless of the number of cells seeded. This simple experiment showed that a single layer of PHBV was capable of preventing cells passing through for at least 6 weeks. Total cell populations appeared to peak at 3 weeks for both cell densities. This could be due to the cells becoming confluent and then senescent. Some similar instances are investigated in the literature, fibroblasts have been shown to undergo a form of programmed cell death known as anoikis. Anoikis is triggered when anchorage dependent cells such as fibroblasts detach from the surrounding extracellular matrix.[243] So, if the cells reached confluence, and insufficient extracellular matrix deposition had occurred in the time it took to reach confluence, this could be an explanation of the drop in cell numbers observed.

Alternatively, decreases in fibroblast proliferation has been observed on poly(ether imide)/poly(benzimidazole) blended scaffolds after a period of incubation.[244] Altankov explains such instances as possibly due to membrane-promoted cellular aggregation, leading to easier cell detachment from the substratum. This

could mean that after a period of incubation cells may only be weakly attached to a scaffold, and hence could fall off during media changes *etc.*

Aside from this fibroblasts have a fixed life time *in vitro* and cease proliferation following a number of cell division.[245] This occurs through the process of senescence, which was first described in fibroblasts by Hayflick in 1961.[180] Hayflick notes after continuous incubation for 1 month, fibroblast cultures form sheets of cells that curl up, and peel away from the glass substrate, on agitation of the culture medium. This time scale is shorter than that attempted in this experiment, and therefore is perhaps the most compelling reason for the drop in cell number observed around the 3 week mark.

There is a clear difference between PCL nanofibrous scaffolds and nanofibrous scaffolds of PHBV. Fibroblasts were able to squeeze through the PCL scaffolds, although this could be due to the PCL scaffolds being more fragile, and holes developing when placing them in the cell crowns.

4.8.5 Cell migration into scaffolds up to 6 weeks

Barrier membranes form a big part of the GTR area of dentistry (Section 1.5.2). Gingivitis is a growing problem, this is a disease where bacteria cause the bone around teeth to erode, resulting in tooth loss. It is estimated that around 10%-15% of adults worldwide have advanced gingivitis (6 mm or greater periodontal defects).[246] The idea of GTR is to keep fast growing soft tissues at bay and allow bone to regrow. There is some literature on a collagen bilayer, designed for this purpose.[247] This is able to prevent cell cross over for up to

3 weeks. However, bovine collagen as a material is disliked by surgeons due to the possibility of prion disease transmission. This study presents a totally synthetic, biocompatible, and biodegradable electrospun membrane of PHBV, which was developed to keep two different cell types separate. On one side hESMPs (shown to have osteogenic potential) while on the other, fast growing dermal fibroblasts.[227,228]

Investigations into cell penetration into nanofibrous scaffolds long term are promising (Section 4.4). A single layer of electrospun PHBV scaffold is capable of preventing cells passing through it for at least 6 weeks. Total cell populations on the scaffold appeared to peak at 3 weeks for both high and low concentrations of cells, this could be due to the cells becoming confluent or senescent, as they would in normal culture. There is a clear difference between performance of cells on a PCL nanofibrous scaffold and on a PHBV scaffold. Fibroblasts are able to squeeze through the PCL nanofibres due to mechanical damage, which could be due to the PCL scaffold being more fragile, and holes developing when placing it in the CellCrowns^{TM} prior to cell seeding.

Penetration of scaffolds by cells has received a lot of attention in the literature.[237,248,249] However, the main focus of these papers is to improve or tailor cell penetration into the scaffold. This is typically achieved through the use of sacrificial fibres to increase porosity (as described in Section 4.8.3). One thing that all these papers agree on is that nanofibrous networks are effective at preventing cell ingress. Shalumon *et al.* use a co-spun nanofibrous/microfibrous PLA network and report improved cell infiltration.[237] This is a potential problem for the concurrent electrospun PLA/ PHBV-PLA/ PLA composite trilayer scaffold reported here. The combination of micro and nano fibres may facilitate cell infiltration. However, the proportion of nano to micro fibres used

by Shalumon *et al.* is not reported.[237] Their method merely states that "microfibres were continuously electrospun whereas nanofibres were intermittently depositing on the same target". If the quantity of nanofibres was sufficently low, the microfibres may act as supporting beams, and open up the structure, allowing cell migration into the scaffold. The 50:50 micro:nano fibre network, reported in this project, appears as a much denser network and should be proven to be a barrier to cells in the future.

4.8.6 Electroweaving of PLA fibres

To the best of my knowledge the simultaneous deposition of aligned and random fibres to create a pseudo woven network has not been reported previously. PLA was chosen as it readily formed into uniform microfibres, but when spun as a random network it is notoriously difficult to handle, and an improvement was required. When produced using this method, the resulting scaffold was much easier to handle. It had improved E in the direction of the aligned component, compared to the random form of the same scaffold. The use of fluorescent dyes to label the weft and warp strands respectively, showed that the fibres are deposited in the desired manner, with one set of fibres exhibiting a distinct orientation, while the other set randomly whip across creating a tight interwoven network. This process is ideal for creating scaffolds that require additional strength in one direction, such as required by pelvic floor repair.

4.8.7 Electrospinning and electroweaving of PLA and PLA-(PMSSQcoPFPA) blended fibres

Another potential use of pseudo-woven scaffolds is for incorporating functional agents to promote specific cell responses. If the aligned fibres were functionalised to promote angiogenesis for example, this could be a simple way to encourage vessel formation through a scaffold. As proof of concept, PMSSQcoPFPA was incorporated into the aligned set of PLA fibres, and regular PLA was electrospun as the random weft fibres. PMSSQcoPFPA was selected as it can be used as a method to introduce functional peptide motifs on the scaffold, such as heparin and VEGF. This is important in that it may encourage angiogenesis. To be able to selectively functionalise parts of a scaffold is even better. Using the technique of electroweaving the PMSSQcoPFPA should only be incorporated in the aligned component. This is hard to prove *in situ* in the scaffold. A second scaffold of just randomly oriented PLA and PMSSQcoPFPA blended fibres was created to act as a positive control, and regular PLA as a negative control. Using the toluidine blue assay it was shown that a detectable amount of heparin was bound to the scaffolds containing PMSSQcoPFPA, in contrast to the PLA only scaffolds where no heparin was detected.

4.8.8 Cell culture on electrowoven PLA-co-(PLA/PMSSQ-co-PFPA)

Functionalising scaffolds with heparin is not new. Wang *et al.* demonstrated that heparin could be bound to bulk electrospun PCL scaffolds by washing with an ethylenediamine solution (to aminate the scaffold), and then washing

for a second time with a solution containing heparin.[250] This produced a scaffold with heparin immobilised on the surface. However, the benefit of incorporating PMSSQcoPFPA into a scaffold is that only the fibres containing the dopant are capable of binding heparin. This allows the scaffold to be selectively functionalised instead of the bulk scaffold, potentially providing control over how the scaffold forms a vascular network. Culturing cells on PMSSQcoPFPA doped pseudo-woven scaffolds demonstrated a clear change in cell morphology. When a woven scaffold was used, the cells elongated and aligned, but no scaffold out performed any other with regard to cell viability. There is a question over whether this is just due to the cells aligning with the aligned component of the scaffold, or if the PMSSQcoPFPA is having an effect. This should be investigated further.

4.8.9 Electrospinning of an aligned-random-aligned sandwich of PLA fibres

There are a number of scenarios where it is desirable to have a scaffold that will not contract or even expand perpendicular to an applied tension. Such examples are cleft palate repair and pelvic organ prolapse, where delicate tissues need to be supported even when under tension, without the device "necking". A search of the literature reveals very little work on creating electrospun scaffolds or biomaterials that are either auxetic, or have a low bulk Poisson's ratio. One example applies a pattern to a material imbuing the material with an extrinsic auxetic ability (Figure 4.44).[251] Such methods should definitely be investigated as one solution to this problem.

Figure 4.44: A geometric pattern than can be applied to a material to imbue it with auxetic properties.

Unfortunately, such patterning would render the material unsuitable for a barrier function, as it would create large holes for tissue to penetrate through, but it would be ideal for tissue regeneration that does not require a barrier function. The use of a mixture of aligned and random fibres as a sandwich creates a material that is not auxetic, but it does have a low Poisson's ratio. This behaviour is directly from the aligned component, random scaffolds have high Poisson's ratio and become thinner when stretched. Aligned scaffolds have poor handling properties perpendicular to the axis of the fibres, and are readily split. Sandwich scaffolds of aligned and random fibres exhibit the best of both worlds. They retain good mechanical properties parallel to the aligned component, but also do not fall apart then pulled perpendicular to the aligned fibres, due to the random component. A side effect is that the material also maintains a low Poisson's ratio while under tension, due to the aligned fibres. Materials with low Poisson's ratio are ideal for conditions such as pelvic floor,

as the material will not narrow or neck when under tension. This ensures support to the surrounding organs is maintained, and prevents the erosion observed with polypropylene meshes.[148–150]

4.9 Summary

Described here are simple methods for electrospinning bilayer and trilayer nanofibrous/microfibrous membranes, capable of supporting the culture of two very different cell types, while maintaining segregation between the two. It is hoped that these will prove useful in a range of applications, such as the first step in developing an approach for tissue engineering of cleft palate, and also guided tissue regeneration for periodontal disease, and in the production of tissue engineered skin for treatment of patients with extensive full thickness burns injuries.

Chapter 5

Discussion

Most tissues are not simple monolayers, and contain distinct structures and architectures, which are present for a reason. Designing scaffolds that mirror these should help achieve good incorporation, and eventual renewal of the target tissue. There are some significant challenges in creating a scaffold that can allow two distinct tissues to be cultured, without one tissue over-running the other, by virtue of it possessing a faster growth rate.

A solution to this problem would be applicable to many tissue engineering dilemmas, principally repair of a cleft palate, but the work contained here is also meant to provide a tool kit that can be applied to other situations. Each tissue engineering problem presents its own particular requirements, and a range of methods is required to adapt solutions to meet them. Cleft palate repair requires a barrier to enable slow growing bone tissue to develop preferentially over faster growing soft tissues. This needs to be coupled with a mechanism to allow for growth and expansion of the implanted tissues. Soft

tissue grafts and epidermal models require a cell impermeable barrier, and must be easy to handle. Other problems such as treating pelvic floor prolapse or stress urinary incontinence, require strength in the scaffold in one direction, and architectures designed to minimise construct necking when under tension. Finally, bladder regeneration requires a scaffold that can cyclically inflate and deflate, without fatigue, or a build up of pressure, to ensure protection of the kidneys.

The main hypotheses which were investigated in this PhD, and shall be discussed in turn, are that;

1. Microfibres and nanofibres can be produced in a range of polymers and architectures, by using the technique of electrospinning.
2. Cells perform differently on different architectures and polymers.
3. The scaffold's mechanical properties are dependent on architecture, as well as the polymer's intrinsic properties.
4. Cells respond to mechano-stimulation by up-regulating production of extracellular matrix.

5.1 Microfibres and nanofibres can be produced in a range of polymers and architectures, by using the technique of electrospinning

A range of microfibres and nanofibres can be produced from a range of polymers and in a variety of architectures, by using the technique of electrospinning. The velocity of the electrospinning collector determines if the final scaffold has a random (collector rotated slowly), or aligned (collector rotated fast) architecture. PHBV can be electrospun in DCM as a pearl necklace, but by using mixed solvent systems to increase the permittivity of the solution, nanofibres can be obtained. The solvent used can impact mechanical properties and scaffold architecture (e.g. DMF caused the PHBV fibres to weld together). PLA can be electrospun as microfibres, and a nanofibrous pearl necklace in DCM.

A source of inexpensive PLA has been identified, and has been shown to be identical to that originally used. PCL can be electrospun as microfibres, or a nanofibrous pearl necklace in DCM, and mixed solvent systems. The nanofibrous mixed solvent PCL scaffold produced an interesting "pock" marked architecture. PLGA can be electrospun as a nanofibrous scaffold using a mixed solvent system of DCM and MeOH.

A pseudo-woven architecture can be formed by electrospinning random and aligned fibres of PLA at the same time. This produces a scaffold that is easy to handle, and that has anisotropic mechanical properties. Functionality can be added to these scaffolds by incorporating PMSSQcoPFPA, which allows binding of proteins. This could be used in future to promote angiogenesis through

a scaffold. Finally, nanofibres of PHBV and microfibres of PLA can be combined, either in sequence to form scaffolds with bilayer and trilayer structures, or spun together to produce a trilayer that has microfibres throughout, and a central barrier where nanofibres bind the microfibres together.

5.2 Cells perform differently on different architectures and polymers

Cells perform differently on different scaffold architectures and polymers. Fibroblasts and hESMPs penetrate and fill microfibrous PLA scaffolds, but when cultured on nanofibrous PHBV both cell types form a layer on the surface, and are unable to penetrate the dense nanofibrous network. The PHBV scaffold is capable of preventing fibroblast infiltration for at least 6 weeks. Fibroblasts cultured on pseudo-woven PLA-co-(PLA-PMSSQcoPFPA) align with the grain of the scaffold, and cell viability is as good as scaffolds not containing PMSSQ-coPFPA. Finally, it has been shown that hESMPs cultures are viable on PLA, PCL, and PHBV based scaffolds.

5.3 The scaffold's mechanical properties are dependent on architecture, as well as the polymer's intrinsic properties

A scaffold's mechanical properties is dependent on architecture, as well as the polymer's intrinsic properties. It is possible, through the use of designed architectures, to construct a scaffold with novel mechanical properties. Here, PLA is electrospun as an aligned-random-aligned trilayer. This produces a scaffold with low Poisson's ratio. When the scaffold is placed under tension, the bulk structure does not neck. Such scaffolds have great potential for the problem of pelvic floor repair, where scaffolds that narrow can lacerate the surrounding tissues.

5.4 Cells respond to mechano-stimulation by up-regulating production of extracellular matrix

Cells respond to mechano-stimulation by up-regulating production of extracellular matrix. This was determined using a proof of concept biaxial bioreactors. The design of these were based on the estimated worst case expansion expected for a cleft palate defect (a doubling in surface area). Children's toy balloons were selected as they are inexpensive, can be sterilised by autoclave, and expand multiaxially when inflated. It was shown that balloons expand

anisotropically on inflation, and that the expansion varies between balloons. Balloons can be used as electrospinning collectors by coating with graphite, adding a small volume of a conducting liquid (such as IMS), or inflating with PBS. Sterile balloons filled with PBS could be aseptically coated with a bilayer scaffold, and fibroblasts subsequently cultured on the surface. A syringe pump was used to administer multiaxial distension. Increased elastin deposition was observed in the exercised system, compared to a static control.

This research highlighted the need to design a better culture system with more replicates. This necessitated investigations into alternative incubation chambers that could be adapted to include equipment to administer multiaxial distension. It was shown that an inexpensive propagator or an egg incubator were capable of maintaining the required temperature for cell culture.

A different proof of concept bioreactor (based on Ebers P3D chambers was investigated), to attempt to create a system with increased replicates. Although variability between chambers was high, increased elastin deposition was observed in the exercised system, compared to the static system. Finally, different pH buffer systems were investigated in order to determine if it was feasible to culture keratinocytes in a sealed bioreactor, with no gaseous CO_2 exchange. It was shown that bicarbonate is essential in keratinocyte culture medium, regardless of the pH buffer system used. A double buffer system of HEPES and bicarbonate was found to be the most effective pH buffer system, and could be used to create isolated bioreactor systems.

5.5 Synopsis

This thesis details a tool kit to create scaffolds. The scaffolds are designed to overcome the difficulties in treating problems such as cleft palate, and weakened pelvic floor tissues. This was achieved by investigating a number of hypotheses. Firstly, that microfibres and nanofibres can be produced from multiple polymers, in a variety of architectures, by using the technique of electrospinning. This has been achieved with monolayers of microfibres and nanofibres in a range of polymers. These monolayers can in turn, be combined together into complex multilayers, combining both nanofibres and microfibres, to make bilayer and trilayer scaffolds, that retain aspects of the monolayers' attributes.

The second hypothesis was that that cells perform differently on different architectures and polymers. This research has shown that nanofibres act as barrier membranes and prevent cell ingress, while microfibres encourage the proliferation of cells. Multilayered scaffolds of micro and nanofibres have been shown to have cell penetrable, and cell impenetrable regions, inherent in their design.

The third hypothesis was that a scaffold's mechanical properties are dependent on architecture, as well as the intrinsic properties of a given polymer. Combinations of aligned and random fibres have been investigated to create materials that while not auxetic, have low Poisson's ratio, to tackle the problem of scaffold contraction when under tension. Other methods, such as electrospinning onto a balloon to try to make a scaffold that incorporates corrugations, have been investigated. These furrows can unravel during multi-axial expansion, as

a secondary solution to making an implant that can flex with a patient, in order to minimise growth disturbances. This research shows that a scaffold's mechanical properties can be influenced by scaffold architecture.

The final hypothesis (cells respond to mechano-stimulation by up-regulating production of extracellular matrix), was demonstrated by the creation of proof of concept bioreactors. These can administer multi-axial distension to cells cultured on expanding constructs, continuously over an extended period of time. This work necessitated investigations into economical methods of providing the basic requirements for cell culture. This included maintaining constant temperature and also pH buffering in systems where it is either impracticable, or impossible, to change the medium, or gas in the system. At the time of writing there are no other systems found in the literature that are capable of completing such a task.

Chapter 6

Major findings, limitations and future directions

Through the careful selection and adaptation of key electrospinning parameters, such as concentration and solvent system, a variety of nanofibrous scaffolds can be produced in a number of different polymeric biomaterials.

Cells have been successfully cultivated on all of the scaffolds presented. Viability measurements have shown there is no great difference between cells cultured on microfibres compared to nanofibres. Cells tend to "see" nanofibrous scaffolds as a flat sheet, compared to microfibrous scaffolds that they proliferate through. This extends to attachment of cells on the respective scaffolds, there isn't a distinct difference between attachment to nanofibres or microfibres.

The one thing that does change is the intended use for the scaffold. Microfibres are clearly more suited to problems requiring a space filling aspect, where cells are required to fill a void. Nanofibres are great at providing sheets of cells. Nanofibres also lend themselves to the creation of cell impermeable barriers. When electrospun as dense mats, with demonstrably lower porosity, it is impossible for cells to squeeze through, instead they treat it as a flat surface. While the inherently porous structure of such electrospun scaffolds provide fenestrations not large enough for cells, they are more than large enough for nutrients and cytokines to permeate through.

It has been shown that two distinct cell populations (hESMPs and fibroblasts) can be cultured either side of a nanofibrous electrospun scaffold, without either population meeting by crossing the barrier. One criticism of this work is that although these barriers are impermeable to cells, they are porous enough for bacteria to penetrate into. In the context of surgery, this could result in the scaffold becoming a safe haven where immune surveillance by macrophages cannot reach the bacterial intruders. This should be investigated further, the solution may be as simple as determining how thin this barrier can be made, whilst still being effective as a barrier. An alternative could also be to consider the inclusion of antimicrobial agents, either immobilised within the nanoporous layer, or released over time.

This project showed that the microfibrous and nanofibrous scaffolds can be combined in order to meet more complex tissue engineering problems, that require a multifaceted solution.

One example is culturing, and encouraging, the proliferation of two distinct tissues with different rates of growth next to each other. Scaffolds can be elec-

trospun into bilayers and trilayers, consisting of microfibrous and nanofibrous regions, and then cells cultured on them. The nanofibrous component prevents the faster growing fibroblast over taking the slower developing hESMPs. While the microfibrous component provides the space filling element for cells to proliferate and fill. Ultimately, this is intended to create a substantial tissue as opposed to a thin sheet of cells.

The mechanical properties of composite multilayered scaffolds also change when compared to monolayers of the individual components. The individual scaffolds each contribute a component to the overall mechanical properties of the composite scaffolds, and produce a synergistic effect. This manifests itself in a E that is either an average, or greater than that of the E of the components. The E of the scaffolds produced is appropriate for the tissue engineering of the hard palate, the lead example in this thesis. While it has been demonstrated that materials with a low Poisson's ratio can be created, architectures that are auxetic have not. This area could be expanded with the creation of methods to spin intrinsically auxetic scaffolds, or to apply patterns to the final scaffold, and make an extrinsically auxetic scaffold.

Finally, this project attempted to tackle the issue of how cells could be cultured on scaffolds such as the above and stressed in two dimensions. It also attempted to determine what the effect would be on cellular extracellular matrix production. This is a complex area and no good solutions are currently commercially available.

A system was required that could keep samples in culture for long periods of time, provide replicates, and provide biaxially exercise. A number of proof-of-concept reactors were created. Practical issues, such as how to supply the

cells with everything they require (for example, constant temperature and pH regulation), while working under a strict budget have been discussed, and working solutions developed. The results of culturing cells while stressing them in two dimensions is clear. Cellular extracellular matrix production is up-regulated, as demonstrated in the production of elastin, when compared to a static control.

One criticism of this work is the use of toy balloons. Balloons do not allow for full characterisation of the forces a scaffold undergoes. Also, the size of the forces single cells feel on the scaffolds cannot be easily obtained.

This work is intended as a first step, a proof of concept. It is possible to create a system that can physically culture cells in a 2D dynamic environment for an extended period of time, and there is huge potential for further work in bringing this to maturation. The balloon could be easily substituted for a more predictable and uniform material. Strain gauges and measuring methods (whether mechanical or optical) could be incorporated, and should be investigated. The degree of distension, and regime applied, could be accurately modelled. Finally, the deposition of other extracellular matrix proteins besides elastin, could be investigated, and tuned, depending on the desired tissue engineering solution under investigation.

In order to be able to use such techniques, bioreactor technology needs to be further investigated. It has been shown here that simple designs can maintain cells in culture for a long period, and apply an exercise regime in 2D, but more work is required to enable incorporation of equipment such as strain gauges, and optical measurement devices.

Chapter 7

Bibliography

[1] JC Middleton and AJ Tipton. Synthetic biodegradable polymers as orthopedic devices. *Biomaterials*, 21:2335–2346, 2000.

[2] MI Sabir, X Xu, and L Li. A review on biodegradable polymer materials for bone tissue engineering applications. *Journal of material science.*, 44:5713–5724, 2009.

[3] JH Jang, O Castano, and HW Kim. Electrospun materials as potential platforms for bone tissue engineering. *Advanced drug delivery reviews*, 61:1065–1083, 2009.

[4] Technical data, 12 2013.

[5] Aldrich. *Handbook of fine Chemicals*. Sigma-Aldrich, 2010.

[6] D. Hutmacher, M. B. Hrzeler, and H. Schliephake. A review of material properties of biodegradable and bioresorbable polymers and devices for gtr and gbr applications. *Int J Oral Maxillofac Implants*, 11(5):667–678, 1996.

[7] A.Ni Annaidh, M. Ottenio, K. Bruyere, M. Destrade, and M.D. Gilchrist. Mechanical properties of excised human skin. In C.T. Lim and J.C.H. Goh, editors, *6th World Congress of Biomechanics (WCB 2010). August 1-6, 2010 Singapore*, volume 31 of *IFMBE Proceedings*, pages 1000–1003. Springer Berlin Heidelberg, 2010. ISBN 978-3-642-14514-8.

[8] Pil-Ryung Cha, Hyung-Seop Han, Gui-Fu Yang, Yu-Chan Kim, Ki-Ha Hong, Seung-Cheol Lee, Jae-Young Jung, Jae-Pyeong Ahn, Young-Yul Kim, Sung-Youn Cho, Ji Young Byun, Kang-Sik Lee, Seok-Jo Yang, and Hyun-Kwang Seok. Biodegradability engineering of biodegradable mg alloys: tailoring the electrochemical properties and microstructure of constituent phases. *Sci Rep*, 3:2367, Aug 2013.

[9] D. Puppi, N. Detta, A.M. Piras, F. Chiellini, D.A. Clarke, G.C. Reilly, and E. Chiellini. Development of electrospun three-arm star poly (ε-caprolactone) meshes for tissue engineering applications. *Macromolecular bioscience*, 10(8):887–897, 2010.

[10] K.M. Ainslie and T.A. Desai. Microfabricated implants for applications in therapeutic delivery, tissue engineering, and biosensing. *Lab Chip*, 8 (11):1864–1878, 2008.

[11] Sam Ali, S.P. Zhong, PJ Doherty, and DF Williams. Mechanisms of polymer degradation in implantable devices: I. poly (caprolactone). *Biomaterials*, 14(9):648–656, 1993.

[12] H. Sun, L. Mei, C. Song, X. Cui, and P. Wang. The in vivo degradation, absorption and excretion of pcl-based implant. *Biomaterials*, 27(9):1735–1740, 2006.

[13] Riitta Suuronen, Timo Pohjonen, Jarkko Hietanen, and Christian Lindqvist. A 5-year in vitro and in vivo study of the biodegradation of polylactide plates. *Journal of oral and maxillofacial surgery*, 56(5): 604–614, 1998.

[14] JE Bergsma, WC De Bruijn, FR Rozema, RRM Bos, and G Boering. Late degradation tissue response to poly (l-lactide) bone plates and screws. *Biomaterials*, 16(1):25–31, 1995.

[15] KA Blackwood, R McKean, I Canton, CO Freeman, KL Franklin, A Cole, I Brook, P Farthing, S Rimmer, JW Haycock, AJ Ryan, and S MacNeil. Development of biodegradable electrospun scaffolds for dermal replacement. *Biomaterials*, 29:3091–3104, 2008.

[16] Friederike von Burkersroda, Luise Schedl, and Achim Göpferich. Why degradable polymers undergo surface erosion or bulk erosion. *Biomaterials*, 23(21):4221–4231, Nov 2002.

[17] J. A. Tamada and R. Langer. Erosion kinetics of hydrolytically degradable polymers. *Proc Natl Acad Sci U S A*, 90(2):552–556, Jan 1993.

[18] David J. Walton and J. Phillip Lorimer. *Polymers (Oxford Chemistry Primers)*. Oxford University Press, USA, 2001. ISBN 019850389X.

[19] Yuuki Hirota, Naoko Yoshie, Nariaki Ishii, Ken-ichi Kasuya, and Yoshio Inoue. Correlation between solid-state structures and enzymatic degradability of cocrystallized blends. *Macromolecular Bioscience*, 5(11):1094–1100, Nov 2005.

[20] J. M. Schakenraad, M. J. Hardonk, J. Feijen, I. Molenaar, and P. Nieuwenhuis. Enzymatic activity toward poly(l-lactic acid) implants. *J Biomed Mater Res*, 24(5):529–545, May 1990.

[21] S. A. Ali, P. J. Doherty, and D. F. Williams. Mechanisms of polymer degradation in implantable devices. 2. poly(dl-lactic acid). *J Biomed Mater Res*, 27(11):1409–1418, Nov 1993.

[22] G.-Q. Chen. *Plastics from Bacteria: Natural Functions and Applications (Microbiology Monographs)*. Springer, 2010. ISBN 3642032869.

[23] EI Shishatskaya, TG Volova, and II Gitelson. In vivo toxicological evaluation of polyhydroxyalkanoates. *Doklady Biological Sciences*, 383:109–111, 2001.

[24] S. Rathbone, P. Furrer, J. Lbben, M. Zinn, and S. Cartmell. Biocompatibility of polyhydroxyalkanoate as a potential material for ligament and tendon scaffold material. *J Biomed Mater Res A*, 93(4):1391–1403, Jun 2010.

[25] Luzier WD. Materials derived from biomas/biodegradable materials. *Proceeds of the National Academy of sciences*, 89:839–842, 1992.

[26] D Byrom. Production of poly-β-hydroxybutyrate: polyhydroxy-β-hydroxyvalerate copolymers. *Microbiology Reviews*, 103:247–250, 92.

[27] Bronwyn Laycock, Peter Halley, Steven Pratt, Alan Werker, and Paul Lant. The chemomechanical properties of microbial polyhydroxyalkanoates. *Progress in Polymer Science*, Aug 2013.

[28] SJ Holland, AM Jolly, M Yasin, and BJ Tighe. Polymers for biodegradable medical devices. II. hydroxybutyrate-hydroxyvalerate copolymers: hydrolytic degradation studies. *Biomaterials*, 8:289–295, 1987.

[29] M Yasin, SJ Hollands, and BJ Tighe. Polymers for biodegrable medical devices V. hydroxybutyrate-hydroxyvalerate copolymers: effects of polymer processing on hydrolytic degradation. *Biomaterials*, 11:451–455, 1990.

[30] H Li, W Zhai, and J Chang. In vitro biocompatibility assessment of phbv/wollastonite composites. *Journal of Material Science: Materials in Medicine*, 19:67–73, 2008.

[31] D'Agnostino and William. Recombinant expressed bioadsorbable polyhydroxyalkonate monofilament and multi-filaments self-retaining stutures., 2009.

[32] M Wang. Developing bioactive composite materials for tissue replacement. *Biomaterials*, 24:2133–2151, 2003.

[33] EM Engelhardt, LA Micol, S Houis, FM Wurm, J Hilborn, JA Hubbell, and P Frey. A collagen-poly(lactic acid-co-ε-caprolactone) hybrid scaffold for bladder tissue regeneration. *Biomaterials*, 32:3969–3976, 2011.

[34] LJ Suggs and SA Moore. *Physical properties of polymers handbook*, chapter 55, pages 939–950. Springer, 2 edition, 2007.

[35] TA Telemeco, C Ayres, GL Bowlin, GE Wnek, ED Boland, N Cohen, CM Baumgarten, J Mathews, and DG Simpson. Regulation of cellular infiltration into tissue engineering scaffolds composed of submicron diameter fibrils produced by electrospinning. *Actabiomaterialia*, 1:377–385, 2005.

[36] F Yang, R Maurugan, S Wang, and S Ramakrishna. Electrospinning of nano/micro scale poly(l-lactic acid) aligned fibers and their potential in neural tissue engineering. *Biomaterials*, 26:2603–2610, 2005.

[37] I Canton, R McKean, M Charnley, KA Blackwood, C Fiorica, AJ Ryan, and SM MacNeil. Development of an ibuprofen-releasing biodegradable pla/pga electrospun scaffold for tissue regeneration. *Biotechnology and bioengineering*, 105:396–408, 2010.

[38] H. Pistner, R. Gutwald, R. Ordung, J. Reuther, and J. Mühling. Poly (l-lactide): a long-term degradation study in vivo: I. Biological results. *Biomaterials*, 14(9):671–677, 1993.

[39] H Pistner, D Bendi, J Muhling, and J Reuther. Poly (l-lactide): a long-term degradation study in vivo part III. Analytical characterization. *Biomaterials*, 14(4):291–298, 1993.

[40] H Pistner, H Stallforth, R Gutwald, J Muhling, J Reuther, and C Michel. Poly(l-lactide): a long-term degradation study in vivo part II: Physicomechanical behaviour of implants. *Biomaterials*, 15(6):439–450, May 1994.

[41] M. Labet and W. Thielemans. Synthesis of polycaprolactone: a review. *Chem. Soc. Rev.*, 38(12):3484–3504, 2009.

[42] Daniel Kessler and Patrick Theato. Reactive surface coatings based on polysilsesquioxanes: defined adjustment of surface wettability. *Langmuir*, 25(24):14200–14206, Dec 2009.

[43] Daniel Kessler, Peter J Roth, and Patrick Theato. Reactive surface coatings based on polysilsesquioxanes: controlled functionalization for specific protein immobilization. *Langmuir*, 25(17):10068–10076, Sep 2009.

[44] Daniel Kessler, Florian D Jochum, Jiyeon Choi, Kookheon Char, and Patrick Theato. Reactive surface coatings based on polysilsesquioxanes: universal method toward light-responsive surfaces. *ACS Appl Mater Interfaces*, 3(2):124–128, Feb 2011.

[45] Daniel Kessler, Maria C Lechmann, Seunguk Noh, Rdiger Berger, Changhee Lee, Jochen S Gutmann, and Patrick Theato. Surface coatings based on polysilsesquioxanes: solution-processible smooth hole-injection

layers for optoelectronic applications. *Macromol Rapid Commun*, 30(14): 1238–1242, Jul 2009.

[46] Daniel Kessler and Patrick Theato. Synthesis of functional inorganic-organic hybrid polymers based on poly(silsesquioxanes) and their thin film properties. *Macromolecules*, 41(14):5237–5244, 2008.

[47] John Chiefari, Y. K. (Bill) Chong, Frances Ercole, Julia Krstina, Justine Jeffery, Tam P. T. Le, Roshan T. A. Mayadunne, Gordon F. Meijs, Catherine L. Moad, Graeme Moad, and et al. Living free-radical polymerization by reversible additionfragmentation chain transfer: the raft process. *Macromolecules*, 31(16):5559–5562, Aug 1998.

[48] John Chiefari, Roshan T. A. Mayadunne, Catherine L. Moad, Graeme Moad, Ezio Rizzardo, Almar Postma, , and San H. Thang. Thiocarbonylthio compounds (sc(z)sr) in free radical polymerization with reversible addition-fragmentation chain transfer (raft polymerization). effect of the activating group z. *Macromolecules*, 36(7):2273–2283, 2003.

[49] Y. K. Chong, Julia Krstina, Tam P. T. Le, Graeme Moad, Almar Postma, Ezio Rizzardo, and San H. Thang. Thiocarbonylthio compounds [sc(ph)sr] in free radical polymerization with reversible addition-fragmentation chain transfer (raft polymerization). role of the free-radical leaving group (r). *Macromolecules*, 36(7):2256–2272, 2003.

[50] J Zeleny. The electrical discharge from liquid points, and a hydrostatic method of measureing the electric intensity at their surfaces. *The Physical Review*, 3:69–91, 1914.

[51] Geoffrey Taylor. Disintegration of water drops in an electric field. *Proceedings of the Royal Society of London. Series A. Mathematical and Physical Sciences*, 280(1382):383–397, 1964.

[52] A Formhals. Process and apparatus for preparing artifical threads, 1934.

[53] AE Martin and ID Cockshott. Fibrillar product of electrostatically spun organic material, 1977.

[54] R Hans Tromp, Carolien Vink, and Ann C Stijnman. Encapsulation by electrospinning of live bacteria used in the food industry. *Gums and Stabilisers for the Food Industry Sixteen*, 16:247, 2012.

[55] V Thavasi, G Singh, and S Ramakrishna. Electrospun nanofibers in energy and environmental applications. *Energy & Environmental Science*, 1(2):205–221, 2008.

[56] Luana Persano, Andrea Camposeo, Cagri Tekmen, and Dario Pisignano. Industrial upscaling of electrospinning and applications of polymer nanofibers: A review. *Macromolecular Materials and Engineering*, 2013.

[57] CJ Luo, Simeon D Stoyanov, E Stride, E Pelan, and M Edirisinghe. Electrospinning versus fibre production methods: from specifics to technological convergence. *Chemical Society Reviews*, 41(13):4708–4735, 2012.

[58] JM Deitzel, J Kleinmeyer, D Harris, and NC Beck Tan. The effect of processing variables on the morphology of electrospun nanofibres and textiles. *Polymer*, 42:261–272, 2001.

[59] SV Fridrikh, JH Yu, MP Brenner, and GC Rutledge. Controlling the fiber diameter during electrospinning. *Physical review letters*, 90:1–4, 2003.

[60] T Jarusuwannapoom, W Hongrojjanawiwat, S Jitjaicham, L Wannaton, M Nithitanakul, C Pattamaprom, P Koombhongse, R Ranghupan, and P Supaphol. Effect of solvents on electro-spinability of polystyrene solutions and morphological appearance of resulting electrospun polystyrene fibres. *European polymer journal*, 41:409–421, 2005.

[61] H Fong, I Chun, and DH Reneker. Beaded nanofibres formed during electrospinning. *Polymer*, 40:4585–4592, 1999.

[62] Arkadii Arinstein and Eyal Zussman. Electrospun polymer nanofibers: mechanical and thermodynamic perspectives. *Journal of Polymer Science Part B: Polymer Physics*, 49(10):691–707, 2011.

[63] Jan Pelipenko, Julijana Kristl, Romana Rošic, Saša Baumgartner, and Petra Kocbek. Interfacial rheology: An overview of measuring techniques and its role in dispersions and electrospinning. *Acta Pharmaceutica*, 62 (2):123–140, 2012.

[64] J-H He, Y Liu, and L Xu. Apparatus for preparing electrospun nanofibres: a comparative review. *Materials Science and Technology*, 26(11): 1275–1287, 2010.

[65] Nandana Bhardwaj and Subhas C Kundu. Electrospinning: a fascinating fiber fabrication technique. *Biotechnol Adv*, 28(3):325–347, 2010.

[66] Roya Nezarati, Michelle Eifert, and Elizabeth Cosgriff-Hernandez. Effects of humidity and solution viscosity on electrospun fiber morphology. *Tissue Eng Part C Methods*, Mar 2013.

[67] Chi Wang, Yong-Wen Cheng, Chia-Hung Hsu, Huan-Sheng Chien, and Shih-Yung Tsou. How to manipulate the electrospinning jet with controlled properties to obtain uniform fibers with the smallest diameter? a brief discussion of solution electrospinning process. *Journal of Polymer Research*, 18(1):111–123, 2011.

[68] Songting Tan, Xianwei Huang, and Bolin Wu. Some fascinating phenomena in electrospinning processes and applications of electrospun nanofibers. *Polymer International*, 56(11):1330–1339, 2007.

[69] Gregory C Rutledge and Sergey V Fridrikh. Formation of fibers by electrospinning. *Advanced Drug Delivery Reviews*, 59(14):1384–1391, 2007.

[70] Kenneth Lin, Kian-Ngiap Chua, Gregory T. Christopherson, Shawn Lim, and Hai-Quan Mao. Reducing electrospun nanofiber diameter and variability using cationic amphiphiles. *Polymer*, 48(21):6384–6394, Oct 2007.

[71] Sander De Vrieze, Tamara Van Camp, A Nelvig, B Hagström, Philippe Westbroek, and Karen De Clerck. The effect of temperature and humidity on electrospinning. *Journal of materials science*, 44(5):1357–1362, 2009.

[72] Oliver Hardick, Bob Stevens, and Daniel G Bracewell. Nanofibre fabrication in a temperature and humidity controlled environment for improved fibre consistency. *Journal of materials science*, 46(11):3890–3898, 2011.

[73] X & Lin T Niu, H & Wang. Upward needleless electrospinning of nanofibers. *Journal of Engineered Fibers and Fabrics*, 7:17–22, 2012.

[74] Haitao Niu and Tong Lin. Fiber generators in needleless electrospinning. *Journal of Nanomaterials*, 2012:1–13.

[75] Method of nanofibres production from a polymer solution using electrostatic spinning and a device for carrying out the method, 2009.

[76] Toby D. Brown, Paul D. Dalton, and Dietmar W. Hutmacher. Direct writing by way of melt electrospinning. *Advanced Materials*, 23(47): 5651–5657, Dec 2011.

[77] Tao Sun, David Norton, Robert J McKean, John W Haycock, Anthony J Ryan, and Sheila MacNeil. Development of a 3d cell culture system for investigating cell interactions with electrospun fibers. *Biotechnol Bioeng*, 97(5):1318–1328, Aug 2007.

[78] Cameron Ball, Emily Krogstad, Thanyanan Chaowanachan, and Kim A Woodrow. Drug-eluting fibers for hiv-1 inhibition and contraception. *PLoS One*, 7(11):e49792, 2012.

[79] Elham Hoveizi, Mohammad Nabiuni, Kazem Parivar, Sareh Rajabi-Zeleti, and Shima Tavakol. Functionalisation and surface modification of electrospun polylactic acid scaffold for tissue engineering. *Cell Biology International*, 38(1):41–49, Jan 2014.

[80] Ana Paula Serafini Immich, Manuel Lis Arias, Nria Carreras, Rafael Lus Boemo, and Jos Antonio Tornero. Drug delivery systems using sandwich configurations of electrospun poly(lactic acid) nanofiber membranes and ibuprofen. *Mater Sci Eng C Mater Biol Appl*, 33(7):4002–4008, Oct 2013.

[81] Larissa G. Santos, Daniel C. Oliveira, Michele S L. Santos, Lia Mara G. Neves, Fernanda O G. de Gaspi, Fernanda A S. Mendona, Marcelo A M.

Esquisatto, Glucia M T. Santos, M. A. d'Avila, and Lucia H Innocentini Mei. Electrospun membranes of poly(lactic acid) (pla) used as scaffold in drug delivery of extract of sedum dendroideum. *J Nanosci Nanotechnol*, 13(7):4694–4702, Jul 2013.

[82] Beom-Su Kim, Ko Eun Park, Won Ho Park, and Jun Lee. Fabrication of nanofibrous scaffold using a pla and hagfish thread keratin composite; its effect on cell adherence, growth, and osteoblast differentiation. *Biomedical Materials*, 8(4):045006, Jun 2013.

[83] Dario Puppi, Nicola Detta, Anna Maria Piras, Federica Chiellini, David A. Clarke, Gwendolen C. Reilly, and Emo Chiellini. Development of electrospun three-arm star poly(-caprolactone) meshes for tissue engineering applications. *Macromol Biosci*, 10(8):887–897, Aug 2010.

[84] Paul D. Dalton, Tim Woodfield, and Dietmar W. Hutmacher. Snapshot: Polymer scaffolds for tissue engineering. *Biomaterials*, 30(4):701–702, Feb 2009.

[85] Andrew Krishna Ekaputra, Yefang Zhou, Simon McKenzie Cool, and Dietmar Werner Hutmacher. Composite electrospun scaffolds for engineering tubular bone grafts. *Tissue Eng Part A*, 15(12):3779–3788, Dec 2009.

[86] Dietmar W. Hutmacher, Kee Woei Ng, Christian Kaps, Michael Sittinger, and Svea Klring. Elastic cartilage engineering using novel scaffold architectures in combination with a biomimetic cell carrier. *Biomaterials*, 24(24):4445–4458, Nov 2003.

[87] D. W. Hutmacher. Scaffold design and fabrication technologies for engineering tissues–state of the art and future perspectives. *J Biomater Sci Polym Ed*, 12(1):107–124, 2001.

[88] D. W. Hutmacher. Scaffolds in tissue engineering bone and cartilage. *Biomaterials*, 21(24):2529–2543, Dec 2000.

[89] T H B. Eriksen, E. Skovsen, and P. Fojan. Release of antimicrobial peptides from electrospun nanofibres as a drug delivery system. *J Biomed Nanotechnol*, 9(3):492–498, Mar 2013.

[90] M. Rampichova, J. Chvojka, M. Buzgo, E. Prosecka, P. Mikes, L. Vyslouzilova, D. Tvrdik, P. Kochova, T. Gregor, D. Lukas, and E. Amler. Elastic three-dimensional polycaprolactone nanofibre scaffold enhances migration, proliferation and osteogenic differentiation of mesenchymal stem cells. *Cell Prolif*, 46(1):23–37, Feb 2013.

[91] Ho-Wang Tong and Min Wang. Electrospinning of fibrous polymer scaffolds using positive voltage or negative voltage: a comparative study. *Biomed Mater*, 5(5):054110, Oct 2010.

[92] Ho-Wang Tong and Min Wang. An investigation into the influence of electrospinning parameters on the diameter and alignment of poly(hydroxybutyrate-co-hydroxyvalerate) fibers. *Journal of Applied Polymer Science*, 120(3):1694–1706, 2011.

[93] Ho-Wang Tong and Min Wang. Electrospinning of poly(hydroxybutyrate-co-hydroxyvalerate) fibrous tissue engineering scaffolds in two different electric fields. *Polymer Engineering & Science*, 51(7):1325–1338, 2011.

[94] Weiwei Zuo, Meifang Zhu, Wen Yang, Hao Yu, Yanmo Chen, and Yu Zhang. Experimental study on relationship between jet instability and formation of beaded fibers during electrospinning. *Polymer Engineering & Science*, 45(5):704–709, 2005.

[95] Ivan Martin, David Wendt, and Michael Heberer. The role of bioreactors in tissue engineering. *Trends in Biotechnology*, 22(2):80–86, 2004.

[96] Federico Vozzi, Maria Angela Guzzardi, Arti Devi, Giovanni Vozzi Ahluwalia, and Claudio Domenici. Cell cross-talk analysis in static and dynamic multi-compartmental bioreactor. *IEEE*, 2007.

[97] Brandon D Riehl, Jae-Hong Park, Il Keun Kwon, and Jung Yul Lim. Mechanical stretching for tissue engineering: two-dimensional and three-dimensional constructs. *Tissue Eng Part B Rev*, 18(4):288–300, Aug 2012.

[98] Katia Bilodeau and Diego Mantovani. Bioreactors for tissue engineering: focus on mechanical constraints. a comparative review. *Tissue Eng*, 12 (8):2367–2383, Aug 2006.

[99] Richard Balint, Nigel J Cassidy, and Sarah H Cartmell. Electrical stimulation: a novel tool for tissue engineering. *Tissue Eng Part B Rev*, 19 (1):48–57, Feb 2013.

[100] Ralf Portner, Stephanie Nagel-Heyer, Christiane Goepfert, Peter Adamietz, and Norbert M. Meenen. Bioreactor design for tissue engineering. *Journal of Bioscience and Bioengineering*, 100(3):235–245, 2005.

[101] Jan Hansmann, Florian Groeber, Alexander Kahlig, Claudia Kleinhans, and Heike Walles. Bioreactors in tissue engineering -principles, applications and commercial constraints. *Biotechnol J*, 8(3):298–307, Mar 2013.

[102] Fahimeh Sadat Tabatabaei, Marzieh Vahid Dastjerdi, Maryam Jazayeri, Nooshin Haghighipour, Elahe Vahid Dastjerdie, and Marziyeh Bordbar. Comparison of osteogenic medium and uniaxial strain on differentiation of endometrial stem cells. *Dental Research Journal*, 10(2), 2013.

[103] R. M. Delaine-Smith, S. MacNeil, and G. C. Reilly. Matrix production and collagen structure are enhanced in two types of osteogenic progenitor cells by a simple fluid shear stress stimulus. *Eur Cell Mater*, 24:162–174, 2012.

[104] RMH Rumney, A Sunters, GC Reilly, and A Gartland. Application of multiple forms of mechanical loading to human osteoblasts reveals increased atp release in response to fluid flow in 3d cultures and differential regulation of immediate early genes. *Journal of biomechanics*, 45 (3):549–554, 2012.

[105] A. Sittichokechaiwut, J. H. Edwards, A. M. Scutt, and G. C. Reilly. Short bouts of mechanical loading are as effective as dexamethasone at inducing matrix production by human bone marrow mesenchymal stem cell. *Eur Cell Mater*, 20:45–57, 2010.

[106] Christopher J OConor, Natasha Case, and Farshid Guilak. Mechanical regulation of chondrogenesis. *Stem cell research & therapy*, 4(4):1–13, 2013.

[107] Jo A Hannafin, Erik A Attia, Ross Henshaw, Russell F Warren, and Madhu M Bhargava. Effect of cyclic strain and plating matrix on cell proliferation and integrin expression by ligament fibroblasts. *J Orthop Res*, 24(2):149–158, Feb 2006.

[108] Vishal Gupta and K. Jane Grande-Allen. Effects of static and cyclic loading in regulating extracellular matrix synthesis by cardiovascular cells. *Cardiovasc Res*, 72(3):375–383, Dec 2006.

[109] Matthias Chiquet, Laurent Gelman, Roman Lutz, and Silke Maier. From mechanotransduction to extracellular matrix gene expression in fibroblasts. *Biochim Biophys Acta*, 1793(5):911–920, May 2009.

[110] J. Revuz, H. Adhoute, J.P. Cesarini, F. Poli, C. Lacarriere, and C. Emiliozzi. Clinical and histological effects of the lift 6 device used on facial skin ageing. *Les Nouvelles Dermatologiques*, 21:335–342, 2002.

[111] Soroor Sharifpoor, Craig A. Simmons, Rosalind S. Labow, and J. Paul Santerre. A study of vascular smooth muscle cell function under cyclic mechanical loading in a polyurethane scaffold with optimized porosity. *Acta Biomaterialia*, 6(11):4218–4228, Nov 2010.

[112] T-Q. Wei, D-Y. Luo, L. Chen, T. Wu, and K-J. Wang. Cyclic hydrodynamic pressure induced proliferation of bladder smooth muscle cells via integrin alpha5 and fak. *Physiol Res*, Nov 2013.

[113] D T K. Malcolm, P M F. Nielsen, P. J. Hunter, and P. G. Charette. Strain measurement in biaxially loaded inhomogeneous, anisotropic elastic membranes. *Biomech Model Mechanobiol*, 1(3):197–210, Dec 2002.

[114] P M F. Nielsen, D T K. Malcolm, P. J. Hunter, and P. G. Charette. Instrumentation and procedures for estimating the constitutive parameters of inhomogeneous elastic membranes. *Biomech Model Mechanobiol*, 1(3):211–218, Dec 2002.

[115] Y. A. Kvistedal and P M F. Nielsen. Estimating material parameters of human skin in vivo. *Biomech Model Mechanobiol*, 8(1):1–8, Feb 2009.

[116] P. S. Howard, U. Kucich, R. Taliwal, and J. M. Korostoff. Mechanical forces alter extracellular matrix synthesis by human periodontal ligament fibroblasts. *J Periodontal Res*, 33(8):500–508, Nov 1998.

[117] Sarah R. Rathbone, John R. Glossop, Julie E. Gough, and Sarah H. Cartmell. Cyclic tensile strain upon human mesenchymal stem cells in 2d and 3d culture differentially influences ccnl2, wdr61 and bahcc1 gene expression levels. *J Mech Behav Biomed Mater*, 11:82–91, Jul 2012.

[118] R. Langer and J. P. Vacanti. Tissue engineering. *Science*, 260(5110): 920–926, May 1993.

[119] E Simpson, J Weiner, editor. *Oxford English Dictionary*. Clarendon Press, 2 edition, 1989.

[120] LG Griffith and AJ Grodzinsky. Advances in biomedical engineering. *Opportunities for medical research*, 285:556–561, 2001.

[121] Y Ikada. Challenges in tissue engineering. *Interface*, 3:589–601, 2006.

[122] PH Warnke, I Springer, Y Acil, H Bolte, PAJ Russo, E Sherry, H Terheyden, J Wiltfang, H Eufinger, E Behrens, and M Wehmoller. Growth and transplantation of a custom vascularised bone graft in a man. *Lancet*, 364:766–770, 2004.

[123] PH Warnke, J Wiltfang, I Springer, Y Acil, H Bolte, M Kosmahl, PAJ Russo, E Sherry, U Lutzen, S Wolfart, and H Terheyden. Man as living bioreactor: Fate of an exogenously prepared customized tissue-engineered mandible. *Biomaterials*, 27:3163–3167, 2006.

[124] S Terada, M Sato, A Sevy, and JP Vacanti. Tissue engineering in the twenty-first century. *Yonsei Medical Journal*, 41:685–691, 2000.

[125] KC Rustad, M Sorkin, B Levi, MT Longaker, and GC Gurtner. Strategies for organ level tissue engineering. *Organogenesis*, 6:151–157, 2010.

[126] JW Larrick and A Mendelsohn. Applied healthspan engineering. *Rejuvenation research*, 13:265–280, 2010.

[127] W Rowinski. Future of transplantation medicine. *Annals of transplantation*, 12:5–10, 2007.

[128] PH Warnke. Repair of human face by allotransplantation. *Lancet*, 368: 181–183, 2006.

[129] S Bhargava, CR Chappel, AJ Bullock, C Layton, and SM MacNeil. Tissue-engineered buccal mucosa for substitution urethroplasty. *British Journal of Urology*, 93:807–811, 2004.

[130] S Bhargava, JM Patterson, RD Inman, SM MacNeil, and CR Chapple. Tissue-engineering buccal mucosa urethroplasty - clinical outcomes. *European Urology*, 53:1263–1271, 2008.

[131] AH Yen and PC Yelick. Dental tissue regeneration - a mini-review. *Gerontology*, 57:85–94, 2010.

[132] M Retzepi and N Donos. Guided bone regeneration: biological principle and therapeutic applications. *Clinical oral implants research*, 21:567–576, 2010.

[133] JL Moreau, JF Caccamese, DP Coletti, JJ Sauk, and JP Fisher. Tissue engineering solutions for cleft palates. *Journal of oral maxillofacial surgery*, 65:2503–2511, 2007.

[134] S Ivanovski. Periodontal regeneration. *Australian Dental Journal*, 54: S118–S128, 2009.

[135] D Lundgren and C Slotte. Reconstruction of anatomically complicated periodontal defects using a bioresorbable GTR barrier supported by bone mineral. a 6-month follow-up study of 6 cases. *Journal of clinical periodontology*, 26:56–62, 1999.

[136] MM Bornstein, DD Bosshardt, D Buser, ST Chen, SS Jensen, I Rocchietta, RK Schenk, M Simion, and T von Arx. *20 Years of guided bone regeneration in implant dentistry.* Quintessence Publishing Co, Inc, 1994. 86-139 pp.

[137] LC Parrish, T Miyamoto, N Fong, JS Mattson, and DR Cerutis. Non-bioabsorbable vs. bioabsorbable membrane: assessment of their clinical efficacy in guided tissue regeneration technique. A systematic review. *Journal of oral science*, 51:383–400, 2009.

[138] SS Kim and BS Kim. Comparision of osteogenic potential between apatitie-coated poly(lactide-co-glycolide)/hydroxyapatite particulates and bio-oss®. *Dental Materials Journal*, 27:368–375, 2008.

[139] B Wenz, B Oesch, and M Horst. Analysis of the risk of transmitting bovine spongiform encephalopathy through bone grafts derived from bovine bone. *Biomaterials*, 22:1599–1606, 2001.

[140] NHS. NHS choices, 2010.

[141] Richard E Hautmann, Robert C de Petriconi, and Bjoern G Volkmer. 25 years of experience with 1,000 neobladders: long-term complications. *The Journal of urology*, 185(6):2207–2212, 2011.

[142] N. Shakhssalim, M. M. Dehghan, R. Moghadasali, M. H. Soltani, I. Shabani, and M. Soleimani. Bladder tissue engineering using biocompatible nanofibrous electrospun constructs: feasibility and safety investigation. *Urol J*, 9(1):410–419, 2012.

[143] H. H. Ahvaz, M. Soleimani, H. Mobasheri, B. Bakhshandeh, N. Shakhssalim, S. Soudi, M. Hafizi, M. Vasei, and M. Dodel. Effective combination of hydrostatic pressure and aligned nanofibrous scaffolds on human bladder smooth muscle cells: implication for bladder tissue engineering. *J Mater Sci Mater Med*, Jun 2012.

[144] Anthony Atala, Stuart B Bauer, Shay Soker, James J Yoo, and Alan B Retik. Tissue-engineered autologous bladders for patients needing cystoplasty. *The Lancet*, 367(9518):1241–1246, Apr 2006.

[145] A. Atala. Bladder regeneration by tissue engineering. *BJU Int*, 88(7): 765–770, Nov 2001.

[146] A. Atala. Tissue engineering of human bladder. *British Medical Bulletin*, 97(1):81–104, Mar 2011.

[147] Susan L Hendrix, Amanda Clark, Ingrid Nygaard, Aaron Aragaki, Vanessa Barnabei, and Anne McTiernan. Pelvic organ prolapse in the women's health initiative: gravity and gravidity. *American journal of obstetrics and gynecology*, 186(6):1160–1166, 2002.

[148] Ketul Shah, Dmitriy Nikolavsky, Daniel Gilsdorf, and Brian J Flynn. Surgical management of lower urinary mesh perforation after mid-urethral polypropylene mesh sling: mesh excision, urinary tract reconstruction and concomitant pubovaginal sling with autologous rectus fascia. *International urogynecology journal*, pages 1–7, 2013.

[149] B Klosterhalfen and U Klinge. Retrieval study at 623 human mesh explants made of polypropylene–impact of mesh class and indication for mesh removal on tissue reaction. *Journal of Biomedical Materials Research Part B: Applied Biomaterials*, 2013.

[150] Food and Drug Administration. FDA safety communication: update on serious complications associated with transvaginal placement of surgical mesh for pelvic organ prolapse, July 2011. http://www.fda.gov/MedicalDevices/Safety/AlertsandNotices/ucm262435.htm.

[151] VW Diewert. A quantitative coronal plane evaluation of carniofacial growth and spatial relations during secondary palate development in the rat. *Archives of Oral Biology*, 23:607 to 629, 1978.

[152] H Yoon, IS Chung, EY Seol, BY Park, and HW Park. Development of the lip and palate in staged human embryos and early fetuses. *Yonsei Medical Journal*, 41(4):447–484, 2000.

[153] JW Parker. *Gray's Anatomy*. Elsevier, 2008.

[154] P Mossey. Addressing the global challenges of craniofacial anomalies. report of a WHO meeting on international collaborative research on craniofacial anomalies. Technical report, World Health Organisation, 20 Avenue Appia, 1211 Geneva 27, Switzerland, 2004.

[155] J Lilja. Cleft lip and palate surgery. *Scandinavian Journal of Surgery*, 92:269–273, 2003.

[156] FK Wong and U Hagg. An update on the aetiology of orofacial clefts. *Hong Kong Medical Journal*, 10:331 to 336, 2004.

[157] AC Lidral, LM Moreno, and SA Bullard. Genetic factors and orofacial clefting. *Seminars in Orthodontics.*, 14:103 to 114, 2008.

[158] J Little, A Cardy, and RG Munger. Tobacco smoking and oral clefts: a meta-analysis. *Bulletin of the World Health Organisation*, 82:213–218, 2004.

[159] GL Wehby and JC Murray. Folic acid and orofacial clefts: a review of the evidence. *Oral Diseases*, 16:11 to 19, 2010.

[160] MM Yazdy, MA Honein, and J Xing. Reduction in orofacial clefts following folic acid fortification of the U.S. grain supply. *Birth Defects Research*, 79:16–23, 2007.

[161] AE Czeizel and I Dudas. Prevention of the first occurence of neural-tube defects by periconceptional vitamin supplementation. *The New England Journal of Medicine*, pages 1832–1835, 1992.

[162] CY Johnson and J Little. Folate intake, markers of folate status and oral clefts: is the evidence converging? *International Journal of Epidemiology*, 37:1041–1058, 2008.

[163] PR Itikala, ML Watkins, J Mulinare, CA Moore, and L Liu. Maternal multivitamin use in orofacial clefts in offspring. *Tetraology*, 63:79–86, 2001.

[164] JD Atherton. Morphology of facial bones in skulls with unoperated unilateral cleft palate. *Morphology*, 4:18–30, 1967.

[165] JT Lambrecht, T Kreusch, and L Schulz. Position, shape and dimensions of the maxilla in unoperated cleft lip and palate patients: Review of the literature. *Clinical Anatomy*, 13:121–133, 2000.

[166] FE Law and JT Fulton. Unoperated oral clefts at maturation. *American Journal of Public Health*, 49:1517–1524, 1959.

[167] LA Will. Growth and development in patients with untreated clefts. *Cleft Palate-Craniofacial Journal*, 37:523–526, 2000.

[168] BC Sommerland. Surgical management of cleft palate: a review. *Journal of the Royal Society of Medicine.*, 82:677–679, 1989.

[169] G Nellhaus. Head circumference from birth to eighteen years. *Paediatrics*, 41:106–114, 1968.

[170] RJ Langford, S Sgouros, K Natarajan, H Nishikawa, MS Dover, and AD Hockley. Maxillary volume growth in childhood. *Plastic and reconstructive surgery*, 111:1591–1597, 2003.

[171] DH Enlow and MG Hans. *Essentials of Facial Growth*. Saunders, 1996.

[172] AA Delgado, NG Schaaf, and L Emrich. Trends in prosthodontic treatment of cleft palate patients at one institution: A twenty one year review. *Cleft Palate-Craniofacial Journal*, 29:425–428, 1992.

[173] YF Liao, TJ Cole, and M Mars. Hard palate repair timing and facial growth in unilateral cleft lip and palate: a longitudinal study. *Cleft Palate-Craniofacial Journal*, 43:547–556, 2006.

[174] G Semb. Effect of alveolar bone grafting on maxillary growth in unilateral cleft lip and palate patients. *Cleft Palate Journal.*, 25:288–295, 1988.

[175] A Habel, D Sell, and M Mars. Management of cleft lip and palate. *Archives of Diseases in Childhood*, 74:360–366, 1996.

[176] B Gallagher. Prosthesis in velopharyngeal insuffidiency: effect on nasal resonance. *Jounral of Communication Disorders*, 15:469–473, 1982.

[177] H Enemark, S Bolund, and I Jorgensen. Evaluation of unilateral cleft lip and palate treatment: Long term results. *Cleft Palate Journal*, 27: 354–361, 1990.

[178] CP Shah and D Wong. Management of children with cleft lip and palate. *Canadian Medical Association Journal*, 122:19–22, 1980.

[179] *Human Tissue Act*, 2004.

[180] L. Hayflick and P.S. Moorhead. The serial cultivation of human diploid cell strains. *Experimental Cell Research*, 25(3):585 – 621, 1961.

[181] David Janson, Marion Rietveld, Rein Willemze, and Abdoelwaheb El Ghalbzouri. Effects of serially passaged fibroblasts on dermal and epidermal morphogenesis in human skin equivalents. *Biogerontology*, 14 (2):131–140, Apr 2013.

[182] Michael V Lancaster and Rebecca D Fields. Antibiotic and cytotoxic drug susceptibility assays using resazurin and poising agents, March 26 1996. US Patent 5,501,959.

[183] Tim Mosmann. Rapid colorimetric assay for cellular growth and survival: application to proliferation and cytotoxicity assays. *Journal of immunological methods*, 65(1):55–63, 1983.

[184] John Robert Taylor. *An Introduction To Error Analysis: The Study of Uncertainties in Physical Measurements*. University science books, 1997.

[185] C. M. Vaz, S. van Tuijl, C. V C Bouten, and F. P T Baaijens. Design of scaffolds for blood vessel tissue engineering using a multi-layering electrospinning technique. *Acta Biomater*, 1(5):575–582, Sep 2005.

[186] Han Bing Wang, Michael E Mullins, Jared M Cregg, Andres Hurtado, Martin Oudega, Matthew T Trombley, and Ryan J Gilbert. Creation of highly aligned electrospun poly-l-lactic acid fibers for nerve regeneration applications. *J Neural Eng*, 6(1):016001, Feb 2009.

[187] David R Lide and Thomas J Bruno. *CRC handbook of chemistry and physics*. CRC Press PLC, 2012.

[188] FAL Dullien. *Porous media fluid transport and pore structure.* Academic Press, 1979.

[189] Mohammad Chowdhury and George Stylios. Effect of experimental parameters on the morphology of electrospun nylon 6 fibres. *International Journal of Basic & Applied Sciences*, 10(06):116–131, 2010.

[190] Geun Hyung Kim. Electrospun pcl nanofibers with anisotropic mechanical properties as a biomedical scaffold. *Biomedical materials*, 3 (2):025010, 2008.

[191] Khalil Abdelrazek Khalil, H Fouad, T Elsarnagawy, and Fahad N Almajhdi. Preparation and characterization of electrospun plga/silver composite nanofibers for biomedical applications. *Int. J. Electrochem. Sci*, 8:3483–3493, 2013.

[192] Kyunghwan Yoon, Benjamin S Hsiao, and Benjamin Chu. Formation of functional polyethersulfone electrospun membrane for water purification by mixed solvent and oxidation processes. *Polymer*, 50(13):2893–2899, 2009.

[193] Satoru Kidoaki, Il Keun Kwon, and Takehisa Matsuda. Structural features and mechanical properties of in situ–bonded meshes of segmented polyurethane electrospun from mixed solvents. *Journal of Biomedical Materials Research Part B: Applied Biomaterials*, 76(1):219–229, 2006.

[194] Brittany Coats and Susan S Margulies. Material properties of human infant skull and suture at high rates. *Journal of neurotrauma*, 23(8): 1222–1232, 2006.

[195] Xiang Wang, D Sudhaker Rao, Leonardo Ajdelsztajn, Traci E Ciarelli, Enrique J Lavernia, and David P Fyhrie. Human iliac crest cancellous bone elastic modulus and hardness differ with bone formation rate per bone surface but not by existence of prevalent vertebral fracture. *Journal of Biomedical Materials Research Part B: Applied Biomaterials*, 85(1): 68–77, 2008.

[196] S Korossis, F Bolland, E Ingham, J Fisher, J Kearney, and J Southgate. Tissue engineering of the uninary bladder: considering structure-function relationships and the role of mechanotransduction. *Tissue Engineering*, 12:635–644, 2006.

[197] Travis J. Sill and Horst A. von Recum. Electrospinning: Applications in drug delivery and tissue engineering. *Biomaterials*, 29(13):1989 – 2006, 2008.

[198] Mohamed Selim, Anthony J Bullock, Keith A Blackwood, Christopher R Chapple, and Sheila MacNeil. Developing biodegradable scaffolds for tissue engineering of the urethra. *BJU Int*, 107(2):296–302, Jan 2010.

[199] RL Sass and RF Scheuerman. The crystal structure of sodium bicarbonate. *Acta Crystallographica*, 15(1):77–81, 1962.

[200] Frank J Millero. The thermodynamics of the carbonate system in seawater. *Geochimica Et Cosmochimica Acta*, 43(10):1651–1661, 1979.

[201] Sarah Tynan and Bradley N Opdyke. Effects of lower surface ocean ph upon the stability of shallow water carbonate sediments. *Science of the Total Environment*, 409(6):1082–1086, 2011.

[202] Norman E Good, G Douglas Winget, Wilhelmina Winter, Thomas N Connolly, Seikichi Izawa, and Raizada MM Singh. Hydrogen ion buffers for biological research. *Biochemistry*, 5(2):467–477, 1966.

[203] Teresa Mastrocola, Michele De Luca, and Michela Rugolo. Characterization of chloride transport pathways in cultured human keratinocytes. *Biochimica et Biophysica Acta (BBA)-Molecular Basis of Disease*, 1097 (4):275–282, 1991.

[204] Rangaprasad Sarangarajan, Holli Shumaker, Manoocher Soleimani, Caroline Le Poole, and Raymond E Boissy. Molecular and functional characterization of sodium–hydrogen exchanger in skin as well as cultured keratinocytes and melanocytes. *Biochimica et Biophysica Acta (BBA)-Biomembranes*, 1511(1):181–192, 2001.

[205] Albert J Banes. Flexible bottom culture plate for applying mechanical load to cell cultures, April 11 2000. US Patent 6,048,723.

[206] RL Melnick. NTP technical report on toxicity studies of isoprene (cas no. 78-79-5) administered by inhalation to f344/n rats and b6cf$_1$ mice. Toxicity Report Series Number 31 94-3354, United States Department of Health and Human Services, Public Health Service, National Institute of Health, National Toxicology Program, Post Office Box 12233, Research Triangle Park, NC 27709, 1994.

[207] FB Rihani and DM Da'ameh. Intraoral graphite tattoo. *Archives of Diseases in Childhood*, 91:563, 2006.

[208] S Choudhary, ML Elsaie, A Leiva, and K Nouri. Lasers for tattoo removal: a review. *Lasers in medical science*, 25:619–627, 2010.

[209] Gregory E Phillips and Vanchit John. Use of a subepithelial connective tissue graft to treat an area pigmented with graphite. *Journal of periodontology*, 76(9):1572–1575, 2005.

[210] CR Anderegg Jr and MB Lyles. Graphite tattoo: report of a case and differential diagnosis. *Military medicine*, 157(6):323, 1992.

[211] Gwendolen C Reilly and Adam J Engler. Intrinsic extracellular matrix properties regulate stem cell differentiation. *J Biomech*, 43(1):55–62, Jan 2010.

[212] LE Freed, GC Engelmayr, JT Borenstein, FT Moutos, and F Guilak. Advanced material stratagies for tissue engineering scaffolds. *Advanced Materials*, 21:3410–3418, 2009.

[213] J. G. Rheinwald and H. Green. Serial cultivation of strains of human epidermal keratinocytes: the formation of keratinizing colonies from single cells. *Cell*, 6(3):331–343, Nov 1975.

[214] Anthony J Bullock, Michael C Higham, and Sheila MacNeil. Use of human fibroblasts in the development of a xenobiotic-free culture and delivery system for human keratinocytes. *Tissue Eng*, 12(2):245–255, Feb 2006.

[215] Tao Sun, Mike Higham, Chris Layton, John Haycock, Robert Short, and Sheila MacNeil. Developments in xenobiotic-free culture of human keratinocytes for clinical use. *Wound Repair Regen*, 12(6):626–634, 2004.

[216] Jan-Thorsten Schantz, Swee Hin Teoh, Thiam Chye Lim, Michaela Endres, Christopher Xu Fu Lam, and Dietmar Werner Hutmacher. Repair of calvarial defects with customized tissue-engineered bone grafts i. evaluation of osteogenesis in a three-dimensional culture system. *Tissue Eng*, 9 Suppl 1:S113–S126, 2003.

[217] Maria Ann Woodruff and Dietmar Werner Hutmacher. The return of a forgotten polymerpolycaprolactone in the 21st century. *Progress in Polymer Science*, 35(10):1217 – 1256, 2010.

[218] Vincenzo Guarino, Filippo Causa, Paola Taddei, Michele di Foggia, Gabriela Ciapetti, Desire Martini, Concezio Fagnano, Nicola Baldini, and Luigi Ambrosio. Polylactic acid fibre-reinforced polycaprolactone scaffolds for bone tissue engineering. *Biomaterials*, 29(27):3662–3670, Sep 2008.

[219] Sunny A Abbah, Christopher X L Lam, Dietmar W Hutmacher, James C H Goh, and Hee-Kit Wong. Biological performance of a polycaprolactone-based scaffold used as fusion cage device in a large animal model of spinal reconstructive surgery. *Biomaterials*, 30(28):5086–5093, Oct 2009.

[220] Jan-Thorsten Schantz, Thiam-Chye Lim, Chou Ning, Swee Hin Teoh, Kim Cheng Tan, Shih Chang Wang, and Dietmar Werner Hutmacher. Cranioplasty after trephination using a novel biodegradable burr hole cover: technical case report. *Neurosurgery*, 58(1 Suppl):ONS–E176, Feb 2006.

[221] Sheila MacNeil. Progress and opportunities for tissue-engineered skin. *Nature*, 445(7130):874–880, Feb 2007.

[222] FJ Bye, L Wang, AJ Bullock, KA Blackwood, AJ Ryan, and S MacNeil. Post production processing of electrospun fibres for tissue engineering. *J. Vis. Exp*, page e4172, 2012.

[223] Shaun Eshraghi and Suman Das. Mechanical and microstructural properties of polycaprolactone scaffolds with one-dimensional, two-dimensional, and three-dimensional orthogonally oriented porous architectures produced by selective laser sintering. *Acta Biomater*, 6(7):2467–2476, Jul 2010.

[224] OE Öhrn. Thickness variations of paper on stretching. *Svensk Papperstidning*, 68(5):141–149, 1965.

[225] LJ Gibson, KE Easterling, and MF Ashby. The structure and mechanics of cork. *Proceedings of the Royal Society of London. A. Mathematical and Physical Sciences*, 377(1769):99–117, 1981.

[226] A. Cipitria, A. Skelton, T. R. Dargaville, P. D. Dalton, and D. W. Hutmacher. Design, fabrication and characterization of pcl electrospun scaffolds-a review. *J. Mater. Chem.*, 21(26):9419–9453, 2011.

[227] Giuseppe Maria de Peppo, Peter Sjovall, Maria Lenneras, Raimund Strehl, Johan Hyllner, Peter Thomsen, and Camilla Karlsson. Osteogenic potential of human mesenchymal stem cells and human embryonic stem

cell-derived mesodermal progenitors: a tissue engineering perspective. *Tissue Eng Part A*, 16(11):3413–3426, Nov 2010.

[228] Camilla Karlsson, Katarina Emanuelsson, Fredrik Wessberg, Kristina Kajic, Mathilda Zetterström Axell, Peter S Eriksson, Anders Lindahl, Johan Hyllner, and Raimund Strehl. Human embryonic stem cell-derived mesenchymal progenitors -potential in regenerative medicine. *Stem Cell Res*, pages 39–50, May 2009.

[229] Xuejun Xin, Mohammad Hussain, and Jeremy J. Mao. Continuing differentiation of human mesenchymal stem cells and induced chondrogenic and osteogenic lineages in electrospun PLGA nanofiber scaffold. *Biomaterials*, 28(2):316–325, Jan 2007.

[230] Jin Nam, Jed Johnson, John J. Lannutti, and Sudha Agarwal. Modulation of embryonic mesenchymal progenitor cell differentiation via control over pure mechanical modulus in electrospun nanofibers. *Acta Biomater*, 7(4):1516–1524, Apr 2011.

[231] Jiang Hu, Laura A. Smith, Kai Feng, Xiaohua Liu, Hongli Sun, and Peter X. Ma. Response of human embryonic stem cell-derived mesenchymal stem cells to osteogenic factors and architectures of materials during in vitro osteogenesis. *Tissue Eng Part A*, 16(11):3507–3514, Nov 2010.

[232] Jennifer E Phillips, Kellie L Burns, Joseph M Le Doux, Robert E Guldberg, and Andrés J García. Engineering graded tissue interfaces. *Proceedings of the National Academy of Sciences*, 105(34):12170–12175, 2008.

[233] E Kon, A Mutini, E Arcangeli, M Delcogliano, G Filardo, N Nicoli Aldini, D Pressato, R Quarto, S Zaffagnini, and M Marcacci. Novel nanostructured scaffold for osteochondral regeneration: pilot study in horses. *Journal of tissue engineering and regenerative medicine*, 4(4):300–308, 2010.

[234] Scott A Sell, Michael J McClure, Koyal Garg, Patricia S Wolfe, and Gary L Bowlin. Electrospinning of collagen/biopolymers for regenerative medicine and cardiovascular tissue engineering. *Advanced drug delivery reviews*, 61(12):1007–1019, 2009.

[235] Marco C Bottino, Vinoy Thomas, and Gregg M Janowski. A novel spatially designed and functionally graded electrospun membrane for periodontal regeneration. *Acta Biomaterialia*, 7(1):216–224, 2011.

[236] Albino Martins, Sangwon Chung, Adriano J Pedro, Rui A Sousa, Alexandra P Marques, Rui L Reis, and Nuno M Neves. Hierarchical starch-based fibrous scaffold for bone tissue engineering applications. *Journal of tissue engineering and regenerative medicine*, 3(1):37–42, 2009.

[237] KT Shalumon, KP Chennazhi, H Tamura, K Kawahara, SV Nair, and R Jayakumar. Fabrication of three-dimensional nano, micro and micro/nano scaffolds of porous poly (lactic acid) by electrospinning and comparison of cell infiltration by z-stacking/three-dimensional projection technique. *Nanobiotechnology, IET*, 6(1):16–25, 2012.

[238] Brendon M Baker, Albert O Gee, Robert B Metter, Ashwin S Nathan, Ross A Marklein, Jason A Burdick, and Robert L Mauck. The potential to improve cell infiltration in composite fiber-aligned electrospun scaffolds by the selective removal of sacrificial fibers. *Biomaterials*, 29(15): 2348–2358, 2008.

[239] S. D. McCullen, Y. Zhu, S. H. Bernacki, R. J. Narayan, B. Pourdeyhimi, R. E. Gorga, and E. G. Loboa. Electrospun composite poly(l-lactic acid)/tricalcium phosphate scaffolds induce proliferation and osteogenic differentiation of human adipose-derived stem cells. *Biomed Mater*, 4(3): 035002, Jun 2009.

[240] Chao Yan, Yang Wang, Xiao-Yan Shen, Gang Yang, Jia Jian, Hua-Su Wang, Guo-Qiang Chen, and Qiong Wu. Microrna regulation associated chondrogenesis of mouse MSCs grown on polyhydroxyalkanoates. *Biomaterials*, 32(27):6435–6444, Sep 2011.

[241] Jiehong Liao, Xuan Guo, Dan Nelson, F. Kurtis Kasper, and Antonios G Mikos. Modulation of osteogenic properties of biodegradable polymer/extracellular matrix scaffolds generated with a flow perfusion bioreactor. *Acta Biomater*, 6(7):2386–2393, Jul 2010.

[242] M. Farokhi, S. Sharifi, Y. Shafieyan, Z. Bagher, F. Mottaghitalab, A. Hatampoor, M. Imani, and M. A. Shokrgozar. Porous crosslinked poly(-caprolactone fumarate)/nanohydroxyapatite composites for bone tissue engineering. *J Biomed Mater Res A*, 100(4):1051–1060, Apr 2012.

[243] K. Itagaki, T. Naito, R. Iwakiri, M. Haga, S. Miura, Y. Saito, T. Owaki, S. Kamiya, T. Iyoda, H. Yajima, and et al. Eukaryotic translation elongation factor 1a induces anoikis by triggering cell detachment. *Journal of Biological Chemistry*, 287(19):16037–16046, May 2012.

[244] G. Altankov, W. Albrecht, K. Richau, Th Groth, and A. Lendlein. On the tissue compatibility of poly(ether imide) membranes: an in vitro study on their interaction with human dermal fibroblasts and keratinocytes. *J Biomater Sci Polym Ed*, 16(1):23–42, 2005.

[245] T Mammone, D Gan, and R Foyouziyoussefi. Apoptotic cell death increases with senescence in normal human dermal fibroblast cultures. *Cell Biology International*, 30(11):903–909, Nov 2006.

[246] Poul Erik Petersen and Hiroshi Ogawa. Strengthening the prevention of periodontal disease: the who approach. *Journal of periodontology*, 76 (12):2187–2193, 2005.

[247] Shahram Ghanaati, Markus Schlee, Matthew J Webber, Ines Willershausen, Mike Barbeck, Ela Balic, Christoph Görlach, Samuel I Stupp, Robert A Sader, and C. James Kirkpatrick. Evaluation of the tissue reaction to a new bilayered collagen matrix in vivo and its translation to the clinic. *Biomed Mater*, 6(1):015010, Feb 2011.

[248] Angelique Balguid, Anita Mol, Mieke H van Marion, Ruud A Bank, Carlijn VC Bouten, and Frank PT Baaijens. Tailoring fiber diameter in electrospun poly (-caprolactone) scaffolds for optimal cellular infiltration in cardiovascular tissue engineering. *Tissue Engineering Part A*, 15(2): 437–444, 2008.

[249] Maciej Skotak, Jorge Ragusa, Daniela Gonzalez, and Anuradha Subramanian. Improved cellular infiltration into nanofibrous electrospun cross-linked gelatin scaffolds templated with micrometer-sized polyethylene glycol fibers. *Biomedical Materials*, 6(5):055012, 2011.

[250] Zhexiang Wang, Bin Sun, Min Zhang, Lailiang Ou, Yongzhe Che, Jun Zhang, and Deling Kong. Functionalization of electrospun poly (ε-caprolactone) scaffold with heparin and vascular endothelial growth factors for potential application as vascular grafts. *Journal of Bioactive and Compatible Polymers*, 28(2):154–166, 2013.

[251] Murtaza N Ali and Ihtesham Ur Rehman. An auxetic structure configured as oesophageal stent with potential to be used for palliative treatment of oesophageal cancer; development and in vitro mechanical analysis. *Journal of Materials Science: Materials in Medicine*, 22(11): 2573–2581, 2011.

Appendix A

A.1 Material data sheets

Goodfellow 2-December-2013 19:04:28

Technical Information - Polyhydroxybutyrate/Polyhydroxyvalerate 12% - Biopolymer Close

Polyhydroxybutyrate/Polyhydroxyvalerate 12% - Biopolymer
PHB88/PHV12

Standard products are available in these forms

- 

General Description:

General Description : See also PHB. PHB/PHV copolymers are used in preference to PHB homopolymer for general purposes (e.g. moulding containers) in order to obtain a better balance of stiffness and toughness. PHV contents of 5 - 20% give a useful range of properties broadly similar to those of the polyolefins (the polyethylenes and polypropylene). They melt at lower temperatures than the homopolymer, giving a useful improvement in melt-processability. Their other properties are similar to those of PHB.

They are being used for biodegradeable containers (of which shampoo bottles are the most high-profile example) and other articles difficult to recycle e.g. disposable razors or medically contaminated articles.

Chemical Resistance

Acids - dilute	Fair
Alcohols	Fair
Alkalis	Poor
Greases and Oils	Good

Electrical Properties

Dielectric constant @1MHz	3.0
Volume resistivity (Ohmcm)	10^{16}

Mechanical Properties

Elongation at break (%)	35
Izod impact strength (J m^{-1})	200
Tensile modulus (GPa)	0.5
Tensile strength (MPa)	23

Physical Properties

Density (g cm^{-3})	1.25
Resistance to Ultra-violet	Fair

Thermal Properties

Specific heat (J K^{-1} kg^{-1})	1400
Thermal conductivity @23C (W m^{-1} K^{-1})	0.15

Print this page

Close

Goodfellow 2-December-2013 19:00:22

Technical Information - Poly L lactic acid - Biopolymer Close

Poly L lactic acid - Biopolymer
PLLA

Standard products are available in these forms

- 
- 

General Description:

General Description : PLLA is a melt-processable semi-crystalline thermoplastic made by biological fermentation from renewable carbohydrate feedstocks. PLLA is quite stable under everyday conditions, although it does degrade slowly in humid environments at temperatures above its glass transition temperature 55°C. Therefore, composting is usually carried out in professional facilities over a number of week, rather than in garden compost.

Its chemical resistance is somewhat limited although it is said to have good resistance to solvents in general. PLLA is a stiff polymer of high crystallinity (60-70%), whose mechanical properties are similar to those of polystyrene. It can be processed as a classic thermoplastic material and has similar processing characteristics to liquid crystal polymers LCPs.

Applications for PLLA is mostly used in food packaging, envelope windows, floral wrap. It is also being considered for a range of medical applications, such as bioresorbable stitches and anchors, although at the time of writing these applications are very much in the research phase.

Mechanical Properties

Elongation at break (%)	2.4
Tensile modulus (GPa)	3.6
Tensile strength (MPa)	70

Physical Properties

Density (g cm^{-3})	1.25
Resistance to Ultra-violet	Good
Water absorption (%)	0.3
Water absorption - equilibrium (%)	0.3

Thermal Properties

Lower working temperature (C)	-10
Upper working temperature (C)	50

Print this page

Close

SAFETY DATA SHEET

according to Regulation (EC) No. 1907/2006
Version 5.0 Revision Date 05.01.2013
Print Date 10.01.2014

1. IDENTIFICATION OF THE SUBSTANCE/MIXTURE AND OF THE COMPANY/UNDERTAKING

1.1 Product identifiers

Product name : Poly(L-lactide)

Product Number : 93578
Brand : Aldrich
CAS-No. : 26161-42-2

1.2 Relevant identified uses of the substance or mixture and uses advised against

Identified uses : Laboratory chemicals, Manufacture of substances

1.3 Details of the supplier of the safety data sheet

Company : Sigma-Aldrich Company Ltd.
The Old Brickyard
NEW ROAD, GILLINGHAM
Dorset
SP8 4XT
UNITED KINGDOM

Telephone : +44 (0)1747 833000
Fax : +44 (0)1747 833313
E-mail address : eurtechserv@sial.com

1.4 Emergency telephone number

Emergency Phone # : +44 (0)1747 833100

2. HAZARDS IDENTIFICATION

2.1 Classification of the substance or mixture

Not a hazardous substance or mixture according to Regulation (EC) No 1272/2008
This substance is not classified as dangerous according to Directive 67/548/EEC.

2.2 Label elements

Caution - substance not yet tested completely.

2.3 Other hazards - none

3. COMPOSITION/INFORMATION ON INGREDIENTS

3.1 Substances

Synonyms : L-Lactide polymer

Molecular Weight : 10,100 g/mol

4. FIRST AID MEASURES

4.1 Description of first aid measures

If inhaled
If breathed in, move person into fresh air. If not breathing, give artificial respiration.

In case of skin contact
Wash off with soap and plenty of water.

In case of eye contact
Flush eyes with water as a precaution.

If swallowed
Never give anything by mouth to an unconscious person. Rinse mouth with water.

4.2 Most important symptoms and effects, both acute and delayed
To the best of our knowledge, the chemical, physical, and toxicological properties have not been thoroughly investigated.

4.3 Indication of any immediate medical attention and special treatment needed
no data available

5. FIREFIGHTING MEASURES

5.1 Extinguishing media

Suitable extinguishing media
Use water spray, alcohol-resistant foam, dry chemical or carbon dioxide.

5.2 Special hazards arising from the substance or mixture
Carbon oxides

5.3 Advice for firefighters
Wear self contained breathing apparatus for fire fighting if necessary.

5.4 Further information
no data available

6. ACCIDENTAL RELEASE MEASURES

6.1 Personal precautions, protective equipment and emergency procedures
Avoid dust formation. Avoid breathing vapors, mist or gas.

6.2 Environmental precautions
Do not let product enter drains.

6.3 Methods and materials for containment and cleaning up
Sweep up and shovel. Keep in suitable, closed containers for disposal.

6.4 Reference to other sections
For disposal see section 13.

7. HANDLING AND STORAGE

7.1 Precautions for safe handling
Provide appropriate exhaust ventilation at places where dust is formed.Normal measures for preventive fire protection.

7.2 Conditions for safe storage, including any incompatibilities
Store in cool place. Keep container tightly closed in a dry and well-ventilated place.

Handle and store under inert gas. Moisture sensitive.

7.3 Specific end use(s)
no data available

8. EXPOSURE CONTROLS/PERSONAL PROTECTION

8.1 Control parameters

Components with workplace control parameters
Contains no substances with occupational exposure limit values.

8.2 Exposure controls

Appropriate engineering controls
General industrial hygiene practice.

Personal protective equipment

Eye/face protection
Use equipment for eye protection tested and approved under appropriate government standards such as NIOSH (US) or EN 166(EU).

Skin protection
Handle with gloves. Gloves must be inspected prior to use. Use proper glove removal technique (without touching glove's outer surface) to avoid skin contact with this product. Dispose of contaminated gloves after use in accordance with applicable laws and good laboratory practices. Wash and dry hands.

The selected protective gloves have to satisfy the specifications of EU Directive 89/686/EEC and the standard EN 374 derived from it.

Body Protection
Choose body protection in relation to its type, to the concentration and amount of dangerous substances, and to the specific work-place., The type of protective equipment must be selected according to the concentration and amount of the dangerous substance at the specific workplace.

Respiratory protection
Respiratory protection is not required. Where protection from nuisance levels of dusts are desired, use type N95 (US) or type P1 (EN 143) dust masks. Use respirators and components tested and approved under appropriate government standards such as NIOSH (US) or CEN (EU).

9. PHYSICAL AND CHEMICAL PROPERTIES

9.1 Information on basic physical and chemical properties

a)	Appearance	Form: solid
b)	Odour	no data available
c)	Odour Threshold	no data available
d)	pH	no data available
e)	Melting point/freezing point	no data available
f)	Initial boiling point and boiling range	no data available
g)	Flash point	no data available
h)	Evaporation rate	no data available
i)	Flammability (solid, gas)	no data available
j)	Upper/lower flammability or explosive limits	no data available
k)	Vapour pressure	no data available
l)	Vapour density	no data available
m)	Relative density	no data available
n)	Water solubility	no data available
o)	Partition coefficient: n-octanol/water	no data available
p)	Auto-ignition temperature	no data available
q)	Decomposition temperature	no data available
r)	Viscosity	no data available
s)	Explosive properties	no data available

t) Oxidizing properties no data available

9.2 Other safety information
no data available

10. STABILITY AND REACTIVITY

10.1 Reactivity
no data available

10.2 Chemical stability
no data available

10.3 Possibility of hazardous reactions
no data available

10.4 Conditions to avoid
no data available

10.5 Incompatible materials
acids, Bases

10.6 Hazardous decomposition products
Other decomposition products - no data available

11. TOXICOLOGICAL INFORMATION

11.1 Information on toxicological effects

Acute toxicity
no data available

Skin corrosion/irritation
no data available

Serious eye damage/eye irritation
no data available

Respiratory or skin sensitization
no data available

Germ cell mutagenicity
no data available

Carcinogenicity

IARC: No component of this product present at levels greater than or equal to 0.1% is identified as probable, possible or confirmed human carcinogen by IARC.

Reproductive toxicity
no data available

Specific target organ toxicity - single exposure
no data available

Specific target organ toxicity - repeated exposure
no data available

Aspiration hazard
no data available

Potential health effects

Inhalation	May be harmful if inhaled. May cause respiratory tract irritation.
Ingestion	May be harmful if swallowed.
Skin	May be harmful if absorbed through skin. May cause skin irritation.
Eyes	May cause eye irritation.

Signs and Symptoms of Exposure
To the best of our knowledge, the chemical, physical, and toxicological properties have not been thoroughly investigated.

Additional Information
RTECS: Not available

12. ECOLOGICAL INFORMATION

12.1 Toxicity
no data available

12.2 Persistence and degradability
no data available

12.3 Bioaccumulative potential
no data available

12.4 Mobility in soil
no data available

12.5 Results of PBT and vPvB assessment
no data available

12.6 Other adverse effects
no data available

13. DISPOSAL CONSIDERATIONS

13.1 Waste treatment methods

Product
Offer surplus and non-recyclable solutions to a licensed disposal company.

Contaminated packaging
Dispose of as unused product.

14. TRANSPORT INFORMATION

14.1 UN number
ADR/RID: - IMDG: - IATA: -

14.2 UN proper shipping name
ADR/RID: Not dangerous goods
IMDG: Not dangerous goods
IATA: Not dangerous goods

14.3 Transport hazard class(es)
ADR/RID: - IMDG: - IATA: -

14.4 Packaging group
ADR/RID: - IMDG: - IATA: -

14.5 Environmental hazards
ADR/RID: no IMDG Marine Pollutant: no IATA: no

14.6 Special precautions for user
no data available

15. REGULATORY INFORMATION

This safety datasheet complies with the requirements of Regulation (EC) No. 1907/2006.

15.1 Safety, health and environmental regulations/legislation specific for the substance or mixture
no data available

15.2 Chemical Safety Assessment
no data available

16. OTHER INFORMATION

Further information

The above information is believed to be correct but does not purport to be all inclusive and shall be used only as a guide. The information in this document is based on the present state of our knowledge and is applicable to the product with regard to appropriate safety precautions. It does not represent any guarantee of the properties of the product. Sigma-Aldrich Corporation and its Affiliates shall not be held liable for any damage resulting from handling or from contact with the above product. See www.sigma-aldrich.com and/or the reverse side of invoice or packing slip for additional terms and conditions of sale.

A.2 Estimating the change in surface area of a growing cleft defect

Approximating the defect to be a cylindrical hole of radius r, it has a surface area ($S.A.$) and volume (V) of

$$S.A. = 2\pi r^2 + 2\pi rl \tag{A.1}$$

$$V = \pi r^2 l \tag{A.2}$$

As a worst case scenario, we can assume that if all the expansion is taken up by the two circles top and bottom of the cylinder, then l is constant. In other words, this assumes there is no thickening of the maxilla, it just expands outwards, so all the expansion would need to be accommodated by the tissue engineered solution. We know that by the time the child reaches 3 years the volume of the defect will have doubled (Figure A.1):[169,170]

$$V_{final} = 2V_{initial} \tag{A.3}$$

Both volumes can be defined in terms of π, where r and x are the initial and final radii as the defect expands:

$$V_{initial} = \pi r^2 l \tag{A.4}$$

$$V_{final} = \pi x^2 l \tag{A.5}$$

Substituting in these in gives:

$$V_{final} = 2V_{initial} \tag{A.6}$$

$$\pi x^2 l = 2\pi r^2 l \tag{A.7}$$

We can now solve for x and determine the change in radius:

$$x^2 = 2r^2 \tag{A.8}$$

$$x = \sqrt{2}r \tag{A.9}$$

Therefore, if the volume doubles, and all of this is expansion solely occurs as a surface area change in the top and bottom of a cylindrical defect, then the radius will change by a factor of $\sqrt{2}$. We can now work out the proportional change in surface area. The initial surface area of the defect ($S.A._{initial}$) is equal to:

$$S.A._{initial} = 2\pi rl + 2\pi r^2 \tag{A.10}$$

As the radius increased by a factor of $\sqrt{2}$ then the final surface area of the defect ($S.A._{final}$) is equal to:

$$S.A._{final} = 2\pi\sqrt{2}rl + 2\pi(\sqrt{2}r)^2 \tag{A.11}$$

This can be expressed as a factorial change between $S.A._{initial}$ and $S.A._{final}$:

$$S.A._{final} = x(S.A._{initial}) \tag{A.12}$$

The change in surface area is not equal across the whole cylinder. There are two components, the change in top and bottom, and then the change in the cylinder wall. So this equation should be expressed as:

$$2\pi\sqrt{2}rl + 2\pi(\sqrt{2}r)^2 = a(2\pi rl) + b(2\pi r^2) \tag{A.13}$$

We are not too interested in the change in height of the defect (a), as this would occur inside the body, away from the implant interface but for completeness the height of the defect would change by a factor of:

$$a = \sqrt{2} \tag{A.14}$$

The change in the surface area of the top and bottom of the defect would be:

$$2\pi(\sqrt{2}r)^2 = b(2\pi r^2) \tag{A.15}$$

$$2\pi 2(r^2) = b(2\pi r^2) \tag{A.16}$$

Hence:

$$b = 2 \tag{A.17}$$

From this it can be seen that there is a 2 fold change in surface area in the top and bottom of the defect, given the assumptions stated above. So the model will need to be able to produce a doubling in surface area to account for a worst case scenario. This scenario is that as the child grows, the volume of the defect doubles, and all this expansion is exhibited with the maximum surface area change possible.

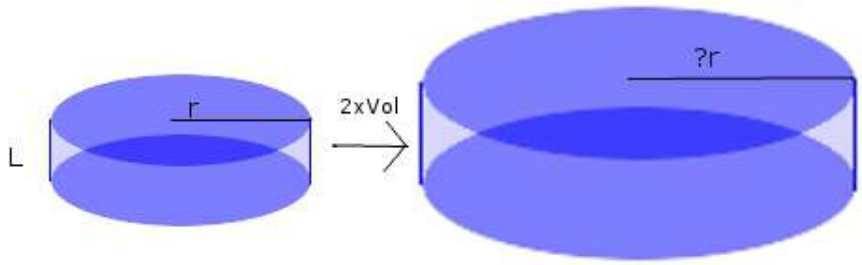

Figure A.1: What is the relationship between surface area and volume change as cleft palate defect grows?

A.3 Required change in balloon volume to give the same expansion as seen in cleft palate defects

If, as shown above, the worst case scenario we can expect is a doubling in surface area, then it is essential to ensure the model distends to the same degree. This leads to the question "What is the change in volume required to produce a doubling in surface area of a balloon?".

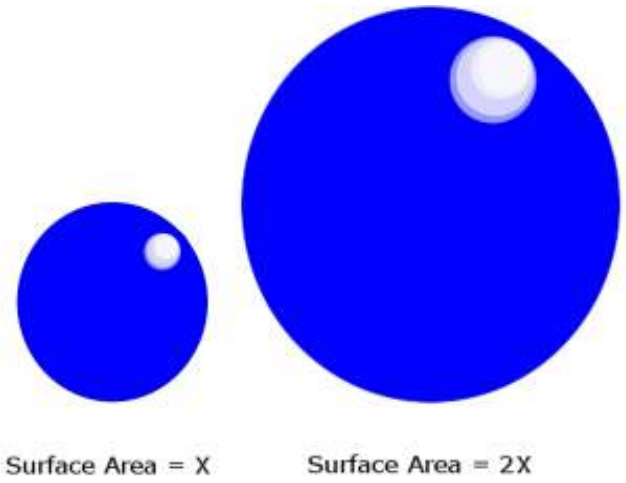

Figure A.2: What is the change in volume of a sphere required to give the same maximum change in surface area as seen in cleft palate cases?

If the surface area increases by a factor of $\times 2$ what change in volume is required to increase the surface area of a balloon by the same amount (Figure A.2)?

The surface area (S.A.) of a sphere is;

$$S.A._{sphere} = 4\pi r^2 \tag{A.18}$$

If the surface area of a sphere doubles, how does the radius change? Initial radius (r) and final radius (x)

$$S.A._1 = 4\pi r^2 \tag{A.19}$$

$$S.A._2 = 4\pi x^2 \tag{A.20}$$

If the surface area doubles then;

$$S.A._2 = 2S.A._1 \tag{A.21}$$

$$4\pi x^2 = 2(4\pi r^2) \tag{A.22}$$

$$x^2 = \frac{8\pi r^2}{4\pi} \tag{A.23}$$

$$x^2 = 2r^2 \tag{A.24}$$

Hence, the radius change required to achieve a doubling in surface area of a sphere is;

$$x = \sqrt{2}r \tag{A.25}$$

The volume (V) of a sphere is calculated as follows;

$$V = \frac{4}{3}\pi r^3 \tag{A.26}$$

If the radius increases by $\sqrt{2}$ then the volume changes as;

$$V_{initial} = \frac{4}{3}\pi r^3 \tag{A.27}$$

$$V_{final} = \frac{4}{3}\pi\sqrt{2}r^3 \tag{A.28}$$

$$V_{final} = xV_{initial} \tag{A.29}$$

$$\frac{4}{3}\pi(\sqrt{2}r)^3 = x(\frac{4}{3}\pi r^3) \tag{A.30}$$

$$V_{final} = 2\sqrt{2}V_{initial} \tag{A.31}$$

So, in order to achieve a doubling in surface area, the volume of a sphere needs to be increased by a factor of $2\sqrt{2}$.

The approximations used in this calculation are rather extensive, they assume that the defect is a perfect cylinder, and that it only expands at its ends, and not at the side. This is an area where clear modelling is required to establish exactly what the worst case scenario is. However, there is limited data on what happens as a child grows, and more-so, how this changes given the current treatment regime. Much of this data is not available as most cleft cases are either treated early, (the defect is filled with soft tissues only) or observed at maturation (only in parts of the world with poor availability of health care). The best data at the present time states that a hard palate

defect doubles in volume as the child ages. This is the value underpinning the estimation used here, and is based upon reasonable evidence. The other assumptions made in the estimate are to ensure this volume change occurs in the most detrimental manner, with maximum impact on the proposed implant. This would be observed as a surface area change only, and that an implant would directly have to cope with that change, *i.e.* the implant would have to expand to cope with that change.

A.4 Published outputs

Video Article

Postproduction Processing of Electrospun Fibres for Tissue Engineering

Frazer J. Bye[1], Linge Wang[2], Anthony J. Bullock[1], Keith A. Blackwood[1], Anthony J. Ryan[3], Sheila MacNeil[1]

[1]Materials Science and Engineering, University of Sheffield

[2]Department of Biomedical Science, University of Sheffield

[3]Department of Chemistry, University of Sheffield

Correspondence to: Sheila MacNeil at s.macneil@sheffield.ac.uk

URL: http://www.jove.com/video/4172/

DOI: 10.3791/4172

Keywords: Bioengineering, Issue 66, Materials Science, Biomedical Engineering, Tissue Engineering, Medicine, Chemistry, Electrospinning, bilayer, biaxial distension, heat and vapour annealing, mechanical testing, fibres

Date Published: 8/9/2012

Citation: Bye, F.J., Wang, L., Bullock, A.J., Blackwood, K.A., Ryan, A.J., MacNeil, S. Postproduction Processing of Electrospun Fibres for Tissue Engineering. *J. Vis. Exp.* (66), e4172 10.3791/4172, DOI : 10.3791/4172 (2012).

Abstract

Electrospinning is a commonly used and versatile method to produce scaffolds (often biodegradable) for 3D tissue engineering.[1, 2, 3] Many tissues *in vivo* undergo biaxial distension to varying extents such as skin, bladder, pelvic floor and even the hard palate as children grow. In producing scaffolds for these purposes there is a need to develop scaffolds of appropriate biomechanical properties (whether achieved without or with cells) and which are sterile for clinical use. The focus of this paper is not how to establish basic electrospinning parameters (as there is extensive literature on electrospinning) but on how to modify spun scaffolds post production to make them fit for tissue engineering purposes - here thickness, mechanical properties and sterilisation (required for clinical use) are considered and we also describe how cells can be cultured on scaffolds and subjected to biaxial strain to condition them for specific applications.

Electrospinning tends to produce thin sheets; as the electrospinning collector becomes coated with insulating fibres it becomes a poor conductor such that fibres no longer deposit on it. Hence we describe approaches to produce thicker structures by heat or vapour annealing increasing the strength of scaffolds but not necessarily the elasticity. Sequential spinning of scaffolds of different polymers to achieve complex scaffolds is also described. Sterilisation methodologies can adversely affect strength and elasticity of scaffolds. We compare three methods for their effects on the biomechanical properties on electrospun scaffolds of poly lactic-co-glycolic acid (PLGA).

Imaging of cells on scaffolds and assessment of production of extracellular matrix (ECM) proteins by cells on scaffolds is described. Culturing cells on scaffolds *in vitro* can improve scaffold strength and elasticity but the tissue engineering literature shows that cells often fail to produce appropriate ECM when cultured under static conditions. There are few commercial systems available that allow one to culture cells on scaffolds under dynamic conditioning regimes - one example is the Bose Electroforce 3100 which can be used to exert a conditioning programme on cells in scaffolds held using mechanical grips within a media filled chamber.[4] An approach to a budget cell culture bioreactor for controlled distortion in 2 dimensions is described. We show that cells can be induced to produce elastin under these conditions. Finally assessment of the biomechanical properties of processed scaffolds cultured with or without cells is described.

Video Link

The video component of this article can be found at http://www.jove.com/video/4172/

Protocol

1. Electrospinning of Random and Aligned Fibres

Electrospinning creates fine fibrous networks by using electric potential to draw a polymer solution towards an earthed collector. Collectors can be in very many shapes and can be static or, more commonly, rotating. The solvent evaporates before the solution arrives at the collector and the jet solidifies into a fibre.

Each polymer requires its own set of conditions to produce a given type of fibre. The concentration of the polymer, the solvent, the distance between the pumped solution and the earthed collector, the potential difference between the two, the velocity of the rotating collector, the flow rate, temperature and humidity will all affect electrospinning. There are many studies describing the selection of electrospinning parameters and how these impact on the scaffolds produced (e.g. fibre diameter, morphology, and orientation).[5, 6, 7, 8] In these experiments scaffolds were spun based on conditions selected in our previous studies.[2, 9]

The following methods are suitable for the production of electrospun scaffolds from PLGA, poly lactic acid (PLA), poly ε-caprolactone (PCL) and poly hydroxybutyrate-co-hydroxyvalerate (PHBV) using a rotating collector as shown in **Figure 1**. Throughout the solvent dichloromethane

(DCM) is used. The method here produces microfibrous PLGA, PLA and PCL and nanofibrous PHBV scaffold with micro-sized beads ('pearl necklace' morphology).

1. Coat the rotating mandrel collector with aluminium foil, with the polished/shiny side facing outwards. Our mandrel was 20 cm wide, and 10 cm in diameter.
2. Prepare polymer solutions; PLA, PCL and PHBV are made up as a 10 wt% solution in DCM. PLGA is made up as a 20 wt% solution in DCM.
3. Place 4 syringes of 5 ml volume on a syringe pump. Syringes are loaded to contain 5 ml of the polymer each, giving 20 ml in total.
4. For PLA, PCL and PHBV use a flow rate of 40 $\mu Lmin^{-1}$ per syringe.
5. For PLGA use a flow rate of 30 $\mu Lmin^{-1}$ per syringe.
6. For PLA, PCL and PLGA use a working distance of 17 cm from needle tip to mandrel.
7. For PHBV use a working distance of 10 cm from needle tip to mandrel.
8. Charge the syringe needles to +17000 V (73030 P, Genvolt, Shropshire, UK) and electrospin from the appropriate distance onto the aluminium foil coated mandrel.
9. For random fibres rotate the mandrel at 200 rpm.
10. For aligned fibres rotate the mandrel at 1000 rpm.
11. Scaffolds can be stored on the aluminium foil under dry conditions. Recommended storage is in a sealed container at 4 °C in the presence of desiccant. In our experience scaffolds remain stable for at least 4 months (possibly much longer) under these conditions (we are not aware of any published studies on long term storage conditions for scaffolds).

2. Production of Complex Scaffolds by Sequential Spinning

Sequential spinning provides a method of combining the properties of different materials to create a material that has the best of both properties. PHBV produces a flat, dense, brittle sheet whereas PLA or PCL spinning produces low density elastic sheets. Both materials support cell attachment. Consecutively spinning these materials results in a dense cell-impermeable membrane that is elastic.

1. Set up the electrospinning rig as per Section 1, with PHBV spinning conditions.
2. Electrospin PHBV as above.
3. Without changing the aluminium foil, electrospin a second polymer on-top using the parameters and normal conditions for that polymer (e.g. 17 cm drum to needle, 17000 V, 200 rpm for PLA). This additive process builds up a double layer of scaffold producing a bilayer.

3. Production of Multilayered Scaffolds by Annealing Several Layers Together

1. Scaffolds can be multilayered through the use of heat annealing. To do this 4 sheets of PLGA are placed on top of each other and then heat annealed at 60 °C for 3 hours.
2. Scaffolds can also be annealed by vapour annealing. Here 4 sheets of PLGA are placed on top of each other and suspended 2 cm above a pool of DCM (10 ml) for 1 hour. This is performed in a sealed container at room temperature.

4. Aseptic Production and Postproduction Sterilisation of Electrospun Scaffolds

1. Aseptic scaffold production can be achieved by electrospinning in an aseptic environment of a laminar flow hood inside a clean room environment. To do this either sterile polymers of medical grade or polymers sterilised by incubation in DCM can be used. Once dissolved, polymers are electrospun onto sterile foil wrapped around a sterilised mandrel. Scaffolds are then handled aseptically. Sterility is verified by incubating samples of the scaffold in antibiotic-free growth media for the appropriate period.
2. For ethanol disinfection (this is of use experimentally but is not a recognised methodology of sterilisation which could be taken to the clinic) scaffolds are placed briefly (15 min) in a 70% v/v solution of ethanol in distilled water. For practical experimental purposes this is usually sufficient to disinfect scaffolds so that they can then be combined successfully with cultured cells.
3. For peracetic acid sterilisation scaffolds are immersed in peracetic acid (0.1% v/v in phosphate buffered saline (PBS)) and incubated for 3 hours at room temperature as described in Selim *et al.*[9]
4. For gamma sterilisation scaffolds are irradiated with a dose of 3 kGy using a caesium source as described in Selim *et al.*[9]

5. Biomechanical Testing of Scaffolds

1. Scaffolds are cut into rectangles 5 mm x 20 mm, measured for thickness using a micrometer, and placed into a Bose Electroforce 3100 instrument. This machine applies a force of 0-22 N up to a displacement of 6mm and plots the load vs. displacement as a stress/strain curve. This allows the Young's modulus and elasticity to be calculated.

6. Visualising Cells on Scaffolds and Assessing ECM Production

Cells can be stained with vital fluorescent dyes which allow one to see cells on the scaffolds as they attach, migrate and proliferate. Post culture the presence of cells on scaffolds can be determined by staining for cell nuclei with 4',6-diamidino-2-phenylindole dihydrochloride (DAPI). The production of ECM by cells on the scaffold can be assessed by staining cells for a range of ECM proteins including elastin as shown in this example. All scaffolds used were measured to have a thickness of at least 0.2 mm and cut into squares 1.5 cm x 1.5 cm prior to seeding.

In these studies human dermal fibroblasts are used throughout because of the role they play in soft tissue reconstruction which is our laboratory's primary research interest.

Cells are obtained from skin samples from patients undergoing elective surgery for breast reduction or abdominoplasty (consent was given for their tissue to be used for research purposes). Tissues are collected and used anonymously under Research Tissue Bank Licence 12179. Tissues are washed with PBS containing streptomycin (0.1 mg/ml) and penicillin (100 IU/ml) and amphotericin B (0.5 µg/ml). Tissue samples are incubated in 0.1% w/v trypsin and 0.1% glucose in PBS (12-18 hours, 4 °C). The dermis is peeled off, minced finely and incubated with 10 ml of collagenase (0.5% w/v in DMEM and 10% FCS, 37 °C for 18 hours). Centrifugation of the resulting cell suspension (400 g for 10 mins), produces a pellet of cells that can be cultured and subcultured in DMEM supplemented with fetal calf serum (FCS, 10% v/v), streptomycin (0.1 mg/ml), penicillin (100 IU/ml) and amphotericin B (0.5 µg/ml). Only fibroblasts of passage 4-9 are used in experiments.

1. Human dermal fibroblasts, once confluent in a T75 (EasyFlask, Nunc, New York, US) are seeded by adding trypsin/EDTA (5 ml, 5 mg/ml trypsin, 2 mg/ml EDTA in saline), incubating for 5 minutes at 37 °C. The suspension is centrifuged for 10 minutes (150 g). The cells are resuspended in 5 ml of DMEM (supplemented with FCS (10% v/v), streptomycin (0.1 mg/ml), penicillin (100 IU/ml) and amphotericin B (0.5 µg/ml)) and counted using a haemocytometer, and the concentration is adjusted for seeding. Cells are normally seeded at 50,000 cells per well.
2. If required, prior to seeding cells on the scaffold, cells can be pre-labelled using CellTracker red or green. The cells are washed with 3 x 5 ml PBS. A solution of 10 mM CellTracker in serum free, cell-appropriate, medium (10 ml) is added and the cells are incubated for 45 minutes at 37 °C. After incubation, the cells are washed in 3 x 5 ml PBS following which they are seeded onto scaffolds. Following this the surface of the scaffolds can be imaged in an Axon ImageExpress microscope (Molecular Devices, Sunnyvale, US) at 570 nm λex - 620 nm λem (CellTracker red) and 480 nm λex - 533 nm λem (CellTracker green). To investigate the penetration of cells deeper into scaffolds a multiphoton confocal microscope can be used. This can achieve around 200 micron penetration into most scaffolds with or without cells.
3. Post culture samples are fixed in 1 ml 3.7% formaldehyde in PBS at 37 °C for 20 minutes and then washed with 3 x 1 ml PBS.
4. 200 µL of elastin primary antibodies are added to each sample (5% v/v in PBS, rabbit anti-human alpha elastin, AbDserotec, Kidlington, UK) and incubated at 37 °C for 30 minutes.
5. Samples are washed with 3 x 1 ml PBS and then incubated in a solution of secondary antibody (0.5% v/v goat anti-rabbit IgG (FC):FITC) in PBS containing DAPI (1 µg/ml) for 30 minutes.
6. Following this the samples are washed with 3 x 1 ml PBS.
7. DAPI and secondary antibody stained samples are then imaged on an Axon ImageExpress fluorescent microscope, 365 nm λex - 460 nm λem for DAPI and 480 nm λex - 533 nm λem for the secondary antibody. DAPI stains the nuclei and allows one to see the distribution of cells within the fibres very readily.

7. Subjecting Cells on Scaffolds to Biaxial Dynamic Conditioning

To examine the effect of dynamic conditioning on fibroblast ECM production we developed a simple proof-of-concept bioreactor to explore this.

1. Assemble balloon and flow regulation apparatus and prepare system so it can be readily placed into a sterile vessel suitable for cell culture once it is coated.
2. Autoclave the apparatus including the balloon (122 °C, 220 mBar for 1 hour). We can confirm that balloons survive autoclaving without adversely affecting their function by inflating and deflating them repeatedly.
3. In a clean room, unpack the apparatus in a laminar flow hood in position to be electrospun onto.
4. Inflate the balloon to the required surface area (remember the balloon still needs to fit into the culture vessel) with phosphate buffered saline and connect the PBS to an electrical earth at a point in the apparatus that does not need to be sterile (branch pipe on 3-way tap).
5. Electrospin the required polymer onto the balloon using the normal spinning conditions, using a working distance of 10 cm. Allow the scaffold to dry for 1 hour. The 'wet' fibres are 'sticky' enough to adhere to the surface of the balloon without subsequently detaching.
6. Place the balloon into a sterile vessel and transport it to a laminar flow hood suitable for cell culture.
7. Remove the balloon from the vessel and place onto a sterile surface (Petri dish) and repeatedly (every 20 seconds) pipette a cell suspension (1×10^6 cells in 5 ml of DMEM) onto the coated balloon for 20 minutes to attempt to distribute cells evenly over the surface.
8. Place balloon into the culture vessel, and add pre-warmed media appropriate to the cell type.
9. Connect the inflation apparatus to a syringe pump (Kent Scientific, Genie Plus, Connecticut, US) and inflate/deflate the balloon as required to give biaxial distension. A computer controlled syringe pump can be used to achieve a more complex distension regime.

8. Representative Results

The following figures are representative results that can be expected if the above methods are followed.

Electrospinning can be utilised to create scaffolds with random and ordered architectures (**Figure 1**), this is repeatable and the fibres are uniform. Many types of polymers can be electrospun with characteristics which can vary considerably as shown in **Figure 2** for PHBV, PLA or PCL. Electrospinning can produce light fluffy scaffolds or dense cell impenetrable membranes (see **Figure 3**). All scaffolds shown here facilitated cell attachment and proliferation. Previous work has shown that cells can migrate through these scaffolds up to a depth of at least 500-600 µm.[9] For PLA the average fibre diameter is 3 µm; for PHBV it is 0.3µm with pearls ranging from 5-20 µm; for PCL it is 3 µm; and for PLGA it is 11 µm. Other studies using other solvent systems report that PHBV can be electrospun as fibres without beads or polymer pearls.[10,11]

If thicker scaffolds are required vapour and heat annealing can be employed to anneal layers of scaffolds together (see **Figure 4**). These scaffold layers do not delaminate and it can be very difficult to find the junction between layers.

We show that bilayer membranes can be made where cells A and B can each be cultured on a separate membrane without intermingling as shown in **Figure 5**. Here we demonstrate this by using human dermal fibroblasts coloured with two different fluorescent cell tracker dyes. Such a bilayer membrane would be useful when culturing cells to form a hard tissue such as bone or cartilage on one side separated from cells designed to form a soft (and usually faster growing) tissue on the other side such as cleft palate repair or reconstructive periodontal surgery.[12, 13]

With respect to the impact of sterilisation on electrospun scaffolds we have previously reported that the method of sterilisation impacts on the scaffold and subsequent cell culture.[9] This is illustrated in **Figure 6** which shows the effects of peracetic acid, gamma irradiation and ethanol on the fibre diameter and ultimate tensile strength and Young's modulus of a PLGA scaffold.

Gamma irradiation has no significant effect on fibre diameter whereas peracetic acid and ethanol reduce fibre diameter by approximately 50%. With respect to ultimate tensile strength each of the methods of sterilisation changed the ultimate tensile strength and the elasticity of the scaffolds. Culture of cells on these scaffolds further reduced the ultimate tensile stress, but increased the elasticity.

Finally, a method of testing the effect of dynamic biaxial distension on cells cultured on electrospun scaffolds is presented. This proof-of-concept approach shows that cells remain viable during dynamic distension but also produce increased amounts of elastin under these conditions. This contrasts markedly to the lack of elastin when the same cells on the same scaffold are maintained under static conditions (see **Figure 7**).

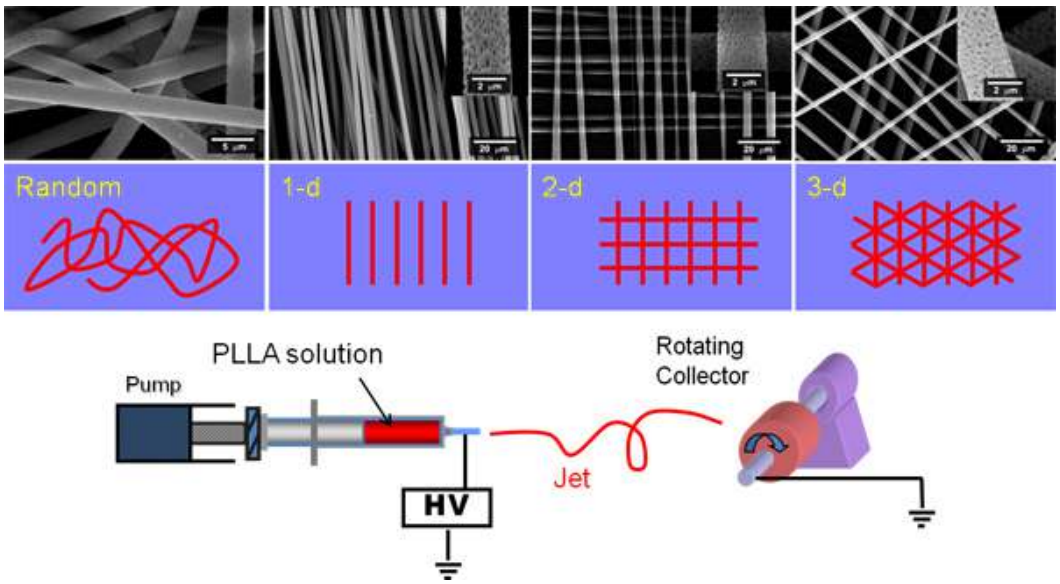

Figure 1. Shows a cartoon of an electrospinning rig and of the spinning of random and parallel fibres and then layers of fibres placed over each other. Perpendicular fibres can be created by electrospinning a set of aligned fibres onto aluminium foil, rotating the foil by 90° and then immediately electrospinning a second set of aligned fibres on top of these.

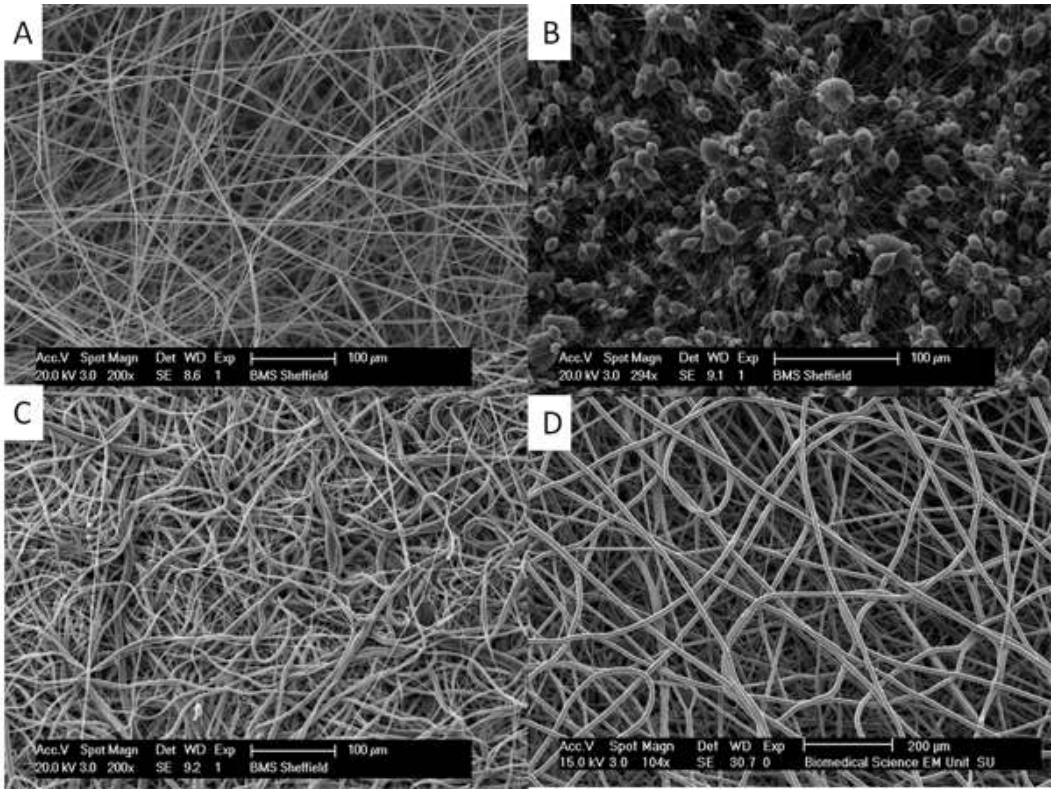

Figure 2. Shows the morphology of random electrospun mats of (A) PLA (scale bar is 100 µm), (B) PHBV (scale bar is 100 µm), (C) PCL (scale bar is 100 µm) and (D) PLGA (scale bar is 200 µm). Note that PLA, PCL and PLGA are all microfibrous uniform scaffolds. PHBV is spun as a 'pearl necklace' with nanofibres connecting 5-20 µm sized beads. Click here to view larger figure.

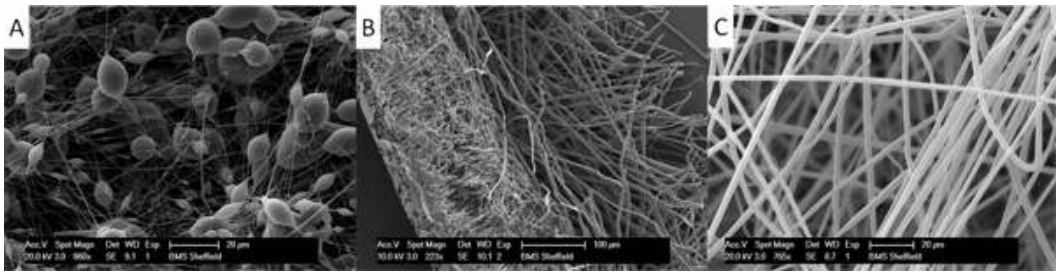

Figure 3. Production of a multilayered scaffold. Here the scaffolds are initially spun using PHBV and then syringes filled with PLA or PCL are used. These are spun on top of the PHBV scaffold. The figure shows the appearance of these multilayered scaffolds, (A) A single PHBV layer, (B) A cross section of a PHBV-PLA bilayer, showing the dense nanofibrous, 'pearl necklace' PHBV layer (left) and more open microfibrous PLA layer (right) and (C) A single PLA layer. Click here to view larger figure.

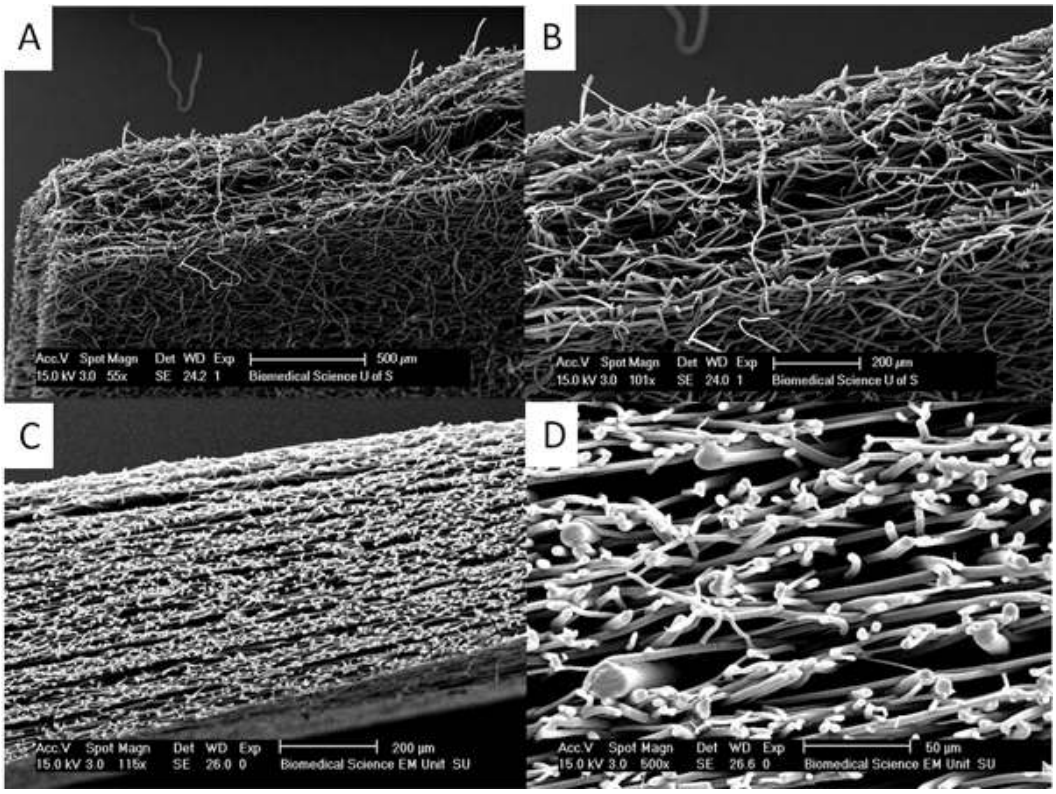

Figure 4. Thicker scaffolds can be produced by heat annealing and vapour annealing. (A) and (B) show a section through a vapour annealed PLA scaffold where initial fibrous scaffolds of approximately 150 µm are been placed together and dichloromethane vapour is used to make much thicker scaffolds of up to 500 µm. In (C) and (D) one can see that the scaffold consists of layers of much thicker fibres interspersed with layers of thinner fibres created by heat annealing layers of thin and thick fibres together. This approach can be used to produce scaffolds of complex mechanical properties. Click here to view larger figure.

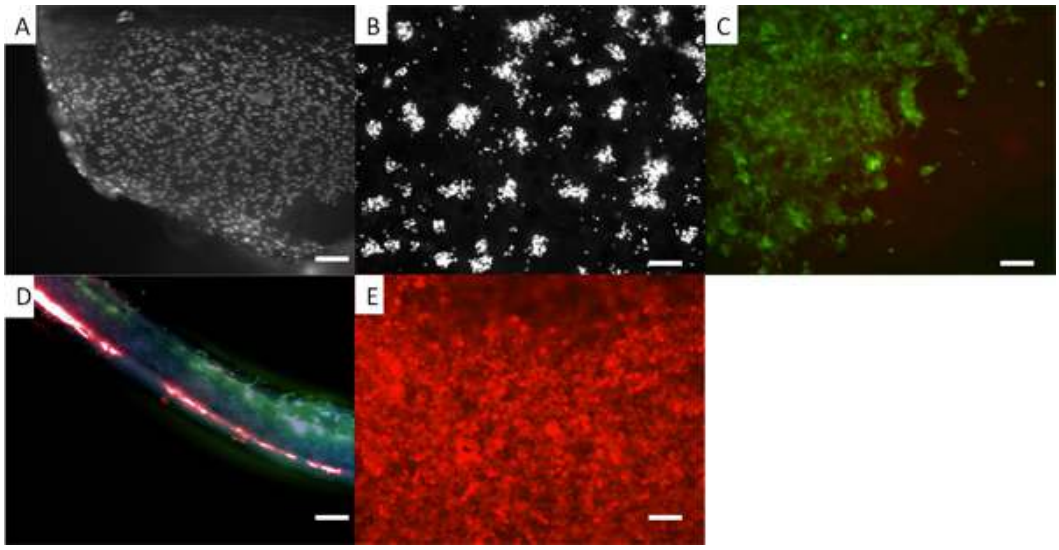

Figure 5. Appearance of cells on a bilayer scaffold. In all cases the cells present are human dermal fibroblasts. (A) Fibroblasts on electrospun PLA where the cells are fixed and stained with DAPI. (B) DAPI stained cells on PHBV. In (C) the fibroblasts are pre-stained with a vital dye, CellTracker green, and you can see the appearance of them on the PLA side of the bilayer. (D) A section through the bilayer with red stained fibroblasts on the lower PHBV surface and green stained fibroblasts on the upper PLA surface. (E) Fibroblasts pre-stained with CellTracker red grown on the PHBV surface. The use of vital fluorescent dyes provides a convenient methodology for looking at the distribution of cells on the scaffold while the cells are still growing. One can routinely use these dyes for at least 7 days. However the concentration of dye becomes diluted as the cells divide. Scale bars are equal to 0.1 mm.

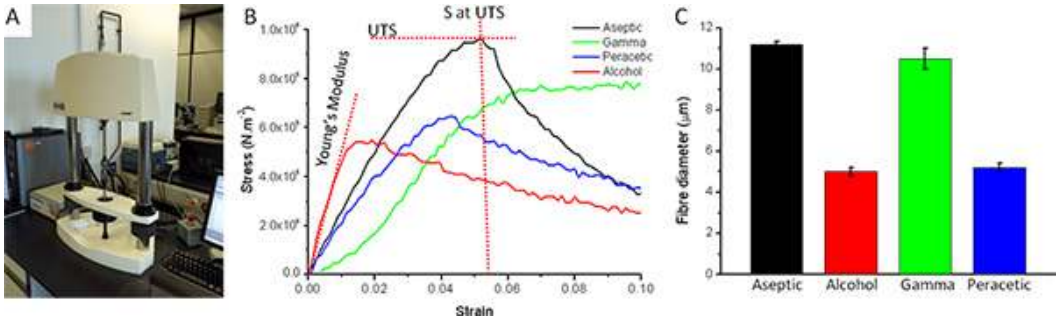

Figure 6. Biomechanical properties of electrospun scaffold are obtained using a Bose Electroforce tensiometer device (A). (B) Stress/strain curves of PLGA scaffolds sterilised by gamma irradiation, alcohol, peracetic acid, or aseptically produced. Three measurements can be obtained from such a graph: the ultimate tensile stress (UTS) to which the fibre can be subjected before it breaks, the ultimate tensile strain and the Young's modulus. The latter gives an indication of the elasticity of the scaffold. (C) The effect of each sterilisation method on PLGA fibre diameter in μm. Each sterilisation methodology decreased UTS. Both peracetic acid and gamma irradiation decrease the Young's modulus giving a more elastic scaffold, alcohol makes the scaffold particularly brittle. Click here to view larger figure.

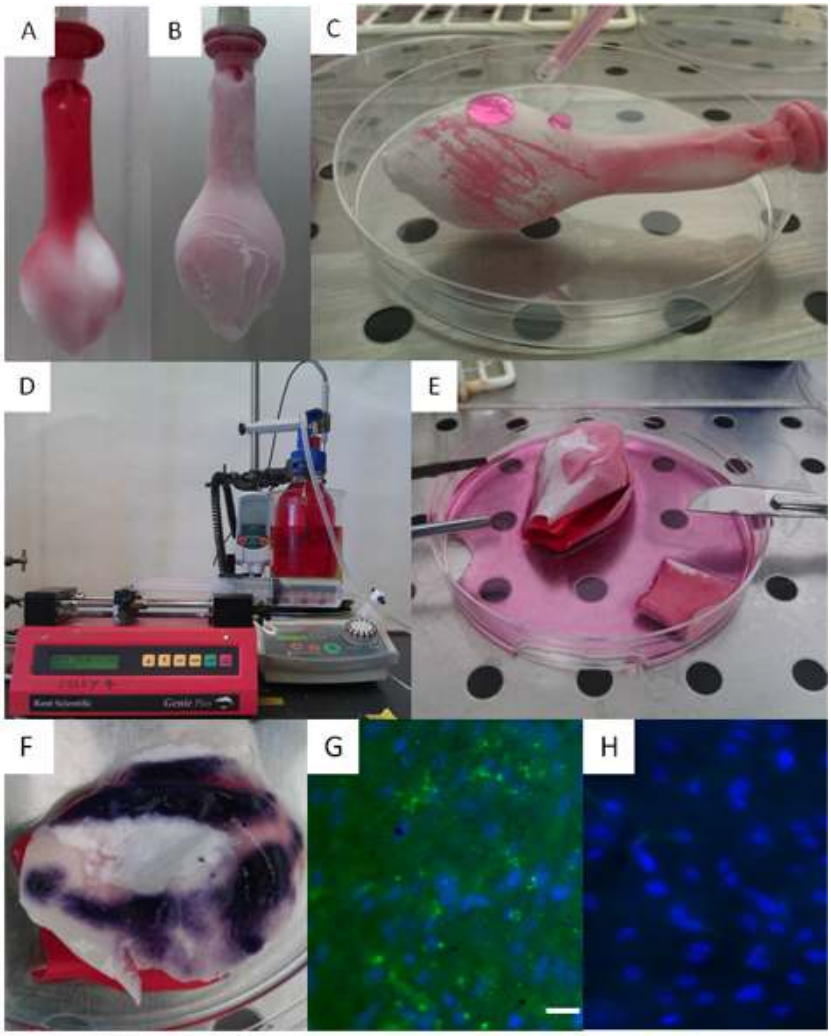

Figure 7. This figure shows the use of a simple balloon to provide a biaxial bioreactor on which scaffolds (and cells growing within the scaffolds) can be subjected to biaxial distension for periods of time. (A) A deflated balloon onto which electrospun fibres, PHBV, have been deposited. At this stage the balloon is partially covered with fibres. (B) A balloon fully coated with PHBV and PLA fibres. (C) A cell suspension is repeatedly pipetted onto the balloon. (D) A balloon placed within a bottle of sterile media where the balloon is connected to a syringe pump and PBS (used as a conducting electrolyte) is used to gently inflate and allow deflation of the balloon against a programmed schedule. (E) Cells on scaffolds being removed from the balloon at the end of the experiment and analysis undertaken for cell viability shown in (F) where viable cells develop a dark blue colour using the metabolic indicator 3-(4,5-dimethylthiazol-2-yl)-2,5-diphenyltetrazolium bromide. (G) Shows that cells (blue) cultured

on this balloon and subject to biaxial distension develop elastin fibres (green, stained using elastin specific antibodies), whereas the same cells on an identical scaffold (H) cultured under static conditions have negligible elastin production. Scale bars are equal to 0.025 mm.

Discussion

Electrospinning is a very popular technique for producing scaffolds for tissue engineering.[14, 15, 16] While it is relatively simple to produce basic electrospun scaffolds for experimental use the technique is also complex and multifaceted with many variables.[6] There are many studies describing how the electrospinning parameters determine the scaffold produced. In this study the focus is on the considerable challenges post production to make scaffolds of appropriate architectures and mechanical properties and to encourage cells within them to make extracellular proteins to achieve tissue fit for implantation in man.

Our aim in this article is to describe methods to equip readers to design and characterise scaffolds for a wide range of purposes. In this article we describe methodologies to make complex and thicker scaffolds and to sterilise scaffolds for experimental and clinical use. We also describe imaging cells on the scaffolds and the induction of elastin fibre production by subjecting cells to biaxial distension.

Many of the desired features of scaffolds can be achieved post production (such as annealing several layers) and sterilisation. However these in turn will affect the mechanical properties of scaffolds. We report that sterilisation methodologies all tend to change ultimate tensile strength and Young's modulus to varying extents. A recent study from our group compared gamma irradiation, peracetic acid and ethanol for their effects as potential sterilising regimes for PLGA scaffolds.[9] The adverse effects of sterilisation techniques can be avoided by producing scaffolds under aseptic conditions - the latter requires the use of a cleanroom. Different users may select different methodologies but all should be aware that current sterilisation methodologies will impact negatively on the properties of the scaffolds.

Culture of cells on scaffolds also affects the scaffolds' mechanical properties. Induction of ECM production by subjecting cells on scaffolds to biaxial distension may be used to affect the mechanical properties.

The methodology of spinning one scaffold over another to make a bilayer membrane is easily understood and we describe bilayer scaffolds capable of supporting two diverse populations of cells illustrated in this paper by pre-labelling cells with two vital cell tracker dyes. These were used to illustrate that the bilayer membrane achieved its stated purpose.

Finally the budget biaxial distension rig described in this study can be used to deliver a range of regimes. Cyclic, linear, and random regimes can be readily programmed and applied. This versatility will allow the system to be utilised for many of the problems faced in tissue engineering such as, cleft palate, pelvic floor, bladder, and skin.

In the tissue engineering literature the use of uniaxial testing systems for culturing cells on scaffolds has been reported.[4] However we were unable to find any published literature dealing with how soft tissues respond to biaxial distension. This simple approach demonstrates that cells respond to biaxial distension with the production of elastin - a key component of the extracellular matrix which gives soft tissues elastic recoil. This gives a clear indication of how conditioning soft tissues as they grow in the laboratory offers a route to produce tissues appropriate for implantation for areas of the body where the native tissues have intrinsic elasticity. This is an area where further development will clearly be merited by the tissue engineering community and bioreactor manufacturers.

Disclosures

No conflicts of interest declared.

Acknowledgements

We thank BBSRC for funding a PhD for Mr. Frazer Bye.

References

1. Canton, I., McKean, R., Charnley, M., Blackwood, K., Fiorica, C., Ryan, A., & MacNeil, S. Development of an Ibuprofen-releasing biodegradable PLA/PGA electrospun scaffold for tissue regeneration. *Biotechnology and bioengineering*. **105**, 396-408 (2010).
2. Blackwood, K., McKean, R., Canton, I., Freeman, C., Franklin, K., Cole, A., Brook, I., Farthing, P., Rimmer, S., Haycock, J., Ryan, A., & MacNeil, S. Development of biodegradable electrospun scaffolds for dermal replacement. *Biomaterials.* **29**, 3091-3104 (2008).
3. Yang, F., Maurugan, R., & Wang, S. Electrospinning of nano/micro scale poly(L-lactic acid) aligned fibers and their potential in neural tissue engineering. Ramakrishna, S. *Biomaterials*. **26**, 2603-2610 (2005).
4. Sittichokechaiwut, A., Edwards, J.H., Scutt, A.M., & Reilly, G.C. Short bouts of mechanical loading are as effective as dexamethasone at inducing matrix production by human bone marrow mesenchymal stem cell. *Eur. Cell Mater.* **20**, 45-57 (2010).
5. Sill, T.J. & von Recum, H.A. Electrospinning: applications in drug delivery and tissue engineering. *Biomaterials*. **29** (13), 1989-2006 (2008).
6. Deitzel, J., Kleinmeyer, J., Harris, D., & N.C., N.B.T. The effect of processing variables on the morphology of electrospun nanofibers and textiles. *Polymer.* **42**, 261-272 (2001).
7. Fridrikh, S., Yu, J., Brenner, M., & Rutledge, G. Controlling the fiber diameter during electrospinning. *Physical review letters.* **90**, 1-4 (2003).
8. Fong, H., Chun, I., & Reneker, D. Beaded nanofibers formed during electrospinning. *Polymer*. **40** (16), 4585-4592 (1999).
9. Selim, M., Bullock, A.J., Blackwood, K.A., Chapple, C.R., & MacNeil, S. Developing biodegradable scaffolds for tissue engineering of the urethra. *BJU Int.* **107** (2), 296-302 (2010).

10. Tong, H.-W. & Wang, M. An investigation into the influence of electrospinning parameters on the diameter and alignment of poly(hydroxybutyrate-co-hydroxyvalerate) fibers. *Journal of Applied Polymer Science.* **120** (3), 1694-1706 (2011).
11. Tong, H.-W. & Wang, M. Electrospinning of poly(hydroxybutyrate-co-hydroxyvalerate) fibrous tissue engineering scaffolds in two different electric fields. *Polymer Engineering & Science.* **51** (7), 1325-1338 (2011).
12. Retzepi, M. & Donos, N. Guided Bone Regeneration: biological principle and therapeutic applications. *Clinical oral implants research*. **21**, 567-576 (2010).
13. Moreau, J., Caccamese, J., Coletti, D., Sauk, J., & Fisher, J. Tissue engineering solutions for cleft palates. *Journal of oral maxillofacial surgery.* **65**, 2503-2511 (2007).
14. Yang, F., Both, S., Yang, X., Walboomers, X., & Jansen, J. Development of an electrospun nano-apatite/PCL composite membrane for GTR/GBR application. *Acta biomaterialia*. **5**, 3295-3304 (2009).
15. Yoshimoto, H., Shin, Y., Terai, H., & Vacanti, J. A biodegradable nanofiber scaffold by electrospinning and its potential for bone tissue engineering. *Biomaterials.* **24**, 2077-2082 (2003).
16. Telemeco, T., Ayres, C., Bowlin, G., Wnek, G., Boland, E., Cohen, N., Baumgarten, C., Mathews, J., & Simpson, D. Regulation of cellular infiltration into tissue engineering scaffolds composed of submicron diameter fibrils produced by electrospinning. *Acta biomaterialia*. **1**, 377-385 (2005).

Biomaterials Science

RSC Publishing

PAPER

Development of bilayer and trilayer nanofibrous/microfibrous scaffolds for regenerative medicine

Cite this: *Biomater. Sci.*, 2013, **1**, 942

Frazer J. Bye,[a] Julio Bissoli,[a] Leanne Black,[a] Anthony J. Bullock,[a] Sasima Puwanun,[a] Keyvan Moharamzadeh,[b] Gwendolen C. Reilly,[a] Anthony J. Ryan[c] and Sheila MacNeil*[a]

Received 17th March 2013,
Accepted 22nd May 2013

DOI: 10.1039/c3bm60074b

www.rsc.org/biomaterialsscience

Many biomaterial scaffolds have been developed for use in tissue engineering usually for populating with a single cell-type. In this study we demonstrate the production of bilayer and trilayer nanofibrous/microfibrous biodegradable scaffolds suitable for the support, proliferation and yet segregation of different tissues – here used to separate soft tissue from bone forming tissue and keratinocytes from fibroblasts. Essentially we describe a nanofibre barrier membrane which is permeable to nutrients coupled with attached microfibers (either on one side or both sides) to support the proliferation of different cell types either side but prevents migration of cells across the barrier. Such membranes would be suitable for guided tissue regeneration in areas where one wishes to support both soft and hard tissues but keep them separated. We describe a sterile bilayer membrane electrospun from polyhydroxybutyrate-*co*-hydroxyvalerate (PHBV) (nanofibres) and polylactic acid (PLA) or poly ε-caprolactone (PCL) (microfibres) and a trilayer membrane electrospun in layers of PLA, PHBV, then PLA. These membranes are biocompatible, biodegradable and capable of supporting two different cell populations.

Introduction

Biomaterial scaffolds are extensively used as carriers for cells and as 3D scaffolds for the regeneration of new tissue. They are commonly tailored to specific tissue types. Thus they are designed to have the necessary mechanical properties for the tissue that they are seeking to repair or replace. All scaffolds must be biocompatible to avoid provoking an adverse immune response to be successful post-implantation. The majority of scaffolds (but not all) are designed to be biodegradable with the intention that cells introduced in the scaffolds will form a new tissue and supporting tissue matrix, replacing the implanted scaffold as it degrades, for a long term successful repair. Biodegradable devices also negate the necessity for a second surgical operation to remove the implant.[1] There are many polymers that can be used to create a biocompatible and degradable implant.[2,3]

[a]*Kroto Research Institute, University of Sheffield, Broad Lane, Sheffield, South Yorkshire S7 1LN, United Kingdom. E-mail: s.macneil@sheffield.ac.uk; Fax: +44 (0) 114 222 5943; Tel: +44 (0) 114 222 5995*
[b]*Academic Unit of Restorative Dentistry, The School of Clinical Dentistry, The University of Sheffield, Claremont Crescent, Sheffield, S102TA, United Kingdom. E-mail: k.moharamzadeh@sheffield.ac.uk; Fax: +44 (0) 114 226 5484; Tel: +44 (0) 114 271 7931*
[c]*Department of Chemistry, University of Sheffield, Sheffield, S3 7HF, United Kingdom. E-mail: a.ryan@sheffield.ac.uk; Fax: +44 (0) 114 222 9346; Tel: +44 (0) 114 222 9300*

The ultimate goal of tissue engineering is to be able to regenerate or replace diseased or damaged tissues.[4,5] Tissue engineering, based on autologous laboratory expanded cells and scaffolds, is most commonly used but sometimes scaffolds are designed to promote the in growth of the surrounding tissue *in vivo*.[6,7] Here the approach is essentially to concentrate on using the patient's own tissues in conjunction with scaffolds to regenerate the areas in need of repair.[8–12]

Thus in tissue engineering very often the patient's own tissues are biopsied, cells expanded in the laboratory and combined with scaffolds to regenerate tissues for repair of damaged areas. However there are many conditions when one needs to look at replacing both soft tissues and adjacent hard tissues or to introduce a scaffold that could promote the intrinsic repair of soft tissues and hard tissues.[13,14]

While it is entirely possible to culture skin cells or even epithelia it has been difficult to make more complex tissues. The last decade has seen a growing realisation that the 3D environment of the extracellular matrix in which cells live is far from passive. Not only are the cells receiving signals from the extracellular matrix proteins but the composition of the matrix and it's stiffness give major signals which guide the differentiation and performance of cells within this matrix.[15] Thus bone was originally repaired using metal splints, providing the structural and mechanical support while allowing the bone to heal.[16] There are now ceramics and osteoinductive materials which can be used to aid bone repair. Tissue

guidance membranes have been developed, for example for use in periodontal defects seeking to achieve guided tissue regeneration.[17–19] The problem of one tissue growing much faster than another, invading and preventing the appropriate expansion of the slower growing tissue needs to be considered.

One area where tissues require segregation is in the treatment of cleft palate. This condition affects 1 in every 500–700 live births worldwide.[20] The current standard treatment is protracted, involving many stages. While soft tissue defects can be readily repaired within a few months, defects of the hard tissue of the alveolar ridge (which bears teeth) and the hard palate are much more challenging. After birth a cleft lip is repaired at 3 months, and then the defect in the hard palate is covered with soft tissue at around 1 year. This results in the child having to use custom made acrylic moulded prosthesis known as an obturator.

Bone grafts to fill the hard palate defect are currently not used as an option as they have actually been found to lead to distortion of the maxilla and the results can be worse than no surgery.[21,22] Bone grafts appear to be satisfactory, immediately after implantation, but then the bone cells fuse and this tissue does not grow at the rate of the child's head causing major facial disfigurement. The subsequent complications and distortions to the maxilla are unacceptable and explain why the hard tissues of the palate are currently mostly left untreated and an obturator used.

The problem of treating hard tissue defects in the cleft palate is twofold. Firstly, hard tissues grow at a rate far slower than soft tissue. An implant must account for this and prevent the invasion of the much faster growing soft tissues into regions where the hard tissues are desired. The implant must also allow for the flow of nutrients in order to allow the separated tissues to proliferate. Secondly, the implant must be compatible with the growth of the patient. The area of a cleft defect approximately doubles in volume from birth to the age of 5 and this must be taken into consideration in developing materials and procedures for treatment of hard palate defects.[23,24] The implant must also be biocompatible and biodegradable as it would be undesirable to remove an implant at a later stage disturbing the new tissues and risking the formation of disfiguring scar tissue.

An ideal solution would be an approach that could treat both soft and hard palate defects early in the child's life requiring very minimal follow up. We emphasise that we are not aware of any such solution on the horizon at present. To achieve an early stage repair for soft and hard palate, the biomaterial to be introduced must be able to cope with the dramatic growth of the child's palate up to the age of five. For bone to form it is highly likely that bone forming tissue or cells will need to be introduced into the defect; one common source for similar surgery are bone chips from the femoral head. It would be quite possible to culture bone forming cells (bone marrow MSC for example) on a scaffold for use in the hard palate. However introduction of soft tissue, such as tissue engineered buccal mucosa or in growth of soft tissues from the periphery of the defect could threaten the development of hard palate tissues as soft tissues will grow throughout such a scaffold almost certainly forming a fibrotic scar. Scar tissue can contract extensively, distorting the growth of the palate, hence one requirement in developing materials for treatment of soft and hard palate defects is a biocompatible and resorbable tissue segregating membrane which should separate and yet still allow the proliferation of soft tissues on one side and hard tissues on the other without allowing in growth of soft tissues into the hard palate area.

A second area is tissue engineering of skin for burns or diabetic ulcer repair. A biopsy of healthy skin is taken, cultured and expanded in the laboratory on a scaffold ready for implantation back on the patient. Normally in the laboratory we culture keratinocytes under long-established conditions using murine fibroblast feeder cells and media with bovine foetal calf serum.[25] However, for use in the clinic, it would be preferable to achieve keratinocyte culture without the need for any animal products and the chance of viral or prion infection they may bring. We have had some success previously, using autologous fibroblast feeder cells (instead of murine cells) and omitting bovine serum in the initial expansion of keratinocytes.[26,27] Building on this a scaffold designed to provide a synthetic basement membrane would be advantageous as it would give the cells a framework around which to start producing the required extracellular matrix. If the scaffold was designed to be porous, fibroblasts cultured on the lower surface could act as a feeder layer, and culture may be achieved without the need for animal products.

With respect to choice of scaffolds, PHBV was selected for use as a barrier membrane due to its slow degradation time and ease of synthesis through phosphate starving the bacteria *Alcaligene eutrophus*.[28–30] Toxicological assessment of the polymer *in vitro* and *in vivo* has shown no negative effects or abnormalities when tested with cultured cells or in animal experiments and it has been patented for use as bioresorbable sutures.[31–33] Poly L-lactic acid is well known as a biodegradable biomaterial with good biocompatibility.[2,34–38] It has been used for several years in the MacNeil group and a knowledge base has been established, making it a good candidate for further investigation.[39,40] PCL was included in this study as it has been successfully used as a scaffold for production of bone, as extensively reviewed by Woodruff and Hutmacher.[41–45] We have experience of culturing autologous buccal mucosa based on de-epidermised acellular human dermis, and of taking this to the clinic for replacing scarred tissue of the urethra.[13,14,46] We also have previously developed synthetic electrospun scaffolds for soft tissue reconstruction.[40,47]

Against this background; our approach to designing a tissue barrier membrane is to harness electrospinning to produce bilayer and trilayer nanofibrous/microfibrous scaffolds suitable for separating and independent proliferation of two distinct tissue types such as soft tissue on one side and bone tissue on the other side. These scaffolds are designed for culturing a range of tissues under different situations. Thus we describe a bilayer structure made to segregate bone and soft tissues. We describe a trilayer structure intended to

support soft tissue growth either side. For example two populations of cells such as epithelial and stromal cells as shown here, require an open network (microfibers) to grow into but still require segregation (nanofibres). These scaffolds are also designed to be capable of plastic deformation so that they can grow with the growth of the child's skull.[48] These scaffolds are the first step towards developing a synthetic solution to tissue separation.

Methods and materials

Electrospinning of PHBV, PCL, and PLA monolayers

All electrospinning was conducted in an aseptic cleanroom environment.

10 wt% PLA, PCL (Sigma Aldrich, Dorset, UK) solutions were made by dissolving the bulk polymer in dichloromethane (DCM, Sigma Aldrich, Dorset, UK). 10 wt% PHBV (12 : 1 PHB–PHV, Goodfellow, Huntingdon, UK) solutions were made by dissolving the bulk polymer in a mixed solvent of 10 wt% methanol and 80 wt% DCM (solvent ratio 88.8 : 11.1 DCM–MeOH, Sigma Aldrich). These solutions were loaded into 4 × 5 ml syringes (20 ml in total), fitted with blunt-tip needles (0.6 mm ID), and placed onto a single syringe pump (40 μL min^{-1}, Genie Plus, Kent Scientific, Connecticut, USA). A mandrel, 20 cm wide and 10 cm in diameter, coated in aluminium foil and rotated at 200 rpm, was used to collect the fibres. A working distance of 17 cm from the needle tip to the mandrel was used for PLA and PCL and 10 cm for PHBV. A potential of +17 000 V was used (73030P, Genvolt, Shropshire UK).

Electrospinning of PHBV–PLA and PHBV–PCL bilayers

Bilayer membranes were electrospun by consecutively spinning a PHBV layer as above and then, without changing the aluminium foil, immediately spinning either PCL or PLA on-top using the conditions appropriate to PCL/PLA.

Electrospinning of PLA–PHBV–PLA trilayers

Trilayer membranes were electrospun by consecutively spinning a PHBV–PLA bilayer as above. The bilayer was peeled off the backing foil, turned over to reveal the uncoated PHBV side, and reattached using autoclave tape to the aluminium foil. A final coating of PLA was spun on the exposed PHBV face using the conditions above. This method was adopted to ensure a complete and uniform PHBV layer was produced rather than sequential electrospinning each layer one on top of the other and risking the denser PHBV layer being fragmented across the more open PLA layer. Two further PLA–PHBV–PLA trilayers were produced with decreasing amounts of PHBV to test the impermeability of the scaffold with decreasing PHBV content. This was achieved by loading the syringes with only 4 ml and 1 ml of the PHBV solution (20% and 5% of original volume) respectively.

Scanning electron micrographs of each scaffold were taken (Philips XL-20 SEM).

Porosity measurements

Scaffolds were cut into discs (14 mm diameter) and weighed on a balance. Scaffold thickness was determined by measuring cross section thickness of SEMs. SEM cross sectional thickness was chosen as it prevents scaffold deformation unlike other methods such as using a micrometer, thus allowing the actual volume of the scaffold to be calculated. The density of each scaffold was then calculated and the ratio of scaffold density to bulk polymer density was used calculate the bulk porosity.[49]

Mechanical testing of scaffolds

All scaffolds were cut into rectangles (5 mm × 20 mm) and measured for thickness using a micrometer. These sections were then placed in a Bose Electroforce 3100 instrument. A load of between 0 and 22 N was then applied up to a distension of 6 mm. The Young's modulus (E) was then calculated.

Cell culture and proliferation

Materials were acquired as follows: alizarin red, alkaline phosphatase system for ELISA, ammonium hydroxide, amphotericin B, dexamethasone, Dulbecco's modified Eagle's medium (DMEM), formaldehyde, gelatine type A, L-glutamine, β-glycerolphosphate, penicillin and streptomycin, perchloric acid, tris-HCl, trypsin/EDTA and zinc chloride were all from Sigma Aldrich, Dorset, UK. Fetal calf serum (FCS) was from Biosera, Sussex, UK. Trypsin was from Difco Laboratories, Detroit, USA. Mesenchymal progenitor cells (hES-MP™ 002.5) were obtained from Cellatris®, Göteborg, Sweden. αMEM was from BioWhittaker, Lonza, Switzerland. CellTracker green (CMFDA), CellTracker red (CMTPX) and fibroblast growth factor (bFGF) were from Invitrogen, USA. Magnesium chloride hexahydrate and triton X-100 were from BDH laboratory supplies, Poole, UK.

All experiments unless otherwise stated, were conducted in a class II laminar flow hood (Walker Safety Cabinets, Glossop, UK).

Scaffolds were produced under aseptic conditions in a cleanroom to avoid the detrimental effect that sterilisation methods have on their mechanical properties.[47]

Fibroblasts were obtained from skin samples obtained from patients, undergoing elective surgery for breast reduction or abdominoplasty, who gave consent for their tissue to be used for research purposes. Tissues were collected and used on an anonymous basis under Research Tissue Bank Licence 12179. Tissues were washed with phosphate buffered saline (PBS) containing streptomycin (0.1 mg ml^{-1}) and penicillin (100 IU ml^{-1}) and amphotericin B (0.5 μg ml^{-1}). Tissue samples were incubated in 0.1% w/v trypsin and 0.1% glucose in PBS (12–18 hours, 4 °C). The dermis was peeled off, minced finely and incubated with 10 ml of collagenase (0.5% w/v in DMEM and 10% FCS, 37 °C for 18 hours). Following centrifugation of the resulting cell suspension (400 g for 10 minutes), pelleted cells were cultured in DMEM supplemented with FCS (10% v/v), streptomycin (0.1 mg ml^{-1}), penicillin (100 IU ml^{-1}) and amphotericin B (0.5 μg ml^{-1}) and subcultured as necessary. Only fibroblasts of passage 4–9 were used in experiments.

The hESMPs were seeded into a T75 (EasyFlask™, Nunc, New York, USA) pre coated with gelatine (5 ml, 0.1% w/w in distilled water) and cultured in αMEM supplemented with penicillin (100 IU ml^{-1}), streptomycin (0.1 mg ml^{-1}), bFGF (4 ng mL^{-1}) and L-glutamine (100 mg ml^{-1}) until confluent.

Keratinocytes were obtained from skin samples obtained from patients as above, washed with streptomycin and penicillin (100 mg mL^{-1} and 100 IU ml^{-1} respectively in PBS). Tissue samples were incubated overnight (12 hours) in trypsin and glucose (0.1% w/v and 0.1% w/v respectively) in PBS at 4 °C. The epidermal and dermal layers were separated, and keratinocytes were scraped off of the lower surface of the epidermis and the upper surface of the dermis with a scalpel blade. Keratinocytes were then seeded at a density of 2×10^6 per T75 culture flask pre-seeded with 5×10^5 i3T3 cells in Greens' medium (3 : 1 v/v DMEM and Ham's F12 medium supplemented with 10% v/v FCS, 10 ng mL^{-1} EGF, 0.4 μg mL^{-1} hydrocortisone, 1×10^{-10} mol mL^{-1} cholera toxin, 1.8×10^{-4} mol L^{-1} adenine, 5 μg mL^{-1} insulin, 2×10^{-3} mol L^{-1} glutamine, 0.625 μg mL^{-1} amphotericin B, 100 IU mL^{-1} penicillin and 100 μg mL^{-1} streptomycin). Keratinocytes were maintained in culture and used prior to passage 3 in experiments.

Culture wells (10 mm diameter) were created by placing aseptic electrospun scaffold squares (1.5 × 1.5 cm) under stainless steel rings (internal diameter 10 mm) in a laminar flow hood and placed into a 12 well plate. Each scaffold was seeded with either 50 000 hESMPs or fibroblasts and left for 7 days. Cells were seeded by adding trypsin/EDTA (5 ml, 5 mg ml^{-1} trypsin, 2 mg ml^{-1} EDTA in saline) and incubating for 5 minutes at 37 °C. The suspension was centrifuged for 10 minutes (150 g). The cells were resuspended in 5 ml of cell appropriate medium and counted using a haemocytometer, and the concentration adjusted for seeding.

Resazurin (5 μg ml^{-1} in PBS) was used to assess cell viability on the 7th day. After removal of residual media, 1 ml of solution was added to each scaffold and incubated for 1 hour, following which 150 μL was taken from each sample and the optical density read (570 nm, Bio-Tek ELx800). The media was then replaced (1 ml per sample).

Cell migration into scaffolds at 7 days

Aseptic electrospun scaffold squares (1.5 × 1.5 cm) were fitted into Scaffdex Cellcrowns™24 (Tampere, Finland) in a laminar flow hood and placed into a 24 well plate. The PHBV face of the scaffold was seeded, as above, with 50 000 hESMPs, and left for 24 hours to allow attachment as per normal cell culture process.[39,40,48] The cell crown was then turned over, and the opposite face (PCL or PLA) seeded with 50 000 fibroblasts and left for 7 days (αMEM, 37 °C, 5% CO_2, media was replaced after 3 days).

CellTracker red (CMTPX) or green (CMFDA) were applied to the hESMPs and fibroblasts respectively, prior to seeding. Cells were washed 3 times with 5 ml PBS then 10 ml of serum free cell-appropriate medium containing CellTracker (10 mM) was added and the cells incubated for 45 minutes at 37 °C. After incubation, the cells were washed 3 times with 5 ml PBS following which they were seeded onto scaffolds. Scaffolds could then be imaged in an Axon ImageExpress microscope (Molecular Devices, Sunnyvale, USA) at 570 nm λ_{ex}–620 nm λ_{em} (CellTracker red) and 480 nm λ_{ex}–533 nm λ_{em} (CellTracker green).

Bone forming potential of hESMPs

hESMPs were cultured as above until confluent. And then seeded, as above, onto tissue culture plastic and PCL scaffolds (TCP, 6 well plate, 7500 cells per well) in 2 ml of αMEM supplemented with FCS (10% v/v), L-glutamine (10 mM), penicillin (100 IU ml^{-1}), streptomycin (0.1 mg ml^{-1}), dexamethasone (10 nM), ascorbic acid (50 μg ml^{-1}) and β-glycerolphosphate (5 mM). The cells were assessed for alkaline phosphatase activity by washing 3 times in PBS and adding cell digestion buffer (tris-HCl (0.15 M), zinc chloride (0.1 mM) and magnesium chloride (0.1 mM) in distilled water). Triton X-100 (1% v/v in cell digestion buffer) was added and then the samples incubated (30 minutes, 37 °C). The cell lysate (20 μL) was added to the alkaline phosphatase substrate (180 μL) and the solution vortexed. The solution was pipetted out into a 96 well plate, left for 10 minutes (at room temperature) and then absorbance readings taken every minute for 5 minutes (405 nm, Bio-Tek ELx800). (The plate reader was previously calibrated such that 1 absorbance unit represents 22.5 nM of product.)

The cells were also assayed for calcium mineral deposition by alizarin red. The samples were washed 3 times with 2 ml PBS, fixed with formaldehyde (3.7% in PBS, 10 minutes) and then washed 3 times with 2 ml PBS. 1 ml of alizarin red (40 mM in distilled water adjusted to pH 4.1 with ammonium hydroxide) was added to each sample. The samples were then agitated at room temperature for 20 minutes. Any residual dye was removed, and the samples washed with distilled water (until the water ran clear) and left to dry (4 hours). The bound alizarin red was solubilised by adding 1 ml of perchloric acid (50 mM in distilled water) to each well for 30 minutes and agitated. The absorbance of 200 μL samples were read at 405 nm on a plate reader (Bio-Tek ELx800).

Culture of keratinocytes and fibroblasts on trilayer scaffolds

PLA–PHBV–PLA trilayers and PLA monolayers (2 cm × 2 cm) were sterilised in peracetic acid (0.1% v/v in distilled water) for 3 hours and washed three times in PBS (1 ml). The scaffolds were then placed in 6-well plates. Stainless steel rings with an internal diameter of 1 cm were placed on top of the scaffolds. Human dermal fibroblasts (1×10^5 cells), pre-labelled with CellTracker green as above, were then seeded inside the steel rings and medium topped up to 3 ml. The scaffolds were incubated for 2 days (37 °C, 5% v/v CO_2). Following this, the scaffold was turned over. Human keratinocytes (3×10^5 cells per scaffold), pre-labelled with CellTracker green, were seeded on the reverse side of the scaffold. The steel rings were then removed on the 4th day of incubation. On the 5th day the constructs were raised to an air–liquid interface on stainless steel grids and incubated for 7 days. Culture medium was

replenished twice a week. Cell viability using resazurin was taken as above. Samples were then fixed by incubating at 37 °C, in formaldehyde (3.7% v/v in PBS) and then labelled with DAPI (1 ml of 1 μg ml^{-1} in PBS, 20 minutes, 37 °C). Fluorescence images at 365 nm λ_{ex}–460 nm λ_{em} for DAPI, 570 nm λ_{ex}–620 nm λ_{em} for CellTracker red, and 480 nm λ_{ex}–533 nm λ_{em} for CellTracker green were taken following the culture period. This was also repeated on PLA–PHBV–PLA trilayers using 4 ml (0.4 g) and 1 ml (0.1 g) of PHBV to form the barrier layer.

Statistics

Student's unpaired *t*-test was used to assess the statistical significance of differences between different fibre types.

Results

Fig. 1 and 2 show the fibre diameters that were obtained when a 10 wt% polymer solution was used. Electrospinning 10 wt% PHBV in DCM–MeOH produced fibres of 700 nm in diameter. In contrast a 10 wt% concentration of PLA and PCL in DCM produced 2.5 μm and 4 μm diameter microfibers respectively.

Table 1 shows porosity and mechanical data for the bulk polymer and electrospun scaffolds. Porosity measurements show a significant difference between the microfibrous scaffolds of PLA and PCL compared to the nanofibrous PHBV, with the microfibrous scaffolds being around 20% more porous. The Young's modulus (*E*) of the bulk polymer is higher than the measured *E* of the scaffolds in all cases. The highest *E* was recorded for the PLA–PHBV–PLA trilayer and is approximately 33% more than the next nearest, PHBV. Scaffolds containing PCL had *E* values of around 50% of those scaffolds not containing PCL.

Cell viability on scaffolds was demonstrated using a resazurin salt assay. Fig. 3 shows cell viability on the scaffolds after 7 days of culture compared to the same cells cultured on TCP. With respect to the attachment and expansion of fibroblasts

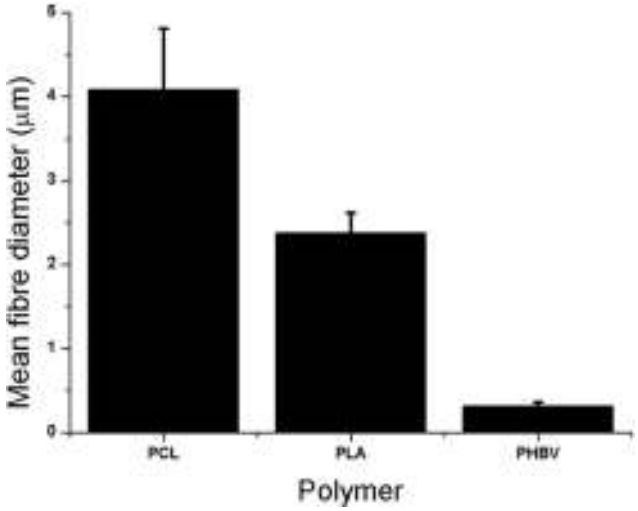

Fig. 2 Mean fibre diameters for PCL, PLA and PHBV of 4 μm, 2.5 μm and 700 nm respectively. Values are taken from measurement of SEM images, presented as average + standard error of the mean (+SEM), $n = 5$.

Table 1 Mechanical properties and porosity of scaffolds and their bulk polymers. Bulk polymer and porosity data is not available for bilayer and trilayer structures as these are composite scaffolds. Porosity measurements are the ratio of scaffold density to bulk density subtracted from 1 and turned into a percent. Bulk polymer Young's modulus (*E*) data is from the respective manufacturers where available or referenced. Values are the mean ± SEM, $n = 3$

Scaffold	Bulk *E*/GPa	Scaffold *E*/GPa	Bulk density/ g ml^{-1}	Scaffold density/ g ml^{-1}	Porosity/ %
PLA	3.6	0.012 ± 0.001	1.25	0.18	85 ± 0.8
PCL	0.3[50]	0.008 ± 0.003	1.145	0.25	78 ± 0.8
PHBV	0.5	0.015 ± 0.002	1.25	0.50	60 ± 1
PHBV–PLA	N/A	0.014 ± 0.008	N/A	0.24	N/A
PHBV–PCL	N/A	0.004 ± 6 × 10^{-5}	N/A	0.30	N/A
PLA–PHBV–PLA	N/A	0.021 ± 0.001	N/A	0.21	N/A

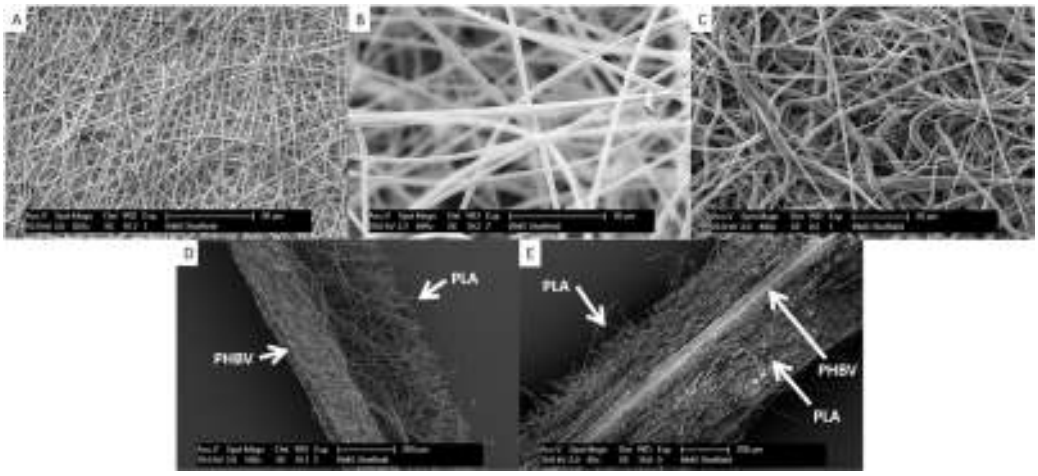

Fig. 1 Scanning electron micrographs (SEMs) of electrospun scaffolds A. PHBV. B. PLA. C. PCL. D. Representative cross-section of PHBV–PLA. The PHBV region on the left is dense while the PLA region has a more open structure. E. Representative cross section of a trilayer of PLA–PHBV–PLA.

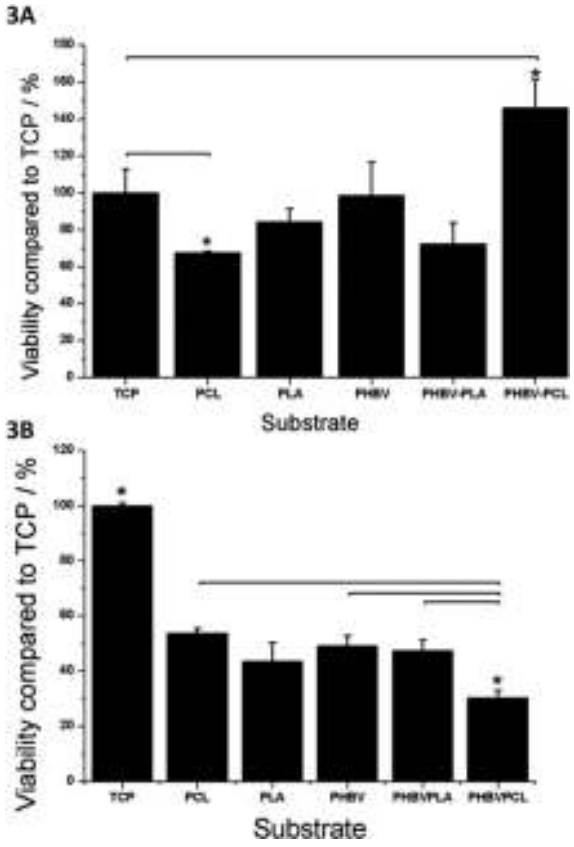

Fig. 3 A. Cell viability (assessed by the resazurin salt assay) of fibroblasts on PCL, PLA, PHBV, PHBV–PLA and PHBV–PCL scaffolds after 7 days. All scaffolds supported cell viability to a similar extent to TCP cells except for PCL on which cell viability was significantly lower (by approximately 30%) and PHBV–PCL where cell viability was approximately 40% better than TCP. B. Cell viability (assessed by the resazurin salt assay) of hESMPs on PCL, PLA, PHBV, PHBV–PLA and PHBV–PCL scaffolds after 7 days. All scaffolds were significantly less effective (approximately 50% as effective) at supporting cell growth compared to TCP except for PHBV–PCL which was only 30% as effective as TCP (significantly lower than PCL, PHBV and PHBV–PLA). Values are mean + SEM, $n = 3$.

all scaffolds compared reasonably well to TCP. Cells on PCL performed significantly worse than on TCP but only by approximately 30%, while cells on PHBV–PCL did significantly better (by approximately 20%). Scaffolds were less supportive of hESMP attachment and expansion with cell performance on all scaffolds being only approximately 50% as good as on TCP (Fig. 3B).

Fig. 4 shows fluorescent images of the cells on TCP (Fig. 4A) and on scaffolds (Fig. 4B–F). When seeded together, there is clear mixing of the cells on TCP, PLA and PCL. On these PLA and PCL scaffolds it is evident that fibroblasts and hESMPs have migrated through the scaffolds, as each face of the scaffold shows both cell types. With PHBV, however, there is a clear segregation of cell types. Even after 7 days of culture of fibroblasts on one face of the PHBV and culture of hESMPs on the opposite face, the cells remain segregated as can be seen in Fig. 4D (for fibroblasts) and Fig. 4E (for hESMPs). Fig. 4F is a cross section of the PHBV with the cells on their respective surfaces. As there was no mixing of the red and green fluorescently labelled cells it appears that PHBV has been successful at both supporting cell attachment and keeping the two cell types segregated for at least 7 days.

PHBV–PLA and PHBV–PCL bilayers were assessed for their ability to maintain cell segregation. Fig. 5A and D show the fibroblasts seeded on the PLA and PCL faces of the bilayers respectively. It is clear that hESMPs have not migrated through to this face. Likewise, Fig. 5B and E show the hESMPs seeded onto the PHBV faces of each bilayer respectively. Fig. 5C and F show cross sections through both bilayers with both the hESMPs and fibroblasts contained on their respective side.

The bone forming potential of hESMPs is demonstrated in Fig. 6. Continuous culture under appropriate conditions resulted in the cells differentiating into bone forming osteoblasts (increased alkaline phosphatase activity with time) and depositing calcium containing bone mineral (alizarin red staining).

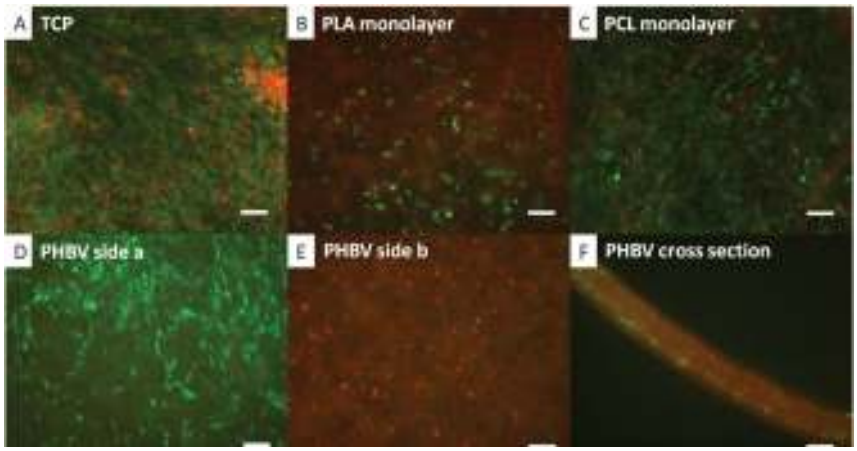

Fig. 4 Co-culture of CellTracker™ labelled fibroblasts (green) and hESMPs (red) on a range of scaffolds. In A hESMPs were seeded on day 1 (red) followed by an equal ratio of fibroblasts on day 2 (green) and cultured for 7 days on TCP. In B–F hESMPs were seeded on one side of the scaffold on day 1, and then fibroblasts on the other side on day 2 and these were then cultured for a further 7 days. The scaffolds used were PLA in B, PCL in C and PHBV in D, E and F. In A, B and C there is a clear mixture of red and green cells. In D and E however cells remain segregated. All fibroblasts (green) are shown on the surface shown in D and all hESMPs (red) are seen on the opposite side (E). F shows a cross section of the PHBV scaffold with clear separation of the hESMPs and fibroblasts. Scale bars 0.1 mm.

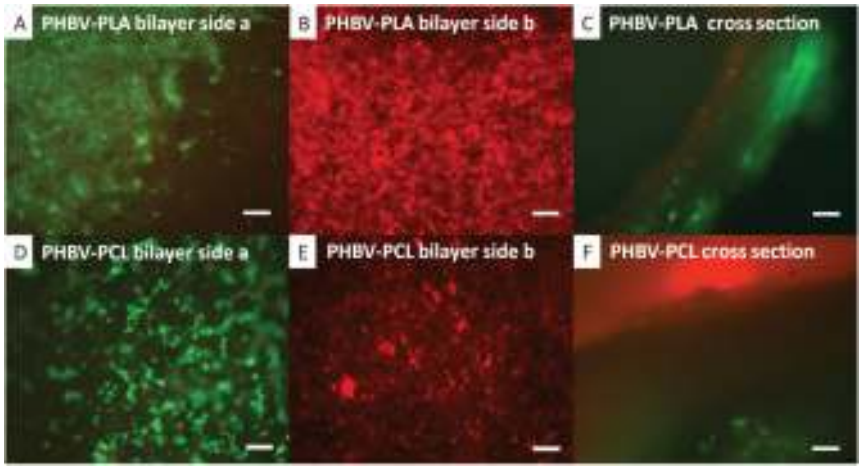

Fig. 5 Co-culture of CellTracker™ labelled fibroblasts (green) and hESMPs (red) on bilayer membranes of either PHBV–PLA or PHBV–PCL. hESMPs were seeded on day 1 (red) onto the PHBV face of each bilayer. Fibroblasts were seeded on either the PLA or PCL face of the bilayer on day 2 (green) and then cultured for a further 7 days. In A fibroblasts (green) are confined to the PLA face after 7 days with no sign of hESMPs (red). On the opposite face (B, PHBV), hESMPs (red) are also present once again with no fibroblasts. A cross section of the PHBV–PLA membrane is shown in C showing each cell type on its respective side after 7 days of culture. In D and E, fibroblasts (green) and hESMPs (red) are shown on the PCL and PHBV faces respectively and there is no mixing across these faces. F shows a cross section of the PHBV–PCL membrane and clearly shows each cell type still confined to their respective faces after 7 days of culture. All scale bars are equal to 0.1 mm.

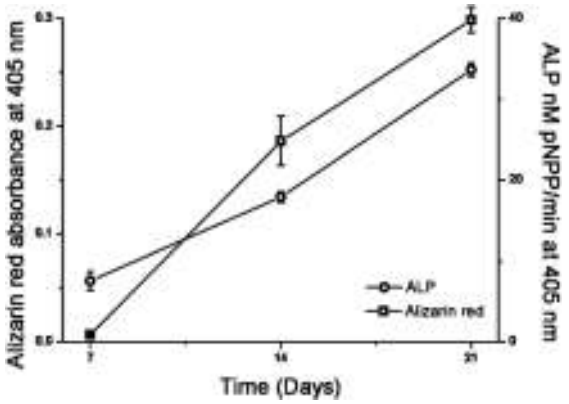

Fig. 6 Alkaline phosphatase activity and quantification of alizarin red staining of hESMPs after 7, 14 and 21 days on TCP. Increasing alkaline phosphatase activity indicates cell differentiation towards osteoblastic (bone forming) cells and increasing alizarin red indicates increased calcium (present in bone mineral) deposition. Values are mean ± SEM, $n = 3$.

The retained barrier properties of the PLA–PHBV–PLA trilayer scaffold are shown by the fluorescent images in Fig. 7. DAPI staining of the cell nuclei (blue) has been added to aid with visualising the cell nuclei. There are nuclei on either side of the scaffold, showing that both fibroblasts and keratinocytes adhere and proliferate. The face seeded with fibroblasts (green) shows no sign of keratinocytes (red) having penetrated through the scaffold. Likewise on the keratinocyte seeded face, there are no fibroblasts present. The final image shows a cross section, with both sides well populated by cells, but the fibroblasts and keratinocytes are confined to their respective sides. The recorded cell viability on the PLA–PHBV–PLA trilayer scaffold is good (around 50% compared to those on TCP). This is comparable to the bilayer scaffolds.

Decreasing the amount of the nanofibrous scaffold to 20% and 5% of the original weight does not appear to affect the barrier qualities of these trilayers with segregation of fibroblasts and keratinocytes maintained after 7 days also (Fig. 8).

Discussion

We demonstrate that a nanofibrous scaffold can act as a barrier to cell penetration while providing a scaffold for cell attachment and proliferation. For cleft palate treatment in the clinic, it would be our intention to culture autologous buccal mucosa on one face (as we have previously demonstrated) and autologous periosteal cells as a bone precursor on the opposite face.[47] These are being investigated for their bone forming ability at present. These could be harvested at the time of a cleft lip repair, expanded in the laboratory, and then re-introduced on a bilayer membrane to encourage the growth of a native hard palate.

The concept of segregating tissue for regenerative purposes is not new. It has been established in dentistry for some time where tissue guides have been developed to segregate soft tissue from bone forming tissue in periodontal repairs.[18,19] Commercial materials include collagen-based membranes, biodegradable polymers and Teflon.[2,51,52] Collagen has a high biodegradation rate, can be difficult to remove when there are problems, and can introduce the risk of infection as it is an animal derived tissue (usually bovine). Therefore, one must be mindful of the source of the collagen to avoid any risk of prion disease transmission.[51] Teflon is a very successful and effective barrier to cells. However, it cannot be left implanted and follow up procedures are required to remove it. This is not

Fig. 7 Co-culture of CellTracker™ labelled fibroblasts (green) and keratinocyte (red) on trilayer membranes of PLA–PHBV–PLA. Fibroblasts were seeded on day 1 (green) onto one face of each trilayer. Keratinocytes were seeded on the opposite face of the trilayer on day 4 (green) and then cultured for a further 7 days. In A, fibroblasts (green) are confined to the PLA face after 7 days with no sign of keratinocytes (red). On the opposite face, keratinocytes (red) are present once again without fibroblasts. A cross section of the PLA–PHBV–PLA membrane is shown in C showing each cell type on its respective side after 7 days of culture. Cell nuclei have been stained using DAPI (blue). All scale bars are equal to 0.1 mm.

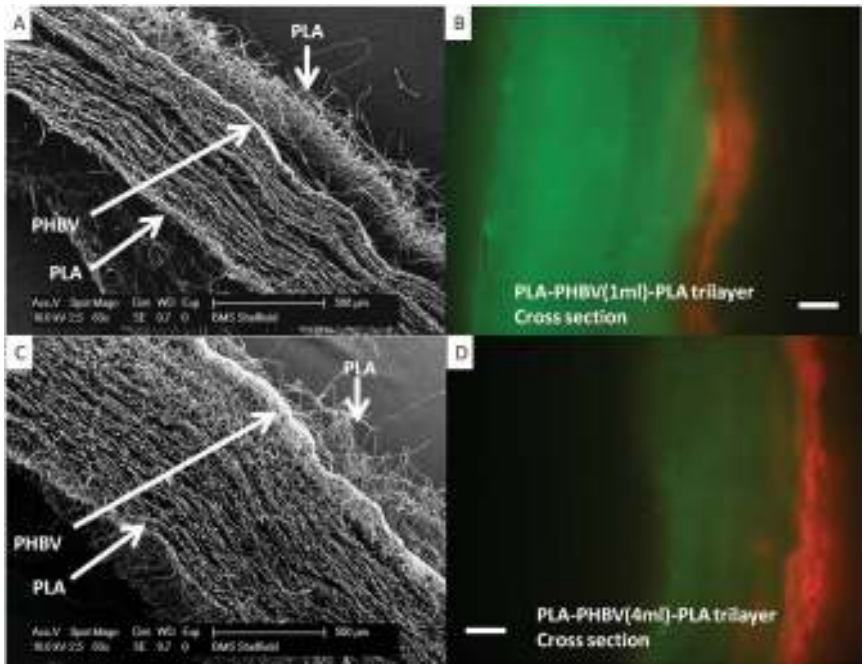

Fig. 8 SEM and fluorescence microscopy of PLA–PHBV–PLA trilayers with reduced PHBV layer thickness. Panels A and C shows SEM cross sections of trilayers made using 1 ml and 4 ml of PHBV respectively (5% and 25% of original volume used in Fig. 4, 5 and 7. Microfibrous PLA is present on the top and bottom of each scaffold, with a dense nanofibrous PHBV slither through the middle of each. Panels B and D show fluorescence microscopy of cross sections with fibroblasts (green) cultured on one face and keratinocytes (red) cultured on the opposite face with separation maintained after a week (demonstrated by no 'bleed though' of the colours to opposite faces).

ideal as it disturbs the newly repaired tissues risking scar formation and infection.[53] Current biodegradable polymer solutions are commonly based on PLA, however, these are not entirely popular with surgeons as they are difficult to handle.[54]

In the current study the nanofibrous component of the bilayer and trilayer makes the material much more user-friendly, it can be readily picked up, shaped and handled without tangling, sticking or loss of shape, unlike microfibrous electrospun scaffolds.

The methodology of spinning one scaffold on top of another is reproducible and consistent. Our data show that by using cell tracker labelled cells it is possible to culture two different cell types on these scaffolds while maintaining segregation for at least 7 days.

The cell tracker fluorescent dyes are very successful at labelling cells through to 7 days, but the intensity of the dye decreases noticeably after longer periods.

In this study we simply examined fibroblast attachment as a soft tissue model. We selected hESMPs as a model bone forming cell as they are capable of forming bone (see Fig. 6), and are also an appropriate cell type against which other candidate cells can be compared.[55,56] Here we present hESMP bone forming potential on TCP, and other studies have shown similar bone forming potential on other well known

biodegradable polymers such as PCL, PLA and PLGA.[57–60] Similarly we confirm that keratinocytes and fibroblasts are effectively segregated when cultured on a trilayer membrane separated by a nanofibrous scaffold layer.

Conclusions

In summary, we describe simple methods for electrospinning bilayer and trilayer nanofibrous/microfibrous membranes capable of supporting the culture of two very different cell types, while maintaining segregation between the two. We hope that these will prove useful in a range of applications such as the first step in developing an approach for tissue engineering of cleft palate and also guided tissue regeneration for periodontal disease and in production of tissue engineered skin for treatment of patients with extensive full thickness burns injuries.

Acknowledgements

We thank the BBSRC for funding a PhD for Frazer Bye and the Narusuan University for funding a PhD for Sasima Puwanun.

Notes and references

1 J. Middleton and A. Tipton, *Biomaterials*, 2000, **21**, 2335–2346.
2 M. Sabir, X. Xu and L. Li, *J. Mater. Sci.*, 2009, **44**, 5713–5724.
3 J. Jang, O. Castano and H. Kim, *Adv. Drug Delivery Rev.*, 2009, **61**, 1065–1083.
4 L. Griffith and A. Grodzinsky, *Oppor. Med. Res.*, 2001, **285**, 556–561.
5 Y. Ikada, *Interface*, 2006, **3**, 589–601.
6 P. Warnke, I. Springer, Y. Acil, H. Bolte, P. Russo, E. Sherry, H. Terheyden, J. Wiltfang, H. Eufinger, E. Behrens and M. Wehmoller, *Lancet*, 2004, **364**, 766–770.
7 P. Warnke, J. Wiltfang, I. Springer, Y. Acil, H. Bolte, M. Kosmahl, P. Russo, E. Sherry, U. Lutzen, S. Wolfart and H. Terheyden, *Biomaterials*, 2006, **27**, 3163–3167.
8 S. Terada, M. Sato, A. Sevy and J. Vacanti, *Yonsei Med. J.*, 2000, **41**, 685–691.
9 K. Rustad, M. Sorkin, B. Levi, M. Longaker and G. Gurtner, *Organogenesis*, 2010, **6**, 151–157.
10 J. Larrick and A. Mendelsohn, *Rejuvenation Res.*, 2010, **13**, 265–280.
11 P. H. Warnke, *Lancet*, 2006, **368**, 181–183.
12 W. Rowiński, *Ann. Transplant.*, 2007, **12**, 5–10.
13 S. Bhargava, C. Chappel, A. Bullock, C. Layton and S. MacNeil, *Br. J. Urol.*, 2004, **93**, 807–811.
14 S. Bhargava, J. Patterson, R. Inman, S. MacNeil and C. Chapple, *Eur. Urol.*, 2008, **53**, 1263–1271.
15 G. C. Reilly and A. J. Engler, *J. Biomech.*, 2010, **43**, 55–62.
16 L. Freed, G. Engelmayr, J. Borenstein, F. Moutos and F. Guilak, *Adv. Mater.*, 2009, **21**, 3410–3418.
17 A. Yen and P. Yelick, *Gerontology*, 2010, **57**, 85–94.
18 J. Moreau, J. Caccamese, D. Coletti, J. Sauk and J. Fisher, *J. Oral Maxillofac. Surg.*, 2007, **65**, 2503–2511.
19 M. Retzepi and N. Donos, *Clin. Oral Implants Res.*, 2010, **21**, 567–576.
20 P. Mossey, Addressing the global challenges of craniofacial anomalies. Report of a WHO meeting on international collaborative research on craniofacial anomalies, World health organisation technical report, 2004.
21 B. Sommerland, *J. R. Soc. Med.*, 1989, **82**, 677–679.
22 J. Lilja, *Scand. J. Surg.*, 2003, **92**, 269–273.
23 G. Nellhaus, *Paediatrics*, 1968, **41**, 106–114.
24 R. Langford, S. Sgouros, K. Natarajan, H. Nishikawa, M. Dover and A. Hockley, *Plast. Reconstr. Surg.*, 2003, **111**, 1591–1597.
25 J. G. Rheinwald and H. Green, *Cell*, 1975, **6**, 331–343.
26 A. J. Bullock, M. C. Higham and S. MacNeil, *Tissue Eng.*, 2006, **12**, 245–255.
27 T. Sun, M. Higham, C. Layton, J. Haycock, R. Short and S. MacNeil, *Wound Repair Regen.*, 2004, **12**, 626–634.
28 WD. Luzier, *Proc. Natl. Acad. Sci. U. S. A.*, 1992, **89**, 839–842.
29 M. Yasin, S. Hollands and B. Tighe, *Biomaterials*, 1990, **11**, 451–455.
30 S. Holland, A. Jolly, M. Yasin and B. Tighe, *Biomaterials*, 1987, **8**, 289–295.
31 H. Li, W. Zhai and J. Chang, *J. Mater. Sci. Mater. Med.*, 2008, **19**, 67–73.
32 D'Agnostino and William, *US Pat.* 20090112259, 2009.
33 E. Shishatskaya, T. Volova and I. Gitelson, *Dokl. Biol. Sci.*, 2001, **383**, 109–111.
34 M. Wang, *Biomaterials*, 2003, **24**, 2133–2151.
35 F. Yang, R. Maurugan, S. Wang and S. Ramakrishna, *Biomaterials*, 2005, **26**, 2603–2610.
36 T. Telemeco, C. Ayres, G. Bowlin, G. Wnek, E. Boland, N. Cohen, C. Baumgarten, J. Mathews and D. Simpson, *Acta Biomater.*, 2005, **1**, 377–385.
37 L. Suggs and S. Moore, in *Physical Properties of Polymers Handbook*, ed. J.E. Mark, Springer, 2nd edn, 2007, ch. 55, pp. 939–950.
38 E. Engelhardt, L. Micol, S. Houis, F. Wurm, J. Hilborn, J. Hubbell and P. Frey, *Biomaterials*, 2011, **32**, 3969–3976.
39 I. Canton, R. McKean, M. Charnley, K. Blackwood, C. Fiorica, A. Ryan and S. MacNeil, *Biotechnol. Bioeng.*, 2010, **105**, 396–408.
40 K. Blackwood, R. McKean, I. Canton, C. Freeman, K. Franklin, A. Cole, I. Brook, P. Farthing, S. Rimmer, J. Haycock, A. Ryan and S. MacNeil, *Biomaterials*, 2008, **29**, 3091–3104.
41 J.-T. Schantz, S. H. Teoh, T. C. Lim, M. Endres, C. X. F. Lam and D. W. Hutmacher, *Tissue Eng.*, 2003, **9**(Suppl 1), S113–S126.
42 M. A. Woodruff and D. W. Hutmacher, *Prog. Polym. Sci.*, 2010, **35**, 1217–1256.
43 V. Guarino, F. Causa, P. Taddei, M. di Foggia, G. Ciapetti, D. Martini, C. Fagnano, N. Baldini and L. Ambrosio, *Biomaterials*, 2008, **29**, 3662–3670.

44 S. A. Abbah, C. X. L. Lam, D. W. Hutmacher, J. C. H. Goh and H.-K. Wong, *Biomaterials*, 2009, **30**, 5086–5093.
45 J.-T. Schantz, T.-C. Lim, C. Ning, S. H. Teoh, K. C. Tan, S. C. Wang and D. W. Hutmacher, *Neurosurgery*, 2006, **58**, ONS-E176.
46 S. MacNeil, *Nature*, 2007, **445**, 874–880.
47 M. Selim, A. J. Bullock, K. A. Blackwood, C. R. Chapple and S. MacNeil, *Br. J. Urol. Int.*, 2010, **107**, 296–302.
48 F. Bye, L. Wang, A. Bullock, K. Blackwood, A. Ryan and S. MacNeil, *J. Vis. Exp.*, 2012, e4172.
49 F. Dullien, *Porous Media Fluid Transport and Pore Structure*, Academic Press, 1979.
50 S. Eshraghi and S. Das, *Acta Biomater.*, 2010, **6**, 2467–2476.
51 M. Bornstein, D. Bosshardt, D. Buser, S. Chen, S. Jensen, I. Rocchietta, R. Schenk, M. Simion and T. von Arx, *20 Years of Guided Bone Regeneration in Implant Dentistry*, Quintessence Publishing Co, Inc, 1994, pp. 86–139.
52 D. Lundgren and C. Slotte, *J. Clin. Periodontol.*, 1999, **26**, 56–62.
53 S. Ivanovski, *Aust. Dental J.*, 2009, **54**, S118–S128.
54 A. Cipitria, A. Skelton, T. R. Dargaville, P. D. Dalton and D. W. Hutmacher, *J. Mater. Chem.*, 2011, **21**, 9419–9453.
55 G. M. de Peppo, P. Sjovall, M. Lenneras, R. Strehl, J. Hyllner, P. Thomsen and C. Karlsson, *Tissue Eng. Part A*, 2010, **16**, 3413–3426.
56 C. Karlsson, K. Emanuelsson, F. Wessberg, K. Kajic, M. Z. Axell, P. S. Eriksson, A. Lindahl, J. Hyllner and R. Strehl, *Stem Cell Res.*, 2009, 39–50.
57 X. Xin, M. Hussain and J. J. Mao, *Biomaterials*, 2007, **28**, 316–325.
58 J. Hu, L. A. Smith, K. Feng, X. Liu, H. Sun and P. X. Ma, *Tissue Eng. Part A*, 2010, **16**, 3507–3514.
59 J. Nam, J. Johnson, J. J. Lannutti and S. Agarwal, *Acta Biomater.*, 2011, **7**, 1516–1524.
60 R. M. Delaine-Smith, S. MacNeil and G. C. Reilly, *Eur. Cell Mater.*, 2012, **24**, 162–174.